US Army Corps of Engineers

UNIVERSITY OF MINNESOTA
MINNEAPOLIS

HYDRAULICS LABORATORY

ENVIRONMENTAL LABORATORY

(2)

WATER QUALITY
RESEARCH PROGRAM

MISCELLANEOUS PAPER EL-90-13

ABSTRACTS OF THE SECOND INTERNATIONAL SYMPOSIUM ON GAS TRANSFER AT WATER SURFACES

FILE COPY

Hydraulics and Environmental Laboratories

DEPARTMENT OF THE ARMY
Waterways Experiment Station, Corps of Engineers
3909 Halls Ferry Road, Vicksburg, Mississippi 39180-6199

US ARMY ENGINEER WATERWAYS EXPERIMENT STATION

August 1990

Final Report

Prepared for DEPARTMENT OF THE ARMY
US Army Corps of Engineers
Washington, DC 20314-1000

Unclassified

SECURITY CLASSIFICATION OF THIS PAGE

REPORT DOCUMENTATION PAGE

Form Approved OMB No. 0704-0188

1a. REPORT SECURITY CLASSIFICATION Unclassified	1b. RESTRICTIVE MARKINGS
2a. SECURITY CLASSIFICATION AUTHORITY	3. DISTRIBUTION/AVAILABILITY OF REPORT Approved for public release; distribution unlimited.
2b. DECLASSIFICATION/DOWNGRADING SCHEDULE	
4. PERFORMING ORGANIZATION REPORT NUMBER(S) Miscellaneous Paper EL-90-13	5. MONITORING ORGANIZATION REPORT NUMBER(S)
6a. NAME OF PERFORMING ORGANIZATION USAEWES, Hydraulics and Environmental Laboratories 6b. OFFICE SYMBOL (If applicable)	7a. NAME OF MONITORING ORGANIZATION
6c. ADDRESS (City, State, and ZIP Code) 3909 Halls Ferry Road Vicksburg, MS 39180-6199	7b. ADDRESS (City, State, and ZIP Code)
8a. NAME OF FUNDING/SPONSORING ORGANIZATION US Army Corps of Engineers 8b. OFFICE SYMBOL (If applicable)	9. PROCUREMENT INSTRUMENT IDENTIFICATION NUMBER
8c. ADDRESS (City, State, and ZIP Code) Washington, DC 20314-1000	10. SOURCE OF FUNDING NUMBERS PROGRAM ELEMENT NO. / PROJECT NO. / TASK NO. / WORK UNIT ACCESSION NO.

11. TITLE (Include Security Classification)

Abstracts of the Second International Symposium on Gas Transfer at Water Surfaces

12. PERSONAL AUTHOR(S)

13a. TYPE OF REPORT	13b. TIME COVERED	14. DATE OF REPORT (Year, Month, Day)	15. PAGE COUNT
Final report	FROM ____ TO ____	August 1990	252

16. SUPPLEMENTARY NOTATION

Available from National Technical Information Service, 5285 Port Royal Road, Springfield, VA 22161.

17. COSATI CODES			18. SUBJECT TERMS (Continue on reverse if necessary and identify by block number)
FIELD	GROUP	SUB-GROUP	Chemical processes, Water surfaces Gas transfer Physical processes,

19. ABSTRACT (Continue on reverse if necessary and identify by block number)

The Second International Symposium on Gas Transfer at Water Surfaces was held 11-14 September 1990 in Minneapolis, MN. The symposium was sponsored by the US Army Engineer Waterways Experiment Station and Professional Development and Conference Services, University of Minnesota, and focused on (a) improvements in the ability to describe the physical and chemical processes associated with gas transfer and (b) applications of process knowledge to solve engineering problems. Eighty-eight papers were selected for presentation at the symposium in the following topic areas: (a) fundamentals of physical phenomena, (b) modeling, (c) laboratory and field measurement techniques; and (d) applications to streams and rivers, lakes and reservoirs, hydraulic structures, unit processes, water and wastewater treatment, biogeochemical cycles, seas and oceans, and artificial aeration. Contained herein are the abstracts of those papers selected for presentation. The papers for the symposium, which are subject to peer review and acceptance, will be published by the American Society of Civil Engineers.

20. DISTRIBUTION/AVAILABILITY OF ABSTRACT ☒ UNCLASSIFIED/UNLIMITED ☐ SAME AS RPT ☐ DTIC USERS	21. ABSTRACT SECURITY CLASSIFICATION Unclassified
22a. NAME OF RESPONSIBLE INDIVIDUAL	22b TELEPHONE (Include Area Code) / 22c. OFFICE SYMBOL

DD Form 1473, JUN 86 Previous editions are obsolete SECURITY CLASSIFICATION OF THIS PAGE

Unclassified

SUMMARY

The Second International Symposium on Gas Transfer at Water Surfaces was held 11-14 September 1990 in Minneapolis, MN. The symposium was sponsored by the US Army Engineer Waterways Experiment Station (WES) and Professional Development and Conference Services (PDCS), University of Minnesota. The First International Symposium on Gas Transfer at Water Surfaces, held at Cornell University in 1983, focused on an improved understanding of the physical and chemical processes controlling gas transfer. As a natural progression, the Second International Symposium focused on (a) improvements in the ability to describe the physical and chemical processes associated with gas transfer and (b) applications of process knowledge to solve engineering problems.

The purpose of the symposium was to provide a forum for interdisciplinary exchange of knowledge about the physicochemical processes that influence gas transfer and the subsequent engineering applications of that state-of-the-art knowledge to solve or mitigate environmental quality problems and improve process design. The scope of disciplines involved in the investigation of the gas transfer process is broad, including fluid mechanics, physical chemistry, chemical engineering, environmental engineering, biogeochemistry, hydraulics, physical oceanography, etc. The topic areas and abstracts presented herein reflect this broad scope of disciplines as applied to gas transfer at water surfaces.

This Miscellaneous Paper contains the abstracts of those papers that were selected for presentation at the symposium. Not included in these abstracts are two keynote addresses, "Equilibria and Partitioning at the Air-Water Interface," by Donald Mackay, University of Toronto, and "Effect of Gas Flow on Adsorption," by Thomas J. Hanratty, University of Illinois. The symposium papers, which are subject to peer review and acceptance, will be published by the American Society of Civil Engineers.

Topic areas included in the symposium were (a) fundamentals of physical phenomena: turbulence, waves, wind, convection, density stratification, bubbly flows; (b) modeling: numerical, conceptual, semiempirical, and empirical; (c) laboratory and field measurement techniques; and (d) applications to streams and rivers, lakes and reservoirs, hydraulic structures, unit processes, water and wastewater treatment, biogeochemical cycles, seas and oceans, and artificial aeration.

The breadth of abstract topics, submitted in response to the call for papers, indicated that the emphasis of gas transfer research has expanded from its traditional applications of unit processes and stream reaeration. Following the trend of the First International Symposium held in 1983, air-sea transfer was a major focus of the symposium. Seventeen of 88 accepted abstracts were related to applications of air-sea gas transfer. In addition, field and laboratory measurement techniques comprised 17 of the 88 accepted abstracts, indicating a need for improved measurements of air-water gas transfer and related processes. Two new areas of emphasis were artificial aeration techniques (with ten papers) and gas transfer at hydraulic structures (with eight papers). One research area for which only a few abstracts were submitted was groundwater applications, an emerging field in air-water gas transfer. It is likely that the applications in groundwater have not developed to the extent required to present results at the symposium.

The technical organization of this symposium was supported by the WES through funding provided by the US Army Corps of Engineers Water Quality Research Program. Administration of the symposium was supported by PDCS. Drs. John S. Gulliver, University of Minnesota, and Jeffery P. Holland, WES, were symposium organizers and directed the overall organizational efforts. Members of the Symposium Organizing Committee were:

Steve Wilhelms, Chair, WES
Bill Boyle, University of Wisconsin
Steve Eisenreich, University of Minnesota
Ed Holley, University of Texas
Steve McCutcheon, US Environmental Protection Agency
Gene Parker, US Geological Survey

The following persons comprised the Symposium Technical Advisory Group:

Thomas Hanratty, University of Illinois
Dean Harshbarger, Tennessee Valley Authority
Bernd Jahne, Universitat Heidelberg
Perry Johnson, US Bureau of Reclamation
Don MacKay, University of Toronto
Edward Monahan, University of Connecticut
Ron Rathbun, US Geological Survey
Richard Speece, Vanderbilt University
Ray Whittemore, Tufts University
P. Novak, University of Newcastle Upon Tyne

The symposium was cosponsored by the following professional organizations and societies:

American Geophysical Union
American Institute of Chemical Engineers
American Society of Civil Engineers

American Water Resources Association
International Association for Hydraulic Research
North American Lake Management Society
International Association for Great Lakes Research
Water Pollution Control Federation

Appreciation is expressed to the University of Minnesota Professional Development and Conference Services and to the Corps of Engineers Water Quality Research Program for sponsoring this symposium; to the cosponsors for providing their professional support; and to the authors and coauthors, who made the effort to share their knowledge. Special thanks are extended to Mses. Maria Juergens and Lori Gravens of PDCS for their logistical and administrative support and to Ms. Lulu Krogh, University of Minnesota St. Anthony Falls Hydraulic Laboratory, and Ms. Barbara Parsons, WES, for all their clerical efforts. Special appreciation is expressed to Ms. Laurin Yates, for her hard work and dedication in helping organize the exchange of information between the Organizing Committee, authors, session cochairs, and PDCS.

PREFACE

This report presents the abstracts of the Second International Symposium on Gas Transfer at Water Surfaces, which was held in Minneapolis, MN, on 11-14 September 1990. Organization of the symposium was funded by the US Army Corps of Engineers Water Quality Research Program (WQRP) and the University of Minnesota (UM) Department of Professional Development and Conference Services (PDCS). The technical aspects of the Symposium were organized by personnel of the US Army Engineer Waterways Experiment Station (WES) and the UM Department of Civil and Mineral Engineering. Arrangements for facilities and symposium administration were handled by PDCS. Dr. Jeffery P. Holland, Chief, Reservoir Water Quality Branch, Hydraulics Laboratory (HL), WES, and Dr. John Gulliver, UM, were symposium organizers. Mr. Steve Wilhelms, WES, chaired the Organizing Committee. Dr. Gulliver and Mr. Wilhelms prepared the executive summary.

Messrs. Glenn Pickering and Frank Herrmann, WES, were Chiefs of the Hydraulic Structures Division and HL, respectively. Mr. J. Lewis Decell, Environmental Laboratory, WES, was Manager of the WQRP. Technical Monitors of the WQRP for the Headquarters, US Army Corps of Engineers, were Messrs. David Buelow and James Gottesman and Dr. John Bushman.

COL Larry B. Fulton, EN, was the Commander and Director of WES. Dr. Robert W. Whalin was Technical Director.

This report should be cited as follows:

Hydraulics and Environmental Laboratories. 1990. "Abstracts of the Second International Symposium on Gas Transfer at Water Surfaces," Miscellaneous Paper EL-90-13, US Army Engineer Waterways Experiment Station, Vicksburg, MS.

CONTENTS

PHYSICAL PHENOMENA

Formation of droplets from bursting bubbles at an air-water interface

George M. AFETI*

School of Engineering, Abubakar Tafawa Balewa University, P.M.B. 0248, Bauchi, NIGERIA.

Abstract

A gas bubble formed in water will, in general, rise to the water surface and burst. The bubble breakup process leads to the formation of a liquid aerosol composed of droplets produced by the shattering of the thin liquid film that constitutes the bubble cap and the drops generated from the disintegration by instability of the vertical water jet that rises from the collapsing bubble cavity, once the bubble cap has disappeared. These two droplet families, known respectively as "film drops" and "jet drops" are capable of transporting across the water-air interface, traces of any chemical or biological substances that may be present in the liquid surface or sub-surface layers.

The droplet production mechanism is investigated using the principles of phenomenological analysis. It is shown that the bursting of bubbles greater than about 6mm in diameter produces only film drops and no jet drops. For smaller bubbles, jet drop formation lags film drop production by about 7ms. Experimentally, the various stages in the bubble breakup process are visualised using laser holographic techniques. The results suggest that the film drops are the end product of a chain of events, taking a total time of about 300µs, which begin with the formation of a number of liquid filaments in the bubble cap.

The bubble-droplets phenomenon finds practical relevance in environmental pollution studies, sea-to-air transfer of particles through the breaking of oceanic bubbles, and in the bubbling processes associated with certain chemical engineering systems and water treatment plants.

Research Fellow, Laboratoire d'Océanographie Physique de Toulon, Université de Toulon, 83597 La Garde Cedex, France.

The Effect of Surface Films on Near-Surface Aqueous-Phase Concentration Fluctuations

W. E. Asher* and J. F. Pankow

Oregon Graduate Institute of Science and Technology, 19600 N.W. Von Neumann Dr., Beaverton, OR 97006-1999

*Present address: Battelle/Marine Sciences Laboratory, 439 W. Sequim Bay Rd., Sequim, WA 98382

The behavior of concentration fluctuations very near a gas/liquid interface is of considerable importance in understanding gas/liquid mass transport. Previous studies of surface concentrations have been performed indirectly (Springer and Pigford, 1970) or directly using invasive techniques such as oxygen microelectrodes (Lee and Luk, 1982). However, it is not clear that the gas/liquid interfaces studied in these earlier experiments were free of adventitious surface films. Because Goldman et al. (1988) have shown that surface films can have a large effect on gas/liquid mass transport rates, it is appropriate to understand how concentration fluctuations differ between clean and film-covered gas/liquid interfaces.

In these experiments, carbon dioxide (CO_2) concentration fluctuations were measured at clean and film-covered CO_2/water interfaces. The water surface was cleaned by removal of surface water using 100% rayon lens paper followed by vacuuming with a Pasteur pipette. Surface films were deliberately created by addition of sufficient quantities of 1-octadecanol to form a monolayer on the water surface. Concentration fluctuations were measured using the noninvasive laser induced fluorescence (LIF) technique of Asher and Pankow (1989) that tracks CO_2 concentrations in unbuffered aqueous solutions using pH-sensitive fluorescent dyes. Varying turbulence intensities and length scales were studied using turbulence generated by a vertically oscillating grid.

Use of the LIF method permitted calculation of concentration fluctuation depths for a range of turbulence conditions for clean and film-covered interfaces. The concentration fluctuation depths were calculated using an empirical pH versus fluorescence intensity calibration curve and an assumed concentration profile in the aqueous boundary layer. Analysis of the results suggests that the calculational procedure was not sensitive to the functional form of this profile.

The calculated fluctuation depths show that the 1-octadecanol film increased the concentration boundary layer depth over that observed at a rayon/vacuum cleaned interface for a given set of turbulence conditions. Furthermore, the calculated concentration boundary layer depths for the film-covered surfaces agree with those measured by Lee and Luk (1982) under similar turbulence intensities. This suggests that the procedure used here to calculate the concentration fluctuation depths provided reasonable estimates of those depths.

The concentration fluctuation depths near a 1-octadecanol film-covered interface show that the aqueous surface was never fully renewed regardless of turbulence intensity. In contrast, at high turbulence intensities the concentration fluctuation depths at the rayon/vacuum cleaned surface indicated that the water surface was completely renewed by the turbulence motions of the water. However, as the turbulence intensity decreased, the number of surface renewal events also decreased. This suggests that the less-energetic turbulence eddies were not able to penetrate the concentration boundary layer.

The concentration fluctuation depths calculated here and concentration fluctuation timescales measured by Asher and Pankow (1989) were used in the surface penetration model of Harriott (1962) to predict the aqueous phase gas/liquid mass transport coefficient, k_L. The predicted k_L values were compared to k_L measured by Asher and Pankow (1986) under identical turbulence and interfacial conditions. This comparison shows that the surface penetration model can accurately predict k_L at both clean and film-covered interfaces for a wide range of turbulence conditions.

References

Asher, W. E.; Pankow, J. F.; Chem. Eng. Sci. 1989, 44, 1451-1455.

Asher, W. E.; Pankow, J. F.; Tellus 1986, 38B, 305-318.

Goldman, J. C.; Dennet, M. R.; Frew, N. M.; Deep Sea Res. 1988, 35, 1953-1970.

Harriott, P.; Chem. Eng. Sci. 1962, 17, 149-154.

Lee, Y. H.; Luk, S.; Ind. Eng. Chem. Fund. 1982, 21, 428-434.

Springer, T. G.; Pigford, R.; Ind. Eng. Chem. Fundam. 1970, 39, 458-465.

IMPACT OF THERMAL STRATIFICATION IN A SURFACE WATER LAYER ON THE RATE OF GAS EXCHANGE BETWEEN THE ATMOSPHERE AND THE WATER

V.F.Brekhovskikh, Dr. of Engineering, Deputy Director,
Z.V.Volkova, Cand. Sci. (Eng.), Senior Research Associate

Water Problems Institute of the USSR Academy of Sciences:
13/3 Sadovo-Chernogriazskaya, 103064, Moscow, USSR

Among the factors affecting the rate of mass transfer at the atmosphere-water interface the impact of the thermal structure of the surface water layer is yet poorly studied. The latter manifests itself clearly in calm weather and under weak winds.

Laboratory investigations show that thermal stratification has an appreciable effect on oxygen exchange between the atmosphere and water under the conditions of water heating and cooling. The experiments revealed empiric relations connecting the rate of mass transfer K_L and the Viasal - Brent frequency for the stable stratification and with the Raley number Ra for the unstable one:

$$K_L = f(E) = 1{,}46 \cdot 10^{-4}(1{,}01 - g\beta \Delta T/\delta_T), \quad cm/s, \tag{1}$$

$$K_L = f(Ra) = (3{,}40 - 0{,}0066\, g\beta \Delta T\, \delta_T^3/a\nu) \cdot 10^{-4}, \quad cm/s. \tag{2}$$

Here $g\beta\Delta T/\delta_T$ is the square of the Viasal-Brent frequency E ; $g\beta\Delta T\delta_T^3/a\nu$, the Raley number; ΔT , temperature overfall in the layer δ_T ; β , ν , a , coefficients of volumetric expansion, kinematic viscosity and thermal conductivity of water, respectively; g , gravity acceleration; ρ , water density.

Under the consitions of unstable stratification (with the cold water layer on the surface) the rate of oxygen mass transfer can be 21.5 - 2 times as large as under natural conditions. At the same time under stabvle stratification (with the warm layer on the surface) it is 2 - 3 times less.

Many in-situ observations show that different patterns of temperature distribution in the surface water layer, depending on the prevailance of certain processes of energy exchange between the water body and the atmosphere, exist. These patterns are: 1) $T_o < T_z$; 2) $T_o \simeq T_z$; 3) $T_o > T_z$; 4) distribution with subsurface temperature maximum.

Formation of the warm surface layer is most probabale for the spring-summer water heating in daytime, when the greater part of solar radiation is absorbed by the surface water layer. When more heat is lost for evaporation and radiation, than absorbed in the surface layer and under small values of contact heat exchange, the cold layer is formed. A model, taking into account the impact of unstable over-water air layer z/L and radiation factor, is developed to describe temperature overfall in the surface layer:

$$\Delta T = f\left[z/L;\ \frac{\sin^2 h(1 - 0{,}38n - 0{,}26n^2)}{\sin h + 0{,}07} - K_1 K_2 (1 - 0{,}5n)\right]. \tag{3}$$

Here h is the height of the Sun above the horizon; n , cloudness; K_1 and K_2 , coefficients.

The dependence of the coefficient of mass transfer on the thermal stratification, obtained as a result of laboratory expe-

riments allows us to describe the rate of mass transfer as a function of meteorological conditions. The obtained dependence also allows for the investigation of the diurnal dynamics of oxygen exchange between the water and the atmosphere, basing on the characteristics of the temperature overfall. Calculations show that the rate of mass transfer (and, therefore, oxygen inflow from the atmosphere into the water), can vary 2-3 times a day.

Thus, thermal stratification in the surface layer has an appreciable effect on gas exchange between the water body and the atmosphere, that should not be neglected in calculating the oxygen water balance. Under the conditions of calm weather and weak wind oxygen exchange can be determined using the information on the characteristics of the surface water layer, obtained on the basis of meteorological parameters.

When calculating oxygen regime in water bodies for the cases when photosynthesis is irrelevant in the dissolved oxygen balance and can be neglected, one should necessarily take into account and introduce corresponding corrective coefficients into the calculations.

HYDRODYNAMICS AND MASS TRANSFER
ON A MOVING DROP OF WATER

B. CAUSSADE and A. SABONI

Institut de Mécanique des Fluides
Avenue du Professeur Camille Soula - 31400 TOULOUSE - France

Fluid dispersion to drops is one of the mechanisms participating to the global gas exchange phenomenon between atmosphere and water surfaces by means of : Spray from breaking waves, Acid rain and Smog. The spray may be considered as an efficient participant in the ecological equilibrium favouring the transfer of oxygen and carbon dioxide which are the most important gases in the biological equilibrium. On the contrary acid rain and smog participate in the scavenging of toxic gases for the environment emitted by industrial countries. These acidic precipitations are strongly implicated in aquatic deterioration, material degradation, reduced agricultural productivity, including impaired forest growth and probably damage human health. Many studies confirm the acidity enhancement in country lakes which are exposed to abundant rain fall (Northern Europe ; Canada ; United States). For those reasons, it is important to understand the transfer mechanism in dispersed phase.

In this study we analyse the hydrodynamics and its influence on the transport phenomenon for a single moving drop which is falling through a polluted atmosphere. Although realistic situations demand the consideration of different drop sizes, evaporation or condensation, break-up and coalescence phenomena, still it is important to comprehend the single drop problem before attempting a more general analysis.

The mass transfer can be described by a classical convective-diffusion equation. An analytical solution exists in the absence of convection (Newman (1931)). In the other cases numerical resolution is the only way and it requires the knowledge of the flow fields inside and outside the drop. When the Reynolds number of drop motion is in the range $N_{Re}O(0)$ (N_{Re} based on terminal velocity and a droplet diameter), the flow fields were carried out analytically by Hadamard-Rybczinski (H-R) (1911). For the intermediate Reynolds $N_{Re}O(100)$ the flow fields are obtained by the numerical resolution of the Navier-Stokes equations. We have obtained the flow fields inside and outside the drop for N_{Re} ranging from 0 to 400 (eg. figure 1). For N_{Re} larger than 400 the model becomes inaccurate because flow instabilities such as drop oscillations and vortex shedding are known to occur.

Concerning the transport equation we have adopted a two step algorithm (explicit Mac Cormack scheme).

The model has been tested in the case of absorption and desorption of two pollutant gases (sulfur dioxide and carbon dioxide) by water drop and gives :

- Total concentration (sulfur or carbon)
- Species concentration ($SO_2.H_2O$; HSO_3^- ; $SO_3^=$ or $CO_2.H_2O$; HCO_3^- ; $CO_3^=$)
- pH

The main conclusions of our study are :

1) Drop size, fall velocity and fluids physico-chemical properties influence significantly the absorption capacity
2) Concerning the sensitivity to flow fields : the concentrations are understimated if the velocity is considered vanishing or is given by an analytical solution (figure 2)
3) Comparison with the experimental results of Walcek (1934) shows a good concordance (figure 3)
4) Comparison with a "film" theory and analytical solution shows a large discordance (figure 3)
5) The comparison with the numerical results given by Walcek (1984) shows some discordance in the case of absorption.

The main reasons are :

- The previous author has adopted the flow field computed by Leclair (1972) wich present some discrepancies with our results. This is mainly due to the interfacial conditions wich we have taken into account without analytical approximation.
- The method we have adopted (Mac Cormak scheme) to solve the transport equation is well adapted to this kind of problem. In effect, the equation is changing from parabolic to hyperbolic type when the convective term is predominant.

a) 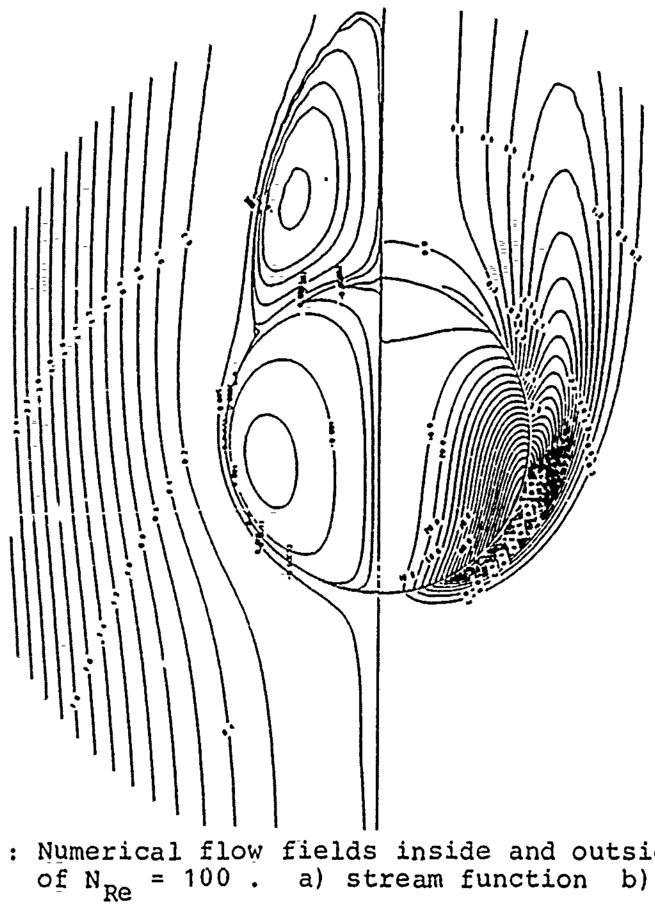 b)

Figure 1 : Numerical flow fields inside and outside the drop of N_{Re} = 100 . a) stream function b) vorticity

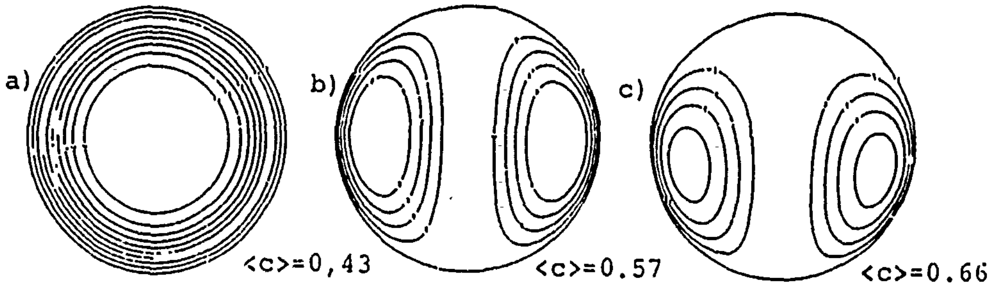

Figure 2 : Concentration field of CO_2 inside a drop
N_{Re} = 100 ; t = 1s ; P_e = 7.8 10^5
a) stagnant drop b) H.R. flow c) numerical flow field

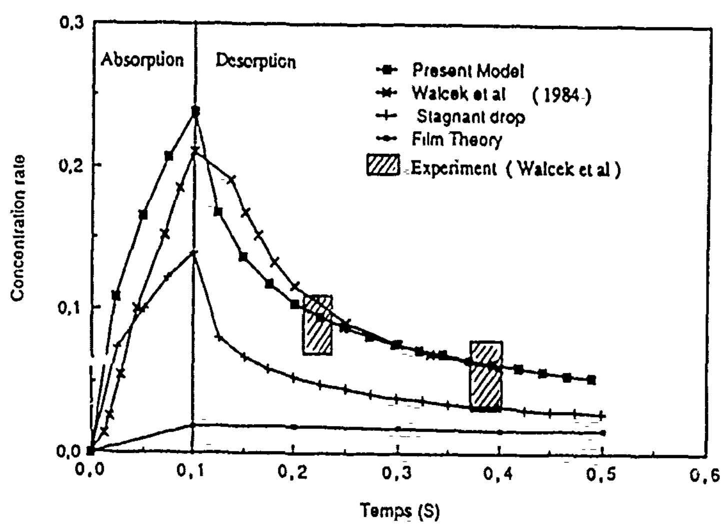

Figure 3 : Concentration within a drop (Re = 100) as a function of time during absorption (Cg = 10%) and desorption. Comparison with literature studies (in the case of SO_2)

REFERENCES

- HADAMARD, J. 1911, Mouvement permanent lent d'une sphère liquide et visqueuse dans un liquide visqueux. C.R.A.S. 152, 1735-1738
- LECLAIR, B.P., HAMIELEC, A.E., PRUPPACHER, H.R. and HALL, W.D. 1972 A theoretical and experimental study of the internal circulations in water drops falling at terminal velocity in air. J. Atmos. Sci 29, 728-740
- NEWMAN, A.B., Trans. inst. Chem. Eng., V27, 1931, 310
- RYBCZINSKI, Bull Acad Cracovie, Ser. A, P40, 1911, referred in lamb H : Hydrodynamics Cambridge University Press, pp 738
- WALCEK, C.J., PRUPPACHER, H.R., TOPALIAN, J.H. and MITRA S.K., 1984 On the scavenging of SO_2 by cloud and rain drops. II : An experimental study of SO_2 absorption and desorption for water drops in air. J. Atmos. Chem., 1, 290-306

EXPERIMENTAL STUDY OF MASS TRANSFER AND HYDRODYNAMICS IN A JET - AGITATED VESSEL

M. Grisenti, J. George

Institut de Mécanique des Fluides
Avenue du Professeur Camille Soula - 31400 - TOULOUSE

INTRODUCTION

Gas absorption studies carried out in the agitated vessel presented below were meant to characterize the role of internal liquid phase turbulence and its relation to the mass transfer coefficient K_L. In classical experiments liquid turbulence inside the parallelepipedic tank is provided by means of impellers : Chen et al. (1985), Komori and Murakami (1988), or by means of oscillating grids : Hopfinger and Toly (1976). So, turbulence is produced without average interfacial shear stress or average flow rate. In the present study turbulence is created by upflowing microjets of water inside the liquid phase, thus mechanical vibrations or imposed frequency problems observed in former studies are avoided. In revenge there exists a recirculation flow rate outflowing through a specially designed input-output device (figure 1). Velocity fluctuation measurements showing a good homogeneity and isotropy level in the intermediate zone close to the free surface, our process is thus validated authorizing further investigation in order to describe the turbulence behaviour and its relation to K_L.

HYDRODYNAMIC STUDY

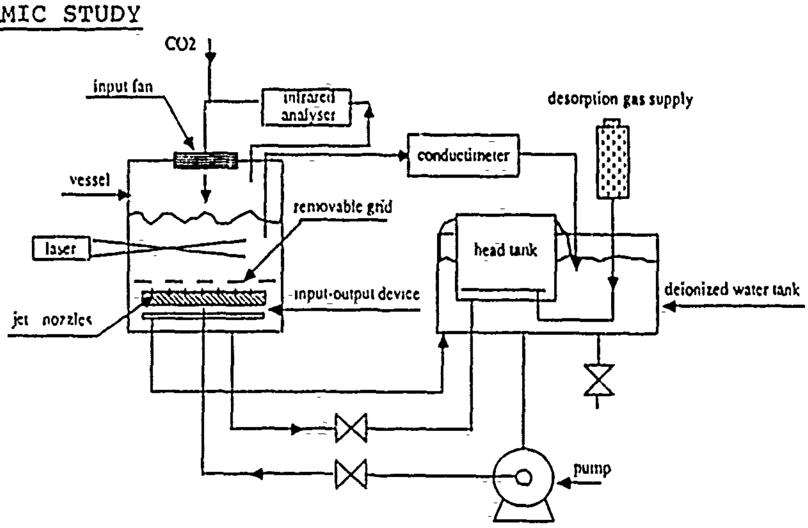

Figure 1 : Experimental setup

Differentruns, carried out for four different surface levels (ranging from 8 to 30 cm depth), correspond to free surface shapes varying from smooth to strongly agitated when two phase dispersed bubbles appear. Vertical $\sqrt{\overline{w'^2}}$ and horizontal $\sqrt{\overline{u'^2}}$ average fluctuation velocity profiles along the vertical axis show the three different steps described by Thompson and Turner (1975). A generation zone in which each jet is independent and turbulence in the outer region is weak ; an intermediate zone in which turbulence is satisfactorily homogeneous and isotropic and decays regularly ; an interfacial zone in which surface interactions occur (figure 2).

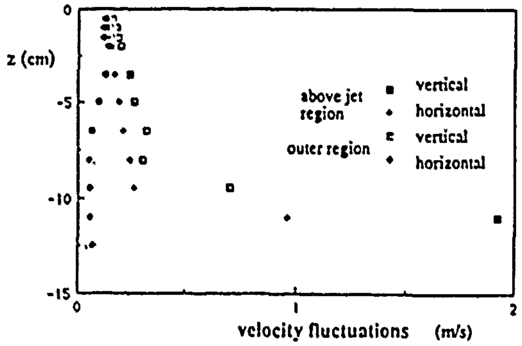

Figure 2 : Horizontal and vertical RMS velocity fluctuations vs distance to the interface

When the interface is rough, a well marked peak corresponding to the surface fluctuations dominant frequency (4Hz) appears in the liquid velocity power spectrum close to the interface (Figure 3a). In all runs for higher frequencies the classical -5/3 decay slope is encountered (Figure 3b).

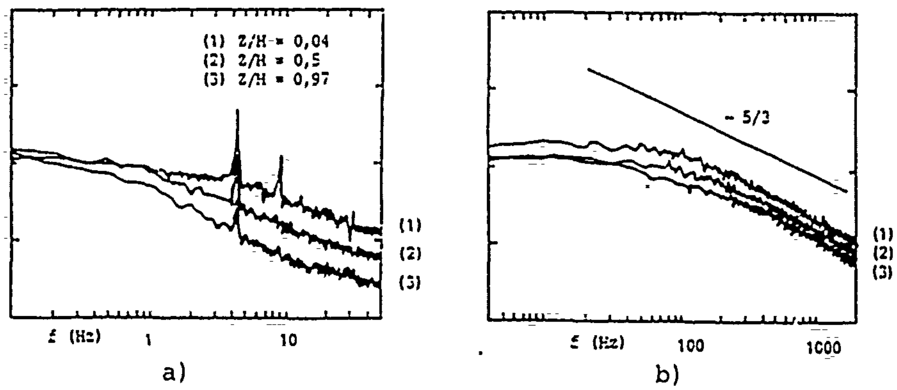

Figure 3 : Velocity power spectrum a) rough surface b) smooth surface

MASS TRANSFER STUDY

The volumic mass transfer rate K_LA is determined by analysing the carbon dioxide budget inside the liquid phase (A represents the free surface area, the value of which is difficult to obtain precisely for a rough surface). As is shown in figure 4, K_LA is well related with the turbulent kinetic energy value k_I reached at the top of the intermediate region

$$(k_I = \frac{2\overline{u'^2} + \overline{w'^2}}{2})$$

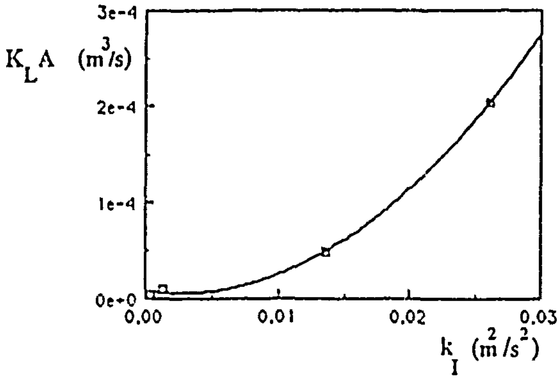

Figure 4 : Volumic gaz absorption rate vs turbulent kinetic energy

This result is in good agreement with the conclusions reached by Caussade et al (1990) and velocity measurements in the interfacial region using the double decomposition $V' = V_V + V_T$ are expected to show the role played by the turbulent fluctuations V_T and by wave surface oscillations induced velocity components V_V.

LITERATURE CITED

Caussade B. George J. Masbernat L.
"Experimental study and parametrization of interfacial gas absorption" N° 2024 to appear in the Feb. issue of the AIChE Journal (1990)

Chen B.H. Mallas K. Mc Millan A.F.
"Gas absorption across a free surface of a stirred vessel"
AIChE Journal 31, 3, 510-512 (1985)

Hopfinger E. Toly S.A.
"Spatially decaying turbulence and its relation to mixing across density interfaces"
J.F.M. 78, 1, 155 (1976)

Komori S. Marakami Y.
"Turbulent mixing in baffled stirred tanks with vertical blade impellers"
AIChE Journal 34, 6, 932 (1988)

Thompson S.M. Turner J.S.
"Mixing across an interface due to turbulence generated by an oscillating grid"
J.F.M. 67, 349 (1975)

SIMULTANEOUS MEASUREMENTS OF TEMPERATURE EFFECT ON GAS TRANSFER AT LOW SURFACE RENEWAL RATES

Niels Aagaard Jensen
Environmental Engineering Laboratory
University of Aalborg, DK-9000 Aalborg, Denmark

ABSTRACT

Laboratory experiments were conducted in order to investigate the temperature dependence of oxygen and krypton-85 gas transfer at water surfaces. These investigations were performed using simultaneous measurements at low surface renewal rates.

For several phenomena related to environmental engineering a [illegible]nship between temperature and gas transfer is needed. Examples are stream reaeration and aeration processes in wastewater treatment facilities. This investigation was performed in connection with a study on reaeration in gravity sewers.

For decades the empirical equation proposed by Streeter et al. (1936) has been used to relate the gas transfer to water temperature.

$$K_La(T) = K_La(20) * \theta^{(T-20)}$$

Until recently it was generally accepted that the gas transfer coefficient increases with temperature under all conditions. Although the value of the temperature correction factor, θ, has been reported within a range from 1.012 to 1.047, all investigators agree that the temperature correction coefficient is higher than unity. However, recently Chao and co-writers, Chao et al. (1987a) and Chao et al.(1987b), have presented both theoretical explanations and experimental verifications for the statement, that gas

transfer decreases with increasing temperature under conditions of low turbulence. If true, this finding creates a new concept for studies of rivers and similar waterbodies with low surface renewal rate.

The theoretical basis for gas transfer is described and evaluated with special attention to the equation for temperature dependence of reaeration derived by Chao et al. (1987a). Furthermore, the experimental verifications derived by Chao et al. (1987b) are discussed.

Gas transfer measurements are very sensitive and therefore easily susceptible to experimental errors. Therefore, experimental data are normally found with considerable scatter. In this paper laboratory studies on the effect of temperature on gas transfer under conditions of low turbulence using dual measurement of gas transfer will be presented. Under carefully controlled conditions gas transfer coefficients for oxygen and krypton-85 were measured simultaneously within a temperature range from 5 to 37 °C. Investigations were carried out in a circular laboratory vessel, diameter 0.25 m, hight 0.25, containing 6 L of clean water. The water was mixed with a magnetic stirrer at a constant rate, and precaution was done to avoid a major vortex at the water surface. The temperature was held constant by a water bath.

At the beginning of a test, the water was deoxygenated by stripping with N_2-gas: Furthermore, a portion of the radioactive gas, krypton-85, was added to the vessel. Using syringes samples for dissolved oxygen (DO) and krypton-85 were taken simultaneously during the test. Each test was run over a period of 2 to 4 hours. Because of the low gas transfer coefficients, some tests were continued for 24 hours in order to obtain equilibrium conditions. The DO samples were analysed by a modified Winkler procedure using a small volume of sample, and the reaeration coefficient was determined by the log deficit methode. Samples taken for krypton-85 determination were analysed using liquid scintillation technique. By analysing the degassing of krypton-85 from the water phase the gas transfer coefficient for krypton-85 was determined. For a series of 22 test the temperature correction factor was found to be 1.031 and 1.032 for oxygen and krypton respectively. Special attention will be devoted to the discussion of the temperature correction factor for oxygen above 20 °C.

In connection with the clean water tests a corresponding series of 10 wastewater tests were conducted using krypton-85 within a temperature range from 5 to 25 °C. The temperature dependence derived from these tests was found to be in accordance with that for clean water.

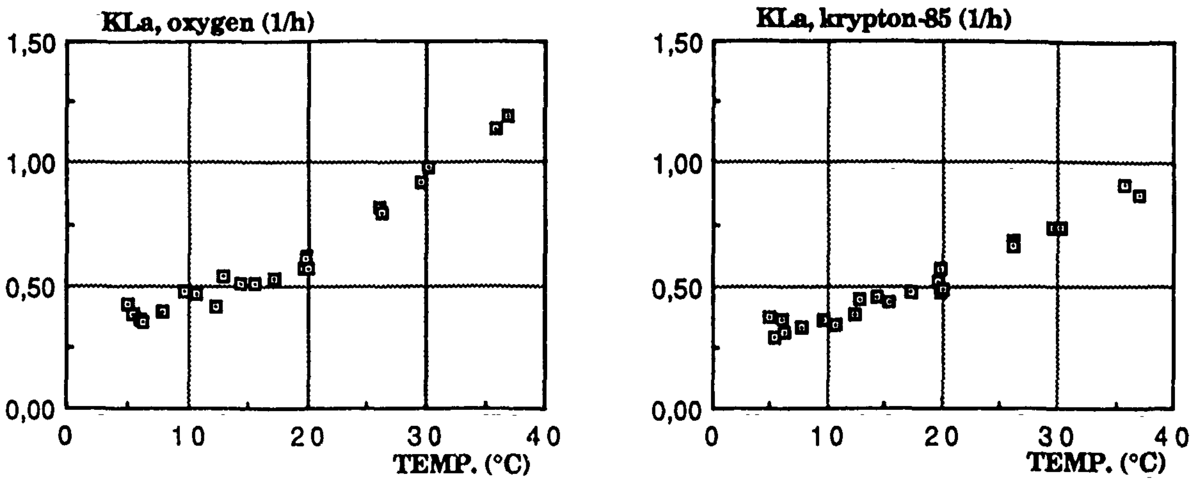

Figure - Results from the clean water tests.

The gas transfer coefficient for krypton-85 is reported by Tsivoglou et al.(1965) as constant relative to that of oxygen under most conditions. Therefore, the temperature dependence of krypton-85 transfer should be identical with that of oxygen. By measuring gas transfer coefficients simultaneously for two gasses (oxygen and krypton-85) with different analytical methods, basic analytical and experimental errors can be reduced, and the temperature dependence of gas transfer for oxygen and krypton-85 can be compared.

Investigation were carried out with K_L values lower than those reported by Chao et al. (1987b), i.e. ~ 0.1 m/h and 0.3 m/h respectively. Based on the investigation, it can be concluded, that there is no reason to believe that gas transfer decreases by increasing temperature under conditions of low turbulence.

Properties of Small-Scale Waves in Sheared Gas-Liquid Flows

M. J. McCready, M. Gupta, and K. Bruno

Department of Chemical Engineering

University of Notre Dame

Notre Dame, IN USA

It is generally recognized that the interfacial transfer of slightly soluble gases is controlled by velocity fluctuations within the liquid in the near vicinity of the interface. What is not clear however, is whether the source of these important fluctuations is associated with turbulence generated below the interface or if it originates with interfacial waves. Furthermore, different mechanisms (Coantic, 1986, McCready and Hanratty, 1985) have been proposed for how small scale waves may produce velocity fluctuations capable of controlling mass transfer. To resolve some of these issues, we have extensively examined the qualitative and quantitative behavior of interfacial waves in a small gas-liquid flow system and developed a theoretical basis for interpretation of wave data.

Figure 1a shows an interfacial wave spectrum very close to the point of neutral stability. Visual observations indicate that these waves are two-dimensional. The salient features of the spectrum are the dominant peak at 8.5 Hz (which corresponds to the fastest growing mode from linear stability theory), symmetric "bumps" at 7 and 11 Hz which indicate the presence of "side bands" and two visible overtone peaks at 17 and 25 Hz. Energy from the gas flow is fed primarily into the dominant peak; the others occur because of

nonlinear inertial interactions. After an initial growth distance, the wave field saturates and then evolves only very slowly with distance. No waves are observed to grow until breaking, indicating that energy fed into the fundamental is transferred to higher frequency modes which can then dissipate it. By including energy input and dissipation from linear stability theory into the nonlinear mode interaction theory derived by Kim and Hanratty (1971), it is possible to produce reasonable quantitative predictions for the magnitude of the wave peaks as shown in figure 1b.

As interfacial shear is increased, waves begin to show transverse variations and the spectrum broadens considerably indicating that many more modes are needed to describe the wave field. However, the same qualitative picture, where energy is transferred from the dominant waves to higher frequencies, remains. For this more complex situation, we describe the waves quantitatively in terms of a dynamic energy balance which includes input and dissipation. The nonlinear interactions are represented in lumped form by a transfer function so that a complete continuous spectrum can be calculated. The wave energy balance approach provides reasonable agreement with measurements and provides a good wave of demonstrating how various physical parameters will influence the spectrum.

How the small scale experiments fit into wave structure found on large bodies of water with long wind histories will also be discussed. The most important consideration is the production of parasitic capillary waves by steep gravity waves (examined by Longuet-Higgins, 1963). For sufficiently steep gravity waves, the parasitic

capillary waves have amplitudes comparable to those which form as a result of direct wind generation.

References:

Coantic, M. (1986) J. Geophys. Res. 91 (C3) p3925.

Kim, Y. Y. and T. J. Hanratty (1971) , J. Fluid Mech. 50, p107.

Longuet-Higgins, M. S. (1963), J. Fluid Mech. 16, p138.

McCready, M. J. and T. J. Hanratty (1985), AIChE J. 31, p2066.

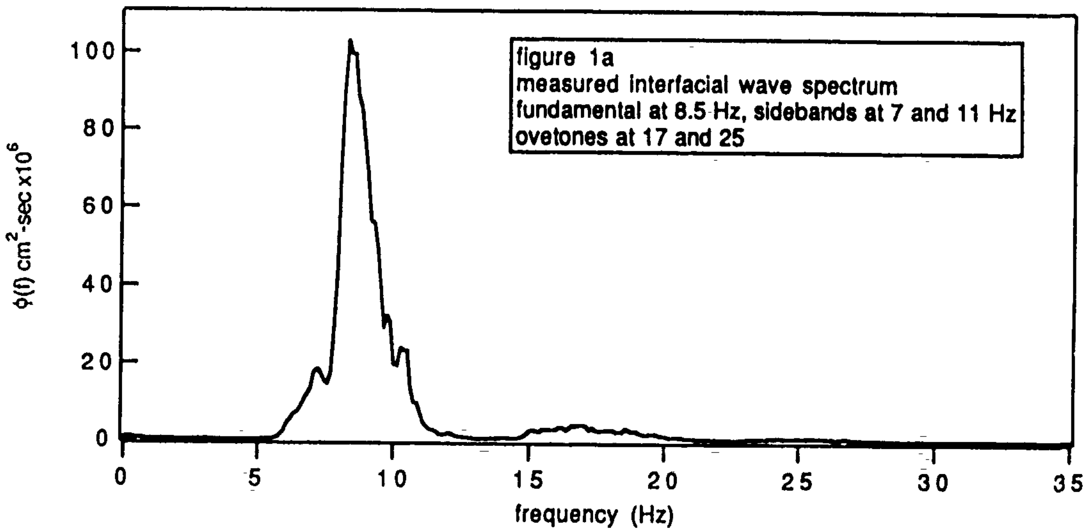

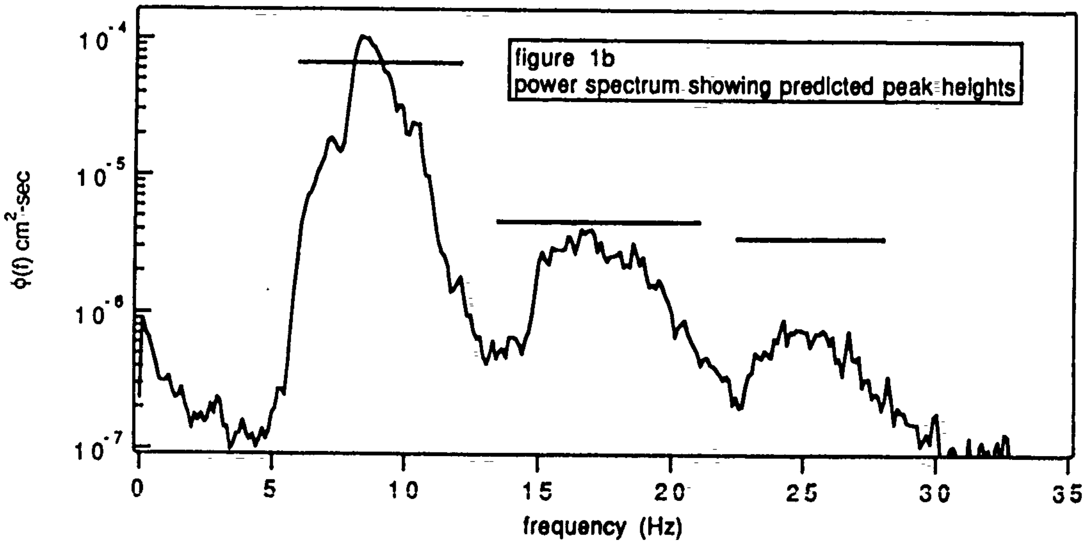

GAS TRANSFER AT HIGHLY AGITATED LIQUID SURFACES

BY

HARRY EDMAR SCHULZ

Professor, São Carlos School of Engineering,

São Carlos, São Paulo, Brazil

The search of a relationship for describing gas transfer at water surfaces has led to a continuing discussion on the values of the exponent in the "power law" which relates the gas absorption coefficient and the molecular diffusivity. The major point in this debate concerns the predictions obtained from the two-film theory and those from the penetration - renewal theories, giving rise to a series of models which try to unify both tendencies. Not much attention has been given in these discussions to the observations of Kishinevsky and Serebriansky (1955) which seem to indicate that the gas transfer in highly agitated liquids follows laws different from those applied to the "normally" agitated case and that the molecular diffusivity is irrelevant in the former.

A mathematical model is construted from a new conceptual sheme which does not use molecular diffusivity. This model furnishes a relationship for the mass transfer coefficients of different gases which was compared with the experimental data from various sources, confirming the present formulation as a limiting case for intense agitation. The model is based on the transfer of gas molecules from the gaseous to the liquid phase.

Mathematical Models

In a previous study where the conditions of concentration of the gas at the water surface were considered, it was possible to obtain the following relationship for the absorption coefficient. (Schulz (1989)).

$$K = \frac{8\ \bar{R}\bar{V}G}{3\ \bar{L}} \left(1 - \exp(-S\bar{L}/\bar{V})\right) \qquad (1)$$

K = Gas transfer coefficient (m/s)
$\bar{V}$ = Mean velocity of liquid elements (tangential to the water surface) (m/s)
$\bar{L}$ = Mean lenght traveled by a liquid element (tangential to the water surface) (m)
$\bar{R}$ = Molecular radium of the gas (m)
G = Area magnification factor (a function of the agitation of the system)
S = A measure of the rate at which the gas molecules "fix" themselves at the liquid surface.

If S is high, it is possible to assume that the surface is instantaneously satured with the gas, giving:

$$K = \frac{8\ R\overline{V}G}{3\ \overline{L}} \tag{2}$$

Defining $\gamma = 8\ GR/3$ and $x = \overline{V}/\overline{L}$ and plotting K from equations 1 and 2 against x, we obtain the graph of figure 1:

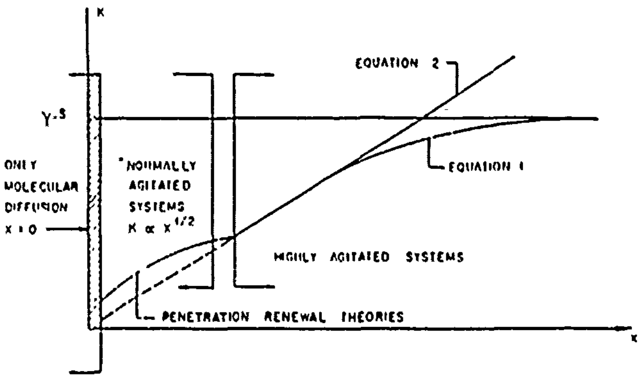

FIGURE 1 GRAPH OF EQUATIONS 1 AND 2 (FOR CONSTANT G)

For two different gases being absorbed by the same liquid, subjected to the same agitation conditions, the relation 3 is obtained:

$$\frac{K_1}{K_2} = \frac{R_1}{R_2} \quad \frac{(1 - \exp(- S_1\ \overline{L}/\overline{V}))}{(1 - \exp(- S_2\ \overline{L}/\overline{V}))} \tag{3}$$

For high values of S_1 and S_2 (surface instantaneously satured) it follows inmediatly that.

$$K_1/K_2 = R_1/R_2 \tag{4}$$

This result shows that, for highly agitated systems, a limiting relation between mass transfer coefficients and molecular radii is obtained, which is different from that established for "normaly" agitated systems. For the last it is accepted that (see Rainwater and Holley (1983), for example):

$$K_1/K_2 = R_2/R_1 \tag{5}$$

<u>Comparison with experimental results of different Sources:</u>

Equations 4 and 5 suggest that if for normaly agitated gas-liquid systems we have

$$\frac{K_1}{K_2} = \text{Constant} \tag{6}$$

then, for higly agitated systems we can expect a tendency to

$$\frac{K_1}{K_2} = (\text{Constant})^{-1} \tag{7}$$

The behavior of experimental data produced by different authors indicates that the above conclusion is confirmed. For example, figure 2 is reconstruded with

the data of Kishinevsky and Serebriansky (1955) and those of Ljubisavljevic (1989).

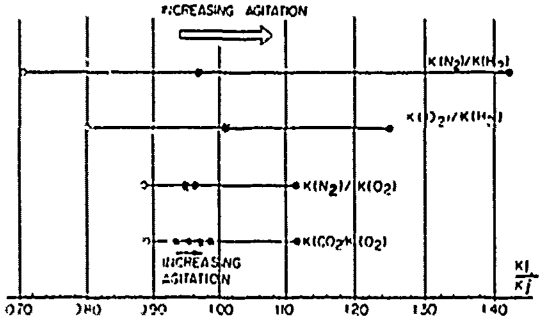

FIGURE 2 DATA OF KISHINEVSKY AND SEREBRIANSKY (1955) AND LJUBISAVLJEVIC (1984)

o = EQUATION 4 (OR 6) •• EQUATION 5 (OR 7) •• MEASURED POINT

The analysis of other experimental data shows similar behaviors.

REFERENCES

KISHINEVSKY, M. Kh. & SEREBRIANSKY, V. T. (1955) - "The Mechanism of Mass Transfer at The Gas - Liquid Interface with Vigorous Stirring". Jour. Appl.Chemistry, U.S.S.R., 29: 29-33.

LJUBISAVLJEVIC, D. (1984) - "Carbon Dioxide Desorption from the Activated Sludge at the Waste Water Treatment Plants". In BRUTSAERT, W. & JIRKA, G. H., ed. Gas Transfer at Water Surfaces, Dordrecht, D. Reidel Publishing Company, p. 613-620.

RAINWATER, K. A. & HOLLEY, E. R. (1983) - "Laboratory Studies on the Hydrocarbon Gas Transfer Technique for Reaeration Measurement". Center for Research in Water Resources, Bureau of Engineering Research, Austin, December, Technical Report 189, 114 p.

SCHULZ, H. E. (1989) - "Investigation of the Flowing Water Reoxigenation Mechanism and its Correlation with the Turbulence Level near the Surface". Doctor-Thesis. University of São Paulo, Brazil, 915 p.

MECHANISMS OF SURFACE RENEWAL IN OPEN CHANNELS

ALDO TAMBURRINO, Research Assistant

JOHN GULLIVER, Associate Professor

Saint Anthony Falls Hydraulic Laboratory
Department of Civil and Mineral Engineering
University of Minnesota
Minneapolis, MN 55454, Phone (612) 627-4600

Gas transfer across the air-water interface plays an important role in the mass balance for many chemicals. Surface gas transfer is explained by the surface renewal theory, in which water from lower levels replace that close to the free surface. Usually, the gas transport in water (represented by the liquid film coefficient) has been expressed in terms of the molecular diffusivity of the gas in water and another variable depending on the global characteristics of the flow, such as mean velocity, average depth, slope,etc. However, the results obtained from this approach present a large scatter in the data.

The paper is focussed on the flow mechanism by which surface renewal originates. An insight on the process has been obtained by flow visualization and velocity measurement experiments carried out in a moving-bed flume. The moving-bed flume is an unique facility which permits to change a moving frame of reference into one that is fixed to the laboratory frame. The advantage of using the moving-bed flume is that the net flow in any cross section is zero, permitting one to perform experiments that, in traditional flumes, require movement of the instrumentation with the bulk velocity of the flow.

Flow visualization experiments have shown the presence of large streamwise vortices scaling with the flow depth similar to those presented by Imamoto and Ishigaki (1984) in a traditional flume or by Gulliver and Halverson (1987) in the moving-bed flume. The large streamwise vortices can be considered as structures of the flow that are not stable in time or space. The structures shift back and forth across the flume.

The upwelling regions of the large streamwise vortices carry fluid particles from the lower regions of the flow to higher levels and to the free surface, constituting the main mechanism of the surface renewal phenomenon. The upwelling region is associated with high vorticity on the free surface and rows of eddies alternating with zones of low vorticity (associated to the downwelling region) is inferred from free surface flow visualization. Free surface flow visualization also reveals the replacement of free surface particles by others coming from lower levels.

The surface renewal mechanism proposed here is different

to that indicated by Rashidi and Banerjee (1988). They link the renewal phenomen to the bursting process ocurring very close to the wall. However, their flow depth of between 1.84 - 2.85 cm. was two or three times the vertical dimension of the bursts. Our experiments, however, have a flow depth which is around eighty times higher than the burst dimension with an observed transverse spacing equal to approximately one houndred times the burst spacing.

Analysis of velocity measurements taken with a two component fiber-optic LDV system reveals that the velocities associated with the large streamwise vortices are more than 2.5 times the velocities associated to secondary currents (which are the temporal mean values of the large streamwise vortices). That analysis was carried out by splitting the velocity in three components: one corresponding to the temporal mean value, another corresponding to fast fluctuations and a third one related to the flow structures. Fast fluctuations were removed by means of moving averages. In this way, it is possible to get a better parameter - the velocity associated with the large streamwise vortice, rather than a bulk velocity- to be related to the liquid film coefficient.

REFERENCES

GULLIVER, J.S. and M.J. HALVERSON (1987) "Measurements of large streamwise vortices in an open-channel flow", Water Resources Research, Vol. 23, No. 1, pp. 115-123.

IMAMOTO, H. and T. ISHIGAKI (1984) "Visualization of longitudinal eddies in an open channel flow", Proc. Fourth Int. Symposium on Flow Visualization, pp. 333-337.

RASHIDI, M. and S. BANERJEE (1988) "Turbulence structure in free-surface channel flows", Phys. Fluids, Vol. 31, No. 9, pp. 2491-2503.

THE EFFECT OF MARANGONI FLOW ON GAS TRANSFER PROCESS

Wei Tong
Creare Inc.
Hanover, NH 03755

The fluid flow induced by the surface tension gradient on a liquid/vapor interface is known as Marangoni flow. Surface tension gradients can be caused by temperature, concentration, or electric potential gradients along the interface. Thus, Marangoni flow can be further divided into three categories: thermocapillary, concentration–capillary and thermoelectric flows according to the corresponding gradient mentioned above.

The surface tension gradient leads to movement of the interface which induces circulating flow in the liquid. This results in the transport of dissolved gas from the liquid surface to its bulk. In the present study, the effect of Marangoni flow on gas transport process is addressed. The theoretical analysis has shown that the presence of the Marangoni flow can strongly influence the gas diffusion process.

MODELING

MATHEMATICAL MODEL OF AERATED JET PROPAGATION WITHIN FLUID MASSIF

Achmetoх V.K.,Candidate of physico-mathematical sciences
Volshanik V.V.,Candidate of technical sciences
Karelin V.Ya., Doctor of technical sciences
Mordasov A.P., Candidate of technical sciences

Moscow Engineering and Construction Institute, the USSR

Method of fluid forced aeration by way of aerated jet may be effectively applied to water enrichment with dissolved oxygen in natural and man-made water reservoirs and water courses, in biological treatment facilities, in basic eguipment of chemical and microbiological industries. Hydraulical and mass-transferal analyses of jet aeration systems suppose that mechanisms of aerated jet propagation within fluid massif are known.Theoretical and experimental information about features of aerated jets propagation is for the present not enough in the contemporary hydromechanics and engireering hydraulics. It makes in practice impossible to use extencive data available in the field of unaerated jets propagation within the same fluid massif for analyses of aerated jets. Among the studies of aerated jets propagation works of Hsia A.H. may be noted.

Broad possibilities of fluid jet aeration system application and the necessity of their close engineering analysis have forced us to start thorough theoretical and experimental study of this hydravlical phenomenon.This report contains some results of initial stages of hydromechanical examination of aerated jets propagation within fluid massif.

As a mathematical model of water reservoir aeration process let us consider the problem on propagation of submerged aerated turbulent jet conteining of uniformly distributed in sections air bubbles and flowing out from the pipe D_o in diameter into homogeneous motionless liquid condition at angle ($0 \angle \theta_o \angle 90^o$) and with speed of U_o. By virtue of the fact that aerated jet density is less than that of motionless liquid condition the trajectory of the jet central line (line of symmetry) will be in the general case curvilinear.That is why it will be convinient to introduce curvlinear coordinates S,n,θ, where S - coordinate along the jet central line, n - normal to it and θ - angle between the motionless liouid condition surface and the jet central line. For simplicity let us consider that axial component of velocity in each section of the jet is constant value, that is U = U(S).

Equations of mass and mmentum balance for aerated jet control volume under the method of integral relationship may be written as following:

$$\frac{d}{ds}\left[\rho_L U_L (1-\alpha) A\right] = E, \qquad (1)$$

$$\frac{d}{ds}\left[\rho_L U_L^2 (1-\alpha) A\right] + \frac{d}{ds}\left[\rho_B \alpha U_B^2 A\right] = (\rho_L - \rho_B)\alpha A g \sin\theta, \qquad (2)$$

$$\frac{d}{ds}\,[\rho_B U_B \alpha A] + \rho_B V_B \alpha D = 0 \;, \qquad (3)$$

$$A[\rho_L(1-\alpha)U_L^2 + \rho_B \alpha U_B^2]\,\frac{d\theta}{ds} = \alpha(\rho_L-\rho_B)\,Ag\cdot\cos\theta + \rho_B \alpha D V_B^2 \qquad (4)$$

where V - velocity lateral component, D - jet diameter, ρ - density, $A=\pi D^2/4$ - section area of the jet, - parameter evaluating "volume-mixture volume unit" ratio, g - free fall acceleration, indexes"L"and"B" relate to liquid and bubble phases correspondingly. Value E evaluates jet ejectional properties in its propagation and it is in proportion to the jet local section perimeter, its speed and density.

Equations of bubbles motion may be obtained from consideration of interphases relationship forces balance.These forces include: frictional force (Stokes force),Archimedes and gravitational forces as well as force connected with the relationship of associated masses.Writting these relationsras axial and lateral components we shall have the following:

$$(\rho_B + k\rho_L)U_B\frac{dU_B}{ds} - k\rho_L U_L\frac{dU_L}{ds} = 3/4\; C_{D_S}\rho_L(U_L - U_B)\,|U_L - U_B|\,\frac{1}{d_B} +$$

$$+(\rho_L - \rho_B)\;g\cdot\sin\theta \;, \qquad (5)$$

$$\rho_B U_B\frac{dV_B}{ds} = -\;3/4\; C_{D_n} V_B\,|V_B|\,\frac{1}{d_B} + (\rho_L - \rho_B)\,g\cdot\cos\theta - k\rho_L U_B\frac{dV_B}{ds} \qquad (6)$$

Here C_{D_S}, C_{D_n} - coefficient of resistance to bubbles motion in axial and lateral directions, d_B - bubble diameter, k - associated masses coefficient.

Adding relations for determination of rectangular coordinates x_c, y_c of the jet central line $\frac{dx_c}{ds} = \cos\theta$, $\frac{dy_c}{ds} = \sin\theta$, (7) to these equations we obtain the closed system of equations (1) ...(7) with respect to unknowns $U_L, U_B, V_B, \theta, \alpha, D, x_c, y_c$,describing aerated jet motion in motionless fluid.

For the system (1)...(7) the initial-value problem (Cauchy problem) was considered. Solution of this system after its reduction to nondimensional form was defined by numerical integration under Runge-Kutta method.

Special attention was paid to the case when aerated jet was conveyed perpendicularly to water reservoir surface ($\theta_0 = 90^o$). At Froude number variuos values ($F_r = U_0^2/g\cdot D_0$) and initial air concentration in the jetαit was obtained data showing the jet aeration effect upon its propagation process. Hereat one of the most important characteristic is a water reservoir working up depth in the capacity of which the maximum depth of air bubbles dive is taken. In the case at issue the jet central line trajectory is rectilinear there is no in practice air bubbles diffusion through the jet side surface and value $\alpha(s)$ reduces mainly at the expense of the jet ejectional properties. Therefore at the depth where speed U_B become near to zero the jet buoyancy, when there is a specific combination of parameters F_r and α_0, may be proved to be great enough to promote the jet turning by 180^o. By examination and integration of obtained numerical data universal relations $H/D_0 = f(F_r, \alpha_0)$ were ploted. Their comparison with the results of experimental studies conducted at the model bench with the stream parametres α_0= 0,4; 0,5; 0,6 and $5 \leq F_r \leq 50$ have shown close correspondence between theory and experiment. Similar re-

lations have been ploted for the cases of aerated jet propagation at angles $\Theta_0 = 30^o; 45^o$ and 60^o with respect to motionless body of water. Results of theoretical analysis and experimental data have corroborated the considerable effect of jet density defining by the air (gas) bubbles saturation ratio upon the trend of the jet propagation within fluid massif and the impossibility of use of relationships describing the unaerated jet within the same fluid massif for analysis of aerated jets

Balancing the Advective and Diffusive Fluxes of Hydrophobic Organic Contaminants Across Natural Water Surfaces

Joel E. Baker, Chesapeake Biological Laboratory, Center for Environmental and Estuarine Studies, The University of Maryland System, P.O. Box 38, Solomons, MD 20688

Steven J. Eisenreich, Environmental Engineering Sciences, Department of Civil and Mineral Engineering, University of Minnesota, 500 Pillsbury Drive, S.E., Minneapolis, MN 55455

Long range atmospheric transport and subsequent deposition of hydrophobic organic contaminants (HOCs) such as polycyclic aromatic hydrocarbons (PAHs) and polychlorinated biphenyls (PCBs) is a major source of these chemicals to remote environments, including the upper Great Lakes (e.g., Eisenreich *et al.*, 1981) and the open ocean (Atlas *et al.*, 1986). Atmospheric deposition of these chemicals results primarily from their washout by precipitation, although dry deposition of HOC-laden aerosols may also contribute significantly to deposition. Once deposited, however, these slightly soluble chemicals are sufficiently volatile that revolatilization may be an important pathway. The net HOC flux from the atmosphere to surface waters depends upon the balance between deposition and volatilization. In this paper, a model based upon the conceptual framework of Mackay *et al.* (1986) and calibrated with our field measurements of PCBs and PAHs in the Great Lakes (Baker and Eisenreich, 1990) is employed to determine which parameters control the dynamic, non-equilibrium exchange of HOCs across the air-water interface.

The fugacity-based model of Mackay *et al.* (1986) calculates the total depositional flux (N, mol/m^2·s) resulting from wet deposition (vapor dissolution and aerosol washout) and aerosol sedimentation as the product of the vapor phase HOC fugacity (f_A, Pa) and the respective transport parameters (D, mol/(m^2·s·Pa)):

$$N_{deposition} = f_A D_R + f_A D_P + f_A D_D,$$

where D_R, D_P, and D_D are the transport parameters for vapor dissolution, aerosol sedimentation, and aerosol washout, respectively. Similarly, diffusive HOC fluxes across the air-water interface (i.e., volatilization or vapor absorption) are modelled as the product of the concentration gradient (or the fugacity difference) and the mass transfer coefficient D_{AW} (mol/(m^2·s·Pa):

$$N_{volatilization} = D_{AW}(f_W - f_A).$$

Combining these two equations results in an expression for the net HOC flux from water to air:

$$N_{total} = f_W D_{AW} - f_A(D_{AW} + D_R + D_P + D_D).$$

At steady state, $N_{total} = 0$, and:

$$f_W/f_A = 1 + (D_R + D_P + D_D)/D_{AW}.$$

At steady state, higher contaminant fugacities in surface waters

relative to overlying vapor drive HOC volatilization fluxes equal in magnitude to the gross total HOC deposition rate. The steady state HOC fugacity gradient across the air-water interface can be estimated if all the transport parameters are accurately known. Conversely, measurement of vapor and dissolved HOC fugacities allows the ratio of the mass transport parameters to be calculated from the above equation.

Fugacity gradients measured across the air-water interface of Lake Superior strongly suggest that PCB congeners were volatilizing from surface waters in August, 1986 (Baker and Eisenreich, 1990). The ratio of dissolved and vapor-phase HOC fugacities was generally greater than 1 and often greater than 10. The mean volatilization flux of total PCBs was 19 ng/m^2·day, which is similar to estimates of gross atmospheric deposition to the lake, supporting the hypothesis of nonequilibrium, steady-state PCB exchange across the air-water interface over long (e.g. weeks to years) time scales.

The transfer equations presented above have been used to simulate the response of the air-water interface to episodic HOC deposition during precipitation events and the subsequent revolatilization (Figure 1). Precipitation efficiently transfers HOCs from the atmosphere, elevates HOC concentrations in surface waters, and increases the fugacity gradient. After the precipitation event is over, the system responds by slowly releasing HOCs from surface waters back to the atmosphere.

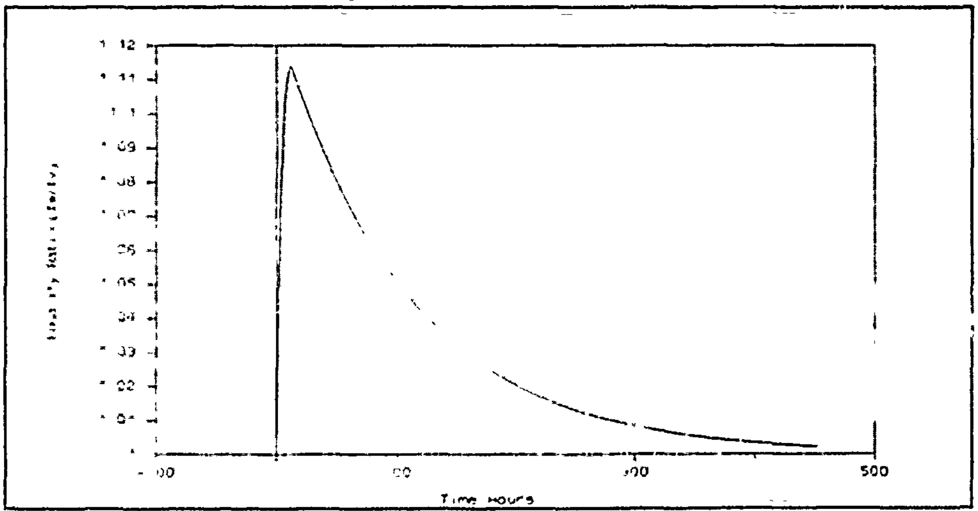

Figure 1. Response of HOC fugacity ratio to a precipitation event at time = 0.

Several parameters strongly influence both the steady state and dynamic solutions to this model. The strong dependence of HOC vapor pressures and, to a lesser degree, solubilities on temperature results in the strong influence of temperature on vapor-aerosol distributions, vapor scavenging efficiencies and aqueous fugacity capacities. Effects of temperature on mass transport parameters are of secondary importance. A second controlling parameter is the physicochemical speciation of HOCs within rainfall and surface waters. As only dissolved and vapor phase HOCs are directly available for diffusive exchange across the water surface, HOC partitioning or complexation

within aqueous phases reduces fugacity gradients. HOCs bound to aerosols which are washed from the atmosphere by precipitation may not be available for revolatilization.

This model demonstrates the largest uncertainties in our understanding of HOC exchange at water surfaces and may be used to further refine the design of both field and laboratory studies.

References

Atlas, E.L., Bidleman, T., Giam, C.S., "Atmospheric Transport of PCB to the Oceans," in *PCBs in the Environment*, Volume I. J.S. Waid, Ed., CRC Press, Inc., pp. 79-100.

Baker, J.E. and Eisenreich, S.J., "Concentrations and Fluxes of Polycyclic Aromatic Hydrocarbons and Polychlorinated Biphenyls Across the Air-Water Interface of Lake Superior," *Environ. Sci. Technol.*, Vol. 24, 1990, in press.

Eisenreich, S.J., Hollod, G.J., Looney, B.B., "Airborne Organic Contaminants in the Great Lakes Ecosystem," *Environ. Sci. Technol.*, Vol. 15, pp. 30-38.

Mackay, D., Paterson, S., Schroeder, W.H., "Model Describing the Rates of Transfer Processes of Organic Chemicals between the Atmosphere and Water," *Environ. Sci. Technol.*, Vol. 20, No. 8, 1986, pp. 810-816.

TURBULENCE LEVEL BELOW THE WAVES : THEORETICAL MODEL AND INFLUENCE ON ABSORPTION

J. MAGNAUDET - J. GEORGE - L. MASBERNAT and B. CAUSSADE

Institut de Mécanique des Fluides
Avenue du Professeur Camille Soula - 31400 TOULOUSE, France

The mass transfer rate K_L across a free gas-liquid interface depends altogether on physical parameters and dynamic scalings. In geophysical situations as was shown by Caussade et al. (1990) on simultaneous carbon dioxide and Helium absorption experiments carried on cocurrent gas-liquid flumes, the physical parameters influence is not independent of that of dynamic parameters characterizing interfacial agitation. On the contrary, K_L is found proportional to $S_c{}^n$ with a -2/3 n exponent for weaker winds (<4 m/s) which happens at a solid wall : and with a -1/2 n exponent for higher winds. These results, in good agreement with observations of Jähne et al (1987) show there is a dramatic change of interfacial behaviour with wind wave occurence. Hence dynamic scalings have to be defined properly.

For most authors, working on horizontal cocurrent gas-liquid flumes, u_* is characteristic of interfacial dynamic scalings, the non dimensional value of K_L ranging between $0{,}1 < K_L S_c{}^n / u_* < 0{,}2$ for laboratory experiments. However for other gas absorption experiments u_* is not relevant. For free falling films without wind, Henstock and Hanratty (1971) showed K_L is related to an artificial friction velocity based on u_* and the wall friction velocity. On a narrow channel (George 1987) two-dimensional waves were found to develop, increasing the liquid turbulent kinetic energy level ; therefore K_L values are higher than predicted according to those of u_*. Hence when the liquid phase turbulence is more important than normally created by the wind stress (i.e. wall upwelling turbulence for thin falling films ; superimposed fluctuations due to developed wind waves) u_* is not adapted. For experiments on a vessel agitated by liquid microjets K_L is well correlated to liquid turbulent kinetic energy close to the interface. Same results were observed by Chen et al. (1985) in a stirred vessel even if their conclusions on the charasteristic turbulent eddies size is not very convincing. Those different experimental results show that u_* is not the only scaling of K_L and that in presence of big waves turbulence is strongly increased.

Thus, it is of fundamental importance to explain rationally the origin of this enhancement of turbulence. Wave breaking is often invoked (Kitaïgorodskï and Lumley 1983, Chalikov 1978). However convincing measurements were obtained without significant breaking : Kitaïgorodskï et al. (1983) on Lake Ontario and Cheung and Street (1988) in the Stanford air-water facility. In both cases, the fluctuating data were processed by classical linear filtration techniques in order to separate the orbital motion and the turbulent contribution. The results

show that below the interface the ratio k/u_*^2 takes unusual values ranging approximately between 9 and 50. This demonstrates that there exist indeed a mechanism capable of extracting energy from the waves and changing it into turbulence in the absence of wave breaking.
In the case of deterministic waves, this mechanism can be explored by using the phase average concept (Reynolds and Hussain 1972). The instantaneous velocity field is written under the classical form :
$V = \langle V\rangle + V'$ where $\langle V\rangle = \overline{V} + \tilde{V}$ ($\langle V\rangle$ represents the phase averaged velocity, V' the turbulent fluctuation, $\overline{V}$ the time averaged velocity and $\tilde{V}$ the orbital fluctuation). Introducing the orbital vorticity $\tilde{\omega} = \nabla \times \tilde{V}$, the $\tilde{\omega}$ balance is shown to be :

$$\frac{\partial\tilde{\omega}}{\partial t} + \nabla \times (\overline{\omega} \times \tilde{V}) + \nabla\tilde{\omega}.\overline{V} - \nabla \overline{V}.\tilde{\omega} = \nabla \times (\overline{\tilde{\omega} \times \tilde{V}} - \tilde{\omega}\times \tilde{V}) + \nu\nabla^2\tilde{\omega} - \nabla\times(\nabla.\tilde{\mathbb{R}})$$

where $\tilde{\mathbb{R}} = \langle\mathbb{R}\rangle - \overline{\langle\mathbb{R}\rangle}$ is the orbital part of the turbulent Reynolds stress tensor. $\nabla \times (\nabla . \tilde{\mathbb{R}})$ represents the vortex-stretching due to the orbital motions and is the key term in order to explain a nonzero $\tilde{\omega}$.
Using the eddy viscosity concept :

$$\langle\mathbb{R}\rangle = 2/3\ (\overline{k} + \tilde{k})\, \mathbb{I} - 2\ (\overline{\nu}_T + \tilde{\nu}_T)\ (\overline{\mathbb{S}} + \tilde{\mathbb{S}})$$

$$\text{where } S_{ij} = 1/2\ \left(\frac{\partial V_i}{\partial x_j} + \frac{\partial V_j}{\partial x_i}\right)$$

In order to perform an asymptotic study of the $\tilde{\omega}$ equation two different velocity scales and two different length scales are introduced : the reduced wave length $\lambda/2\pi$ and the relative phase velocity $C-\overline{V}_o$ in the streamwise direction ; the turbulent length scale $l_T = \overline{\nu_T}/u_*$ and u_* in the vertical direction. According to the values of the different parameters in the usual physical situations, Magnaudet (1989) showed that for a two-dimensional flow :

$$(\overline{V_o} - C)\ \frac{\partial\tilde{\omega}}{\partial x} \cong 2\ \frac{\partial^2\overline{\nu_T}}{\partial z^2}\ \tilde{S}_{xz}\ e_Y$$ (e_Y being the unit vector in the spanwise direction).
By integration in the case of a fully developed flow :

$$\overline{\tilde{u}\tilde{w}} = \int \overline{\tilde{w}\tilde{\omega}}\ .\ e_Y\ dz = -2\ \frac{\partial\overline{\nu_T}}{\partial z}\ \frac{\overline{\tilde{w}^2}}{C-\overline{V_o}}$$

Immediately below the waves $\overline{\nu_T}$ is decreasing with Z, so $\frac{\partial\overline{\nu_T}}{\partial z} < 0$ and $\overline{\tilde{u}\tilde{w}} > 0$ in conformity with the measurements of Cheung and Street (1988). So the vortex stretching mechanism can explain the appearance of a positive $\overline{\tilde{u}\tilde{w}}$ cross-correlation below the waves.
Moreover, at high Reynolds number, the streamwise momentum balance writes approximatively : $-\overline{u'w'}\ (z) = u_*^2 + \overline{\tilde{u}\tilde{w}}\ (z) > u_*^2$.
This increase of $\overline{u'w'}$ implies of course an increase of the turbulence production which leads to the enhancement of $\overline{k}$. This conceptual model was checked with the aid of the classical $k - \varepsilon$ model (the interfacial conditions being $d\overline{k}/dz = 0$, $d\overline{\varepsilon}/dz = -\overline{\varepsilon}/z$).
The results agree well with the data of Cheung and Street (1988). In particular the level of $\overline{k}$ near the interface is well reproduced.
Following the same analysis, the balance of the orbital concentration fluctuation $\tilde{c}$ is :

$$\frac{\partial\tilde{c}}{\partial t} + \nabla\ .\ (\overline{c}\tilde{V} + \tilde{c}\overline{V} + \tilde{c}\tilde{V} - \overline{\tilde{c}\tilde{V}}) = \nabla\ .\ (-D\nabla\tilde{c} - \widetilde{c'V'})$$

According to the eddy diffusivity concept :

$$- \widetilde{c'V'} = \frac{\overline{\nu_T}}{Sc_T} \nabla \tilde{c} + \frac{\tilde{\nu}_T}{Sc_T} \nabla \bar{c}.$$ The asymptotic study leads to :

$$(\overline{V_o} - C) \frac{\partial \tilde{c}}{\partial x} \simeq \tilde{w} \frac{\partial \bar{c}}{\partial z}$$ which immediately gives by integration that $\tilde{c}$ is 90° out of phase with $\tilde{w}$, so that $\overline{\tilde{c}\tilde{w}} = 0$.

Therefore, within the frame of this model, it is shown that the obvious increase of K_L in presence of wind waves is not caused by a direct coupling between concentration fluctuations and orbital motion, but really by the enhancement of the turbulent flux $\overline{c'w'}$ resulting from the increase of $\bar{k}$ explained by the orbital vortex-stretching mechanism.

LITERATURE CITED

Caussade B., George J., Masbernat L. (1990)-"Experimental study and parametrization of interfacial gas absorption". To appear in the AIChE Journal

Chalikov D.V. (1978) - "The numerical simulation of wind-wave interaction". J.F.M. 87, pp 561-582

Chen B.H., Mallas K, Mc Millan A.F. (1985)- "Gas absorption across a free surface of a stirred vessel". AIChE Journal. 31, 3, pp 510-512

Cheung T.K., Street R.L. (1988) - "The turbulent layer in the water at an air-water interface". J.F.M. 194, pp 133-151

George J. (1987) - " Etude de l'absorption d'un gaz peu soluble à une interface gaz-liquide". Internal Report n° 336 EME. IMF Toulouse

Henstock W.H., Hanratty T.J. (1979) - "Gas absorption by a liquid layer flowing on the wall of a pipe". AIChE Journal, 25, pp 122-131

Kitaïgorodskiï S.A., Lumley J.L. (1983)- "Wave-turbulence interactions in the upper ocean. Part I : the energy balance of the interacting fields of surface wind waves and wind-induced three-dimensional turbulence". J. Phys. Ocean, 13, pp 1977-1988

Kitaïgorodskiï S.A., Donelan M.A., Lumley J.L., Terray E.A. (1983)- "Wave-turbulence interactions in the upper ocean. Part II : Statistical characteristics of wave and turbulent components of the random velocity field in the marine surface layer. J. Phys. Ocean, 13, pp. 1988-1999

Magnaudet J. (1989)- "Interactions interfaciales en écoulement à phases séparées". PhD Thesis. INP Toulouse

Reynolds W.C., Hussain A.K.M.F. (1972)- "The mechanics of an organized wave in turbulent shear flow. Part III : Theoretical models and comparisons with experiments". JFM 54, pp 263-288.

SOME IMPORTANT PARAMETERS ON THE TURBULENT REAERATION OF WATER: AN ANALYTICAL APPROACH AND EXPERIMENTAL RESULTS

Harry E. Schulz. Universidade de Sao Paulo, Escola de Engenharia de Sao Carlos, Depto. de Hidraulica e Saneamento, 13560 Sao Carlos, SP, Brazil.
Jose R. Bicudo. Universidade de Sao Paulo, Escola de Engenharia de Sao Carlos, Depto. de Hidraulica e Saneamento, 13560 Sao Carlos, SP, Brazil.
Antenor R. Barbosa. Universidade Federal de Ouro Preto, Escola deMinas, Ouro Preto, MG, Brazil.
Marcius F. Giorgetti. Universidade de Sao Paulo, Escola de Engenharia de Sao Carlos, Depto. de Hidraulica e Saneamento, 13560 Sao Carlos, SP, Brazil.

Introduction

Analytical studies based on the statistical theory of turbulence (Corrsin, 1964) were carried out in order to identify some relevant parameters which may be associated with the reaeration rate coefficient of turbulent waters. These led to the conclusion that the energy dissipation and a length scale (segregation scale) may be among those parameters. Mathematical models expressing the relationship between the reaeration coefficient and the above mentioned parameters were developed.

The trend observed for model results related to energy dissipation was verified for independent experimental systems. The trend observed for other model results, related to the segregation scale, could not be experimentally verified. However, the dimensional similarity between the length scale and artificial roughness allowed a preliminary estimate of the suggested trend.

Theoretical Models

The mathematical expressions which relate the reaeration rate coefficient to the energy dissipation and segregation scaleparameters are given below (Schulz, 1985):

For low agitation:

$$K_2 = A \int_0^{\infty} k^6 \, \mathrm{EXP}\,(-B\,\nu\,k^2)\, dk \qquad (1)$$

where K_2 is the reaeration coefficient, k is the wave number, ν is the kinematic viscosity and A and B are constants.

For high agitation:

$$K_2 = \frac{C}{\left[3 \left(\frac{5}{\pi}\right)^{2/3} \left(\frac{L_s^2}{\varepsilon}\right)^{1/3} + \left(\frac{\nu}{\varepsilon}\right)^{1/2} \mathrm{LN}\,(Sc) \right]} \qquad (2)$$

where C is a constant, L_s is a segregation scale, ε is the energy dissipation by unit mass and Sc is the Schmidt Number.

From the above expressions, it is possible to suggest that $K_2 \alpha \varepsilon^0$ (for very low disturbances), $K_2 \alpha \varepsilon^{1/3}$ and $K_2 \alpha \varepsilon^{1/2}$ (for intermediate disturbances), and $K_2 \alpha \varepsilon^{1/2} L_*^{-2/3}$ (for very high disturbances) without any further consideration regarding the segregation scale L_*, which may be either constant or variable for most situations.

Experimental Results

Four different and independent sets of experiments were conducted and are briefly described here.

Bicudo (1988) carried out reaeration studies in an annular channel where turbulence was induced by a submerged jet. Energy dissipation results were re-analysed based on point velocity measurements made at four different cross sections along the flume for various hydraulic situations. Calculations were made according to the first law of thermodynamics and the relationship between the reaeration rate and the energy dissipated by the system is given by:

$$K_2 \ \alpha \ \varepsilon^{0.33} \tag{3}$$

Barbosa (1989) conducted reaeration experiments in a stainless steel mixing tank working with different gases. His results were analysed by Schulz (1989) who obtained the following relationship for the energy dissipation:

$$K_2 \ \alpha \ \varepsilon^{0.257} \quad \text{for low agitation} \tag{4}$$

$$K_2 \ \alpha \ \varepsilon^{0.500} \quad \text{for high agitation} \tag{5}$$

Bicudo et al.(1989) conducted a series of reaeration experiments in a straight channel with strip bed roughness. Energy dissipation was estimated from an approximation of the first law of thermodynamics and the Darcy-Weisbach equation. The relationship obtained for a set of 36 experiments was as follows:

$$K_2 \ \alpha \ \varepsilon^{0.42} \tag{6}$$

The variation of the reaeration rate coefficient with a length scale, as suggested in equation (2), was also obtained and is as follows:

$$K_2 \ \alpha \ \varepsilon^{0.535} \ \chi^{-0.136} \tag{7}$$

where χ is a strip bed resistance parameter.

Schulz (1989) conducted reaeration studies in a straight recirculation flume working with a set of different sand bed roughnesses. Energy dissipation values were computed from velocity and depth measurements at different cross sections along the channel. Experimental data was then approximated by the same combination of the first law of thermodynamics and the Darcy-Weisbach equation as mentioned above. The following relationshipwas obtained:

$$K_2 \ \alpha \ \varepsilon^{0.49} \tag{8}$$

Schulz (1989) also verified the relationship between the reaeration coefficient and a length scale given by the equivalent sand diameter. The equation obtained was of the type:

$$K2 \propto \varepsilon^{0.49} \phi^{-0.171} \qquad (9)$$

where ϕ is the equivalent sand diameter.

Conclusion

Similar trends were obtained for the reaeration rate coefficient in relation to the energy dissipated in four independent experimental systems. These appear to be concentrated around the following proportionalities:

$$K2 \propto \varepsilon^{1/3} \quad \text{and} \quad K2 \propto \varepsilon^{1/2}$$

The 1/3 power of the energy dissipated by a particular system seems to be associated with low energy dissipation levels, while the 1/2 power seems to be associated with high energy dissipation levels and in agreement with the surface renewal theory.

References

Barbosa, A.R. (1989). Desenvolvimento de Metodologia para a Determinacao do Coeficiente de Reaeracao dos Escoamentos Naturais da Agua com o Emprego de Tracador Gasoso. M.Sc Dissertation, Universidade de Sao Paulo, EESC, Depto. de Hidraulica e Saneamento.

Bicudo, J.R. (1988). The Measurement of Reaeration in Streams. Ph.D Thesis, University of Newcastle upon Tyne, Dept. of Civil Engineering.

Bicudo, J.R., Schulz, H.E. and Giorgetti, M.F. (1989). The Use of Sidewall Correction Procedures for Non-Uniform Roughness Distribution in Open Channel Flow: Energy Dissipation and Mass Transfer Aspects. Paper submitted for presentation at the XIV Latin American Congress of Hydraulics (IAHR) to be held in November, 1990, Montevideo.

Corrsin, S. (1964). The Isotropic Turbulent Mixer: Part II - Arbitrary Schmidt Number. *American Institution of Chemical Engineers Journal*, Vol. 10, No. 6, pp.870-877.

Schulz, H.E. (1985). Investigacao do Mecanismo de Reoxigenacao da Agua em Escoamento e sua Correlacao com o Nivel de Turbulencia junto a Superficie. M.Sc Dissertation, Universidade de Sao Paulo, EESC, Depto. de Hidraulica e Saneamento.

Schulz, H.E. (1989). Estudos Preliminares sobre a Variacao da Dissipacao de Energia nos Casos de Escoamento Turbulento. Internal Report, Universidade de Sao Paulo, EESC, Depto. de Hidraulica e Saneamento.

LABORATORY MEASUREMENT TECHNIQUES

Turbulent Velocity and Gas Concentration Measurements
in the Surface Layers of a Grid-Stirred Experiment

Chia-Ren Chu and Gerhard H. Jirka
DeFrees Hydraulics Laboratory
Cornell University, Ithaca, NY 14853

The transfer of gases across a gas/liquid interface is an ubiquitous and important phenomenon. In most cases, it is desired to predict the transfer rate of a particular substance across the interface. This requires a detailed understanding of the fundamental mechanisms underlying the interfacial mass transfer process. For this reason, an experiment was undertaken to observe the interaction between the liquid turbulence and the concentration fluctuations in the interfacial region.

Because of its well controlled turbulent environment, the stirred cell apparatus has been used in the past by several researchers for the study of gas transfer. Our experiments were performed in a 50 cm-square, 40 cm-deep tank stirred by a vertically oscillating grid, in which turbulent conditions can be reproduced satisfactorily.

This study is mainly concerned with the specific case of oxygen transfer across a reasonable flat and clean, shear free surface. Two types of measurement were carried out. The first type, called the "interfacial concentration measurement", measured the oxygen concentration within 5 mm from the surface with an oxygen microprobe of 5 μm tip size. The other type, called the "simultaneous measurement", used a split hot-film probe and the oxygen microprobe to measure the fluctuations of velocity and oxygen concentration in the interfacial region at the same time. Each type of measurement was carried out for four different turbulence conditions (turbulent Reynolds number are in the range of 80 - 660).

The results of the interfacial concentration measurements show that the mean concentration profiles (see Fig. 1) at the water surface can be approximated by an exponential curve $(C-C_b)/(C_s-C_b) = \exp(z/z_o)$ (the solid line in Fig. 1), where z_o is the thickness constant. The steep gradient at the water surface suggests significant molecular diffusion. Independent bulk concentration measurements can be used to determine the gas transfer velocity K_L for each turbulence condition. From that data, the Lewis-Whitman's film thickness δ is computed, $\delta = D/K_L$ in which D is the molecular diffusivity of oxygen in water. Our observations (see Fig. 2) show that δ and z_o closely agree in trend and magnitude. Fig. 2 also shows that the thickness of the diffusive sublayer $L_D = 2LR_L^{-1/2}S_c^{-1/2}$ suggested by Brumley and Jirka (1988) has a roughly linear relation with z_o and about the same order of magnitude, in which L is the integral length scale of turbulence, R_L is the turbulent Reynolds number, and S_c is the Schmidt number.

Fig. 3 shows the vertical profiles or normalized turbulent fluxes <wc> measured by the eddy correlation method in the simultaneous measurement. The measured fluxes at the surface region are believed to be somewhat in error because of the inaccuracy of vertical velocity measurements caused by a probe surface proximity effect and by surface wave. These profiles show the turbulent flux gradually decays to zero within the bulk region. This is because the

concentration field is well mixed by the turbulence in the bulk region, it is difficult to measure the turbulent flux there. Nevertheless, these measurements are within one order of magnitude compared with the mean flux J computed from the bulk concentration change over 10 hours under the same turbulence condition.

This study was supported by the United States Geological Survey through grant No. 14-08-0001-G1480.

Reference:

Brumley, H.B. and G.H. Jirka, "Air-Water Transfer of Slightly Soluble Gases: Turbulence, Interfacial Processes and Conceptual Models", J. Physico-Chemical Hydro., 10(3), pp.295-319, 1988.

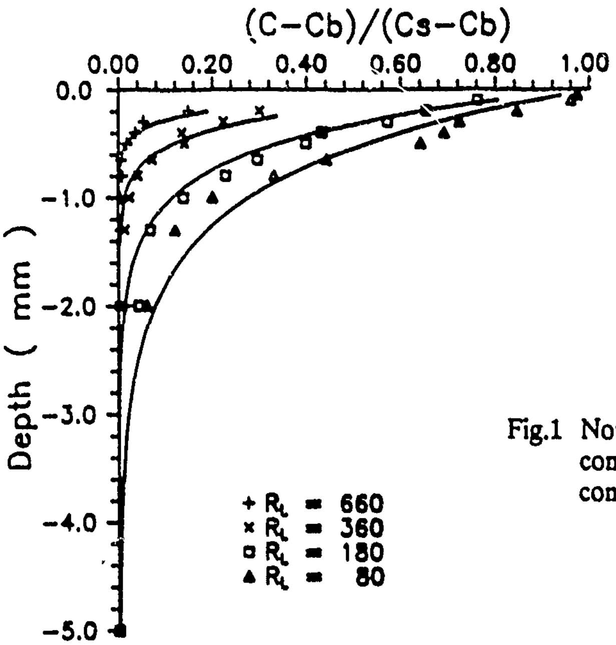

Fig.1 Normalized concentration profiles, in which C_b is the concentration at bulk region, C_s is the saturation concentration

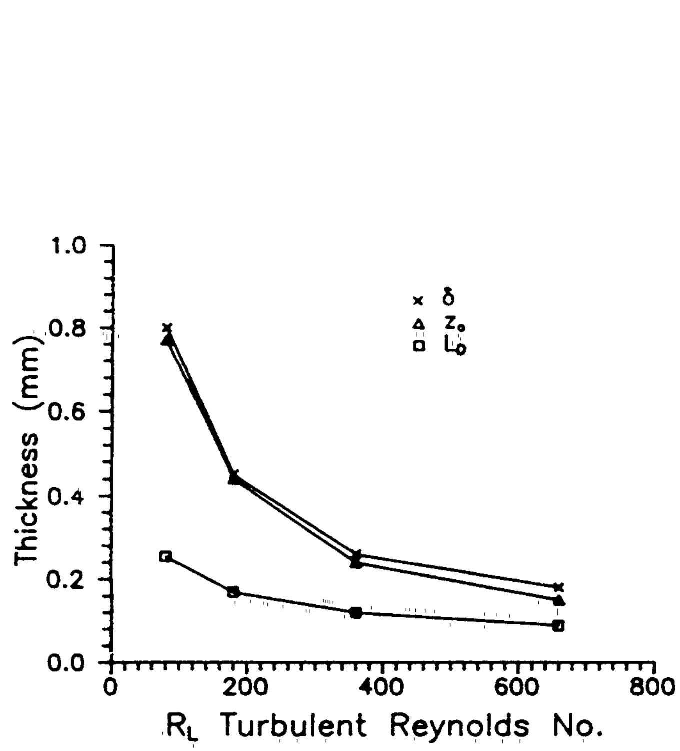

Fig.2 The comparsion of different thickness scale, in which z_o is the thickness constant, δ is the Lewis-Whitman film thickness, and L_D is the thickness of diffusive sublayer.

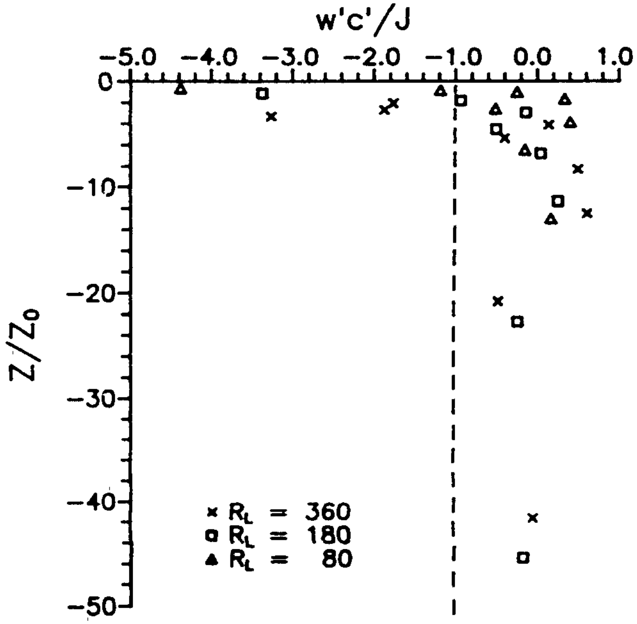

Fig. 3 Vertical profiles of normalized flux, in which J is the mean flux computed from bulk concentration changes

A development of method for measuring near-surface turbulence

by Takeharu ETOH, Professor
and
Kosei TAKEHARA, Research Associate

Department of Civil Engineering, Kinki University,
Higashi-Osaka, Osaka 577 JAPAN

Measurements of turbulence near water surface are essential to study mechanics of gas transfer at water surface. Automatic tracing of small particles in water is one of the most promising methods for the measurement. Use of a video recorder and an image processing computer may provide the best combination for the tracing particles and automatic processing of graphic data. The method, however, has such disadvantages as lower resolution and longer processing time, due to insufficient capacities of current standard video systems and workstations. Technology advancement in electronic industries is day by day improving their capacities. Higher-resolution television with more than one thousand scanning lines, graphic workstations with parallel processing units, etc., will soon be released to market. Software to fully utilize their capacities must be simultaneously developed.

Various element of techniques to support the total system should be developed in parallel and integrated. They may fall into the following three categories.

(1) Development of tracer particle

A tracer particle is expected to accurately follow movement and temperature change of its surrounding water. Thus, the size should be smaller than the micro-scale of turbulence, and the specific gravity, the specific heat,etc., should be as close as possible to those of water. The authors have developed a method to make micro-capsules which are filled with pure water and covered with thin film of polystyrene(See Fig. 1). They may have quite desirable properties as tracer particles.

Fig. 2 shows frequency distribution of specific gravity of the particles. The average is 1.0046, which is very close to that of water, in comparison with that of popularly-used particles for flow visualization of water. For example, the specific gravity of polystyrene is about 1.03 and that of nylon 12 is about 1.02. The standard deviation is 0.0014.

Fig. 3 shows frequency distribution of diameter of the particles. The mean and the standard deviation are 673 μm and 142 μm, respectively. It is easy to make smaller particles.

The manufacturing method is presented in this paper.

(2) Methods to pick up particle-images from background

There have been developed few methods to objectively determine the threshold of brightness which separates particle-image from background. For each frame of picture from which particle-images are

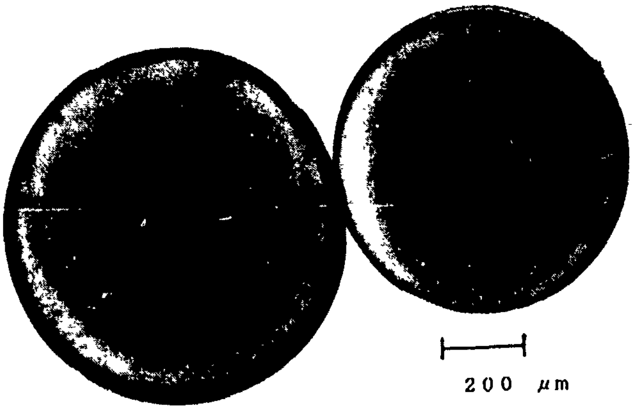

Fig. 1. Photograph of microcapsules taken by a camera with a microscope

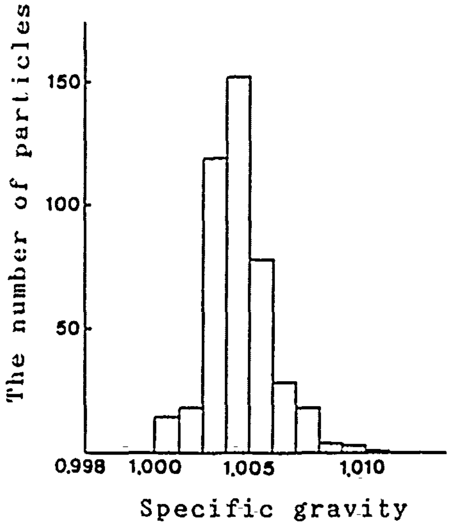

Fig. 2. Frequency distribution of specific gravity of microcapsules

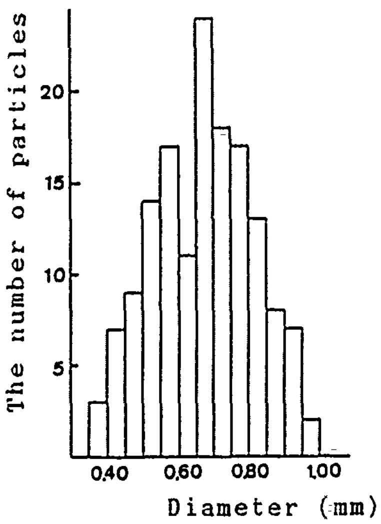

Fig. 3. Frequency distribution of diameter of microcapsules

removed, absolute deviation from local average of the brightness can be calculated. Provided noise in the background distributes normally, the probability that the noise exceeds four times the absolute deviation is practically zero. From this statictical consideration, a new method to objectively determine the threshold is proposed.

(3) Algorithms for tracing particles

At the present time, the number of particles which can be traced by existing algorithms is limited to the order of 10^2, if the color of particles is the same. The number of traceable particles in a frame to keep satisfactory level of resolution may be at least 10^4, which guarantees respective $1/100(\sqrt{10^4})$ and $1/22(\sqrt[3]{10^4})$ line-resolution in two- and three-dimensional spaces. One thousand may be a breakthrough to reach the goal. The proposed algorithm in the paper broke through the limit. It is composed of Kalman's filtering theory to predict location and brightness of each particle in the next frame, and χ^2-test to evaluate the probability that a pair of particle-images in the successive frames represent the same particle. Fig. 4 shows an example

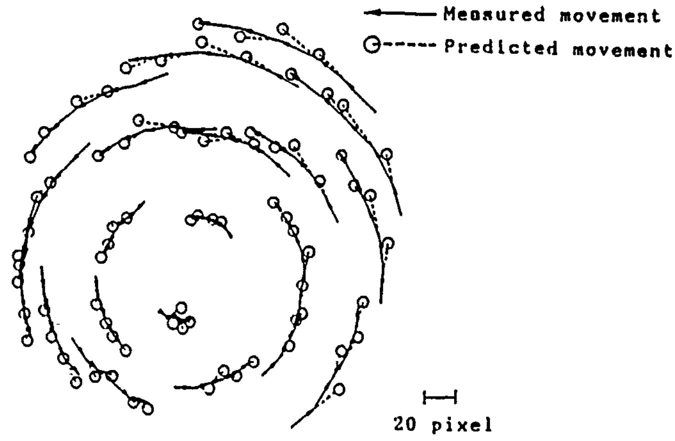

Fig. 4. The result of automatic tracing of particles

of the result of the automatic tracing of particles.

The system is applied to visualize the flow and measure the velocity field at a front where a surface of water submerges and air is entrained along it.

Kinetic isotope fractionation during air-water transfer of oxygen and nitrogen

M. Knox, P.D. Quay, and D.O. Wilbur
School of Oceanography, University of Washington, Seattle

INTRODUCTION

We have performed experiments to determine the kinetic fractionation of oxygen and nitrogen isotopes during gas-water transfer of oxygen and nitrogen gases. The experiments are part of a larger project to use measurements of $^{18}O/^{16}O$ and O_2 saturation as tracers of photosynthesis and respiration rates in the surface ocean. The utility of geochemical tracers in studying biological activity in the upper ocean has been discussed by many researchers (see for example Bender and Grande, 1987; Jenkins, 1982; Jenkins and Goldman, 1985; Schulenberger and Reid, 1981; Emerson, 1987). In order to effectively use measurements of O_2 and $^{18}O/^{16}O$ as biogeochemical tracers, there must be a greater understanding of the effects of air-sea transfer on concentrations and isotopic composition of dissolved gases in the ocean.

Two factors affect the isotopic fractionation of a non-reactive gas during air-sea gas exchange. At equilibrium there is an isotopic fractionation resulting from the difference in the relative free energies of the isotopic species. Benson and Krause (1980) and Klots and Benson (1963) have determined the equilibrium fractionation for oxygen and nitrogen respectively and found that the heavier isotopic species was enriched in the dissolved phase by 1.0 to 0.5‰ over temperatures from 2-30°C. During nonequilibrium gas transfer, there is a fractionation due to the faster transfer rate of the lighter isotopic species versus the heavier. It is this kinetic fractionation that we have determined.

GAS EXCHANGE MODEL FORMULATION

According to the stagnant boundary layer model first described by Whitman (1923), the rate of gas exchange depends on the molecular diffusivity of the dissolved gas, D, and the thickness of the boundary layer, z. In a closed gas-water system, we can write the following equation describing the change in the concentration of the total gas with time.

$$\frac{dG}{dt} = \frac{A}{V}\frac{D_G}{z}\underline{(P\gamma - G_W)} \qquad (1)$$

G and G_W are the concentration of the gas in gas phase and dissolved phase, respectively. A/V is the surface area to volume ratio of the system undergoing gas transfer, P represents the partial pressure of the gas above the liquid, and γ is the gas solubility coefficient. Gas solubility for oxygen and nitrogen are taken from Weiss (1970). Since the light isotope comprises greater than 99.6% of the gas, in the case of both oxygen and nitrogen, the concentration of total gas, G, approximately equals the concentration of the light isotope, and we can rewrite equation (1) to represent the change in the concentration of the light isotopic species, L, with time.

$$\frac{dL}{dt} = \frac{A}{V}\frac{D_L}{z}\underline{(P\gamma - L_W)} \qquad (2)$$

Similarly, we can write the equation describing the rate of transfer of the rare or heavy isotopic species, H, with time.

$$\frac{dH}{dt} = \frac{A}{V}\frac{D_H}{z}\underline{(P\gamma (H/L)_G \alpha_{eq} - L_W (H/L)_W)} \qquad (3)$$

D_H is the molecular diffusivity of the heavy isotope. The ratios of the heavy to light isotopes in the gas and in the dissolved phase respectively are $(H/L)_G$ and $(H/L)_W$. The isotopic fractionation at equilibrium, α_{eq}, is equal to the ratio of the isotopic composition of the dissolved and undissolved gas, $(H/L)_G/(H/L)_W$.

If we allow the kinetic isotopic fractionation, α_k, to represent the ratio of the molecular diffusion rates of the heavy and light isotopes, then $\alpha_k = D_H/D_L$, and equation (2) becomes

$$\frac{dH}{dt} = \frac{A}{V}\frac{D_L}{z}\underline{(P\gamma (H/L)_G\alpha_{eq}\alpha_k - L_W (H/L)_W\alpha_k)} \qquad (4)$$

By measuring the time rate of change of the gas concentration, L, and its isotopic composition, H/L, in the headspace, and by knowing γ and α_{eq}, we can estimate α_k using

$$\frac{dH}{dL} = \frac{\alpha_k(P\gamma (H/L)_G\alpha_{eq} - L_W (H/L)_W\alpha_k)}{(P\gamma - L_W)} \qquad (5)$$

Thus the determination of α_k does not require a measurement of z or A/V.

METHODS

Experiments are performed using a modified version of the system described by Zyakun et al. (1979), see figure (1). Gas exchange takes place in the 4-liter flask, A. The temperature is kept constant with a water bath, B. The sytem is closed to the atmosphere. As gas dissolves into the water, the water level drops in the manometer, C. This enables us to make direct measurements of the volume of gas transferred as the experiment proceeds. The 12-liter flask, D, is large enough to maintain an approximately constant pressure in the system, despite the headspace volume change in flask A.

Samples are drawn by isolating an aliquot of the headspace in section E and then freezing the entire aliquot into liquid helium. Samples of both nitrogen and oxygen gas are run directly on a Finnigan MAT 251 mass spectrometer. All samples are run against a standard gas which is equivalent to the initial gas admitted into the experiment. All data is expressed in the standard del notation: del = $((H/L)_{sa}/(H/L)_{std} - 1) \times 10^3$, where $(H/L)_{sa}$ and $(H/L)_{std}$ indicate the ratio of the heavy to light isotopes in the sample and standard respectively.

Experiments have been run to determine the kinetic fractionation for oxygen and nitrogen at 10 and 20°C, using pure gases containing less than 0.1% impurities. Experiments typically lasted 14 days; water attained >90% saturation after about 6 days, (Figure 2). All experiments were begun with degassed water. The error on the isotopic measurement is ±0.03‰, based on duplicate samples.

RESULTS

Initially the headspace gas becomes enriched in the heavy isotope, indicating a faster rate of transfer of the lighter isotope into water. Typically, this enrichment reaches a maximum of about 0.4‰ above the initial gas for oxygen, and about 0.1‰ for nitrogen (Figures 3 and 4). As equilibrium is approached, particularly after the dissolved gas reaches 40-50% of saturation, the ratio of heavy to light isotopic species in the headspace gas begins to decrease. By 80-90% of saturation, the headspace isotopic ratio is lower than its initial value, indicating that the final isotopic composition of the system is dominated by the equilibrium fractionation, as expected. For each experiment, a best fit line to the data, using equation (5) to describe the time rate of change of the H/L in the gas phase, was used to determine α_k.

Figures (3) and (4) show the change in isotopic composition over the course of experiments run with oxygen and nitrogen respectively. The ratio of heavy to light isotope transfer rates was found to be 0.9973 - 0.997 for oxygen and 0.9989 - 0.9985 for nitrogen. Experimental results to date do not indicate a significant temperature dependence of α_k.

DISCUSSION

In a stagnant boundary layer model, the kinetic fractionation reflects the first power ratio of the molecular diffusivity constants for heavy and light isotopic gas molecules, however this may apply only to situations dominated by molecular diffusion. Ledwell (1984), Wanninkhof (1986), and Danckwertz (1970) have shown that in cases where convective forces affect gas exchange, the relative gas transfer may be more nearly approximated by the 2/3 or the 1/2 power of the molecular diffusivity constants. In a natural setting, it can generally be assumed that some convective flow is occurring and therefore α_k may best represent the 1/2 power of the diffusive coefficient ratio. The experimental system used here was stirred, but there was no visible deformation of the surface, and therefore our values are likely to lie between the first and the 1/2 powers of the D_H/D_G. Experiments to determine the dependence of α_k on degree of stirring are planned.

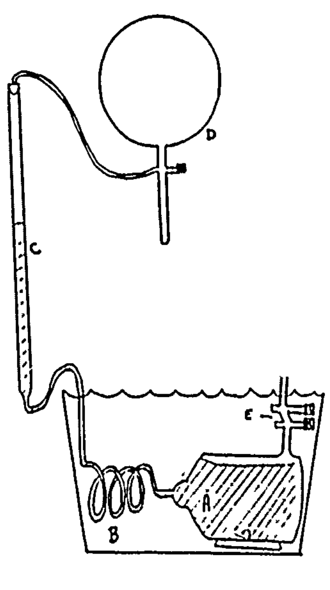

Fig. 1. Schematic diagram of the experimental system used. See text for explanation.

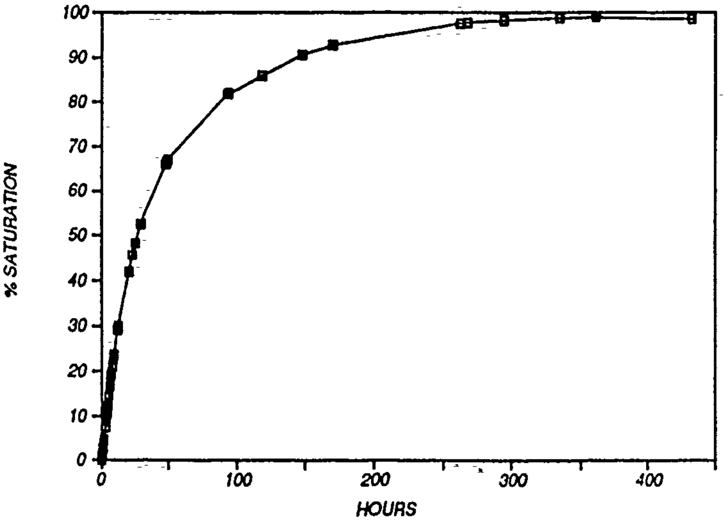

Fig 2. Experimental measurements of percent saturation versus time for an oxygen experiment run at 10°C.

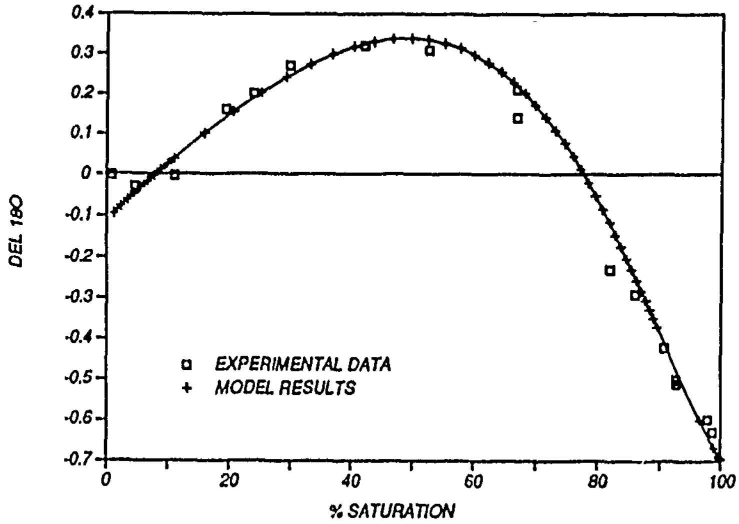

Fig. 3. Experimental measurements of $^{18}O/^{16}O$ (‰) versus percent saturation for an oxygen experiment run at 10°C, plotted with model results obtained using $\alpha_k = 0.9973$. Del ^{18}O values are relative to the $^{18}O/^{16}O$ of the initial headspace gas.

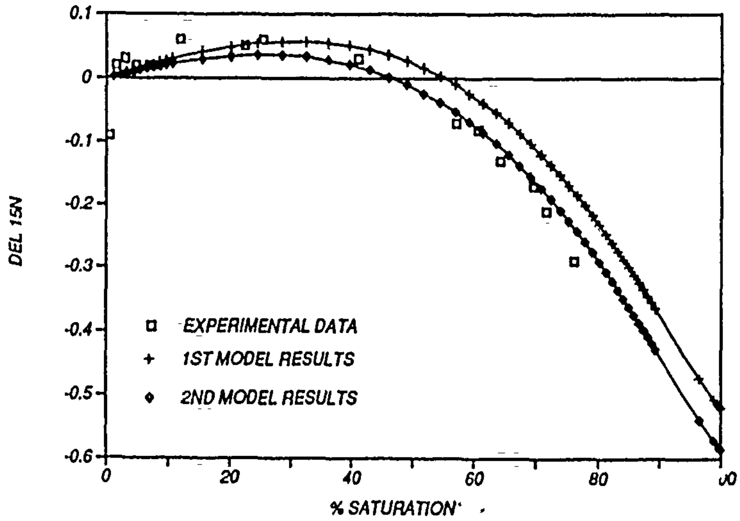

Fig. 4. Experimental measurements of $^{15}N/^{14}N$ (‰) versus percent saturation for a nitrogen experiment run at 10°C, plotted with model results obtained using $\alpha_k = 0.9988$. The first model results here are obtained using the value of α_{eq} given by Klots and Benson (1963), $\alpha_{eq} = 1.00078$. The second results are obtained using $\alpha_{eq} = 1.00088$. Del ^{15}N values are relative to the $^{15}N/^{14}N$ of the initial headspace gas.

REFERENCES

Bender, M.L. and K.D. Grande, Production, respiration, and the isotope geochemistry of O_2 in the upper water column, Global Biogeochem. Cycles, 1, 49-59, 1987.

Benson, B.B. and D. Krause, The concentration and isotopic fractionation of gases dissolved in fresh water in equilibrium with the atmosphere. 1. oxygen, Limnol. Oceanogr., 25, 662-671, 1980.

Danckwertz, P.V., Gas Liquid Reactions, McGraw Hill, New York, 1970.

Emerson, S., Seasonal oxygen cycles and biological new producion in surface waters of the subarctic Pacific Ocean, J. Geophys. Res., 92, 6535-6544, 1987.

Jenkins, W. and J. Goldman, Seasonal oxygen cycling and primary production in the Sargasso Sea, J. Mar. Res., 43, 465-491, 1985.

Klots, C.E. and B.B. Benson, Isotope effect in the solution of oxygen and nitrogen in distilled water, J. Chem. Phys., 38, 890-892, 1963.

Ledwell, J.R., The variation of the gas transfer coefficient with molecular diffusivity, in Gas Transfer at Water Surfaces, ed. by W. Brutsaert and G.H. Jirka, 293-302, Reidel, Dordrecht, 1984.

Wanninkhof, R.H., Gas exchange across the air-water interface determined with man made and natural tracers, Doctoral thesis, Columbia University, 1986.

Weiss, R.F., The solubility of nitrogen, oxygen, and argon in water and seawater, Deep Sea Res., 17, 721-735, 1970.

OPTICAL DETECTION OF TURBULENCE-RELATED PARAMETERS AND CORRELATION WITH REAERATION COEFFICIENT IN GRID-STIRRED TANK

Woodrow N. L. Roma
Marcius F. Giorgetti

School of Engineering at S. Carlos
University of S. Paulo, Brazil

ABSTRACT

An optical sensor has been developed to operate across the free surface of grid-stirred water, based upon the optical refraction of light by moving air-water interface. The objective is the detection of a random electric signal responsive to the water free surface motion.

A light source on the air side sends a beam through the interface to a submerged photocell (Figure 1). Turbulent oscillation of water surface produces local changes in slope of water surface just above the sensor. Light refraction, thus caused, determines oscillation in the electric signal with frequency density distribution representative of the frequencies of deformation of the water surface, as imposed by ascending system of eddies. The hypothesis in this piece of research is that there should be a correlation between the characteristics of the electric signal and those of near surface turbulence, responsible for surface renewal and, therefore, for the rate of reoxygenation.

The experimental apparatus is similar to the one used by Brumley [1,2] except for the grid driving mechanical device, which is operated from underneath the tank through rubber sealed linkages, and powered by a direct current motor. The tank has 0.25 m^2 of water free surface, square in shape, and water depth of 0.70 m. Figure 2 illustrates a typical grid; the bars have square sections with dimensions 10 mm x 10 mm; grid cells are also square in shape with distances between adjoining bars, respectively, 35 mm, 50 mm and 70 mm. For all experiments the grids were set at the mean depth of 500 mm; total amplitude of oscillation was 100 mm ($\pm$ 50 mm from initial mean depth) chosen upon the visual quality of the water surface as determined by the absence of breaking. Each grid was driven at several speeds of oscillation producing differents patterns of turbulence.

The sensor used is a typical germanium transistor, OC71, prepared to react as a phototransistor. The electric signal is digitised directly into a 8 bits microcomputer with 27 readings per second. Times of experimental runs are periods of 155 seconds, with a total of 4100 data points per run.

Water for each experiment is previously de-oxygenized by using the low pressure (cavitation) method as described by MAXWELL & HOLLEY [3]. Reoxigenation is followed-up in each experiment for about 30 hours. Dissolved oxygen is registered by and OD probe (AM 221, Forschungs Institut, GDR) set 300 mm under the water surface near the tank vertical center line. The experimental results are shown in Table 1.

All experiments were run at the temperature of 25 ^{o}C.

Table 1 - Experimental Results

Experiment		V_{RMS} (V)	L_t (V . s)	$K_2 (h^{-1})$
Grid #	Frequency (RPM)			
1	69	0.118	$2.059\ 10^{-3}$	0.0468
1	84	0.176	$3.923\ 10^{-3}$	0.0510
1	108	0.348	$6.080\ 10^{-3}$	0.0778
1	115	0.359	$7.119\ 10^{-3}$	0.0822
1	150	0.619	$10.303\ 10^{-3}$	0.1425
2	90	0.106	$1.234\ 10^{-3}$	0.0509
2	116	0.171	$2.841\ 10^{-3}$	0.0645
2	188	0.366	$5.532\ 10^{-3}$	0.1032
2	198	0.520	$9.943\ 10^{-3}$	0.1279
3	115	0.071	$0.905\ 10^{-3}$	0.0526
3	172	0.108	$3.226\ 10^{-3}$	0.0782
3	198	0.287	$6.274\ 10^{-3}$	0.0845
3	200	0.344	$7.323\ 10^{-3}$	0.0831
3	238	0.389	$5.643\ 10^{-3}$	0.1065

The poor correlation between the true RMS voltage, generated by the optical measurement set, and coefficient of reoxygenation K_2 is shown in Figure 3. The mass transfer coefficient K defined by multiplying K_2 by a pseudo macro scale of turbulence, L_t, obtained through the integration of the autocorrelation of the RMS voltage, produced the much better correlation shown in Figure 4. The best fitted power correlation is

$$K = 0.03118\ V_{RMS}^{5/3} + 0.0004$$

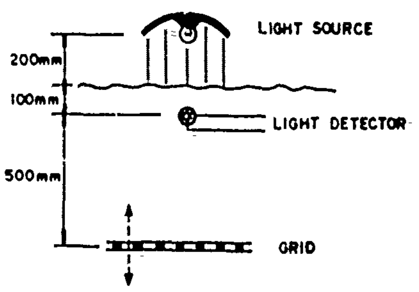

Figure 1 - Optical Set

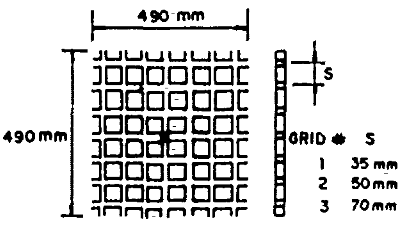

Figure 2 - Typical Grid Set

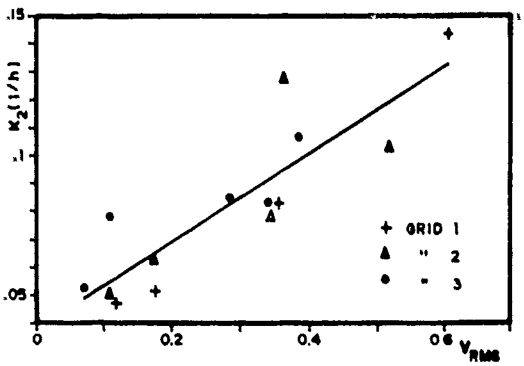

Figure 3 - Coefficient of Reoxygenation K_2 vs . V_{RMS}

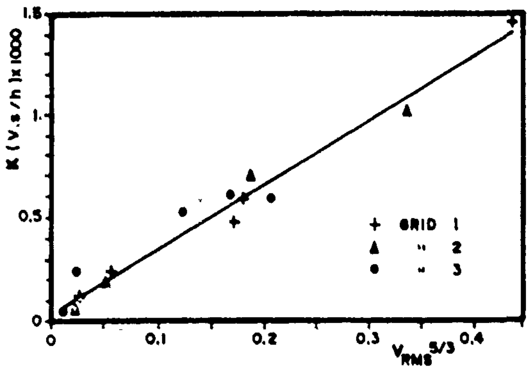

Figure 4 - Mass Transfer Coef. K vs. V_{RMS} to power 5/3

REFERENCES

1 - BRUMLEY, B. Turbulence measurements near the free surface in stirred grid experiments in gas transfer at water surface, 89-92. In: Brutsaert, W. & Jirka, G.H., ed. Gas Transfer at Water Surfaces, D.Reidel Publishing Co.,1984

2 - BRUMLEY, B. Near surface turbulence and associated gas absorption in a grid stirred tank. Ph.D. Thesis, Cornell U., 1983.

3 - MAXWELL, W.H.L. & HOLLEY, E.R. A method for deaerating water. Journal of Hydraulics Division, 95(HY1):577-580, jan, 1969.

PHYSICAL SIGNIFICANCE OF THE PARAMETERS OBTAINED WITH PHOTO-ELECTRIC SENSORS FOR LIQUID SURFACE DISTURBANCES

BY

HARRY E. SCHULZ and WOODROW N. L. ROMA

ABSTRACT

The methodology for studying turbulent liquid surfaces with the aid of photo-electric sensors, proposed by Roma (1988)and described by Roma and Giorgetti (1990), was analised from the point of view of physical phenomena that occur at the gas-liquid interface.This analysis led to an interpretation of the physical meaning of the empirical parameters used to describe the experimental data. Additionally, using this interpretation and the data presented by Roma (1988), it was possible to suggest a treatment of the experimetal observations by dimensional analysis, which shows a good correlation between the nondimensional parameters proposed.

Physical Interpretation of the Measured Parameters

Based on conceptual schemes of the movement and deformation of the free surface of a turbulent agitated liquid, it was possible to show that the variables that are usually calculated from "random" data aquire, in the present case, the following meanings:

(i) Macro-scale of the registred signal, defined by

$$T = \int_0^{\infty} p(t).dt \qquad (1)$$

in which p(t) is the correlation function. It was verified that T is a measure of the mean time for a surface wave to travel through a distance paralel to the surface.

* Department of Hydraulics and Sanitary Engineering, São Carlos School of Engineering, São Paulo University, Brazil.

(ii) Root-mean-square of the registred signal.

It was verified that this r.m.s. value is a measure of the mean angle between surface elements and a horizontal plane, and that, as a first approximation, valid for small angles, the two being related by the following equations:

$$e = I.\sqrt{\overline{E^2}} \qquad (2)$$

Where

$$E = \langle E_i \rangle \qquad (3)$$

$$E_i = 1 + \alpha_i \Big/ \sqrt{n^2 - 1} \qquad (4)$$

The bar indicates a temporal mean and the simbol $\langle\cdot\rangle$ indicates a spatial mean. e is the r.m.s. value of the signal; I,a multiplicative factor; α_i, the angle between the surface element i and the horizontal plane; and n is the refraction index between the gas and the liquid. It is interesting to note that e is related to a mean angle that is a result of two averaging operations, the first over the surface of the water and the second over time.

Correlation with Water Reoxigenation

The experimental data on reoxigenation and surface behavior were obtained by Roma (1988) in a water tank in which the turbulent movements were induced by oscilating grids with different mesh sizes.

Dimensional analysis was formulated, in the present study, in two differents combinations. The first involved two parameters and the second, three parameters which included additionally the mesh size. Good correlations for the experimental data were obtained in both the cases. The analysis with only two parameters was made to verify if the form of the curve so obtained was dependent on the mesh size. Figure 1 shows the dimensionless results of an experiment conducted for a given combination of mesh size and oscillation frequency. The dimensionless parameters used in this figure are

$$\pi_1 = K_2 T \qquad \text{and} \qquad \pi_2 = eT^{3/2} \Big/ \mu\, D^{1/2}$$

K_2 is the reoxigenation coefficient, μ is the viscosity of the liquid and D is the molecular diffusivity of the gas (oxygen) in the liquid (water).

All the experiments were analysed as illustred above. Regression equations were also obtained, showing a good degree of correlation between the nondimensional variables.
The method of analysis offers a means of studying physical surface properties related to transfer processes.

References

ROMA, W.N.L. (1988) - "Measurement of Turbulence Parameters at Water Surfaces and their Relation to the Reaeration Coefficient". Thesis submited to the São Carlos Engineering School, São Paulo, Brazil, 62p. (In portuguese).

ROMA, W.N.L. & GIORGETTI, M.F. (1990) - Abstract of paper proposed for presentation at the 2nd. International Symposium on Gas Transfer at Water Surfaces, September 11-14, 1990, Minneapolis, Minnesota.

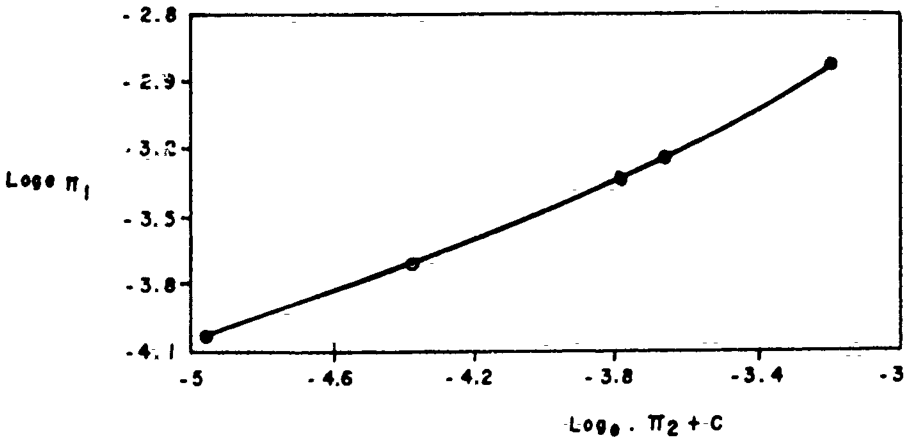

FIGURE 1 : π_1 PLOTTED AGAINST π_2 . C IS A CONSTANT WHICH INVOLVES POWERS OF μ AND D.

Measurement of Wave-Induced Turbulent Flow Structures Using Digital Image Sequence Analysis

Dietmar Wierzimok Institute for Environmental Physics,
University of Heidelberg, Im Neuenheimer Feld 366
D-6900 Heidelberg, West Germany

Bernd Jähne Scripps Institution of Oceanography A-030
La Jolla, CA 92093, USA

Introduction

The interplay between the wind-wave-driven turbulent flow structure close to a free water surface and molecular diffusion determines the gas exchange rate between atmosphere and oceans. Direct measurements of the turbulence from about one meter depth up to the mass boundary layer are one key to proceed knowledge about gas transfer. In conjunction with wave measurements it is the right tool to investigate the influence of waves on the gas exchange process which is one of the most demanding theoretical problems. The method is especially useful to investigate the turbulent patches generated by breaking waves and their influence on the gas exchange process.

Unfortunately, flow measurements close to a moving interface are technically very difficult. Basically, there are two approaches. Firstly, laser doppler anemometry (LDA) could be applied where the measuring position follows the water surface with an optical scanner. This technique has successfully been used by *Cheung and Street* [JGR 93, 14089-097, 1988] with regular mechanical waves but has the disadvantage that no spatial data are gained which are essential to measure the spatial and temporal scales of turbulent patches.

Flow visualization represent an alternative method to measure the turbulent flow close to the water surface. A lot of experimental information could be gained with this method (e.g. the papers of *Okuda et. al.* [J. Oceanogr. Soc. Japan, 32, 53-64, 1976]. Yet the problem here is the enormous work involved in the quantitative evaluation of the images

This paper combines classical flow visualization techniques with modern digital image sequence processing techniques. Thus a new experimental tool is ava..able which allows both Lagrangian and Eulerian analysis of the turbulent flow by automated particle tracking over long image sequences.

Experimental Set-Up

The experiments have been performed in the large circular wind-water tunnel at the Institute of Environmental Physics, Heidelberg University. The annular water channel of the facility has an outer diameter of 4 m, a width of 0.3 m and a maximum water depth of 0.3 m. As tracers for the turbulent flow spherical Latex-particles (polystryrol) have been used, with diameters ranging from $50 - 150\,\mu m$. Since its density is close to the density of water (1.05 g/cm^3) they show only low buoyancy effects and can be used over a long period of time. The particles are illuminated from below by a thin vertical along-wind oriented light sheet of 1.5 cm thickness which is generated by a linear halogen lamp and an optical projection system. Image sequences are taken with a CCD-video camera. The optical axis is oriented perpendicularly to the illuminated plane.

The video data are digitized and stored as binary images in the frame buffer of a PC-based image processing system with a spatial resolution of 512 x 512 pixels. An area of 9 cm by 13.5 cm was observed with a spatial resolution of about 0.2 mm.

Image Sequence Processing

The processing of the image data mainly consists of four steps:

- real time object segmentation
- water surface-particle-segmentation
- particle and water surface tracking
- transformation from image- to world-coordinates

The first two steps include the low level image processing to separate the particles from the background and to determine the water surface. The object segmentation (particles and water surface) reduces the grey value images to binary images in real-time (background to zero, objects to one) using a global threshold. Thus not only a few images can be recorded in real time but a whole sequence of up to 32 consecutive images.

The binary imagery contains particle traces as thin streaklines due to the continuous illumination of 40 ms and a thicker line representing the wavy water surface. This line is separated form the particle traces by use of a morphological opening operation. The direct measurement of the position of the water surface allows a direct determination of the position of the particles relative to the water surface.

The main step, the particle tracking algorithm automatically tracks a particle from image to image through the sequence. As a result, a chain of two-dimensional displacement vectors $\mathbf{u}_p(t_0 + n\Delta t)$ is obtained for every particle p, where n denotes the image number and Δt denotes the reciprocal video image frequency (25 Hz in Europe).

The algorithm uses physical as well as heuristic concepts. The basic idea is to make use of the special pattern of moving objects due to the interlaced video signal. A moving object first appears in odd, then in even lines of a single image. Consequently, all moving particles appear as interleaved patterns which allows an easy discrimination against resting objects. Furthermore it facilitates to find the corresponding particle in the consecutive half frame. In order to avoid faulty correspondences, an additional physical constraint is included. The acceleration between two consecutive particle velocities $\mathbf{u}_p(t)$ and $\mathbf{u}_p(t + \Delta t)$ should be lower than a certain threshold.

By a similar technique, the vertical velocity component of the water surface along the horizontal axis is calculated and later associated with the particles' velocity.

Finally, in order to allow transformation from image- to world-coordinates, the coefficients of the transformation matrix are estimated using a grid, positioned in the light plane for spatial calibration.

Results

Measurements of the two-dimensional velocity vectors at different wind speeds ranging from 0.5 to 6.4 m/s with maximum wave amplitudes of up to 6cm (trough to crest) reveal the advantages of area extended techniques.

Due to the tracking algorithm the velocity vectors are available in Lagrangian as well as Eulerian representation. A typical sequence has a duration of 1.3 seconds (32 images), includes 5000 vectors from 800 recognized particles and requires a computing time of about 4 minutes on a PC-AT-386. The mean distance between different particles has been 1 cm (40 pixels). Depending of the particles' velocities, up to 12 particles within an area of one square centimeter can be resolved.

The tracks, representing the time integrated particles movement, allow calculation of the particles position with subpixel accuracy. Thus, with the used imaging window a maximum error of the velocity estimate is about 2.5 mm/sec for binary images. Using grey value images the error can be reduced by about one order of magnitude.

To demonstrate the far-ranging possibilities of the new technique the obtained particle velocities from test measurements have been evaluated in different ways:

- Height dependent velocity distributions for two velocity component demonstrate the increasing influence of the orbital wave velocity towards the water surface. The most striking effect is the increasing skewness of the distribution.
- Lagragians particle paths are correlated with the water surface motion.
- Calculation of the kinetic energy of the flow turns out to be a good indicator for turbulent patches produced by instabilities of the surface waves.
- An interpolation technique is used to calculate a continuous velocity field with a spatial resolution of about the mean distance of the particles. The curl of this vector field also highlights highly turbulent regions in the flow.

Conclusions

The first results are encouraging and prove that a new experimental tool is available which will be used in the near future for systematic studies of the turbulent water flow close to the water surface in different wind-wave facilities.

Further technical improvements are envisaged. The accuracy of the velocity determination can be improved significantly by the use image processing hardware that allow the recording of long grey value instead of only binary image sequences. Yet it seems to be most important to extend the technique from 2D- to 3D-velocity measurements. One promising proposition is the use of stereo images.

Use of Fluorescence Techniques to Study the Time-Varying Concentration Close to an Interface

Leslie M. Wolff, Zi-Chao Liu and Thomas J. Hanratty

University of Illinois, Urbana, Illinois 61801

Gas absorption at the interface of a stratified gas-liquid flow is controlled by liquid velocity fluctuations close to the interface, within about 300 microns. The main theoretical problem is to identify the source of these fluctuations, to determine their properties and to relate mass transfer rates to the flow. One approach has been to argue that mass transfer can be defined in terms of cellular type eddies close to the interface with certain spatial and temporal characteristics (McCready and Hanratty, 1985). These eddies could originate from the wall; they could be generated by a shearing motion at the interface; they could be generated by shear stress variations at the interface associated with gas phase turbulence or with small wavelength waves.

One of the problems in establishing the credibility of such an approach is the difficulty of obtaining detailed information about the velocity field. An indirect approach, being pursued in this laboratory, is to determine the spatial variation of the concentration field close to the interface. Eddy models predict large spatial variations in the concentration of the diffusing species both in planes parallel and perpendicular to the interface. For example, suppose that oxygen absorption is controlled by an eddy motion at the interface as depicted in figure 1.

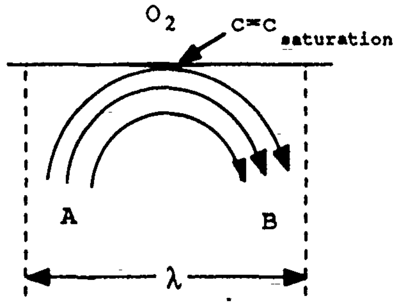

Figure 1: Eddy motion near mobile interface

This eddy is pictured to bring oxygen deficient liquid from A to the interface. It rapidly becomes saturated with oxygen at the interface and carries liquid that has large oxygen concentrations away from the interface at B. This type of considerations suggest that a measurement of the spatial variation in a plane close to the interface should reveal

a spatial variation which is characteristic of the eddy motion controlling oxygen absorption.

This paper describes a fluorescence technique which is being developed to obtain spatial variations near the interface. The experiment was motivated by the interesting work of Pankow et al. (1984) who used a fluorescent dye that is pH sensitive to study changes of CO_2 absorption with time. The technique being explored in this laboratory differs from this previous work in that it focuses on mapping out the spatial variations of the oxygen concentration rather that the bulk-averaged concentration. In addition the technique will use oxygen absorption, which is more easily studied in large flow systems.

Oxygen perturbs the excited states of the fluorescent dye, pyrenebutric acid (PBA) and quenches its fluorescent lifetime (Vaghan and Weber, 1970). Therefore, measurements of the lifetime of PBA can be used to determine oxygen concentration. The Stern-Vollmer equation gives the following relation for the fluorescent lifetime, τ, and fluorescent intensity F:

$$\frac{F_o}{F} = \frac{\tau_o}{\tau} = 1 + k[Q]$$

Here the subscript o indicates a measurement in the absence of oxygen, k is the quenching rate constant and Q is the concentration of the quencher.

In the experiment a PBA solution (10^{-5} M) is dissolved in water and the fluorescent intensity is measured by a scanning camera. The absorption spectrum of this system is such that it can be excited by light with a wavelength of 337 nm. It emits at a higher wavelength in the visible range.

The design of the experiment is depicted below:

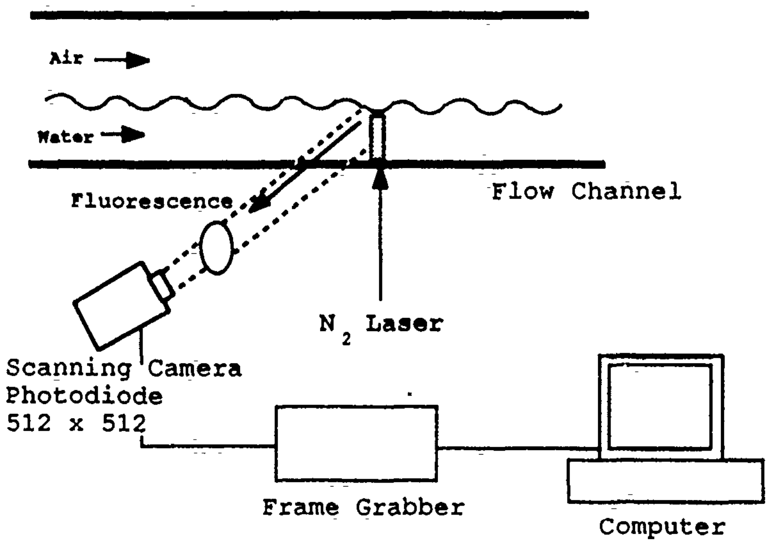

Figure 2. Laser Induced Fluorescence Experimental Set-up

It involves the illumination of the liquid by a thin beam of light or by a thin sheet of light originating from a nitrogen laser with a 250 kW peak power. The light comes from below the transparent rectangular enclosed channel through which the air and water are flowing. This avoids a number of problems associated with diffraction (if waves are present) that would exist if the light entered from the top of the channel. The light emitted by the fluorescent substance in a small region close to the interface is viewed at an angle from below the channel by a scanning camera with a 512 x 512 photodiode array. A discontinuity in the light intensity gives the location of the interface. The variation of the intensity of the light gives the instantaneous spatial variation of the dissolved oxygen.

The use of a beam gives single point variation of height (if waves are present) and the concentration variation, for fixed x and z, in a direction perpendicular to the interface, y. The use of a sheet of light allows the measurement of multipoint liquid height (if waves are present) and of the spatial concentration variation in the x,y or the y,z plane.

Advantage is taken of the fact that the emitted light is at a higher wavelength that the laser to remove effects of extraneous light from the laser (λ = 337 nm). This is accomplished by filtering all light with wavelengths below 370 nm before it reaches the detector elements. Also there is an advantage in using a pulsed light source because higher intensities and a clearer signal can be obtained.

Pyrenebutric acid is particularly amenable to this type of operation. There are a number of fluorescing substances which are quenched by oxygen. The usual fluorescent lifetime is of the order of 10-20 nsec. However, pyrenebutric acid has a lifetime of 100 nsec in air-saturated water solutions. This extra time during which diffusion processes may occur increases the volume of solution that influences the excited state of each pyrenebutric acid molecule from 100 to 1000 times over the volume that can affect the shorter lived molecules. This is why oxygen quenching in a pulsed signal can be studied with PBA, even though it has a negligible effect in most systems.

Initial work with a light beam in a non-flowing system is encouraging. Work in a flowing system (both with light beams and light sheets) will be reported at the symposium.

FIELD MEASUREMENT TECHNIQUES

Regional Estimates of Gas Transfer Using an Airborne System

R. Desjardins[1], H. Hayhoe[1], J.I. MacPherson[2] and P.H. Schuepp[3]

1. LRRC, Agriculture Canada, Research Section, C.E.F., Ottawa, Ontario.
2. NRC, Flight Research Section, Montreal Road, Ottawa, Ontario.
3. Department of Food Science and Chemistry, MacDonald College of McGill University, Ste-Anne-de-Bellevue, Quebec.

ABSTRACT

Recent advances in aircraft-based eddy correlation techniques offer airborne estimates as a possible tool for regional observations of transfer processes of water vapor, carbon dioxide and various trace gases. The limitations and advantages of such a measuring technique will be discussed. Flux measurements of water vapor and carbon dioxide obtained over Wetlands in Northern Ontario will be correlated to features such as surface temperature and vegetation indices (IR/R) in order to attempt to determine the areal extent represented by airborne flux measuremerts under different conditions and to assess recent advances in modeling techniques for footprint prediction. Indications of how such measurements could be used to study man's impact on the atmosphere will be presented.

TRACER GAS TRANSFER TECHNIQUE FOR SHALLOW BAYS

Edward R. Holley
Department of Civil Engineering
The University of Texas at Austin
Austin, TX 78712

Charles W. Downer
Espey Huston and Associates
P. O. Box 519
Austin, TX 78767

George H. Ward
Center for Research in Water Resources
The University of Texas at Austin
Austin, TX 78758

The tracer gas technique was originally developed in the mid-1960s for rivers to provide a means for directly measuring surface gas transfer for situations where reaeration was the primary transfer process of interest. In the method, a conservative tracer and a tracer gas with surface gas transfer characteristics similar to oxygen are simultaneously injected into the river. The two most commonly used gas and conservative tracer pairs are propane with Rhodamine WT and radioactive krypton with tritium. As the tracers move downstream, the concentrations of the tracer gas change due to dilution, mixing, and surface transfer, while the concentrations of the conservative tracer change due to only dilution and mixing. With simultaneous measurements for the two tracers, the conservative tracer can be used to compensate for the effects of dilution and mixing so that the surface transfer of the tracer gas can be isolated. Field techniques have been developed for narrow rivers where the concentration distributions are essentially one dimensional and for wider rivers with two-dimensional distributions. The techniques use either short-duration releases, giving tracer clouds which move downstream, or long-duration releases, giving steady-state tracer distributions. Little previous work has been done on developing field methods for determination of gas transfer coefficients for bays.

The tracer gas method has also been of interest in recent years in conjunction with determining volatilization rate coefficients for some types of volatile dissolved toxics. Although there is sometimes a need to know reaeration rates for bays, it was primarily the interests related to volatilization that prompted this research into the development of tracer gas techniques which can be used in bays. The research has used propane and Rhodamine WT as the tracers and has included both laboratory and field studies.

The laboratory part of the work has been directed at improving the methods used for measuring dissolved propane concentrations and at investigating the influence of salinity on the ratio of transfer coefficients for the tracer gas and other gases.

This paper emphasizes the field work, which has been the primary part of the work. The developmental field tests have been conducted in Lavaca Bay, which is a secondary embayment in the northerly section of the Matagorda Bay system on the Texas coast of the Gulf of Mexico. Astronomical tidal ranges in the Gulf of Mexico are typically 1 to 3 ft and vary between diurnal and semi-diurnal. In the field tests, the

propane is dissolved in the bay water by bubbling the gas through porous stone diffusers.

The first field tests were directed at evaluating the relative benefits of short- and long-duration injections. For long-duration injections, the travel time must be known for the samples which are collected for concentration determination. Both drogues and a second fluorescent tracer were tried for determining travel times. Neither method was satisfactory. Also, reversing tidal flows can cause the tracer plume to double back on itself. Thus, it was decided to use short-duration (15 to 20 minute) injections. During the tests it was observed that if vertical density gradients are present, the rising bubbles cause mixing of the heavier lower and lighter upper water and thereby cause the tracers to gradually sink below the surface. To prevent this problem, a special injection box was built to allow mixing of the tracers during the injection with only the water near the surface. The downward migration of the tracers then is due to only mixing and not density currents. The first tests were also used to determine the time for the tracers to become mixed in the vertical direction. In this bay, the tidally induced velocities are small (on the order of a few hundred feet per hour) and are less effective than wind-induced mixing. For water up to 6 ft deep and wind speeds up to 25 mph, the vertical mixing time varied in the range of approximately one to four hours.

The next sets of tests were aimed at developing methods of sampling the tracer cloud to obtain reliable and consistent results. The first plan was to mark spots in the cloud and to collect samples along vertical profiles at essentially the same relative positions in the cloud each time, with samples being collected at 45-minute to one-hour intervals. No satisfactory method was found for marking a part of the cloud. Thus, sampling is done at a variety of horizontal points in the cloud and also for different depths within the cloud. If data can be collected for st least six hours after the cloud becomes vertically mixed, this sampling method produces generally good results.

Most of the research has been directed at developing testing methods, but some limited quantitative results have been obtained. These results indicate that the surface gas transfer coefficients for a given wind speed for shallow bays are approximately two to four times smaller than would be predicted based on data from either the open sea or laboratory experiments.

From the Measurement of Mean Fluxes to a Detailed Experimental Investigation of the Gas Transfer Process at a Free Wavy Water Surface

Bernd Jähne
Scripps Institution of Oceanography
Physical Oceanogr. Res. Div., A-030
La Jolla, CA 92093, USA

Introduction

Conventional methods to determine the transfer velocity k of gas tracers across the air-water interface are based on mass balance methods of the gas tracer in the water body. As a consequence, the measured transfer velocities are integrated over large temporal and spatial scales. The time constant is in the order of hours in wind-wave facilities and days to weeks in the oceans.

Severe limitations result from these basic facts. In wind-wave tunnel studies, the gas exchange rate can be obtained only as a mean value integrated over the whole water surface of the facility, while the controlling parameters as friction velocity in the air, wave and water flow parameters are measured locally. Thus any parameterization of the measured air-water gas exchange rate becomes questionable if only one parameter changes strongly with fetch.

In large natural water bodies, especially in the oceans, a parameterization of the gas exchange rate is nearly impossible, since the controlling parameters, especially of the wind, are changing much faster than the gas exchange rate can be measured.

Thus the limitations of the conventional measurement techniques seem to be a major obstacle for a better understanding of the gas exchange process. Techniques which involve only the measurement of mean fluxes are obviously not an adequate experimental tool to investigate the mechanisms and parameters controlling the complex transfer processes across the aqueous mass boundary layer at a free water surface. Direct measurements from within the mass boundary layer including the concentration of the gas tracer, water velocities and waves are urgently needed. This paper is a first step in this direction introducing the controlled flux technique.

Instantaneous Transfer Velocities: The Controlled Flux Technique

Principle

The new technique is basically an inversion of the classical mass balance method. A controllable tracer flux density is forced onto the water surface and the surface concentration is monitored continuously. Consider a simple thought experiment. First, let the tracer flux be zero. Then the tracer concentration at the water surface is equal to the bulk water concentration. Now switch on a constant tracer flux density. Immediately, the tracer's concentration at the surface increases; eventually, it reaches an equilibrium value at which the incoming flux is equal to the flux across the boundary layer. In contrast to the mass balance method, the concentration changes are controlled by the time scale of the boundary layer which is in the order of seconds.

By switching the flux density j on and off, the concentration difference across the boundary layer Δc can be derived from tracer surface-concentration measurements. The transfer velocity is then determined by $k = j/\Delta c$.

Measuring the tracer surface concentration at a given constant flux actually monitors the instantaneous transfer velocity which is only spatially and temporally averaged by the characteristics of the used sensor. Moreover, the new technque applies concepts of linear system theory. The features of the "black box" mass boundary layer are investigated by "probing" the system with a known signal and observing its response, i.e. the surface concentration variation as a function of the frequency of the variation of the incoming flux density. In this way, the time constant ("surface renewal rate") can be measured directly. Using different

boundary layer models, theoretical transfer functions of the mass boundary layer have been calculated.

Realization

The controlled flux technique has been realized using heat as a proxy tracer. A system was built which can measure the transfer velocity remotely. It consists of a chopped infrared radiator to force a flux density onto the water surface and an infrared radiometer to measure the water surface temperature. The radiative transfer of the heat to the water surface shortcuts the high atmospheric resistance to heat transport to the water surface. The incoming radiation is absorbed within the first 20 μm of the water surface and almost entirely ($\approx$ 97%) transported across the aqueous boundary layer just as a gas tracer.

The only difference is that the Schmidt (Prandtl) number for heat is about a factor hundred lower than for gas tracers. Careful simultaneous measurements with both tracers however showed that the gas transfer rate can be determined from the measured heat transfer velocities with an uncertainty of less than 10%.

Results

Experiments were performed in different laboratory facilities, including a circular wind-wave tunnel at Heidelberg University, a linear facility at Karlsruhe University, and the large wind-wave flumes of Delft Hydraulics in Delft and de Voorst (partly within the VIERS experiment).

The influence of a number of parameters on the air-sea gas exchange rate has been studied, including the fetch in a range from 2–100 m, regular mechanical waves and thermal stratification of the air flow. These results are discussed in a second paper [*Jähne*, this issue].

Using different chopper frequencies to interrupt the infrared flux, the transfer function of the boundary layer was determined experimentally. While the experimental data agree in general with simple theoretical models, slight but significant deviations show up. A stochastic modeling of the transfer process seems to be necessary to explain these differences.

Finally, some results are discussed which highlight the specific possibilities of the constant flux technique: Direct measurement of the fluctuations of the transfer velocity and the influence of a single breaking wave on the gas transfer rate.

Measurements obtained at the Rhine and Neckar river in June 1988 demonstrate that the constant flux technique can also be applied in the field. The transfer velocities could be determined with a time resolution of four minutes. Thus a large number of measurements was obtained, which allowed to separate flow- and wind-induced gas exchange rates and to establish a simple model for the combined influence of both mechanisms.

Outlook and Conclusions

The controlled flux technique is a first step towards a more detailed investigation of the transfer processes across the aqueous boundary layer. It has sucessfully been used in wind-wave facilities and at rivers. The next step are oceanic measurements which will be performed in 1990 and 1991 at the Scripps Pier (California) and at the Noordwijk Research Platform in the North Sea. As an outlook it is discussed how the concept to control the flux density could be accomplished with gas tracers in wind-wave facilities.

Title Statistical Geometry of a Wind-Swept Sea

Authors Bryan R. Kerman and Lucie Bernier

Affiliations Atmospheric Environment Service
National Water Research Institute
Burlington Ontario Canada

Department of Mathematics and Statistics
University of Ottawa
Ottawa Ontario Canada

The active overturning of the wind-driven lake or ocean surface by breaking waves, or whitecaps, provides a finite volume of the atmosphere temporarily for gas exchange to the surrounding water. The hydrodynamical factors involved in the process include the number and size distribution of bubbles capable of partially dissolving or absorbing gas according to in-water gas concentrations, solubility and diffusivity. They further include the depth to which these bubbles can be delivered, and the number, size, and spatial distribution of the breaking events themselves. This work is directed primarily to addressing the question of understanding the spatial distribution of whitecaps as captured by aerial photography.

Considerable effort has been expended on estimating the fraction of the sea, or lake, which is at an given instant cover by either foam or actively entraining whitecaps or both. Also numerous articles have been written which attempt to relate such observations of whitecap coverage to the dynamics of a breaking wave field. In fact some very recent work has been directed at describing basic breaking wave geometry from wave dynamics. Implicit in all the observations and their comparisons with theoretical models is the accuracy and reliability of the observation technique. The most commonly employed method consists of photographing an ocean or lake surface, either from a ship or airplane, and plenimetering the areas on the developed films which have been identified as foam or whitecaps by some criterion.

Anyone who has the opportunity to sample a given area of a wind-swept sea, particularily one small enough to give adequate spatial resolution, will realize its enormous temporal and spatial variability, as well as the problem of identifying when the breaking wave is actively entraining and when it has become inert foam. The question is further compounded by changes in perceived activity depending on the lighting of the surface, say between bright sunny days and ones which are thickly overcast. Accordingly it seemed appropriate to attempt to develop an objective measure of whitecap activity, as well as one based on automatic extraction techniques so as to accumulate enough data to overcome questions of statistical representativeness. As it turned out just the attempt to develop an objective technique has led to an entirely new concept of the process.

The data for the study were taken over the wind-swept ocean off Halifax, Nova Scotia and over the Bay of Fundy, using a multi-spectral line scanner, mounted on a sufficiently robust and slow

flying DC3 aircraft. The experiment occurred over a span of 7 days in March 1984, when it was possible to capture breaking wave fields associated with estimated over-water wind speeds ranging from 9 to 19 m/sec on 9 occasions. The flight lines were chosen so as to correspond to at least an hourly average at a fixed point. They were flown as close to the sun's direction as feasible. The aircraft was flown at the critical height for contiguous scan lines for a given ground speed.

The multi-spectral scanner utilized a light path originating from the surface to a rotating mirror, through a prism and then onto separate optical channels and photodiodes. In all, 7 channels were recorded, between .57 and 1.64 um. The data were recorded on high density digital data tapes and then transfered to computer-compatible tapes in Ottawa by the Canada Centre for Remote Sensing. Unfortunately inexperience with the intense spiking associated with the signal from isolated breaking waves led to an overreaction in reducing the system gain thus leading to some unnecessary and unrecoverable loss of spatial resolution.

A catastrophic failure of on-board and surface mounted multi-spectral radiometers meant that the original concept of categorizing the surface imagery by its objectively measured reflectivity could not be followed. Various attempts to separate the background from the bubble-rich regions involving factor analysis, using the intensity at all channels, was unsatisfying because the resultant functions were invariably statistically unstable and unreliable. Initial attempts to utilize a spectral decomposition both by a Fourier and a principal components representation of the images promised no penetration of the identification problem and were abandoned.

However experience had shown that a technique was needed which accomodated both the statistical aspects of the intensity variation and the spatial aspects of the rare but significant bubble-rich areas. Just such requirements are central to the very recent and somewhat feverish application of statistical geometry, commonly referred to as fractal geometry. Initial studies, to be discussed, led to an estimate of the covering dimension by a variety of techniques. The results, while inherently interesting from a mathematical and hydrodynamical point of view in light of their possible relationship to ocean wave slope spectra, were somewhat disappointing from the applied point of view, that is how to differente between the elements constituting the field.

The estimated fractal dimensions did not appear to be a function of wind speed as expected, nor were they invariant to a thresholding operation. The later result was directly contrary to the assumed affine similarity with position or amplitude. However initial questions arising from the uni-fractal approach ultimately led to a better definition of the background (a Rayleigh process) and the identification of a distinctly non-cosine cross-scan variation which considerably aided further studies.

Accordingly a new approach was undertaken - that of multi-fractal analysis - in which the inherent (multiplicative) non-linearity of the field is accomodated at the outset. The method of moments and the associated Legendre transforms was utilized to calculate what we call the singularity spectrum. This function is

the fractal dimension of the support of sets which have singularities in their measure characterized by the Lipschitz-Holder exponent, as a function of this exponent. The loss of digital accuracy inherent in the lowering of the sytem's electronic gains and the threshold operation used against the pervasive background, conspire against confidence in the negative order of moments and perhaps in the covering dimension itself. However the information, or entropy, dimension and the correlation dimension, as well as dimensions to moment order about 10, appear to follow a Besicovitch-Cantor process with the spectral flux accumulating measure on the larger of the two non-trivial intervals.

A separate approach to translate such concepts to a workable identication of an image's sub-elements, through a spatial filtering for individual sub-sets based on their order of singularity will also be discussed. If time permits, an analysis of some simple and more commonly understood geometric properties, such as orientation and eccentricity of such connected sub-sets with a given order of singularity will be offered in an attempt to prove the contention that the order of singularity acts as a kinematic parameter akin to a non-dimensional, dynamically defined and measured numbers elsewhere (eg Richardson number) to characterize the wind-swept sea surface. As such it is a quantitative equivalent of the classical Beaufort scale, and one directly measureable through image-processing.

Methane Tracer Technique for Gas Transfer at Hydraulic Structures

John P. McDonald and John S. Gulliver

Research Assistant and Associate Professor
St. Anthony Falls Hydraulic Laboratory
Department of Civil and Mineral Engineering
University of Minnesota
Minneapolis, MN 55454 (612) 627-4600

Hydraulic structures have an impact in the amount of dissolved gases in a river system, even though the water is in contact with the structure for a short time. While water is flowing over . spillway bubbles become entrained in the water, creating more area for gas transfer. Because of this, the same transfer that normally would require several miles in a river can occur at a hydraulic structure.

It would seem natural to use oxygen to measure gas transfer at a structure. However, there are problems associated with using oxygen for measurement. Many times the dissolved oxygen (D.O.) levels are near saturation. The uncertainty associated with estimates of D.O. saturation concentration and with D.O. measurements then results in a large uncertainty in the gas transfer measurement. Also, if the reservoir is stratified it is difficult to predict withdrawl from the various layers with the required accuracy.

Methane is produced in the sediments as a byproduct of the anaerobic decomposition of organic material. Methanogenesis is the terminal process in a chain of decomposition processes and represents a major mechanism by which carbon and electrons leave the sediments. Methane transfer out of the sediments and hypolimnion is by vertical diffusion and, if enough methane is produced, by bubble ebullition (Strayer and Tiedje, 1978). Although methane is oxidized by bacteria to form carbon dioxide and water, the oxidation rate is insignificant over the short residence time of a hydraulic structure. If methane is present in measurable quantities it may prove to be an excellent in-situ tracer of gas transfer.

Transfer efficiency has been used to describe the amount of gas transfer at a structure (Gameson, 1957):

$$E = \frac{C_d - C_u}{C_s - C_u} \qquad (1)$$

where E is the transfer efficiency, C_s is the saturation concentration, C_u is the upstream concentration, and C_d is the downstream concentration. For dissolved gases like methane that do not have an appreciable concentration in the atmosphere, C_s is zero and E is given as:

$$E = \frac{C_u - C_d}{C_u} \qquad (2)$$

Transfer efficiency ranges from zero for no transfer to unity for complete transfer. This variable will be the result measured in this work. Oxygen and methane transfer measurements will be compared through a relationship developed by Gulliver, et al (1990) to index transfer efficiencies for one compound and temperature to another compound at a different temperature.

Field investigations were performed during the summer, fall, and winter to examine the potential use of methane as an in-situ tracer gas for the measurement of gas transfer at hydraulic structures. During an investigation samples were gathered upstream and downstream of the structure and the transfer efficiencies were calculated for oxygen and methane. The mid-winter sampling technique of Rindels and Gulliver (1986) was used to assure accurate oxygen transfer measurements. Various overflow weirs were investigated.

Thene and Gulliver (1989) developed a headspace measurement technique while using propane as a tracer gas for measuring transfer efficiency at hydraulic structures. This measurement technique was adjusted to compute methane concentrations. The measurement technique is also presented.

Methane was found in sufficient quantities for accurate measurements in all but one river/reservoir, where sulfate reduction inhibited the production of methane. Methane was generally unstratified upstream except under ice cover, providing an excellent tracer for gas transfer. The exception was under ice cover, when methane tends to be stratified and accurate transfer efficiency measurements were difficult. Under ice cover, however, the mid-winter oxygen measurements will produce accurate transfer efficiency measurements.

The stratification of methane under ice cover created difficulties with the comparison of oxygen and methane measurements because the field conditions required to accurately measure the transfer of the two gases seems to be mutually exclusive. A technique using oxygen, methane, and temperature measurements with a selective routine (Davis, et al, 1987) was developed to compare oxygen and methane transfer measurements. Oxygen and methane transfer efficiencies, after adjustment for diffusivities, were comparable at a given structure except when the entrained air bubbles were pulled to a depth in the tailwater causing the bubbles to experience a higher pressure. Since the partial pressure in air determines saturation concentration of atmospheric gases, the saturation concentration of oxygen is higher as the bubbles are pulled through the stilling basin. Thus an "effective saturation" concentration must be determined for oxygen at hydraulic structures with a tailwater.

References

Davis, J.E., J.P. Holland, M.L. Schneider, and S.C. Wilhelms, 1987. "Select: A Numerical One-Dimensional Model for Selective Withdraw," Report E-87-2, U.S. Army Engineer Waterways Experiment Station, Vicksburg, MS.

Gameson, A. 1957. "Weirs and the aeration of rivers," Journal of the Institute of Water Engineers, 11, 447-490.

Gulliver, J.S., J.R. Thene, and A.J. Rindels, 1990. "Indexing Gas Transfer in Self-Aerated Flows," Submitted to the Journal of Environmental Engineering, ASCE.

Rindels, A.J., and J.S. Gulliver, 1986. "Air-Water Oxygen Transfer at Spillways and

Hydraulic Jumps," Water Forum '86, ASCE, New York, NY.

Strayer, R.F., and J.M. Tiedje, 1978. "In situ methane production in a small, hypereutropic hard-water lake: Loss of methane from sediments by vertical diffusion and bubble ebullition," Limnology and Oceanography, 23, 1201–1206.

Thene, J.R. and J.S. Gulliver, 1989. "Gas Transfer at Weirs Using the Hydrocarbon Gas Tracer Method With Headspace Analysis," Project Report 273, University of Minnesota, St. Anthony Falls Hydraulic Laboratory, Minneapolis, MN.

ON THE SOLUBLE SOLID FLOATING PROBE METHOD FOR THE INDIRECT DETERMINATION OF GAS-TRANSFER COEFFICIENTS

Harry E. Schulz
Marcius F. Giorgetti

School of Engineering at S.Carlos
University of S.Paulo, Brazil

Analytical and experimental results are presented on the relation between the gas transfer through a gas-liquid interface and the mass transfer (dissolution) from a floating solid probe to the same liquid. References (1) through (6) are previous reports on the same technique.

The experimental results reported are for the absorption of oxygen and the dissolution of oxalic acid in water; they confirm the more general theoretical predictions. Experiments were run in a tank with agitation provided by a propeller, a duplicate of the apparatus described by Rainwater and Holley (7), and in a 20 m long channel specially designed to operate in a loop without interruption of the water free surface.

The basic analytical assumption and results for the modeling of the dissolution of solid probes are:

$$\dot{M} = hA(S_s - S) = hA\ \Delta S \qquad (1)$$

$$\frac{M}{M_o} = 1 - \frac{v_s t}{L_o} \qquad (2)$$

$$\frac{v_s}{h} = \frac{\Delta S}{\rho_s} \qquad (3)$$

$\dot{M}$ = time rate of solid mass dissolution.
h = convection mass transfer coefficient.
A = solid-liquid contact surface area.
S_s = saturation concentration of solid in liquid.
S = concentration of solid in liquid.
M = mass of solid at time t.
M_o = initial mass of solid.
L_o = initial tickness of solid.
v_s = velocity of dissolution; volume flux from solid to dissolved phase.
ρ_s = mass density of solid.

The basic analytical assumption and result for the modeling of gas transfer are:

$$\frac{dC}{dt} = \frac{K}{H}(C_s - C) = \frac{K}{H}\Delta C \qquad (4)$$

K = gas mass transfer coefficient across gas-liquid interface.
C_s = saturation concentration of gas in liquid.
C = concentration of gas in liquid.
H = mean depth of liquid.

$$\frac{v_g}{K} = \frac{\Delta C}{\rho_g} \qquad (5)$$

v_g = gas volume flux across gas-liquid interface.

ρ_g = mass density of gas in gaseous phase.

Analyses of the two processes indicate that the ratio v_s/K can be expressed as the product of two separable functions, the first involving thermodynamic variables, while the second is related only to the fluid-dynamic parameters:

$$\frac{v_s}{K} = f\ (T,\ p)\ .\ g\ (\text{structure of turbulence}) \qquad (6)$$

Figures 2, 3 and 5 illustrate with data obtained at the agitated tank, with eight different speeds, the validity of equations 2, 3 and 4, respectively. Figure 5 is a log-log plot of expression 6 with data from the agitated tank at the channel; it indicates that the function g appears to have characteristics of an universal function, irrespective of the geometry of the hydraulic system.

References

(1) Giorgetti, M.F. and Giansanti, A.E. "Avaliação do Nível de Turbulência em Águas Correntes e sua Correlação com o Coeficiente de Reaeração Superficial"; Proceedings, XII ABES Congress, Camboriú, SC, Brazil, Nov. 1983.

(2) Schulz, H.E. "Investigação do Mecanismo de Reoxigenação da Água em Escoamento e sua Correlação com o Nível de Turbulência junto à Superfície". M.Sc. thesis, University of Sao Paulo, EESC, S.Carlos, Brazil, 1985.

(3) Giorgetti, M.F. and Schulz, H.E. "Contribuição para a Determinação do Coeficiente de Reoxigenação Superficial em Corpos D'Água - I". Proceedings, II Latinamerican Congress of Heat and Mass Transfer, vol.3: 1687-1697, S.Paulo, Brazil, May 1986.

(4) Giorgetti, M.F. and Giansanti, A.E. Evaluation of Turbulence Level in Flowing Water Near The Air-Water Inteface; Paper presented in the International Symposium on Gas Transfer at Water Surfaces, Ithaca, NY, USA, 1983.

(5) Schulz, H.E. and Giorgetti, M.F. "Medida Indireta do Coeficiente de Reoxigenação de Águas Naturais - Modelo Matemático para a Velocidade de Desgaste de Sondas Solúveis". Proceedings, I Brazilian Symposium of Heat and Mass Transfer, 174-187, Campinas, Brazil, July 1987.

(6) Bicudo, J.R.P.W. Measurement of Reaeration in Streams. Ph.D. thesis, University of Newcastle upon Tyne, England, April 1988.

(7) Rainwater, K.A. and Holley, E.R. Laboratory Studies on the Hydrocarbon Gas Tracer Techniques for Reaeration Measurement. Tech. Report, CRWR, University of Texas, Austin, December 1983.

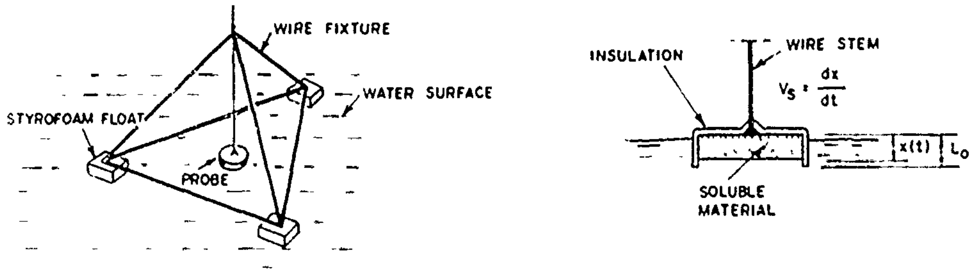

FIGURE 1 - SOLUBLE SOLID FLOAT GENERAL ARRANGEMENT AND DETAIL

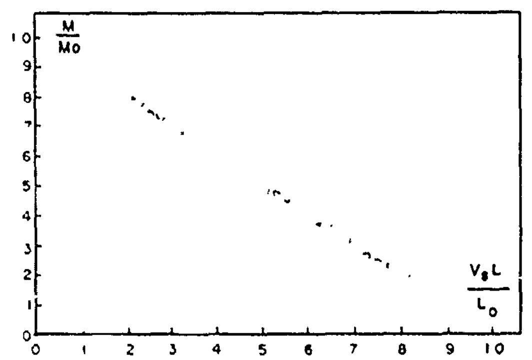

FIGURE 2 - LINEAR TIME VARIATION OF SOLID MASS WITH TIME .

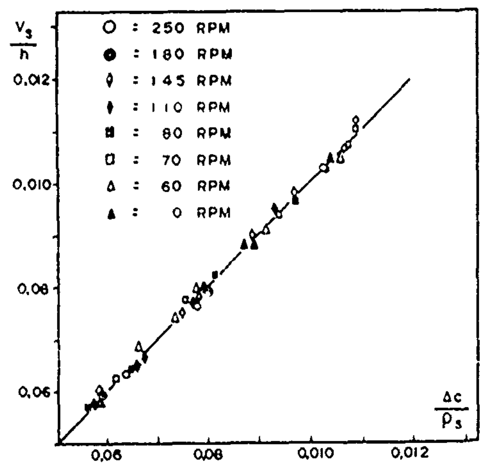

FIGURE 3 - DATA VALIDATION OF EQUATION 3 .

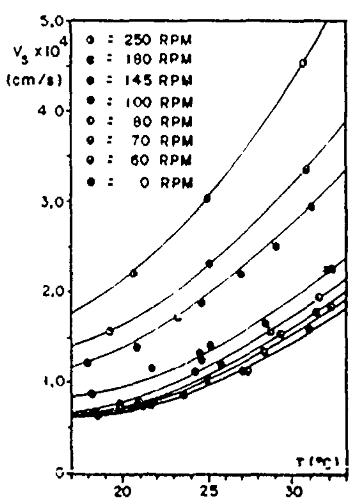

FIGURE 4 - DATA FOR DISSOLUTION OF SOLID PROBE (BENZOIC ACID) IN AGITATED TANK.

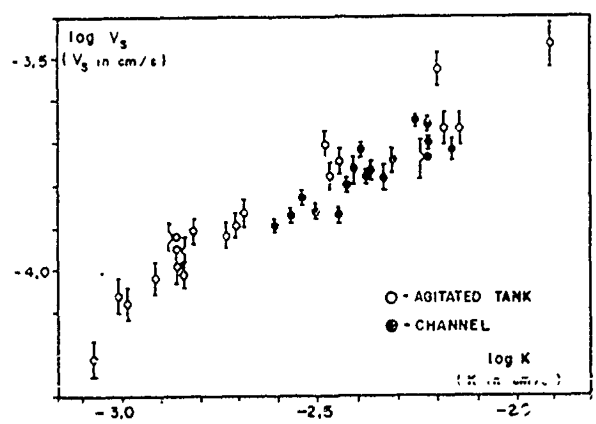

FIGURE 5 - PLOT OF log V_s vs log K . BARS INDICATED CONFIDENCE INTERVALS OF 95 % .

Relationship between Gas Transfer and Radar Backscatter from the Water Surface

R. Wanninkhof[1], L.F. Bliven[2], and D.M. Glover[3]

[1]Lamont-Doherty Geological Observatory of Columbia University, Palisades N. Y. 10964

[2]NASA Goddard Space Flight Center, Wallops Island, VA 23337

[3]Woods Hole Oceanographic Institute, Woods Hole, MA 02543

To determine short term gas fluxes across the air-water interface it is useful to parameterize gas transfer velocities to environmental forcing functions. Attempts to relate gas transfer to wind speed over the ocean has not been very successful because a sensitive technique to measure short term gas fluxes is not available, and because factors other than wind speed influence gas transfer. Turbulence near the surface controls the gas transfer velocities. Waves, in particular the high frequency part of the wave spectrum, can be thought of as a manifestation of this turbulence. Any parameter that yields information about this turbulence can be potentially useful to estimate gas transfer rates.

Radar backscatter is determined for a large part by Bragg scattering from the capillary and capillary-gravity waves with wave lengths of 0.5 to 5 cm (depending on the frequency of the radar unit). Scatterometers have been mounted on aircraft and on a satellite, and used to estimate wind speeds over the ocean. We have investigated if gas transfer velocities can be related to radar backscatter. We hypothesize that these parameters are better correlated than gas transfer to wind speed since factors that interfere in the backscatter wind speed relationship such as surface slicks, water temperature, and air boundary layer stability, influence both backscatter and gas transfer.

The experiments to study gas transfer velocities and radar backscatter were performed in a 18 m long wind-wave tank in Wallops Island, VA and in a 100 m long tunnel in Delft, The Netherlands. Gas transfer velocities of sulfur hexafluoride, methane, and nitrous oxide were determined by measuring the concentration decrease with time of the supersaturated gases in the water. Backscatter values from the surface were obtained from low powered radar units positioned 1 meter above the surface at an incident angle of 30°. For the Wallops Island experiment the 36 gHz unit, operated in VV polarization, was pointed directly upwind. For the Delft experiment two radar units transmitting at 13.5 and 36 gHz were rotated a full 360° to obtain directional response. We performed experiments in which gas transfer and radar backscatter were determined for different wind speeds. In addition we executed several runs in which mechanical waves were generated with a ram at different winds. Previous studies have shown that mechanical waves enhance gas

transfer causing the good correlation between gas transfer and wind speed found in most wind-wave tank studies to break down. We anticipated that the radar backscatter also would change under such conditions, perhaps indicating that the gas transfer could be better related to radar backscatter than to wind speed.

The experiments in Wallops Island showed that gas transfer and radar backscatter increased with increasing wind speed. The influence of mechanical waves of 2.5 Hz on backscatter varied with wind. At low winds a significant increase in backscatter was evident but the enhancement decreased with increasing wind speed. Gas transfer velocities showed a similar trend.

In the Delft experiment, average backscatter and gas transfer increased over a range of friction velocities from 15 to 100 cm/s (wind speeds of 4 to 20 m/s). No significant differences between the two radar units were observed in either the HH or VV polarization except that the response of the 36 gHz unit appeared to reach a plateau at high friction velocities. A relationship of the form $k = a\ 10^{b\ A_0}$, where k is the gas transfer velocity, A_0 is the average directional radar response, and a and b are constants fits the data well. Figure 1 gives the least squares fit to this relationship for the wind-only cases for the 13.5 gHz unit in HH polarization.

The gas transfer velocity increased with mechanical waves. Regular 0.4 Hz and 0.7 Hz waves were created with low (about 10 cm peak to peak) and high (about 25 cm peak to peak) amplitudes. The results were similar to the work at the Wallops Island tank in that at low wind speeds gas transfer and radar backscatter increased significantly. The influence of the 0.4 Hz waves became less at higher winds for both parameters. The 0.7 Hz large amplitude waves gave the largest increase in gas transfer. The radar returns were influenced to a lesser extent by mechanical waves than the gas transfer values. This caused most of the runs with mechanically generated waves to fall above the wind-only cases in the relationship of gas transfer versus backscatter (see Figure 1).

Both tunnel studies clearly show that backscatter and gas transfer velocities are closely correlated. This indicates that both parameters are influenced by the wave field. These first results relating gas transfer to radar backscatter are very encouraging and warrant a similar study in the natural environment.

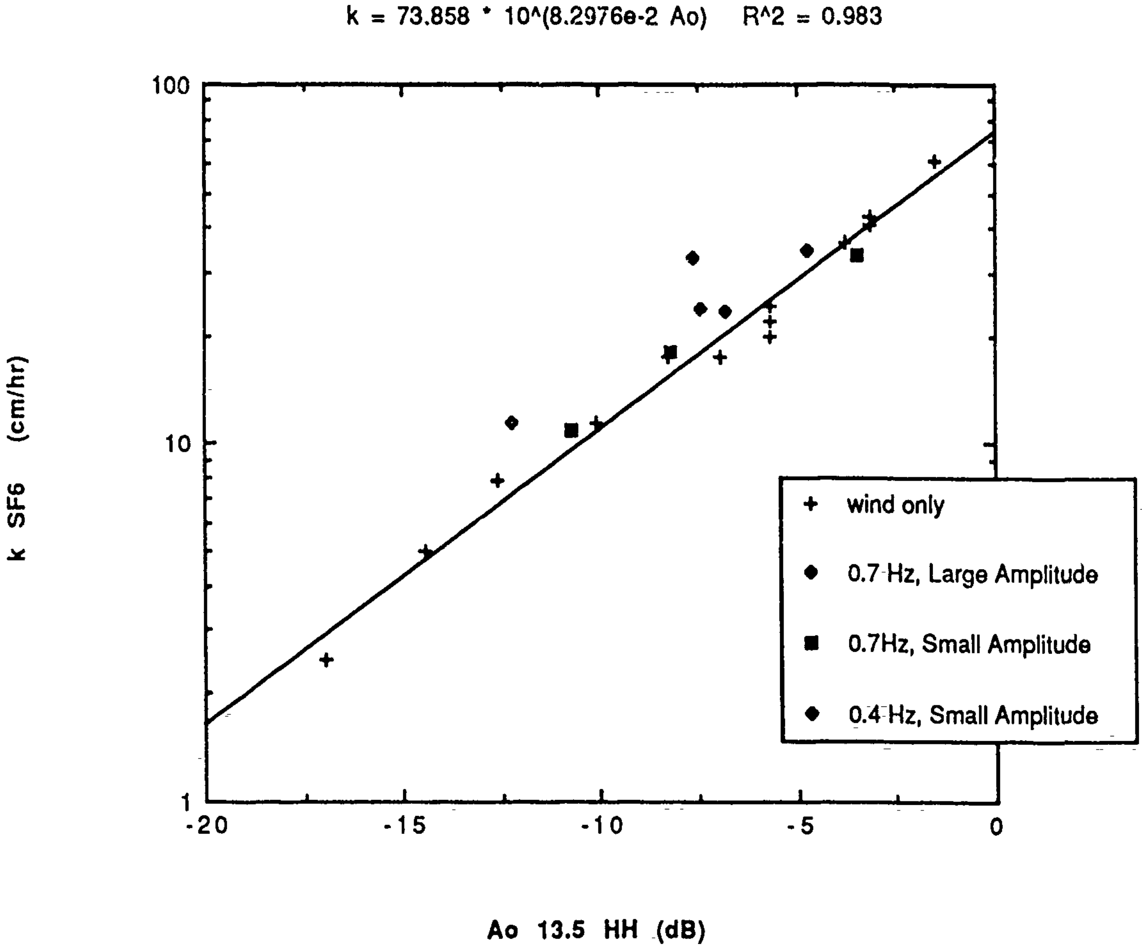

Figure 1. Relationship between the gas transfer velocity and average radar backscatter return, A_0 for the 13.5 gHz radar in HH polarization. The plus symbols are for the wind-only cases. The solid diamonds are for the wind and mechanical wave cases for large amplitude waves generated with 0.7 Hz frequency. The solid squares are for small amplitude waves at 0.7 Hz. The open diamonds are for small amplitude waves at 0.4 Hz. The line is a least squares exponential fit between gas transfer velocity and radar backscatter for the wind-only cases.

DEVELOPMENT OF A GAS CHROMATOGRAPHIC PROTOCOL FOR THE MEASUREMENT OF KRYPTON GAS IN WATER AND DEMONSTRATION OF ITS USE IN STREAM REAERATION RATE MEASUREMENTS

Raymond C. Whittemore, PhD

National Council of the Paper Industry for Air and Stream Improvement, Inc. (NCASI), Tufts University, Medford, MA 02155

Direct measurement of reaeration rates using inert tracers has a long history dating back to the late 1960s. The tracer method which appears to produce the most accurate results is the radioactive technique developed and reported by Tsivoglou in the 1967. This method involves the simultaneous release of three tracers: krypton-85, tritium, and a fluorescent dye. Because of the costs and potential hazards of using these tracers, other tracer techniques have been developed which do not use radioactive materials. These methods have been discussed by Rathbun in 1975. Unfortunately, not all researchers agree on the accuracy of these techniques and they have yet to replace the radiotracer technique as the definitive method.

In 1983-84 NCASI cooperated in a project sponsored by the American Society of Civil Engineers(ASCE) designed to standardize methods for measuring oxygen transfer in wastewater treatment plants. The ASCE project was funded by EPA and managed by the ASCE Committee on Standards via its subcommittee on Oxygen Transfer Measurement. As a result of this cooperative work, NCASI demonstrated field protocols for dosing and sampling for krypton. The krypton isotope was non-radioactive and measured using mass spectrometric isotope dilution. This measurement technique was demonstrated to be highly precise with errors less than 1% for a wide range concentrations in wastewaters.

The basic krypton analytical method consisted of a preparation process gas chromatographic procedure followed by an isotope dilution mass spectrometric technique employing a vacuum cleanup. The isotope dilution technique used a carefully premeasured Kr-78 spike for quantification. The liquid samples were placed inside a unique bottle opener/gas extractor along with the spike material. The dissolved gases from the sample and the spike were vacuum processed through cold traps, a hot titanium furnace and a gas chromatograph to further isolate the krypton fraction. The isotopic ratio of the krypton fraction was then measured on a Nier type mass spectrometer, comparing the ratio of Kr-78(mostly from the spike) to the total Kr-80 to 86(mostly from the sample). From this ratio, and the quantification of the spike, the exact amount of krypton in the sample was calculated.

The significance of this analytical method discussion to the current problem is in the gas chromatograph portion. The GC was added to the processing loop to affect a gross separation of the krypton gases from other noble gases that were present. If the analytical sensitivity of the GC portion could be significantly increased, quantification of krypton could be made directly with the GC. The major advantage would be that the mass spectrometric portion of the analytical train could be eliminated. Since this portion was the most sophisticated and required more highly trained operating personnel, the utility

of the measurement protocol would be greatly enhanced. Initial equipment costs as well as routine operating expenses would be reduced. The net result would be that more krypton tracer studies could be performed at relatively low cost relative to the krypton radiotracer procedure. More significantly, the hazards and concerns of working with radio tracers would be eliminated.

The objective of this work was: (a) to investigate the feasibility of using a gas chromatographic(GC) technique for the measurement of a non-radioactive krypton gas in water, (b) to develop the appropriate gas handling and cleanup apparatus required, and (c) to demonstrate that current GC technology would provide sufficient sensitivity to conduct reaeration measurements on small to medium size streams (10 - 200 cfs).

Partial funding for this work was obtained via a subcontract with Technical Resources, Inc., Rockville, MD and the U.S. Environmental Protection Agency (Contract No. 68-03-3305). The method development work was performed by Dr. Daniel J. Krause, Senior Research Associate, Department of Physics, Amherst College, Amherst, MA.

STREAMS/RIVERS

Title: Measurement of Stream Reaeration Rate Coefficients Using Propane Gas For A Wasteload Allocation

Author: Brian F. Friedmann[1]; Frederic C. Blanc[2]

Affiliation:
[1]Environmental Engineer, Department of Environmental Protection, Massachusetts Division of Water Pollution Control, Westborough, MA 01581;

[2]Professor, Department of Civil Engineering, Northeastern University, Boston, MA 02115.

In order to calculate the waste assimilative capacity of a stream for cost effective waste load allocation purposes, an accurate determination of the reaeration rate coefficient, K_2, is essential. In most instances in the past, a K_2 for a particular situation has been determined through the use of one of a number of predictive equations developed by researchers using a variety of methods under a wide range of conditions. Whether or not the chosen predictive equation accurately reflects the actual K_2 is open to question. A more accurate, site-specific K_2 can be obtained economically and safely using a propane gas tracer technique developed over the last decade primarily by the United States Geological Survey (USGS).

Gas tracer techniques represent an indirect method of determining K_2 based on the stable relationship between the gas exchange characteristics of the tracer gas and oxygen from a solution. Tsivoglou advocated the gas tracer technique in 1965 using radioactive tracer gases. The use of radioactive material as a tracer, however, presents both operator and public safety concerns and involves rigorous licensing requirements. In searching for an alternative tracer, Rathbun conducted laboratory and field experiments which led to the use of propane as a tracer gas. Rathbun's modified general hydrocarbon method has been extensively researched by the USGS for its accuracy and applicability.

The general field technique and basic analysis involved are described by Holley and Yotsukura and are essentially as follows for a one-dimensional stream. A continuous injection of commercially available propane through a system of one or more diffusers into the water column results in a steady state concentration downstream of the injection site. Desorption of the dissolved propane will occur according to first order kinetics. Time of travel between sampling sites is determined using an instantaneous release of Rhodamine WT dye as a tracer. Flow measurements at each sampling site are taken at least once and stage readings should be maintained throughout the study duration. Collection of propane samples at successive downstream sites commences after steady state conditions are obtained as indicated by the passage of the Rhodamine WT dye cloud using the fluorometer. Based on the data collected, a preliminary K_2 is calculated for input into a reiterative equation to calculate the final K_2 which is then temperature corrected as necessary. The relative error in the determination of K_2 is calculated based on estimated relative errors in measured gas concentrations, stream flow, and the number of respective measurements of each.

Using the steady state propane gas tracer technique, three field tests to determine K_2 were made on a 3280 foot reach of the upper Assabet

River. The upper Assabet River, located in Westborough, Massachusetts, has a drainage area of about 10 square miles above the test area. Flow is moderated by a flood control impoundment 1 mile upstream from the test reach. The test reach began approximately 150 feet upstream of the discharge of the Westborough WWTP. The test reach is generally straight due to a channelization effort earlier in the century, 15-20 feet in width, with a slope of 2.4 feet/mile, and a maximum cross-section depth of 3 feet. There is, however, a short riffle reach of approximately 100 feet underneath a highway. Stream flows for the study reach ranged from 6.20-7.26 cfs, 2.98-4.33 cfs, and 1.33-3.70 cfs for the May, August, and October runs, respectively. Time of travels were 3.33 hours, 6.29 hours, and 5.17 hours. Mean reach velocities were 0.27 fps, 0.14 fps, and 0.18 fps. There did appear to be some inexplicable inconsistency for the flows, travel times, and velocities between the August and October runs.

During the three field tests propane concentrations at the sampling sites ranged from 25 to 230 mg/l. Sampling was done at each site for a period of two hours at half-hour intervals to verify steady state conditions. The propane gas samples were analyzed by an USGS laboratory. Final calculations produced K_2s in the range of 2.59 to 5.47 day^{-1} (20^{o}C, base e). Relative errors ranged from 9.2 percent to 15.1 percent.

Over the flow ranges observed, the K_2 increased with flow. The results were not as clear when time of travel or flow velocity were considered due to the inconsistency noted above.

The K_2s obtained were compared with the results of predictive equations and with the K_2s used for the original wasteload allocation. A comparison of the study's K_2s to those calculated by 15 different predictive equations found absolute percentage differences ranging from 2.6% to 92.6% with the majority greater than 30%. Notably, 34 of the 45 predicted K_2s were less than the field-determined K_2s. None of the predictive equations gave consistently good results over the range of conditions for the three studies although this may, in part, be due to the discrepancy between flow and time of travel as noted above.

The K_2s used in the original wasteload allocation were based on Churchill's equation. The K_2s obtained from the study were up to three times higher than those calculated from Churchill's equation. Using a conservative K_2 suggested by the study, 5.00 at 20^{o}C, the wasteload allocation was rerun. While the original wasteload allocation required a level of treatment considered advanced secondary, 10 mg/l BOD5 and 1 mg/l NH_3-N, using the higher K_2 indicated that the treatment level could be relaxed significantly although it still indicated the need for better than secondary treatment (30 mg/l BOD5, approximately 6/mg/l NH_3-N).

Using the propane gas tracer technique to more accurately determine a site-specific K_2 can result in the construction of more reliable models leading to better protection of the in-stream environment and a more refined estimate of the degree of treatment required at wastewater treatment plants. While conditions in this study were assumed to be one-dimensional, the methodology has been used, with adaptations, under two-dimensional conditions.

Percentage Difference Between Predictive Equation and Study Result*

Predictive Equation	May	August	October
1. O'Conner & Dobbins: deep (1958)	-16.8	-15.1	23.6
2. O'Conner & Dobbins: shallow (1958)	-7.1	3.8	68.3
3. Churchill et al (1962)	-61.0	-78.2	-51.9
4. Owens et al I (1964)	2.6	-33.1	47.7
5. Owens et al II (1964)	4.6	-33.1	44.7
6. Langbein & Durum (1967)	-73.1	-84.4	-68.8
7. Isaacs & Gaudy (1968)	-70.9	-83.6	-65.3
8. Negulescu & Rojanski (1969)	-47.0	-62.8	-38.0
9. Bennett & Rathbun I (1972)	-5.1	-20.8	46.4
10. Bennett & Rathbun II (1972)	8.0	-24.4	56.4
11. Bansal (1973)	-72.8	-79.7	-61.9
12. Cadwaller & McDonnell (1969)	-48.3	-56.1	-26.7
13. Krenkel & Orlob (1962)	-9.7	-13.3	27.2
14. Tsivoglou & Neal (1976)	-79.3	-84.6	-78.9
15. Tsivoglou & Neal (1972)	-89.8	-92.6	-89.4

* Percentage difference calculated as:

$$\frac{\text{(predictive equation)} - \text{(study result)}}{\text{(study result)}} \cdot 100$$

Comparison of Study, Wasteload Allocation Model, and Northeastern Reaeration-related Data and K_2s

Data Source	Q cfs	H feet	V feet/sec	W feet	Time of Travel hours	K_2 20°C day^{-1}	K_2 Calculated by
Study:							
May 1986	6.20- 7.26	1.30	0.274	20.4	3.33	5.47	propane tracer[2]
August 1986	2.98- 4.33	1.56	0.145	19.1	6.29	3.90	propane tracer[2]
October 1986	1.33- 3.70	1.14	0.176	18.4	5.17	2.59	propane tracer[2]
Model:							
June 1979	12.32-31.93	2.75	0.435-0.601	14-16	2.32	1.871-2.200	Churchill[1]
August 1979	4.82- 8.48	2.25	0.197-0.240	13-14	5.42	1.701-1.879	Churchill[1]
7Q10y low flow	13.17-14.06	2.63-2.25	0.362-0.371	14-15	3.20	1.830-2.024	Churchill[1]
Northeastern:							
8/20/73	8.8 - 9.1	0.685-0.610	1.066-1.292	12-11	1.80[4]	7.37 -3.68	Tsivoglou[3]
9/11/73	2.0 - 2.2	0.280-0.204	0.594-0.767	12-11	3.09[4]	8.98 -5.07	Tsivoglou[3]

Note: Where a data range is given for a particular parameter, it indicates that more than one measurement or more than one calculation was made over the study reach.

1. $K_2 = 12.9 \cdot V^{0.5} H^{-1.5}$
2. results of this study
3. $K_2 = 0.054 \cdot$ h/(time of travel)
4. calculated from Northeastern University report (Blanc and O'Shaughnessy, 1973)

Propane Concentration vs. Time

August 6, 1986

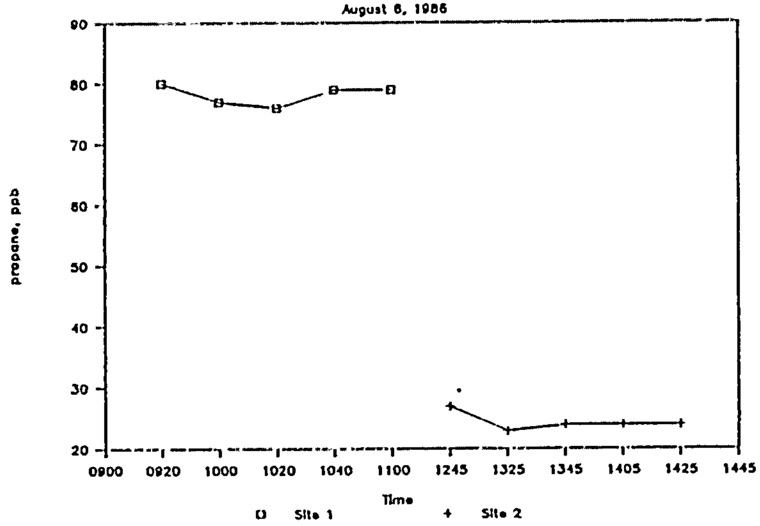

Sensitivity Analysis (STRM7A model)

K2 = 5.86 @ 26.67C

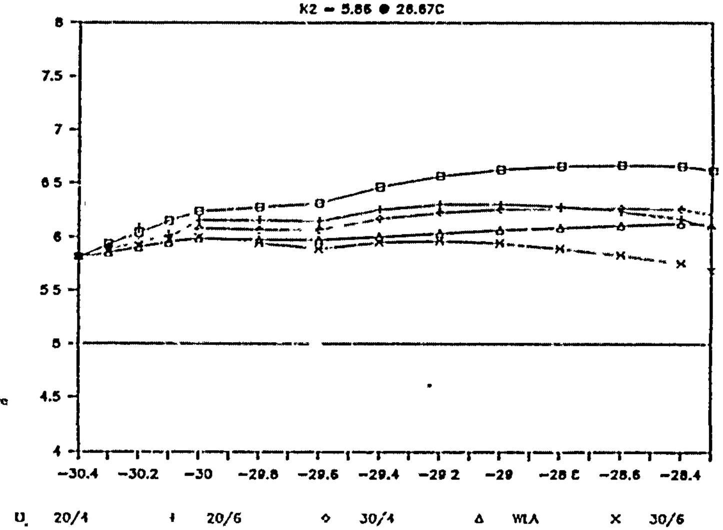

Dissolved Oxygen And Woody Debris: Detecting Sensitive Forest Streams

George G. Ice

National Council of the Paper Industry for Air and Stream Improvement, Inc.

The concentration of dissolved oxygen in forest streams is important for stream organisms including fish. During the Alsea Watershed Study in coastal Oregon (begun in 1959), surface and intergravel dissolved oxygen concentrations were reduced to 2.5 and 1.3 mg/L respectively, following harvesting on the watershed of one small stream. Factors contributing to the low dissolved oxygen for this stream included removal of shade near the stream, introduction of fresh slash, and possibly a decreased reaeration rate. These results led to forest practice rules which maintain shade over and keep organic debris out of streams.

In recent years there has been an increased awareness of the role of large woody debris in providing stream structure and habitat for fish. Recent changes in forest practices rules for Washington, Oregon, and Idaho require that trees be left to provide not only shade but also future sources of woody material for streams. This reverses a trend in stream "enhancement" activities which had resulted in removal or modification of both fresh slash and also large woody material in streams. In some cases, windthrow has resulted in a rapid delivery to streams of trees left for shade and recruitment, with consequent decline in water quality and criticism of the stream management zone policies.

A series of studies was conducted at Oregon State University to determine how dissolved oxygen concentrations could be protected, both in surface and in intergravel water. Stream sensitivity to surface water declines in dissolved oxygen are largely related to the reaeration-rate coefficient, potential for organic contact, and potential for stream heating. Streams with large reaeration coefficients are less susceptible to detrimental oxygen declines.

Slow moving streams that are susceptible to prolonged contact with organic material or heating due to direct solar radiation are potentially sensitive to oxygen deficits.

A study was conducted of seven small streams in western Oregon during low-flow conditions (0.03-0.56 cfs) to develop a semi-empirical equation relating hydraulic conditions with the reaeration rate. Relatively homogeneous stream reaches in typical forested watersheds were identified and hydraulic parameters measured. Of particular concern was the treatment of rapidly varied (nonuniform) flow and especially the presence of hydraulically or thermally isolated pools in the stream reaches. Streams were artificially deaerated using a constant injection of sodium sulfite. The equation developed for the reaeration coefficient (K_2):

$$K_2 = 37 \cdot (E_D^{1/2}/H_D^{2/3})$$

is consistent with theoretical descriptions of gas exchange phenomena. The highest regression coefficient was obtained when large pools were removed from the segment hydraulic parameter calculations. As the rate of energy dissipation increases in a stream segment, the turbulence in the segment also increases. In this study the maximum energy dissipation rate (E_D) was calculated from the apparent maximum velocity and stream slope. Streams with steep slope and high velocities have high E_D values. Turbulence promotes an increase in the liquid-atmosphere interface area (surface roughness and bubbles) and in the exchange rate of volume elements at the interface. Reaeration is stimulated when deaerated water from the bulk flow of the stream replaces the oxygen saturated water in the surface film. As the area of liquid-atmosphere contact increases the total flux of oxygen molecules into the depleted fluid volume increases. The depth term (H_D) used was the discharge divided by the mean width and maximum velocity. This approach adjusts for dead zones that do not actively mix with the bulk flow.

Biochemical oxygen demand (BOD) results from oxidation and respiration of sugars and other organics. Work at Oregon State has identified the relative BOD of forest litter and slash. Although large woody material such as logs and stumps may have large ultimate BOD loads they are often slow to leach or decompose. Water-saturation of downed logs (with resulting anaerobic conditions) is frequently observed to preserve large wood in streams. It is the fine slash such as needles and leaves and especially fresh slash which has not translocated organics that pose the greatest potential oxygen load to streams. Although large woody material often creates a surprisingly small short-term oxygen demand, it can dam streams and cause deep, quiescent pools where more organic material is in contact with the water and reaeration rates are lower. Reaeration may be inhibited by seeping debris jams with coarse and fine slash and sediment.

Using: (a) the equation for the reaeration coefficient, (b) the Brown Equation to predict maximum stream temperature changes due to removal of stream cover, and (c) estimates of organic inputs and flow residence-time in pools, foresters can identify those stream conditions which are sensitive to oxygen depletion. The observations in the Alsea Watershed Study confirm these conditions. In a Canadian study a stream with a slope gradient of less than one percent was loaded with logging debris (some of sufficient size to impound the stream). The dissolved oxygen concentration dropped to zero as a result of these conditions. Conditions which cause streams to be sensitive to management impacts also make streams sensitive to natural organic inputs. For Needle Branch in the Alsea Watersheds, leaf fall from red alder (<u>Alnus rubra</u>) growing in the riparian zone caused a 6 mg/L oxygen deficit during one Fall period.

These results provide some confidence to forest and fisheries managers that large woody debris can generally be introduced into streams for habitat enhancement and improved stream structure without negatively impacting dissolved oxygen concentrations. Streams sensitive to introduction of high BOD slash can be identified and managed using stream management zones, directional felling, and stream clean-up.

GAS TRANSFER MEASUREMENTS ON AN ICE-COVERED RIVER

G. Macdonald[1], E Holley[2], S. Goudey[1]
[1] HydroQual Canada Limited, [2] University of Texas

The Athabasca River in northern Alberta, Canada, has been proposed to receive waste effluent from production of up to 4500 ADMt/d of pulp by 1995. This is an eightfold increase over the 1988 rate of 565 ADMt/d.

The river originates in the Rocky Mountains and flows northeast 1400 kilometers to Lake Athabasca. Mean annual river flows range from 173 m^3/s in the upper basin to 678 m^3/s in the lower basin. However, mean winter flows in the upper basin where most of the pulp mill development will occur are around 30 m^3/s. These low-flows usually last for a four-month period in most years.

In 1987 dissolved oxygen modeling was undertaken to derive effluent standards that would protect the receiving water environment. Unlike southern rivers where low dissolved oxygen occurs during summer when river temperatures and biological activities are high, the Athabasca River experiences low dissolved oxygen in the winter. Despite high dissolved oxygen saturation in the winter, a complete ice-cover inhibits the atmospheric oxygen exchange while biological oxidation of organic materials consumes river oxygen. The result is gradual depletion of dissolved oxygen along the river length. The only appreciable oxygen source appears to be oxygenated tributary inflows.

While modeling the river oxygen profile and determining permissible effluent standards, the atmospheric exchange rate was identified as an extremely sensitive coefficient. The regulatory agency (Alberta Environment) recognized this and provided funding to develop and implement an experimental technique for measuring gas transfer under ice-cover conditions.

To our knowledge, there are no reported studies on under-ice gas transfer measurements. For this reason, we developed an experimental technique, with the assistance of Dr. Holley (University of Texas), to measure gas transfer under ice. The method was based on traditional tracer-gas measurement procedures documented by the USGS. A continuous injunction technique was desirable. However, this was not practical because of the expected very low gas transfer rate and 60 kilometers of river necessary to provide time for a significant change in propane mass. The short duration injection was selected instead.

The diffuser system for the experiment had to release propane and dye, be highly efficient to ensure a sufficient initial concentration that propane would still be detectable after 60 kilometers, and it had to be installed below 1 meter of ice through a 30-cm hole. It was felt that a conventional ceramic diffuser could not be easily manipulated under the ice. After reviewing available products that were marketed as diffusers or could be used as diffusers, we selected a 3-cm-diameter porous rubber hose. The hose is made of recycled rubber and normally used for drip irrigation. The manufacturer had compared the hose with ceramic diffusers aerating a container of water under laboratory conditions and found the hose superior. The final design involved two 3-meter loops of hose, overlaid on top of each other separated by 10 centimeters. Dye was injected through the top hose and dispersed by

propane injected from the lower hose. Both loops were attached to one end of a 10-meter pole.

At the injection point the apparatus was collapsed, forced through the hole in the ice and finally held stationary on the bottom of the river.

Two river reaches were selected for a field trial. A 21-kilometer reach which included a 12-kilometer open-water lead caused by thermal mill effluent. The second reach (58.8 kilometers) was completely ice-covered. Within each reach only two downstream river locations could be accessed for monitoring.

At each downstream monitoring location, samples were collected throughout the dye/propane cloud using a displacement sampler mounted on a 10-meter pole. Roughly half of the sample volume was decanted into two 50-ml glass bottles: one for the field and one for lab Rhodamine analysis. The remaining sample was sealed in the 0.25-L Qorpak bottle with a Teflon septa and cap. Propane was analyzed onsite using a Photovac Model 10A10 portable gas chromatograph equipped with a photoionization detector. Propane was determined by head space analysis with a detection limit of 0.1 nl (1 ml sample volume). Monitoring took up to 20 hours at one location. For this reason, it was important to have immediate information on propane levels in the river.

Peak propane and dye concentrations were well above detection limits at all monitoring sites. Concentration versus time curves were integrated to calculate areas. In the 58.8-kilometer ice-covered reach there was a greater loss of dye than propane mass. At all four monitoring sites the propane centroid passed before the dye centroid. We have attributed the latter to the formation of propane bubbles under the ice surface which could gradually be dissolved into the passing water. As a result of these difficulties, mathematical corrections were applied and transfer rate calculations were restricted to changes in measured propane areas instead of changes in the propane to dry concentration ratio.

The calculated gas transfer rate for oxygen was not significantly different from 0.0 (day^{-1}, 0°C) for the ice-covered reach and was 0.74 (day^{-1}, 0°C) over the open-water reach.

The technique was developed is a viable method for measuring reaeration under ice-covered conditions, particularly under harsh field conditions (air temperature <-30°C). More studies are required, however, to fully assess the magnitude of reaeration that can occur under ice-cover.

Based on the field results, a reaeration rate of 0.001 day^{-1} (0°C) has been used to model dissolved oxygen conditions for wasteload allocation. The result has been a considerable reduction in the predicted assimilative capacity of the Athabasca River and a reduction in the licensed BOD loadings for the proposed and existing pulp mills. Dissolved oxygen monitoring data support these predictions.

TITLE: **Hydraulic, Physical, and Water-Quality Characteristics of Streams That Influence Oxygen Transfer Rates**

AUTHORS: Gene W. Parker and Leslie A. DeSimone

AFFILIATION: Hydrologists, U.S. Geological Survey, W.R.D.,
Marlborough, Massachusetts Office

Abstract for Gas-Transfer Symposium

Multiple regression techniques were used to test which of 14 hydraulic, physical, and water-quality characteristics influence gas transfer rates for low-sloped (water surface slopes less than 0.002 foot per foot) streams in Massachusetts and New York. An empirical equation relating oxygen transfer rates to the 14 stream characteristics was defined. Water surface slope, mean depth, and concentration of surfactants (Methylene blue active substances) were found to show statistically significant correlation with oxygen transfer rates. Twenty-nine oxygen transfer rates were determined using a steady-state, propane gas-tracer method along 24 reaches on 18 streams during the open water periods in 1985 through 1988. Oxygen transfer rates ranged from 0.2 to 11.0 days^{-1} (base e). The hydraulic characteristics tested in the regression analysis were: (1) water surface slope (0.00001 to 0.0017 foot per foot), (2) mean velocity (0.01 to 0.62 feet per second), (3) average wind speed at the closest National Oceanic and Atmospheric Administration station (7.3 to 21.7 feet per second), and (4) resultant wind velocity, parallel to the channel azimuth and corrected for the mean sheltering angle (0.1 to 21.7 feet per second). The physical characteristics tested in the regression analysis were: (5) mean depth (0.23 to 8.7 feet), (6) mean width (19 to 201 feet), (7) channel azimuth (6 to 340 degrees from true North), (8) channel elevation (13 to 1180 feet), (9) mean sheltering angle (25 to 166 degrees). The water quality characteristics tested in the regression analysis were: (10) color (5 to 300 Platinum-cobalt units), (11) total organic carbon concentration (1.4 to 20 milligrams per liter), (12) methylene blue active substances concentration (0.2 to 0.54 milligrams per liter), (13) specific conductance (45 to 647 microsiemens per centimeter), and (14) suspended solids concentration (3 to 350 milligrams per liter).

The weighted, multiple regression analyses defined the empirical relation:

$$K2 = 3.83\,(MBAS)^{-0.410}(SL)^{0.199}(D)^{-0.762}$$

where $K2$ is the oxygen transfer rate, in day^{-1}, $MBAS$ is the methylene blue active substances concentration, in milligrams per liter, SL is the water surface slope, in foot per foot, and D is the mean depth, in feet. The proposed equation has an adjusted coefficient of determination of 0.66 and a standard error of estimate of 71 percent. The concentration of methylene blue active substances is interpreted as an index to the presence of surfactants. Previous researchers have suggested that increased surfactants concentration would reduce oxygen transfer rates in two ways; by increasing the diffusional resistance through a reduction on the surface tension and by decreasing the surface renewal rate (rotation of water within a cross-section) through an increase in viscosity. Water surface slope is an indicator of the energy released along a stream reach and would enhance the transfer process. Mean depth is inversely related to the mean velocity of a stream reach as defined by the continuity equation. Mean velocity is an indicator of the internal energy and turbulence within a cross-section. A decrease in internal energy and turbulence would slow the surface renewal rate. An increase in mean depth would indicate a decrease in the surface renewal rate and would reduce the transfer rate of oxygen throughout the entire water column. The presence of methylene blue active substances concentration as a significant water-quality reach characteristic for estimating reaeration coefficients in low sloped streams was also confirmed by regression analysis of residuals from 20 published equations using reach characteristics not present in the original equations.

DEVELOPMENT OF AN EXPERT SYSTEM FOR ESTIMATING STREAM REAERATION RATES

Raymond C. Whittemore, PhD

National Council of the Paper Industry for Air and Stream Improvement, Inc. (NCASI), Tufts University, Medford, MA 02155

The estimation of reaeration rates in natural streams is an essential, if not critical, element in many water quality models used for wasteload allocation. Model forecasts of dissolved oxygen in rivers are most sensitive to the magnitude of reaeration rates(k2), sediment oxygen demand, and BOD kinetics. Further improvements in the credibility of these models was judged to be linked to a better understanding of these three model parameters.

Based upon an assessment of current modeling state-of-the-art, acceptable methods of estimating reaeration rates include direct measurement with inert gas tracers and computation from numerous semi-empirical and empirical equations. Nearly 20 original equations now appear in the literature. Guidance for using these equations, however, is limited. Covar was the first to provide guidance in selecting an appropriate equation based upon matching stream velocity and average depth to those developed by O'Connor-Dobbins, Churchill, and Owens, et al. Brown and Barnwell incorporated a similar reaeration advisory into the latest documentation manual for the Qual2e water quality model.

The lack of guidance from the scientific community has prompted some state agencies to develop empirical equations for use on rivers and streams within their boundaries. Much of this state work is based upon correlating direct measurements of reaeration rates with the hydraulic parameters used in the various empirical equations cited in the literature. In principle most water quality modelers would agree that the measurement of reaeration rates is desirable, and the standard upon which the validity of empirical equations should be judged. Unfortunately, in most cases, the measurement of reaeration rates is considered too expensive or difficult to implement in spite of the fact that these measurements would remove an element of uncertainty in the model calibration/verification.

Because of the expense of measuring reaeration rates with inert tracers, it is unreasonable to expect direct measurement in all modeling studies. In these situations, it is important that the modeler rely upon all sources of information: including the empirical equations cited in the literature, existing measured values from streams with similar hydraulic characteristics, and the accumulated experience of knowledgeable modelers.

This work presents an overview of an expert system developed by NCASI to assist modelers with estimating stream reaeration rates. The program is based upon a compilation of reaeration rate measurements using either the radiotracer or hydrocarbon tracer techniques. Nearly 1100 k2 measurements are included along with all available hydraulic data at the time of the tracer measurement. These

data include stream temperature, velocity, depth, slope, and flow. In a limited number of cases, wind speed was monitored at the time of the field test. The data base was generated from both published and unpublished literature, and discussion with consultants.

The expert system provides for a rapid search of the data base to extract stream/river reaches that match the range of hydraulic paramet..s provided by the user. Simple statistics and graphics of the corresponding k2 rates can be performed on the extracted results. The expert system also includes a review of 15 empirical equations for k2 estimation. The latter allows the user to select an equation based upon the range of applicability reported in the literature.

LAKES AND RESERVOIRS

Free Water Surface Evaporation In An Arid Area using Different Vapor Pressure Deficit Methods

Abdulaziz S. Al-Turbak
Civil Eng. Dept., King Saud Univ.
P.O. Box 800, Riyadh 11421, Saudi Arabia

The ability to estimate evaporation rates from lakes and reservoirs is important for better management of water resources especially in arid and semi-arid regions of the world. Many approaches have been suggested and used to estimate free water surface evaporation rates. The Penman combination equation for computing evaporation rates is one which is theoreticallly sound. It has been used by many investigators in the past when the required data for its application are available. Penman equation separates the effects of solar energy and advection by dividing evaporation into an energy balance term and an aerodynamic term. The latter has two components. The first is an empirically derived wind function which itself is related to wind velocity at a certain height. The first component is normally multiplied by a second component which is the vapor pressure deficit.

The major problems of applying Penman equation for estimating free water surface evaporation are: availability of required data, the proper choice of the wind function, and deciding on which method to use to calculate the vapor pressure deficit. A major cause of confusion in the application of Penman method is the selection of a wind function that is not suitable for the area. Another difficulty is that many methods exist for the calculation of the vapor pressure deficit. Some of these methods are based on averaging temperatures while others use average vapor pressures. It has been shown by some investigators in the past that using different methods of calculating vapor pressure deficit will result in different predictions of evaporation rates. Some have suggested certain methods of calculating vapor pressure deficit to be used in arid regions.

The major objective of this work is to apply the Penman approach to calculate evaporation at two sites (near two reservoirs that are used for recharge and flood control purposes) in Central Saudi Arabia. The area is in an arid climate. The climatological data required to apply Penman equation are available at the two sites. These include wind

speed (at 2m height), continuous recording of air temperature and relative humidity, solar radiation, and daily Class A pan readings. The data are available from two meteorological stations that were installed few years ago very close to the two reservoirs. A wind function that has been calibrated for arid regions will be chosen and used in the study. Since there are different methods for calculating vapor pressure deficit, the ones that are recommended for arid regions will be used in this work. The results will be evalaution of potential evaporation rates at the two sites. Using available pan evaporation and the Penman results, recommendations will be made on which method (or methods) of calculating the vapor pressure deficit should be used. This will be important contribution toward better evaluation of free water surface evaporation from reservoirs in Central Saudi Arabia.

Rainfall–Reaeration Effects

Thomas V. Belanger, Ph.D.

Department of Chemical and Environmental Engineering
Florida Institute of Technology
Melbourne, Florida

While wind/wave reaeration effects in aquatic systems are currently being

Hamrick (1984), with standard 10 m wind velocity cut-off points of 340 cm/s (200 cm/s at ground level) and 600 cm/s (360 cm/s at ground level) occurring.

The data also indicate a close linear correlation ($r=0.97$) between rainfall intensity and the mass transfer coefficient $K_L(20)$. The measured wind velocities (20 to 67 cm/s) during rainfall events were very low in terms of wind effect on gas transfer and below the critical wind velocity point of 200 cm/s. The contribution from wind velocity, however, was calculated and simply subtracted from values of gas exchange obtained during rainfall events. Although the measured linear relationship between rainfall intensity and $K_L(20)$ appears to be significant ($r=0.97$), more data are needed to adequately define the correlation.

Although reaeration increases due to surface turbulence from rainfall appear obvious, a simple calculation during a high-intensity rainfall event substantiated the significance of the rainfall-reaeration relationship. During that particular rainfall event, 1.3 cm of rain fell in approximately 30 minutes and the average oxygen level in the small experimental pool increased from 3 to 6 mg/L. This rainfall intensity (2.6 cm/hr) represents the average intensity for a one in two year 3.5 hr duration storm in Florida (Wanielista et al., 1981). During this event, 0.0013 m of rain fell on the 0.8172 m^2 pool, increasing the volume of the pool to 0.1332 m^3. Assuming the rain drops are saturated with 8 mg/L of oxygen, 0.085 g of oxygen will be added to the pool and would result in an increase of dissolved oxygen from 3.0 to 3.6 mg/L in the pool. The average measured increase was much larger (3.0 mg/L) however, rising to 6.0 mg/L. In this case, the turbulent mixing caused by the rainfall was responsible for approximately 80 percent of the observed oxygen increase.

The rainfall-reaeration relationship data obtained in this study were applied to actual field data obtained by Belanger and Platko (1986) in a study determining the impact of nutrient loading and vegetation changes on the oxygen dynamics of the Florida Everglades Water Conservation Area 2A (WCA-20). One site was located in an area impacted by nutrient-rich agricultural pumpage from the Everglades agricultural area. This area (nutrient-enriched site) was dominated by cattails and was characterized by depressed oxygen levels. A second study site (sawgrass site) was located in an unimpacted area approximately five kilometers southwest of the nutrient-enriched site.

Oxygen transfer rates were estimated from mass balance calculations from thirteen separate measurements at the study sites in 1985, and averaged 2.64 and 1.94 $gO_2/m^2/day$ for the nutrient enriched and sawgrass sites, respectively. All other sources and sinks of oxygen were measured directly and detailed methodologies are presented by Belanger, Scheidt, and Platko (1989). The only direct measurement reaeration techniques commonly used in lentic systems are methods to measure the rate of concentration changes of carbon dioxide or oxygen inside a floating dome (Copeland and Duffer, 1964; Hood and Kelley, 1976). Problems and errors involved with the use of these techniques are discussed by Broecker and Peng (1983) and Korzun (1986).

The computed dissolved oxygen balance revealed that oxygen sinks such as water column respiration and sediment oxygen demand dominated and resulted in low oxygen saturation levels and suppressed diurnal curves much of the year (Belanger, 1986). The following calculations illustrate the effect different intensity rainfall events would have on the reaeration rate in cattail and sawgrass areas of the Everglades WCA-2A, given the same field conditions. These calculations are based on the experimental pool rainfall data and the average mean depth, temperature, and saturation deficit data collected by Belanger (1986). Oxygen transfer rates can be calculated at various saturation deficits (C_s - C_L), since

$$\frac{dc}{dt} = K_L a \ (C_s - C_L) \qquad (1)$$

where

$\frac{dc}{dt}$ = oxygen transfer rate, mg/L/hr,

K_La = mass transfer coefficient, hr^{-1}, derived from integration of equation 1

C_s = oxygen saturation concentration at test temperature and pressure, mg/L

C_L = oxygen concentration at time t, mg/L

$$K_La = \frac{\ln(C_s - C_1) - \ln(C_s - C_2)}{t} \qquad (2)$$

C_1 = concentration of oxygen at t_1, mg/L

C_2 = concentration of oxygen at t_2, mg/L

t = elapsed time, $t_2 - t_1$, hr

For the sawgrass area of WCA-2A, the mean depth was 0.3 m, the mean temperature was 25° C, and the mean saturation deficit was 4.77 mg/L in 1985. Applying a rainfall intensity of 1.3 cm/hr (0.5 in/hr), the $K_L(20)$ is 12.1 cm/hr. Converting the $K_L(20)$ value to $K_La(20)$ and correcting this value to average field temperature (25° C), using the formula (APHA, 1975)

$$(K_La)_T = K_La(20) \times (1.024)^{T-20} \qquad (3)$$

the K_La equals 2.45 hr^{-1},and from equation 1 the oxygen transfer rate (dc/dt) equals 11.7 mg/L/hr or 84 g/m²/day. If these same calculations are performed for rainfall intensities ranging from 0.64 cm/hr to 2.54 cm/hr (.25 to 1.0 in/hr), the transfer rate varies from 45 to 158 g/m²/day. This represents a 23 to 82 fold increase over the average field transfer rate of 1.94 g/m²/day and shows the dramatic effect rainfall has on reaeration. Calculated rates based on experimental data indicate that extremely high wind velocities of from 233 to 815 cm/s (5.2–18.2 miles/hr) would be required to produce this same oxygen transfer range. At the nutrient-enriched cattail site in Everglades WCA-2A, an area exhibiting an average saturation deficit of 8.27 mg/L, the reaeration increases were even more pronounced since the rate at which oxygen enters a solution is proportional to the degree of undersaturation. At this greater average saturation deficit, reaeration rates ranged from 78 to 273 g/m²/hr for rainfall intensities from 0.64 to 2.54 cm/hr, representing 30 to 103 fold increases over the average reaeration rate of 2.64 g/m²/day. These calculations, and others presented in the paper, indicate the importance of rainfall as a consideration in long-term oxygen budget studies.

Pr... ...!

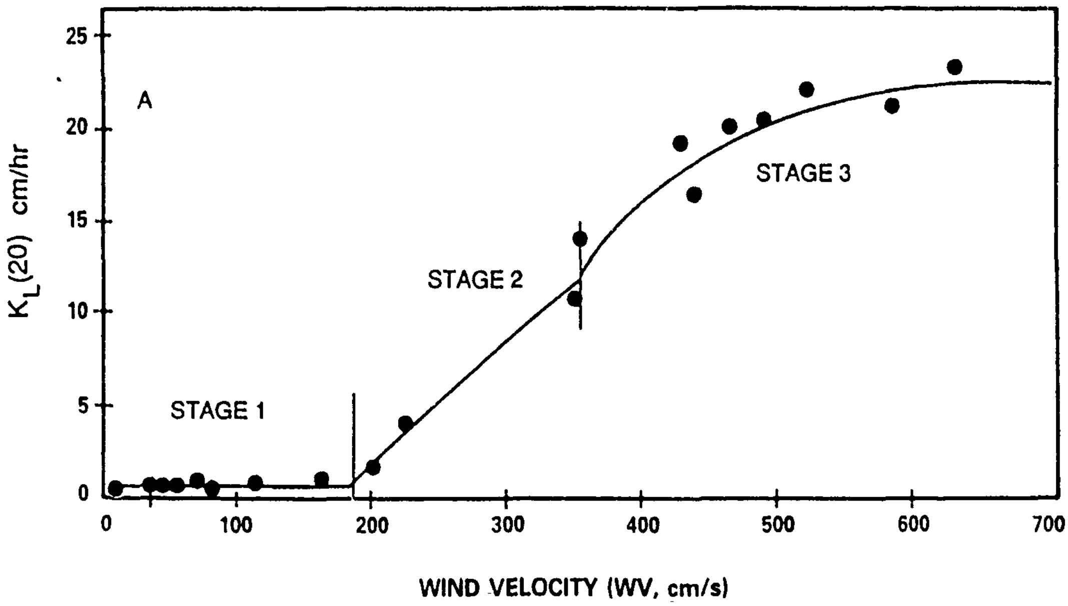

A
STAGE 1
STAGE 2
STAGE 3
$K_L(20)$ cm/hr
0
5
10
15
20
25
0
100
200
300
400
500
600
700
WIND VELOCITY (WV, cm/s)

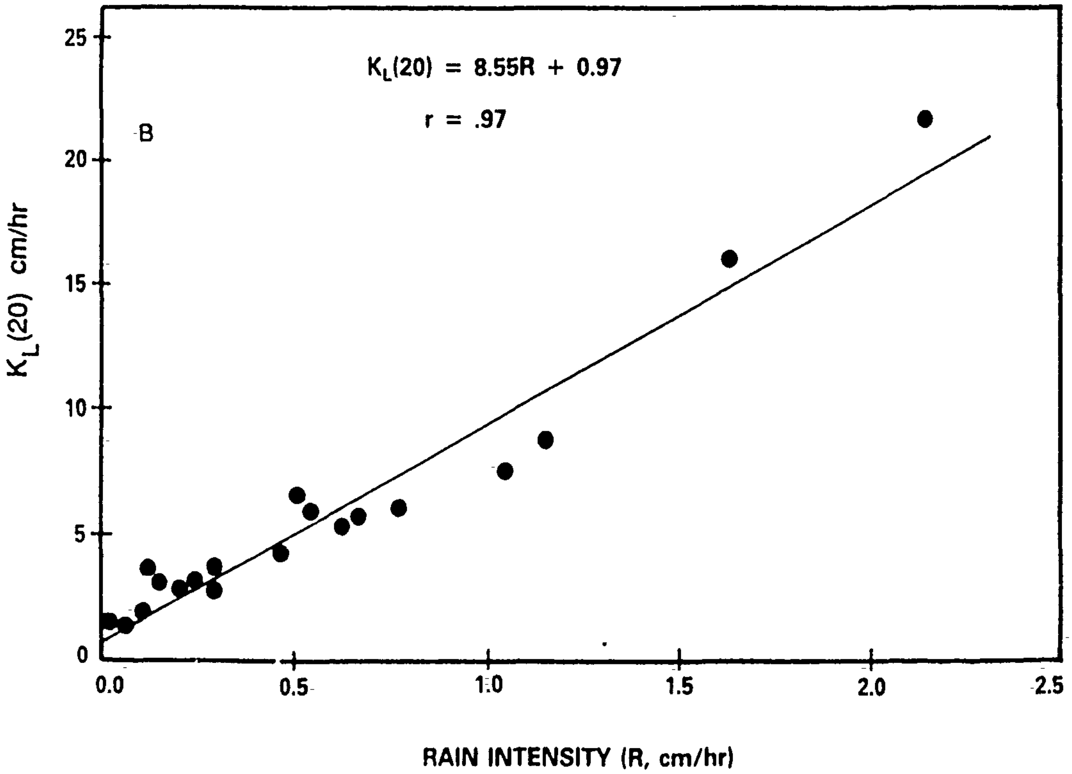

B
$K_L(20) = 8.55R + 0.97$
$r = .97$
$K_L(20)$ cm/hr
0
5
10
15
20
25
0.0
0.5
1.0
1.5
2.0
2.5
RAIN INTENSITY (R, cm/hr)

MEASURING AND MODELING EVAPORATION AT UTAH'S WEST DESERT PUMPING PROJECT - A 500-SQUARE MILE EXPERIMENT

David W. Eckhoff and Karen K. Nichols/Eckhoff, Watson & Preator Engineering
Lloyd Austin/Divison of Water Resources
Gail Bingham/Utah State Climatologist

Beginning in September of 1982, normally desert-like Utah experienced approximately four years of extremely wet weather. In Salt Lake City, the three year average precipitation was approximately 140% of normal. This resulted in annual runoff values in the range of 250%. Moreover, the Great Salt Lake rose from an elevation of 4200 (ft. above MSL) in 1982 to nearly 4212 in 1986. The surface area of the lake expanded by approximately 500,000 acres, and damages to property and public infrastructure extended into the hundreds of millions of dollars. [Note: The Great Salt Lake is a terminal lake.]

The Great Salt Lake had been rising since a low point at elevation 4193 in the year 1963, and the State of Utah had begun planning efforts to deal with The Lake in the event that the rise continued. In 1983 the state funded the West Desert Pumping Project Feasibility Study, which was directed by the Senior Author of this paper. The objective of the West Desert Pumping Project was to pump water from the Great Salt Lake to an engineered evaporation pond in the West Desert of Utah, and thereby to substantially augment evaporation from the lake itself. The Feasibility Study reviewed existing sources of data (relative to evaporation), evaluated alternative configurations for the Evaporation Pond System, diking, canal, and pumping systems. Of major concern was the relative scarcity of data on both the evaporative regime of the West Desert and the specific evaporation rates of high density brines.

As the wet weather continued, the State of Utah invested further funding in the West Desert Pumping Project for project planning and preliminary design work. Additional efforts were directed toward the preparation of an accurate topographic map over the entire area (about 1500 square miles) at a contour interval of 1 foot. This task was made very difficult by the fact that much of the West Desert is a military test range and "Off Limits" to civilian personnel. A variety of procedures were utilized, including inertial surveying and side-scan radar imaging. The significance of this work is exemplified by the fact that a one-foot elevation difference on the evaporation pond represents a volume of 300,000 acre-feet.

Planning was also initiated for the establishment of remote weather monitoring stations in the area of the project. It was determined that a more comprehensive network of precipitation, solar radiation, temperature, wind, and humidity measurements was needed. A preliminary review of evaporation models/formulas was also carried out at this time.

Construction of the West Desert Pumping Project was authorized by the State Legislature in May of 1985. The approved project consisted of one pond, having a nominal surface area of 300,000 acres at a design water surface elevation of 4216 feet. The design fetch and average depth of the pond were 40 miles and 2.1 feet respectively, which created major potential for wind-driven waves (another problem). Seven remote weather monitoring stations were installed in the vicinity of the evaporation pond. Included were a station in the center of the pond, as well as several around the periphery, and one at the pumping station itself. Monitoring included: air and soil temperature, precipitation wind vector, humidity, solar radiation. Generally, the recorded data were hourly averages of samples obtained at one-minute intervals; diurnal highs and lows were also recorded. At four-hour intervals, the data were relayed to Utah State University via GOES.

A precise hydrologic balance on the evaporation pond was maintained. Detailed measurements in the pump discharge canal were used to accurately calibrate the pump curves, and hydraulic modeling tests of the overflow structure were conducted for purposes of calibration of this feature. Digitized satellite imagery was employed for purposes of precisely establishing water surface areas in the evaporation pond. These were then combined with the previously completed side-scan radar topographic work, in order to establish accurate elevation, surface area, volume, relationships tied into the project datum.

Our review of the various evaporation models strongly suggested that the Modified Penman Equation is the most appropriate model for this particular environment. This model was designed for longer-term averaging of pertinent meteorological parameters, and we used the Modified Penman Equation to estimate monthly average evaporation rates. Adjustments were made for both salinity and pond area, with the latter being done by comparative analysis of changes in pond surface elevation. Equivalent Class A pan evaporation rates were also estimated using the Modified Penman Equation and the appropriate pan factors.

Figure 1 shows the measured and computed water surface elevations for the West Desert Evaporation Pond ("West Pond") for the year 1988.

Using the Modified Penman Equation in conjunction with a hydrologic balance on the West Pond, we estimated an annual Potential ET Value of about 72 inches. This translates into an estimated Class A Pan value in excess of 100 inches per year. Taking into account both evaporation pond size and salinity, we computed (and confirmed by measurement and modeling) that the actual pond evaporation was in the range of 36 inches per year. This translated into an annual quantity of 893,000 acre-feet per year for the West Pond, confirming estimates prepared during the design phases of the project.

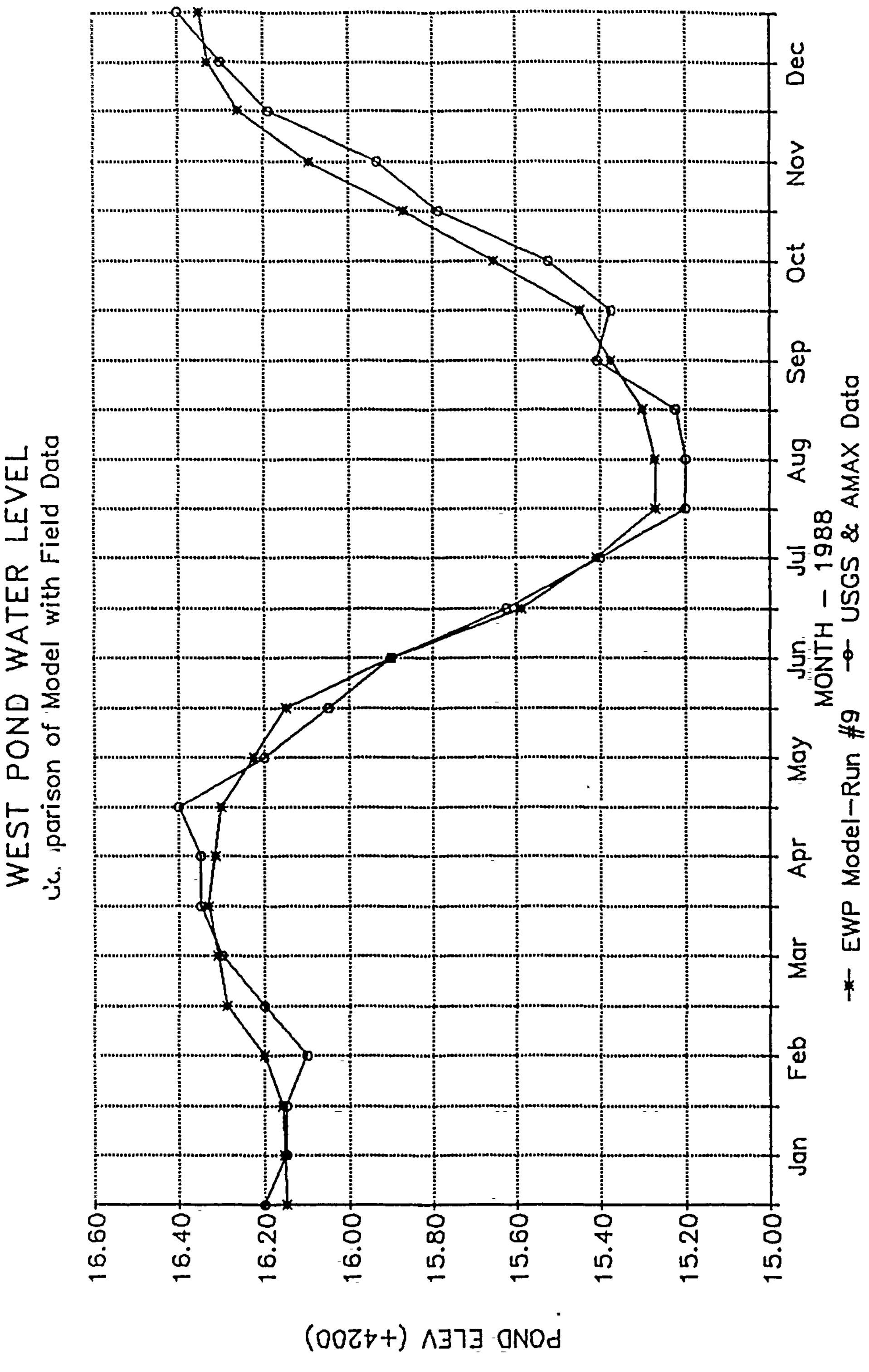
WEST POND WATER LEVEL
parison of Model with Field Data
POND ELEV (+4200)
16.60
16.40
16.20
16.00
15.80
15.60
15.40
15.20
15.00
Jan
Feb
Mar
Apr
May
Jun
Jul
Aug
Sep
Oct
Nov
Dec
MONTH – 1988
EWP Model–Run #9
USGS & AMAX Data

Volatilization of PCBs and PAHs from the Great Lakes

S.J. Eisenreich, D. Achman, K. Hornbuckle
Environmental Engineering Sciences, Department of Civil and Mineral Engineering, University of Minnesota, Minneapolis 55455
J.E. Baker, Center for Environmental and Estuarine Studies, Chesapeake Biological Laboratory, Solomons, MD 20688

Chemical exchange across the air-water interface is one of the major processes that controls concentrations and residence times of semi-volatile organic chemicals (SOCs) in natural waters. SOCs, such as polychlorinated biphenyls (PCBs), organochlorine pesticides (OCs), and polycyclic aromatic hydrocarbons (PAHs), are emitted from ubiquitous sources and transported long distances in the atmosphere. Atmospheric fluxes of SOCs often dominate total inputs to remote lakes, the Great Lakes, and the oceans (1-6). Once in surface waters, dissolved SOCs may revolatilize into the atmosphere, and net atmospheric flux across the air-water interface is the difference between gross deposition and volatilization. Mackay et al (7) and Baker and Eisenreich (8) describe the exchange process as a balance between intense, episodic inputs via precipitation followed by slow, prolonged volatilization during dry periods.

The objective of our studies was to estimate field volatilization rates of PCBs and PAHs from Lake Superior and Green Bay, Lake Michigan. Lake Superior is a cold, oligotrophic, deep lake receiving the majority of its SOC inputs from the atmosphere. Green Bay, Lake Michigan is a relatively large, shallow, eutrophic system receiving the majority of its inputs from the Fox River, its principal tributary. The strategy employed in both areas was the same. Paired water and air samples were collected in the summers of 1986 and 1988 over Lake Superior from aboard the RV Seward Johnson. Paired water and air samples were collected during three cruises in Green Bay, Lake Michigan in 1989. In each case, meteorological and water column data are available. The air samples were collected by passing air at 0.5 m^3/min through a glass fibre filter and a backup adsorbent (polyurethane foam; PUF) plug. The water samples were collected by pumping water from the surface mixed zone and passing it through a glass fibre filter and a backup XAD-2 adsorbent cartridge. The concentration gradient across the air-water interface is taken as the difference in the atmospheric gas-phase concentration and the dissolved-phase water concentration. We maintain that the higher

molecular weight PCBs and PAHs have a portion of their aquatic burden associated with a colloidal phase that passes through the glass fibre filter. Baker and Eisenreich (8,9) provide evidence for this interaction and a model to correct the dissolved phase concentrations for colloidal contributions.

The most complete data set for Lake Superior (1986) indicates that the fugacity of most PCB congeners is greater in the water than the atmospheric gas phase. The mean sum of PCB congeners in the gas and dissolved water phases were 1.25 ng/m^3 and 0.55 ng/L, respectively. We therefore infer that, for most PCB congeners, that the direction of gas transfer in the summer atmosphere is out of the water. For PAHs, the ratio of fugacity in the water phase (f_w) to the fugacity in the atmospheric gas phase (f_a) favors air-to-water transport. Concentrations of gas-phase PAHs ranged from 2650 pg/m^3 for phenanthrene to 1.2 pg/m^3 for benzo[a]pyrene. The dissolved concentrations ranged from 3.5 ng/L for phenanthrene to 0.39 ng/L for benzo[a]pyrene. Calculation of the fugacity gradient requires the availability of accurate Henrys Law constants (K_H)at the ambient water temperature (4 to 25 ^{0}C) for 60 PCB congeners and 17 PAH compounds. The temperature-corrected K_H values for PCBs are now available but their is considerable uncertainty in the K_H values for PAHs. Therefore, PAH air-to-water fluxes are uncertain.

The magnitude of the volatilzation flux of PCBs from Lake Superior was calculated using mass transfer coefficients (K_{OL}) derived from Mackay et al. (10). Both still-air and wind-enhanced fluxes were calculated. The magnitude of the still-air flux of the sum of PCB congeners (19 ng/m^{2}day) is similar to the magnitude of estimated wet and dry deposition (18 ng/m^{2}day). Both of these numbers exceed net sediment accumulation rates for PCBs by a factor of 2 to 3. The wind-enhanced volatilization flux at 5 m/sec was about 7 times greater than the still air value. Preliminary PCB volatilization fluxes from Green Bay are significantly greater due to the 10 to 20 fold increase in the dissolved water concentration while the air concentration remained about the same as the Lake Superior measurements.

This presentation will focus on describing the atmospheric and water column concentrations of PCBs and PAHs in Lake Superior and Green Bay, Lake Michigan, the fugacity ratios as a function of environmental conditions, estimated air/water fluxes, and the role of SOC exchange at the air-water interface of large lakes.

This work has been supported by the US Environmental Protection Agency and the National Oceanic and Atmospheric Administration through its MN Sea Grant and National Undersea Research programs.

References

1. Eisenreich, S.J.; Looney, B.B.; Thornton, J.D. Environ. Sci. Tech., 1981, 15, 30-38.
2. McVeety, B.D.; Hites, R.A. Atmos. Environ., 1988, 22, 511-536.
3. Atlas, E.L.; Giam, C.S. Science, 1981, 211, 163.
4. Atlas, E.L.; Giam, C.S. Water, Air, and Soil Pollution, 1988, 38, 19-36.
5. Swackhamer, D.L.; McVeety, B.M.; Hites, R.A. Environ. Sci. Tech., 1988, 22, 664-672.

6. Strachan, W.M.J.; Eisenreich, S.J. Mass Balancing of Chemical Pollutants in the Great Lakes: the Role of Atmospheric Deposition, International Joint Commission Rept: Windsor, Ontario, 1988, 149 p.
7. Mackay, D.; Paterson, S.; Schroeder, W.H. Environ. Sci. Tech., 1986, 20, 810-816.
8. Baker, J.E.; Eisenreich, S.J. Concentrations and fluxes of PAHs and PCBs across the air-water interface of Lake Superior. Environ. Sci. Tech., 1990, 24, xxx.
9. Baker, J.E.; Capel, P.D.; Eisenreich, S.J. Environ. Sci. Tech., 1986, 20, 1136-1143.
10. Mackay, D.; Yuen, A.T.K. Environ. Sci. Tech., 1983, 17, 211-216.

Carbon dioxide partial pressure in the surface waters of lakes in northwestern Ontario and the Mackenzie delta region, Canada.

Hesslein, Raymond H., J.W.M. Rudd, C. Kelly, P. Ramlal, and K. Hallard.

Department of Fisheries and Oceans, Canada. Freshwater Institute, 501 University Crescent, Winnipeg, Manitoba, Canada R3T 2N6.

Over the past decade, several of us have made measurements of partial pressure of carbon dioxide in the surface waters of lakes studied by our groups at the Freshwater Institute. There have been two main areas of interest in these measurements: 1. Those related to carbon flux in the lakes due to air-water exchange and the biological processes of production and respiration, and 2. The testing of the internal consistency of the pH-carbonate equilibria relationships in low alkalinity waters. As a consequence of the various purposes and timimg of these studies, the measurements have not been put together to give a comprehensive view of the pCO_2 typical of surface waters.

The earliest interest in CO_2 in surface waters by our group came from the dramatic changes in DIC (dissolved inorganic carbon) produced by the fertilization and consequent algal response of Lake 227 (Experimental Lakes Area, northwestern Ontario) in the early 1970s. Gas exchange studies using radon gas were carried out to estimate the CO_2 gas exchange and its enhancement resulting from the pH elevated by algal reduction of pCO_2. The pH in this lake often exceeded 10.5 in the afternoon of a sunny day. The pCO_2 was not measured at this time but DIC values were <20 uMole/L in a lake with and alkalinity increasing from 100 to 300 uEquiv/L over the first several years of the experiment due to fertilization with sodium nitrate. In a subsequent eutrophication study in Lake 226 (also ELA) measurements of pCO_2 in 1979 showed values below 20 ppm-atm, again in the afternoon of sunny days. Even in the basin of Lake without added phosphorous and only a very mild algal response, pCO_2 of <100 ppm-atm were measured. A few measurements of pCO_2 in unperturbed lakes in 1979 suggested that typical values were near or below atmospheric equilibrium.

Previously, in 1976, a ^{14}C tagged sodium bicarbonate was added to the surface of Lake 224 (ELA) to study algal uptake and gas exchange. The loss rate of ^{14}C to the atmosphere was 5% per day in this lake with a DIC value of 80 uMole/L and a mean mixed layer depth of 6 meters. At the time we had no method to measure pCO_2 so it was calculated from the pH (6.8) and the DIC. This calculation gave a pCO_2 value in the range of 700-1000 ppm-atm., or 2-3 times atmospheric equilibria. While this seemed odd the values were accepted at the time as the lake had very low algal productivity and respiration of allocthonous carbon could have resulted in the estimated net evasion.

As a consequence of this disagreement in pCO_2 measured by equilibration of gas with surface water and that calculated from pH

and DIC, a number of studies were carried out during 1980-1984 on the internal consistency of among the components of carbonate equilibria. For these studies acid/base titrations of lake water were performed in closed systems. Changes in pH, DIC, pCO_2, and alkalinity were monitored. These studies concluded that the calculation of pCO_2 from pH, alkalinity, and DIC was risky due to difficulties in measuring pH in low alkalinity waters especially those with important contributions of organic anions from dissolved humic substances. Actually, pH could be more consistently calculated from pCO_2 and DIC than measured by glass electrode. These conclusions lead us to develop some simple methods for the measurement of pCO_2 in lakes.

All the measurements of pCO_2 that we have made have used some form of equilibration with a gas headspace. Detection has been by gas chromatograph, both thermal conductivity and methanizer-flame ionization, or infrared absorbtion. Early measurements at ELA and those in the Mackenzie Delta were made by field equilibration of a 500 or 1000 ml sample with a gas headspace of <5% of the liquid volume so that the carbonate equilibria would not by greatly affected. The equilibration chamber was thermally insulated to insure equilibration at the in situ temperature. After equilibration headspace gas was removed into a syringe and sometimes an evacuated serum bottle for transport to the laboratory. The measurements for the Red Lakes area in northwestern Ontario were made on samples drawn into evacuated 150 ml serum bottles, leaving a headspace of 5-10 ml into which CO_2 free nitrogen was introduced at atmospheric pressure in the lab. These samples were preserved from biological production or respiration prior to analyses by the addition of 8 grams KCl to the bottle prior to evacuation. Corrections were then made to in situ conditions. Samples for pCO_2 in air were taken approximately 2 meters above the lake surface (standing, arms extended up, at the upwind end of the boat or airplane pontoons) by syringe or evacuated bottle.

A study of surface water pCO_2 in Lake 239, ELA from May to September 1980 showed the dramatic effect of the seasonal mixing cycle of the lake. Early May pCO_2 was approximately twice atmospheric equilibrium as a result of the mixing of deep waters high in accumulated CO_2 from winter respiration. The pCO_2 dropped rapidly to near atmospheric equilibrium by the end of May, primarily due to gas exchange, but also influenced by phytoplankton photosynthesis. The pCO_2 stayed near atmospheric equilibrium through June and July before rising through August due to deepening of the mixed layer and decreasing photosynthesis. A boundary film thickness for gas exchange of 200 microns can be calculated from the rate of decline of the pCO_2 in the Spring.

The pCO_2 data from the Mackenzie Delta lakes showed a similar cycle to that in Lake 239. The spring values were high and rapidly declined. Two differences are important in this data set. The delta lakes are high in nutrients and thus have potentially very high photosynthetic rates especially due to dense macrophyte beds. However, these lake have a high silt load due to spring flooding of the Mackenzie River, so that photosynthesis is light limited. As the water cleared faster in some of the lakes, photosynthesis was much greater in those, and the pCO_2 decreased to very low levels in those lakes. In NRC Lake the pCO_2 was below 10 ppm-atm on some occasions. Gas exchange influxes of CO_2 were calculated for these lakes and compared to estimates of the net photosynthesis in the lakes. The agreement was very good. The CO_2 measurements in the air over the Mackenzie Delta lakes was about 400 ppm-atm which is higher than expected for average air, but local influences may have influenced this as the measurements were again made at a height of two meters.

The PCO_2 data from the Red Lakes area in northwestern Ontario showed that values during the open water season in lakes of a wide range of sizes is generally near or slightly below atmospheric equilibrium. Models using independent measures of gas exchange, photosynthesis, and benthic respiration give estimates of pCO_2 which are entirely consistent with the measured values. These modelling efforts suggest that gas exchange coefficients calculated from daily wind measurements using the published wind vs. boundary layer relationships are acceptable for calculating gas fluxes at lake surfaces.

EPILIMNETIC DISSOLVED OXYGEN CONTENT AND SURFACE WATER PUMP PERFORMANCE

Mark H. Mobley

Tennessee Valley Authority
Engineering Laboratory
Norris, Tennessee 37828

Surface water pumps have been operated and monitored at TVA's Douglas Dam since 1987. The purpose of these pumps is to improve the dissolved oxygen (DO) content of the hydropower releases. The epilimnetic DO content is the input variable for a properly designed surface water pump installation at a hydropower facility. Changes in this variable directly effect the performance of the pumps. Therefore, changes in this variable and the reasons for these changes are of interest to those interested in using surface water pumps for reservoir release improvements.

Graphs are presented that document the continuous changes in the epilimnetic DO content at Douglas. Reasons for these changes including diurnal cycles, sunlight variations, wind mixing, weather conditions, and algal population are presented. The effects of these changes on the performance of the surface water pumps are discussed.

The continuous monitoring data presented in this paper will hopefully provide a well-documented example of the effects of epilimnetic DO content on surface water pump performance.

Determination of Gas Transfer Velocities on Lakes Using Sulfur Hexafluoride; an Overview of Experimental Methods and Results

R. Wanninkhof, J.R. Ledwell, and J. Crusius

Lamont-Doherty Geological Observatory of Columbia University, Palisades N. Y. 10964

Gas exchange experiments have been performed by the deliberate tracer technique on five lakes ranging in size from 0.13 km^2 to 300 km^2. This technique involves injecting the man-made tracer gas sulfur hexafluoride into the lake and measuring the decrease in tracer concentration with time. In all lakes the gas transfer was strongly dependent on wind speed. The overall trend as well as the absolute gas transfer velocity values are similar for all the lakes. The larger lakes showed slightly higher gas transfer rates and a stronger dependence on wind speed than the smaller ones.

Sulfur hexafluoride, SF_6 exhibits several characteristics that facilitates its use as a tracer in gas transfer studies. The gas is chemically inert at ambient temperatures and pressures, it has little affinity for particles, and it is non-toxic. It can be measured by headspace analyis or cryogenic purge and trap methods over a range of 10^{-10} mol/L to 1.5 x 10^{-16} mol/L on a gas chromatograph with electron capture detector (ECD-GC). The Ostwald solubility of SF_6 is 7 x 10^{-3} at 20 °C, which simplifies extraction from the water. Headspace analyses by ECD-GC are performed within three minutes; purge and trap analyses take about 12 minutes. Samples can be stored in Pyrex® glass containers submerged under water for at least a month without noticeable change in concentration. Thus experiments can be performed without analysis equipment on site.

In the lake experiments the SF_6 was injected from a compressed gas cylinder into the water. Dispersion stones at 4 m to 12 m depth were towed around the lake. Injection efficiencies ranged from 5 to 30 % depending on depth of injection and salinity of the water. To obtain initial concentrations of around 10^{-11} mol/L, injection volumes from 0.5 L to 3 x 10^3 L (STP) pure SF_6 were used, depending on lake volume. This concentration was sufficient to follow the change in gas concentration for about 2 months by headspace analysis.

The water was sampled by drawing it from depth with a peristaltic pump into 50 mL glass syringes or by taking discreet samples with a Niskin® sampler. If samples could not be analyzed within 12 hours,

they were collected in 60 mL BOD bottles, which were stored in batches of 8 in 2-L Nalgene® containers, completely filled with lake water. At the laboratory the bottle samples were transferred to syringes. The syringes were emptied to a predetermined volume and the headspace was filled with nitrogen. The headspace was injected into a sample loop which was subsequently switched in line with a molecular sieve 5-A column. SF_6 eluted from the column in less than a minute, after which the column was backflushed with carrier gas for two minutes.

The initial streaks of tracer mixed throughout the lake on a time scale of 2 to 10 days depending on lake size. The mixing rate of the small lake (less than 1 km^2) was rapid enough that no concentration variations greater than 5 % throughout the lakes were observed. Such a variation in concentration can be attributed to errors caused by sampling, storage and analysis. The larger lakes showed lateral variation of about 10 to 15 % around the lake based on surveys of 30 to 50 samples. All lakes were well mixed vertically with respect to tracer down to the bottom or down to the bottom of the epilimnion for stratified lakes.

The change in lake averaged concentration was determined from the SF_6 concentration depth profiles taken at one to eight locations around the lake. These average concentrations were used to calculate the gas transfer velocity, k according to:

$$k = h/\Delta t \ln (C_i/C_f)$$

where h is the average (mixed layer) depth of the lake, C_i is the average lake concentration at the start of interval Δt, and C_f is the final concentration. The interval over which k was calculated ranged from 1 day to 2 weeks. The concentrations changed at a slower rate for the deeper lakes requiring longer time intervals to determine gas transfer velocities accurately.

A summary of the data is presented in Figure 1 that includes a least squares linear fit through the gas transfer velocities at wind speeds greater than 2.5 m/s. The experiments lasted from one to three months. All wind speeds are corrected from height of measurement (1 to 3 m) to 10 m. Gas transfer velocities have been normalized to a Schmidt number, Sc (which equals the kinematic viscosity of water divided by the molecular diffusion coefficient) of 600 assuming that k is proportional to $Sc^{-1/2}$. The data show that the absolute gas transfer values are slightly higher for the larger lakes. The dependence of gas transfer on wind speed is also slightly stronger for these lakes. These small differences could be caused by errors in the wind speed measurement, conversion of the data to a Schmidt number of 600 or perhaps by a fetch dependence of gas transfer. Scatter in the data especially at low wind speeds might be caused by variability in wind speed over the measurement interval and because factors other than wind speed, such as surface contamination influence gas transfer rates across the air-water interface.

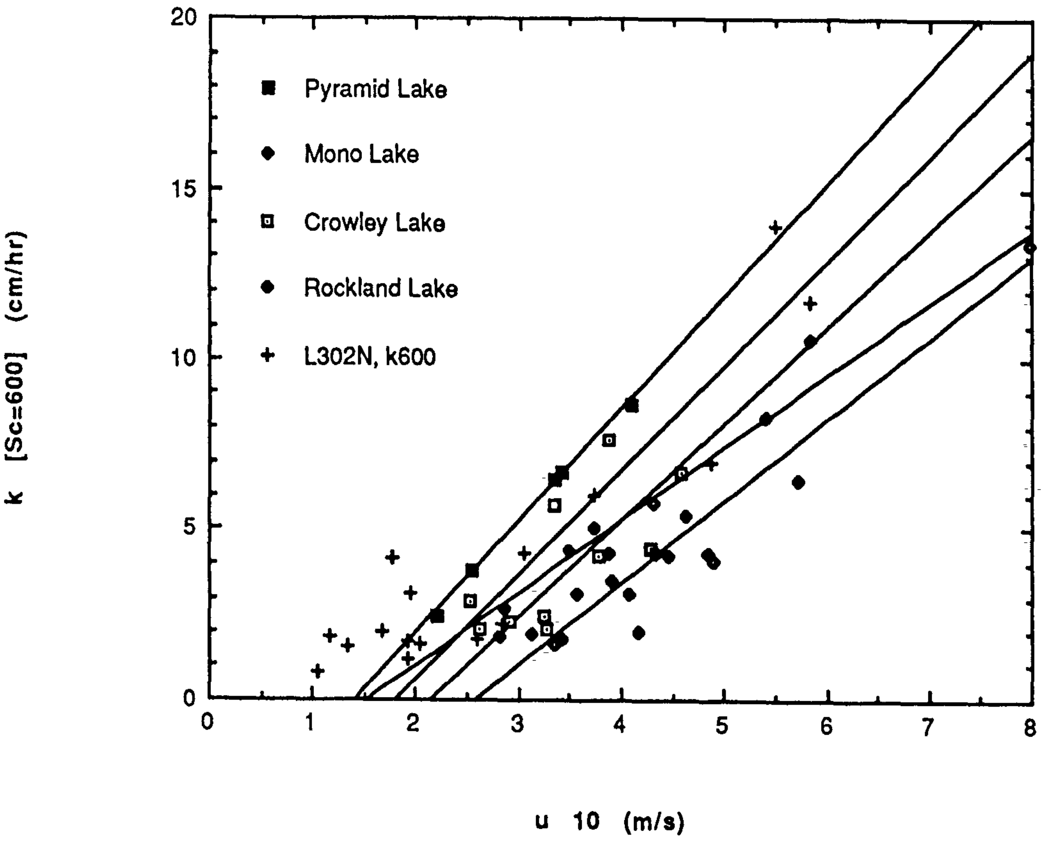

Figure 1. Summary of gas transfer velocity experiments on lakes. The open diamonds and the lowest least squares linear fit line are for Rockland Lake, N.Y., which has a surface area of 1 km^2. The open squares and the line with the smallest slope are for Crowley Lake, CA. (surface area of 20 km^2). The solid diamonds and middle line are for Mono Lake, CA. (surface area of 200 km^2). The plus symbols and the next to highest line are for Lake 302N in the experimental lakes area of Canada (surface area of 0.13 km^2). The solid squares are the results of Pyramid Lake NV. (surface area of 300 km^2). All results are normalized to a wind speed of 10 m/s assuming neutral air boundary layer conditions and a drag coefficient of 1.5 x 10^{-3}. All gas transfer coefficients have been normalized to a Schmidt number of 600.

HYDRAULIC STRUCTURES AND
TURBINE AERATION

TITLE: MONITORING SYSTEM DEVELOPMENT IN SPILLWAYS WITH AERATION DEVICES.

AUTHORS: ANGELACCIO,C.M.-BACCHIEGA,J.D.-TATONE,G.-VERNET,G.F.

AFFILIATION: LABORATORIO DE HIDRAULICA APLICADA.
INSTITUTO NACIONAL DE CIENCIA Y TECNICA HIDRICAS.
EZEIZA, ARGENTINA.

The high head dams show discharge structures (spillways and outlet structures) under very high velocity flow, that are exposed of having the risk of suffering cavitation erosion.

Experience has shown that the air entrainment is one of the technique-economical means more adecuate and safeter to avoid this kind of problems. In 1953 Peterka showed that air concentration in 8% order, eliminates completelly such erosion. For this reason is important to count on adecuate methodologie to obtain the air entrainement devices design. Many authors had spoken about this subject from a teorical and empirical point of view, being indispensable the confirmation and quality of the results obtained by computation or mesurements over phisical models.

This contrast will by done by field mesurements that can be developed in operation dams, giving out a data base that will allow the computation methodology ajustment used for the aerators design.

In this sence, Consultores Patagonia (the Advisor Engineering group formed by IECO and HIDROPROYECTO S.A.), as Piedra del Aguila Dam proyectist, over the Limay river in Argentina, has asked the Applied Hydraulic Laboratory of INCyTH (LHA) the development of the field measures that have conection with the air entrainement devices of the spillway (Figure 1), including the engineering development, the instrumental supply, measurement and interpretation of the data to be obteined.

Under this requarement the LHA has developed the monitoring sistem engineering and also the specific instrumentation for concentration measure near the solid boundary frontiers. The purpose of this paper is of exposing the methodology sugested and toshow the measurement instrumental to be used in this case.

The aerator performance can be shown by the interaction in an air supply sistem formed by the towers and the distribution ducts, and other demand sistem defined by the hidrodinamic characteristics of the flow. That why, for a given

hydraulic condition performance, it will exist an only equilibrium point characterized by an air flow and a pressure in the aerator cavity (Figure 2).

Based on the performance characteristics of the device seems indispensable to do a measurement of the following parameters:

a) Air flow suction by the supply towers.
b) Pressure distribution in the supply sistem and the self formed cavity by the jet.
c) Air concentration in the solid boundary proximities, down stream the aerator device.

For the measurement of these parameters the use of different instrument type such as Pitot-Prandtl tubes, piezometers and air concentration transducers are needed.

In this paper the instrument disposition criterium will be shown (Figure 3) together with its use in work. The especific instrumental development for the concentration measurements consisting in probes without flou interference based in the resistivity measurement of the air-water mixture, and its calibration in Laboratory will be also shown (Figure 4).

--

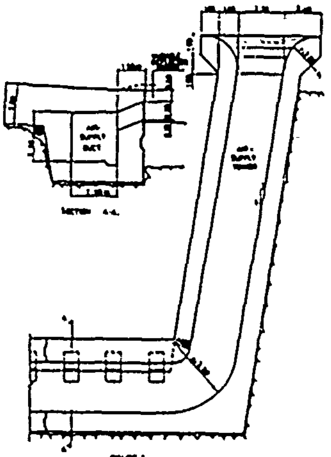

FIGURE 1

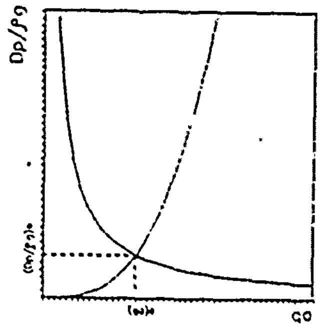

Figure 2

S= CONCENTRATION TRANSDUCERS

G=E= PRESSURE TAPS

P= PITOT-PRANDTL TUBES

ES= MEASUREMENT STATIONS

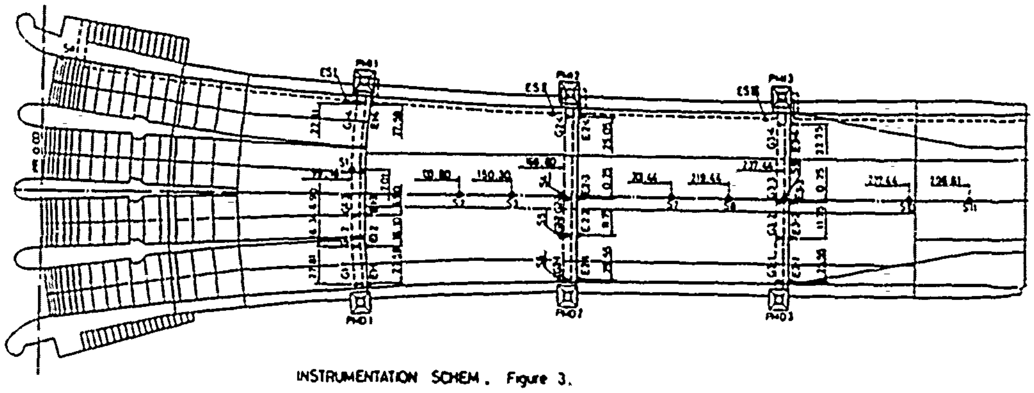

INSTRUMENTATION SCHEM. Figure 3.

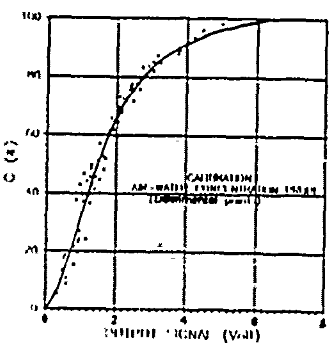

Figure 4

Gas Transfer at Hydraulic Structures

Task Committee on Gas Transfer at Hydraulic Structures*
Technical Committee on Hydraulic Structures
American Society of Civil Engineers

Presently, one of the most cited water quality parameters in our freshwater hydrosphere (rivers, lakes, and reservoirs) is dissolved oxygen (DO). Indeed, the oxygen concentration in our surface waters is a prime indicator of the quality of that water for human use as well as use by the aquatic biota. Many naturally occurring biological and chemical processes, including respiration by aquatic life, use oxygen, thereby diminishing the dissolved oxygen (DO) concentration in the water. The physical process of gas transfer or oxygen absorption from the atmosphere or air bubbles, acts to replenish the used oxygen. The effects of gas transfer involve much more than just oxygen absorption and include such phenomena of interest as the volatilization of industry-produced organic pollutants and absorption of atmospheric nitrogen to supersaturation levels.

A flood-control, navigation, or multi-purpose dam impounds water for subsequent release. From a gas transfer perspective, the effect of the deeper, slower pools is to reduce gas transfer and natural reaeration as compared to the open river. Furthermore, the concentration and accumulation of biological and chemical oxygen demands in the impoundment may degrade the DO concentration in the stored water. Release of this water may pose an environmental and water quality concern in the downstream receiving water.

Some hydraulic structures at reservoirs or impoundments, however, possess the characteristic of providing some degree of gas transfer and oxygen absorption during the release of water. With the wide variety of release structures, one would expect some structures to exhibit remarkable reaeration, while others would do very little to increase release DO. If the DO in releases is lower than desired, then if warranted, methodologies and techniques, such as operational or structural modifications or artificial aeration can be employed to improve the release DO concentration. In any engineering application of such techniques,

*The Task Committee on Gas Transfer at Hydraulic Structures consists of the following people: Steven C. Wilhelms, Control Member, Chair, US Army Engineer Waterways Experiment Station, Vicksburg, MS; Charles E. Bohac, Control Member, Tennessee Valley Authority, Chattanooga, TN; Perry Johnson, Control Member, Bureau of Reclamation, Denver, CO; Mahmood Naghash, Control Member, Bechtel Corporation, Gaithersburg, MD; Alan Rindels, Member, St. Anthony Falls Hydraulic Laboratory, Minneapolis, MN.

it is imperative to possess a clear definition of the processes that affect water quality and the expected change as a result of implementing the particular improvement technique. Hence, for evaluating dissolved oxygen improvement, the impacts of the alternative techniques on the reaeration processes must be thoroughly understood and quantifiable.

In the next decade, as never before, engineers will be asked to provide the technological expertise to accurately evaluate and solve or mitigate a myriad of water quality problems within our surface water environment. What are now seemingly intractable questions regarding the impacts of nature and man on air-water gas transfer must soon be answered. These questions include topics such as improved descriptions of the physio-chemical processes that affect gas transfer; improved descriptions of gas transfer in streams, rivers, and open water; and, last but not least, describing gas transfer at hydraulic structures. The design engineer will be faced with the need to evaluate the gas transfer characteristics of existing conditions at a hydraulic structure for comparison with the characteristics of a proposed modification. Such modifications could be (1) structural, as the retrofit of a navigation or other low-head structure with a hydropower facility or (2) operational with the associated impacts on reaeration and assimilative capacity.

It would be extremely valuable to the practicing professional to possess a technical evaluation of the information currently available for design and assessment of alternatives. The preparation of such a summary became the primary objective of the American Society of Civil Engineers Task Committee on Gas Transfer at Hydraulic Structures, which authors this paper.

The overall purpose of this two-paper series is to define the state-of-the-art in gas transfer at hydraulic structures and to transfer this information to the practicing professional. The objective of this first paper is to identify and briefly summarize the state-of-the-art in measuring and understanding gas transfer at hydraulic structures. The objective of the second paper will be to evaluate the existing state-of-the-art, critically review the work identified in the first paper, recommend the more appropriate evaluation and prediction methodologies, and identify voids in the sphere of knowledge that could be addressed in research.

In this first paper, basic theory of mass transfer at the air-water interface is presented. The physical processes at hydraulic structures, such as air entrainment and turbulent mixing, open channel flow, closed-conduit (two-phase flow), and effects of sub- and super- atmospheric pressures, that significantly impact gas transfer are identified. The fluid mechanics of flow at hydraulic structures is reviewed. Structures are categorized based on these physical processes. Existing data and current measurement, evaluation, and predictive techniques are identified.

DEVELOPMENT OF A NUMERICAL MODEL TO PREDICT THE OXYGENATION OF WATER IN VERTICAL CIRCULAR CONDUITS

Paul N. Hopping

Tennessee Valley Authority
Engineering Laboratory
Norris, Tennessee 37828

To increase the level of dissolved oxygen in hydropower releases, the Tennessee Valley Authority has initiated a research program to help develop design techniques for the autoventing turbine. A major part of the research involves the development of state-of-the-art numerical models to predict the behavior of air/water flow in a hydroturbine, including the oxygen transfer. To test proposed formulations for two-phase flow, preliminary work has focused on the problem of the downward flux of an air/water mixture in a simple, vertical, circular conduit. In the laboratory, this situation is created by introducing air into water through an injection collar situated around the periphery of the conduit (see Figure 1).

In the numerical model described herein, computations were performed for a formulation based on mixture theory. The model solves simultaneously the equations for mean mixture momentum, mixture continuity, air continuity, and mixture density. The individual air and water components are assumed to be incompressible; however, since variations in the mean mixture density can be large, the effect of air is retained in the inertial terms for mean mixture momentum (i.e., the Boussinesq assumption is not utilized). The velocity of air relative to water is estimated based on observations of the motion of air bubbles in water. Turbulent correlations for the radial diffusion of mixture momentum and air are approximated using the isotropic k-ϵ model. Assuming axisymmetric conditions, and assigning appropriate boundary conditions, the numerical solution of the governing equations is obtained using a forward marching, upwind, finite volume procedure.

In the model, the injection collar is simulated by an inward radial flux of air at the wall boundary. Upstream of the collar, the water flow in the conduit is assumed to be fully developed. The formulation is limited to parabolic situations, hence to insure negligible backpressures, the rate of injection of air must be small compared to the axial velocity of the flow in the conduit. To compute the oxygen content, the mass transfer from air to water is assumed to be proportional to the difference between the existing concentration and the equilibrium saturation concentration of the gas. The dynamical behavior of the air/water mixture is assumed to be unaffected by dissolved gasses, hence the governing equation for the oxygen mass transfer is solved after completing the computations for the flow field. The formulation includes the effect of mean
0044r

mixture pressure on the saturation concentration; however, to estimate the gas surface area density, the mean diameter of the entrained air bubbles must be assumed.

Preliminary simulations with the model have given reasonable results for the mean velocity, air concentration, and dissolved oxygen; however, the $k-\epsilon$ formulation is found to overpredict turbulent diffusivities near the center of the conduit. To improve the turbulence model, anisotropic effects at the conduit wall and axis of symmetry are to be considered. Other problems that need attention are related to the energy dissipation caused by the entrained air bubbles, which is not correctly represented in the model. These and other concerns are to be investigated based on measurements to be performed in an aerated conduit in the laboratory. Once the model calibration and verification are complete, it should prove to be a useful tool for future parametric studies, such as the effect of turbulence on bubble size and oxygen mass transfer coefficient. The model should also serve as a good foundation for the more advanced formulations that will be needed to simulate the behavior of air/water flow in an autoventing turbine.

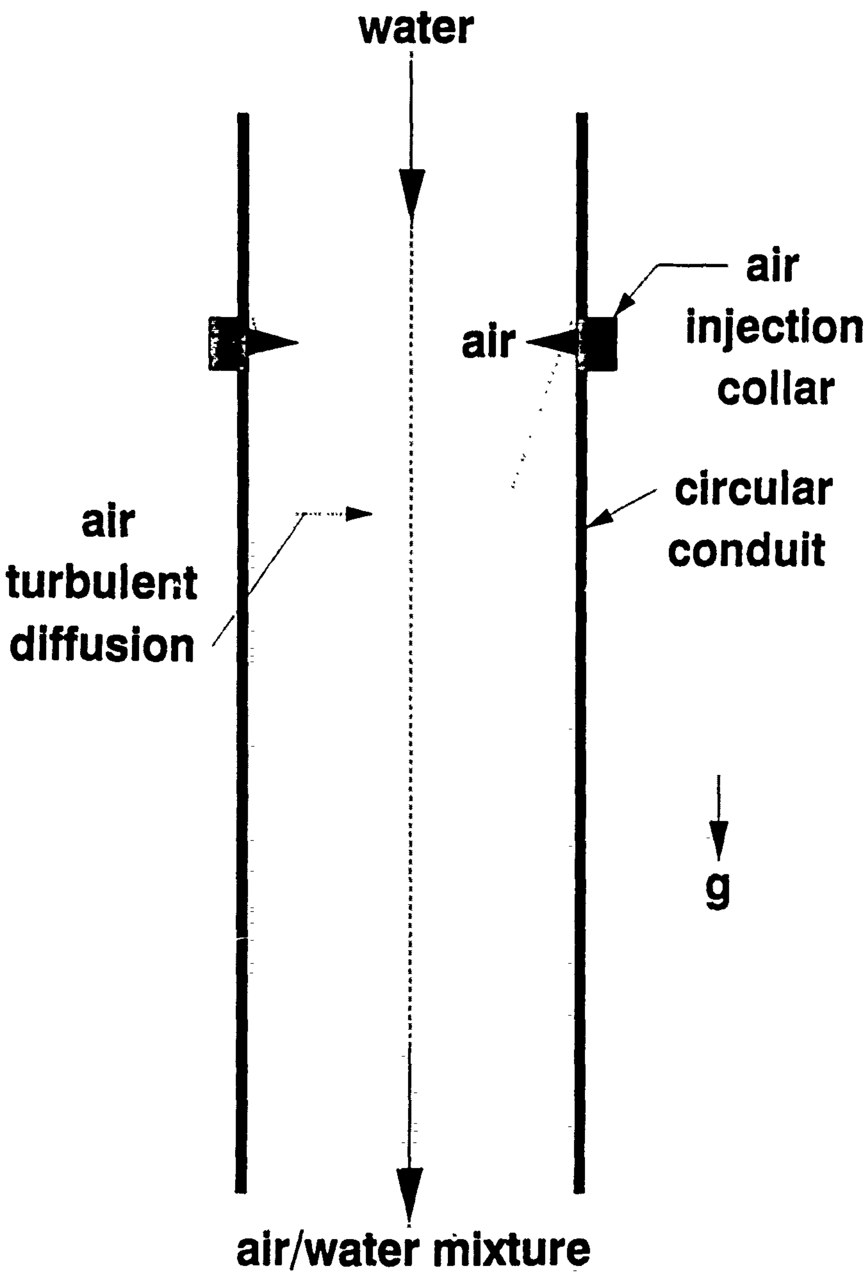

Figure 1 Air injection in vertical conduit.

OXYGEN TRANSFER IN TURBULENT SHEAR FLOWS

Kyung Soo Jun and Subhash C. Jain
Iowa Institute of Hydraulic Research
The University of Iowa
Iowa City, Iowa 52242

ABSTRACT

A typical hydroturbine draws its flow from lower levels of reservoirs where water may be severely depleted of dissolved oxygen (DO). Low DO in hydropower releases causes adverse environmental impacts. Recent environmental regulations require that the DO content of the discharges from hydroturbines be increased to a certain minimum level. Current techniques to enhance DO in hydropower releases are expensive and often ineffective. One of the most promising solutions to the DO enhancement problem is to develop an efficient autoventing hydroturbine which would allow aspiration of air at desired flow rates. One of the several research aspects need to be addressed in the development of autoventing turbines is the understanding g of the oxygen transfer process to maximize the oxygen transfer between air and water after the air is introduced in the flow through the turbine.

Most of the oxygen transfer in turbine venting takes place within the draft tubes in which the flow is essentially turbulent shear flow. Experimental data on oxygen transfer coefficient for turbulent shear flows are sparse. The principal objective of the study reported in this paper was to conduct fundamental laboratory experiments to elucidate and quantify the phenomenon of oxygen transfer from air injected into turbulent shear flows.

A schematic of the experimental set-up, which is currently being used to determine oxygen transfer coefficient for turbulent flows, is shown in the enclosed figure. It is a closed recirculating system consisting of a vertical test pipe of constant diameter which discharges into a basin. The air to the flow is injected through a number of orifices around the periphery of the pipe near its upstream end. The elbow and the conical diffuser at the downstream end of the pipe are provided to release the injected air through an air vent. A series of laboratory experiments are being conducted for a range of values of flow velocity and air flow rate. Experimental data include water discharge, air discharge, DO concentration with time, average bubble size, and water temperature. The paper would present the results of these tests.

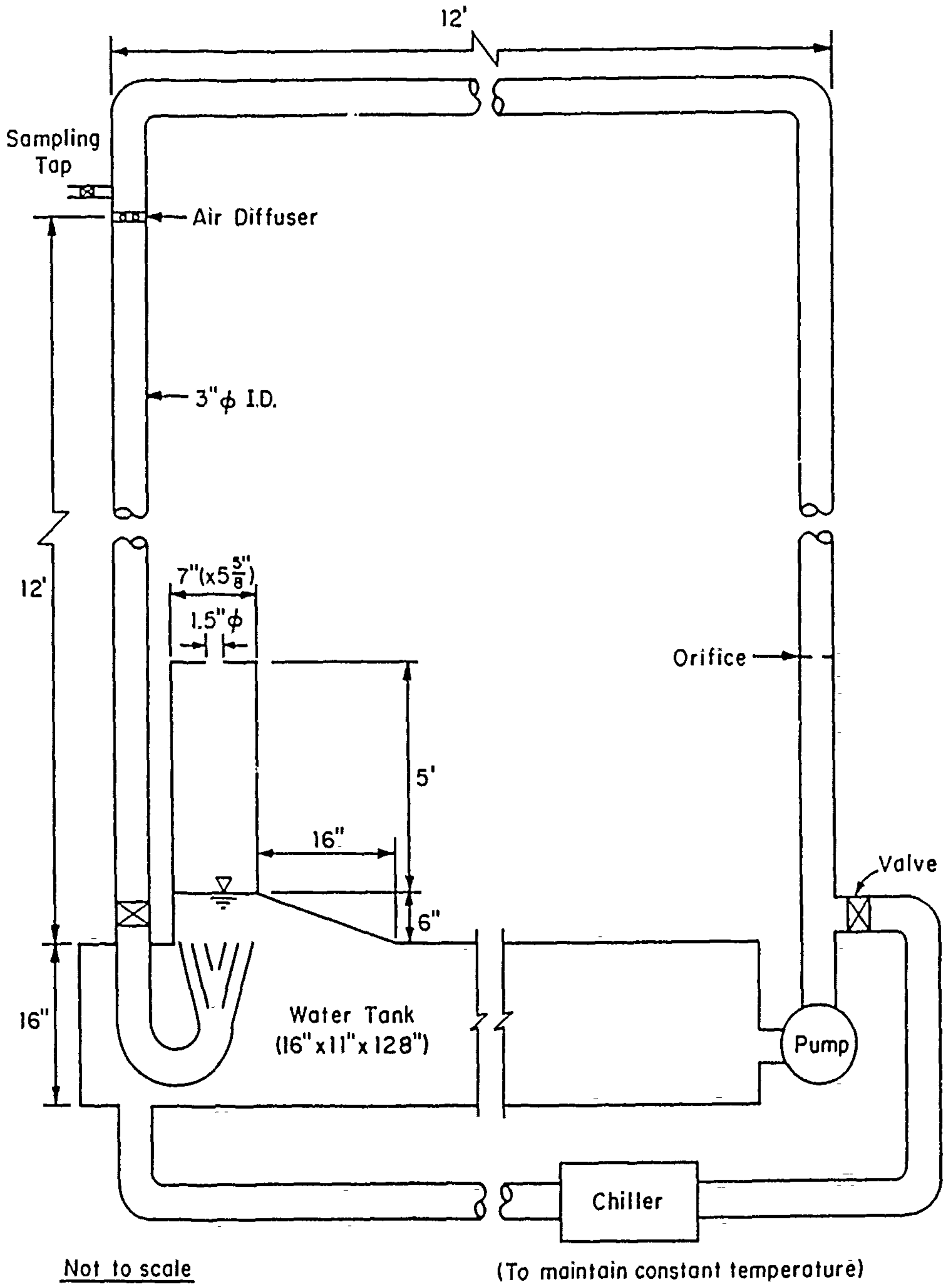

EXPERIMENTAL SET-UP

A SIMPLE EMPIRICAL MODEL OF AERATION AT NAVIGATION DAMS

Steven F. Railsback

Environmental Sciences Division
Oak Ridge National Laboratory
P.O. Box 2008, Oak Ridge, TN 37831-6036

Hydroelectric power plants have been proposed at many existing navigation dams on large rivers. Quantifying the aeration provided by such dams is important in assessing the environmental impacts of hydroelectric development. A hydroelectric project that reduces highly aerated spillage at a navigation dam can significantly reduce downstream dissolved oxygen (DO) concentrations, while a project at a dam that provides little aeration would have little effect on DO concentrations.

Several mathematical models of aeration at dams have been proposed (e.g., Mastropietro 1968; Gameson 1957; Wilhelms unpublished). These models commonly include terms for fall height or head loss, water temperature, and sometimes water quality; and they include dam-specific parameters that must be measured or estimated for each dam. Commonly used models such as Gameson's equation predict a value for the aeration ratio r, which is the ratio of the DO deficit [the difference between the saturation concentration of DO and the actual concentration, in milligrams per liter (mg/L)] upstream of the dam (D_a) to the DO deficit downstream of the dam (D_b). Under a given set of physical conditions (temperature, flow rate, head loss, etc.), r is assumed to be constant. The use of r as an aeration parameter includes the implicit assumption that as D_a approaches zero, D_b approaches zero, or that no aeration takes place when the water upstream of the dam is saturated with DO.

Aeration measurements from 28 navigation dams in the upper Ohio River basin were examined. The number of independent paired measurements of D_a and D_b varied between dams from 6 to 66, with an average of 21 per dam. Since aeration theory and previous studies indicated that aeration may depend on D_a, temperature, or flow rate (head loss being relatively constant at a navigation dam), stepwise linear regression modeling was used to determine which of these three parameters empirically predict D_b. The regression analysis showed that at most dams D_b could be predicted as a linear function of D_a only, with expected errors that are relatively small compared to other uncertainties in DO modeling. For example, the standard error (the square root of the sum of squared errors in the regression model divided by the degrees of freedom) was less than 0.2 mg/L at 9 dams and less than 0.5 mg/L at 26 of the 28 dams (Railsback et. al., in press).

The regression analysis showed that, at a number of dams, significant aeration takes place when the water upstream of the dam is saturated with DO (i.e., the intercept of the regression line is significantly less than zero, as in Fig. 1; the regression lines are included in the figures). Downstream supersaturation of 0.5 to 1 mg/L occurs at six of the dams when D_a is zero. Because aeration models that use r as an aeration parameter (such as Gameson's equation) implicitly assume that D_b is zero when D_a is zero, such models would be inappropriate at these dams where the intercept on the D_b axis is less than zero.

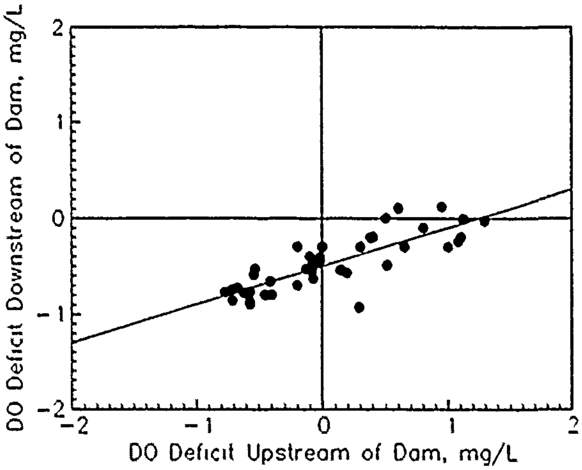

Fig. 1. Aeration at New Cumberland Lock and Dam, Ohio River.

Besides pointing out dams where supersaturation occurs, the linear models clearly distinguish between dams that do and do not aerate well. Dams where the slope of the regression line is nearly equal to one and the intercept is approximately zero (e.g., Fig. 2) provide little aeration since D_b is nearly equal to D_a. Dams where the slope is much less than one (slopes as low as 0.1 were obtained) and/or where the intercept on the D_b axis is significantly less than 0 (e.g., Fig. 1) are effective aerators.

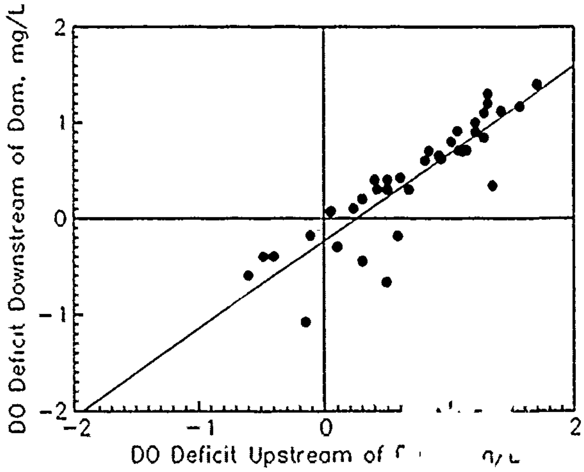

Fig. 2. Aeration at Hannibal Lock and Dam,

At two dams the regression analysis showed that D_b is essentially uncorrelated with D_a and approximately constant (e.g., Fig. 3). Because Gameson's equation approximates a linear relation between D_a and D_b, it would also be inadequate to model aeration at these two dams.

Regression analysis is a simple and appropriate way to model aeration at dams where field measurements of D_a and D_b are available. The regression analysis illustrates the aeration characteristics of a dam (i.e., whether or not a dam is an effective aerator and whether it provides supersaturation). Common regression analysis techniques can readily quantify the uncertainty in linear aeration models. No aeration models have been shown to model aeration adequately without field data for calibration, so the requirement for field data is not a disadvantage of regression analysis, compared to using other available models.

This research was sponsored by the Federal Energy Regulatory Commission, Office of Hydropower Licensing, and by the U.S. Department of Energy, under contract DE-AC05-84OR21400 with Martin Marietta Energy Systems, Inc.

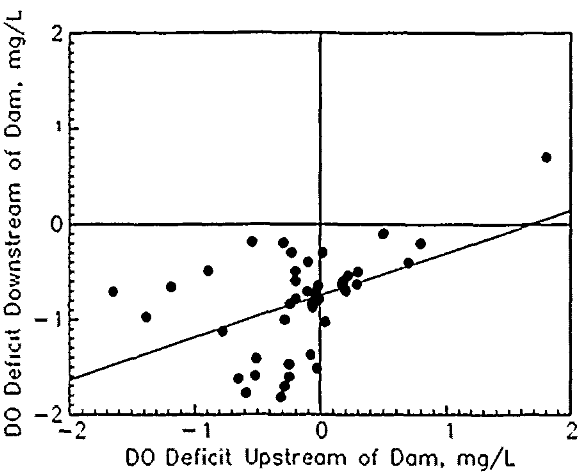

Fig. 3. Aeration at Allegheny River Lock and Dam No. 2.

REFERENCES

Gameson, A. L. H. (1957). "Weirs and Aeration of Rivers." Journal of the Institution of Water Engineers, 6(11), 477-490.

Mastropietro, M. A. (1968). "Effects of dam aeration on waste assimilation capacities of the Mohawk River." Proc. 23rd Industrial Waste Conference-- Part Two, Engineering Extension Series No. 132, Purdue University, Lafayette, Indiana, pp. 754-765.

Railsback, S. F., J. M. Bownds, M. J. Sale, M. M. Stevens, and G. H. Taylor (in press). Aeration at navigation dams in the upper Ohio River basin. Journal of Environmental Engineering.

Wilhelms, S. C. (unpublished). "Reaeration at low-head structures: preliminary results. Reservoir Water Quality Branch, Hydraulics Laboratory, U.S. Army Engineer Waterways Experiment Station, Vicksburg, Mississippi.

OXYGEN TRANSFER AT LOW HEAD DAMS

Alan J. Rindels and John S. Gulliver
Graduate Student and Associate Professor
St. Anthony Falls Hydraulic Laboratory
Department of Civil and Mineral Engineering
University of Minnesota
Minneapolis, Minnesota 55414 (612)627–4600

The oxygen transfer across the air–water interface at a spillway with a hydraulic jump or plunge pool, is an important source or sink of dissolved oxygen in a river–reservoir system. Normally, many river miles are required for a significant air–water transfer of oxygen to occur, but at a spillway this same oxygen transfer may occur in a short residence time of the spillway/hydraulic jump. The primary reason for this oxygen transfer is that air is entrained into the flow, producing a large number of bubbles. These air bubbles greatly increase the surface area available for mass transfer. In addition, the bubbles are pulled to various depths downstream of the hydraulic jump, increasing gas transfer and the possibility of supersaturation because of an increased saturation concentration at the higher pressures.

Because of the significant influence a hydraulic structure has on the downstream dissolved gas levels, engineers being required to predict these levels for a particular mode of hydraulic structure operation. In particular, some hydropower developments are being required to improve the downstream dissolved oxygen level, or show that development will not result in unacceptable dissolved oxygen concentrations. This is not currently possible with the predictive equations available in the literature.

A semi–empirical equation is developed for oxygen transfer using data taken by the authors at 11 sites with 37 individual field surveys (Rindels and Gulliver, 1986, 1989). All transfer efficiencies were converted to 20°C using the indexing relationship of Gulliver, et al. (1990). Head (or the difference between headwater and tailwater elevation) varied from 2.2 ft (.67 m) to 60 ft (18 m). Specific discharge varied from 0.6 cfs/ft (.06 m²/sec) to 35 cfs/ft (3.3 m²/sec). Tailwater depth varied from 0.80 ft (0.24 m) to 13 ft (4.0 m).

The resulting semi–empirical equation for transfer efficiency E is:

$$E = \frac{C_d - C_u}{C_s - C_u} = 1 - \exp\left[\frac{-0.082H}{1+0.2q} - 0.62d\right] \tag{1}$$

where C_d = downstream concentration of oxygen, C_u = upstream concentration, C_s = saturation concentration at the water surface, H = head (ft), q = specific discharge (cfs/ft) and d = effective tailwater depth (ft). Equation 1 was developed for low head dams which used a spillway and hydraulic jump to dissipate excess kinetic energy, and performs properly at the limits of the independent parameters. At large H or d, $E \rightarrow 1$. At small H and d, $E \rightarrow 0$. At large q, $E \rightarrow 1$, and at small q, $E \rightarrow E(H,d)$. The regression was log–linear, with a standard error of .07 percent in the units of E. The measured and predicted valves of E are given in Figure 1.

The equation was verified using data from 11 prototype spillways reported in Evans (1978) and from 1 prototype spillway reported in Daniil and Gulliver (1989). The measured and predicted valves of E for this data are given in Figure 2. The standard error was 0.16 in units of E.

Equation 1 may be used to predict oxygen transfer efficiency at low head spillways. The transfer efficiency of other compounds may be determined from the equations proposed for indexing gas transfer of self–aerated flows by Gulliver, et al. (1990).

References

Butts, T. A. and R. L. Evans, 1978. "Effect of Channel Dams on Dissolved Oxygen: Concentrations in Northeastern Illinois Streams", Illinois State Water Survey Circular 132, Urbana, IL.

Daniil, E. I. and J. S. Gulliver, 1989. "Impact on Hydroplant Operation on Dissolved Oxygen Concentration at the Blanchard Dam: Supplemental Findings", St. Anthony Falls Hydraulic Laboratory External Memorandum M–216, University of Minnesota, Minneapolis, Minnesota.

Gulliver, J. S., J. R. Thene, and A. J. Rindels, 1990. "Indexing Gas Transfer in Self–Aerated Flows", *Journal of Environmental Engineering*, Vol. 116, No. 3.

Rindels, A. J. and J. S. Gulliver, 1986. "Air–Water Oxygen Transfer at Spillways and Hydraulic Jumps", *Water Forum '86*, ASCE, New York, NY.

Rindels, A. J. and J. S. Gulliver, 1989. "Measurements of Oxygen Transfer at Spillways and Overfalls", St. Anthony Falls Hydraulic Laboratory Project Report No. 266, University of Minnesota, Minneapolis, Minnesota.

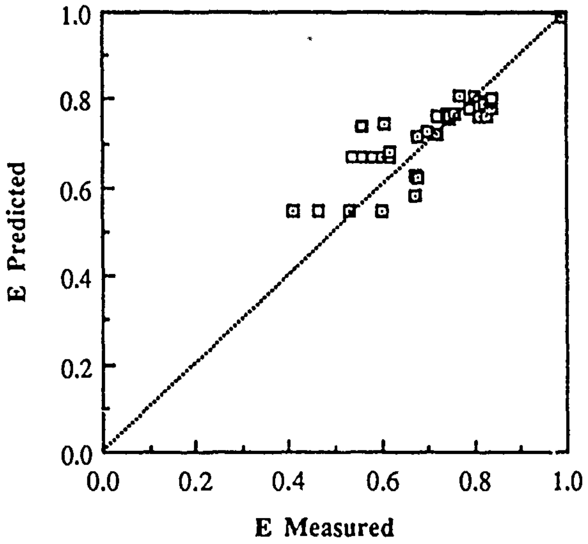

Figure 1 Predicted versus measured oxygen transfer efficiency(E) adjusted to 20° C for 30 surveys at 11 low head spillways.

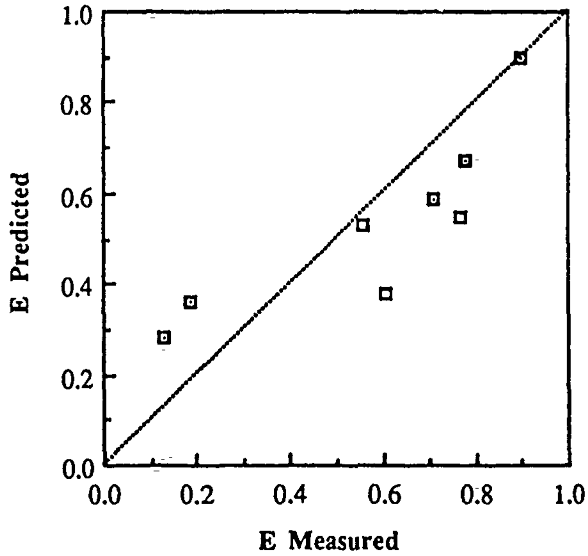

Figure 2 Predicted versus measured oxygen transfer efficiency(E) adjusted to 20° C for 8 additional surveys from the literature used to verify Equation 1.

TECHNOLOGY DEVELOPMENT FOR AUTOVENTING TURBINES

William R. Waldrop and Patrick A. March

Tennessee Valley Authority
Engineering Laboratory
Norris, Tennessee 37828

Experimentation with venting air into the hydroturbines at Norris Dam have convinced TVA that this is a viable method for increasing dissolved oxygen (DO) in the discharge of hydroelectric power plants. TVA has initiated an innovative research project that ultimately will provide industry-wide technology for the design and analysis of autoventing turbines. The goals of this research are threefold:

- To develop mathematical models of the flow of air/water mixtures through a turbine;

- To develop methods to analyze the oxygen transfer between air bubbles and water for the purpose of enhancing the process; and

- To develop test procedures for interpreting results of scale models on hydroturbines with mixtures of air and water.

To assist in this technology development, TVA has solicited and obtained cooperation from the U.S. Bureau of Reclamation, U.S. Corps of Engineers, and the Iowa Institute of Hydraulic Research. TVA is providing overall coordination of the research activities of these organizations as well as performing key elements of the research. This research program is designed to assure integration with the turbine upgrade program for Norris Dam which will include model testing and implementation of an autoventing turbine. The plans and status of the various components of this technology development program will be presented.

THE AERATION PERFORMANCE OF TRIANGULAR LABYRINTH WEIRS

Peter R. Wormleaton and Ebrahim Soufiani

Dept. of Civil Engineering
Queen Mary and Westfield College
London University, UK

INTRODUCTION

The use of weirs or free overfalls in the aeration of river flows has been the subject of a fair amount of laboratory and field study. Novak [1], provides a good summary of published work in this area. Most of the measurements to date, however, relate to the performance of rectangular notch type weirs.

Labyrinth weirs are hydraulic structures with their crests arranged in a variety of plan-forms (Fig. 1). They have the hydraulic advantage of extending the crest length, which at low heads will result in reduced variation in upstream water levels over a range of discharges. However, this advantage is gradually lost as the head increases, due to interference between the downstream nappes. The hydraulic performance of labyrinth weirs has been investigated by Hay and Taylor [2] amongst others. Whilst the collision and interference of the downstream nappes raises upstream heads, it also considerably increases downstream turbulence. The aim of this research was to investigate the effect of this increased turbulence upon the aeration capacity of these weirs.

EXPERIMENTAL METHOD

The experimental rig consisted of a recirculating system feeding a 2.5-m-long, 0.65-m-wide and 0.5-m-deep header tank. The test weirs were fixed into one end of this tank, whilst water levels were controlled by an overflow weir at the other end. The header tank was mounted upon a framework 2.5 m above ground level. Water overflowed the test weirs into a 0.75-m-long by 0.87-m-wide by 0.74-m-deep receiving tank, which was set on a steel frame that could be raised or lowered to adjust the drop height of the weir nappe. The water level in the receiving tank was adjustable. Dissolved oxygen concentration was read upstream and downstream of the test weirs using pHOX electronic probes, and the values read directly into a computer. The upstream dissolved oxygen level was maintained by controlled dosing with sodium sulphite in the presence of cobalt chloride.

The complete experimental programme encompassed both rectangular and triangular weirs with a variety of geometries, although this paper will concentrate on the latter. Six triangular weirs were tested in this series, all of which had the same crest length but the included angle θ (Fig. 1b) varied from 30 to 180 deg (i.e. a straight weir). Each weir was observed with flows ranging from 1 l/s to 4 l/s and drop height between 70 and 150 cm. The receiving pool depth was set so that in each case it just exceeded the penetration depth of the overfall jet.

RESULTS

One of the most commonly used parameters of aeration performance of weirs is the DO deficit ratio, which is defined as upstream DO deficit/downstream DO deficit. Clearly, the greater the value of this ratio, the better the performance of the weir in this respect. Plots were drawn for each weir (Fig. 2) showing the variation in DO deficit ratio with drop height for a range of flows. In each case the DO deficit ratio was shown to increase with drop height. The variation with discharge, on the other hand, was somewhat more interesting. For the larger weir angles, the DO deficit ratio decreased with increasing discharge over the whole range of drop heights considered (Fig. 2a). However for the smaller angles (Fig. 2b), the variation with discharge was seen to reverse at greater drop heights. The explanation of this is to be found in the nature of the overfall jet and the mechanisms of aeration.

The aeration process at a weir is complex, but it can be considered to take place in three phases: (1) during fall, (2) via the free surface of the receiving pool and (3) in the air-water bi-phasic zone due to air entrainment. Phase 3 is governed by the air entrainment rate and the bubble contact time in the water. Clearly, a compact high-velocity jet will tend to carry the bubbles to a greater depth than a slower disintegrated jet. For the larger angle weirs, observations and photographs showed that the jet remained sensibly smooth and compact over the range of drop heights used. However, for the smaller angles of weir, the colliding nappes caused the jet to disintegrate at a certain distance below the weir crest (the break-up length) and then fall in a dispersed manner. The bubble penetration in this latter case was less, and so the DO deficit ratio for such jets was reduced. It can be seen from Fig. 2b that the variation of DO deficit with drop height is less pronounced at drop heights greater than the break-up length. This causes the reversal of DO deficit variation with discharge, since the break-up lengths are shorter for lower flows. It should be noted that no break-up was observed for the 120-deg weirs in Fig. 2a.

Fig. 3 shows the variation in DO deficit ratio with weir angle for two discharges, each at two different drop heights. Clearly, in all cases, the DO deficit increased as the weir angle θ decreased to 45 deg. This is essentially due to the impinging downstream nappes, which increase the turbulence and surface roughness of their combined resultant jet. Provided this jet remains unbroken, it then carries more air into the receiving pool, so encouraging aeration. It is noticeable that for the 700-mm drop height, where the height of fall was always less than the break-up length, the aeration performance was better for the lower discharge throughout. However, at the drop height of 1400 mm, the DO deficit for the 1 l/s discharge does not increase with the smaller weir angle to the same extent as it does for 4 l/s, the reason being that the drop height exceeds the break-up length at weir angles less than 90 deg for this lower discharge.

It is clear from these results that aeration is considerably enhanced at a particular discharge and height of fall by using a triangular labyrinth weir. However, for lower flows, this advantage may be lessened if the drop height exceeds the break-up length.

The full paper considers relationships between the break-up length, discharge and weir geometry. Similar relationships to determine DO deficit ratio are also given.

REFERENCES

1) Novak, P. "Improvement of Water Quality in Rivers by Aeration at Hydraulic Structures," veroff. inst. f. siedl. wass. wirtsch. No. 14, tech. univers. graz, 1988.

2) Hay, N. and Taylor, G. "Performance and Design of Labyrinth Weirs," J. Hyd. Div., Proc. ASCE, Vol. 96, HY11, Nov. 1970.

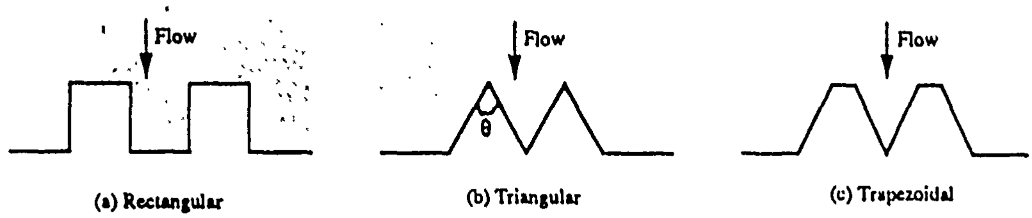

Figure 1. Labyrinth Weir Planforms.

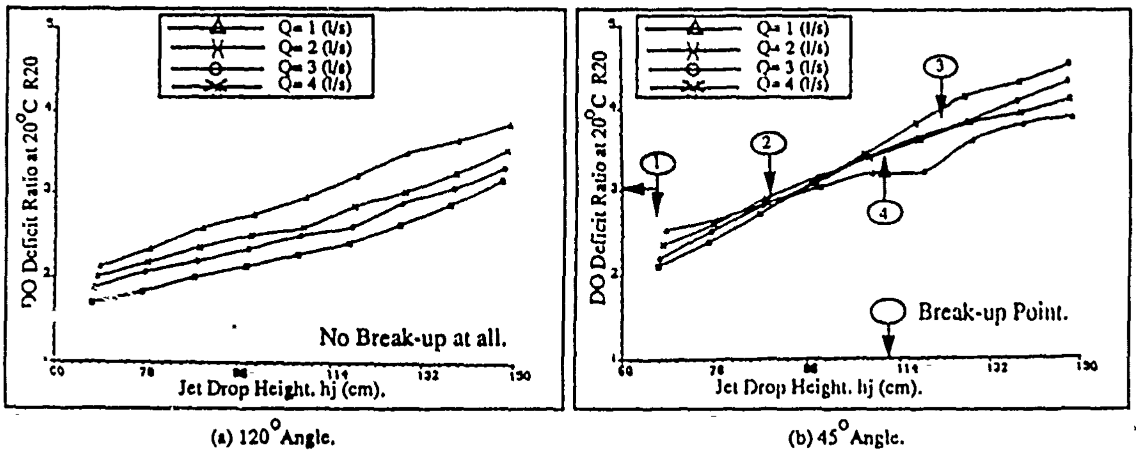

Figure 2. DO Deficit Ratio V Drop Height for Varying Discharge.

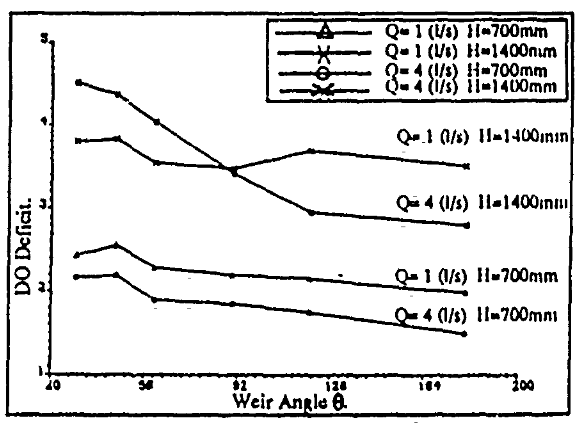

Figure 3. DO Deficit Ratio V Weir Angle θ for Varying Discharge and Drop Height.

GROUNDWATER

The Volatilization Rate Constant for Organic Compounds in Unsaturated Porous Media during Infiltration

H. Jean Cho and Peter R. Jaffé
Department of Civil Engineering and Operations Research
Princeton University

1 Abstract

A column study is being conducted to quantify mass transfer processes between gaseous phase and aqueous (dissolved) phase organic contaminants in the soil system during infiltration. In an isothermal, isobaric, non-reacting soil system in the absence of an advective flow of the soil gas or soil liquid phase, the distribution of a water-soluble organic compound among phases will approximate the distribution at thermodynamic equilibrium. Thus the ratio of gas concentration to water concentration will be equal to the ratio defined by Henry's constant. However, when advection becomes important, either in the gas phase (e.g. in soil venting) or in the liquid phase during infiltration, deviation from Henry's law can and does occur.

This deviation from Henry's law has been observed in preliminary small-scale sand column experiments which were conducted to measure gas phase fluxes from homogeneous, unsaturated porous media during steady state infiltration of water. The glass columns were 30 cm in height and had an inner diameter of 2.5 cm. They were packed with coarse sand from 5 cm from the bottom to 5 cm from the top of the column, for a total sand depth of 20 cm. A volatile, slightly water-soluble compound, trichloroethylene (TCE), was chosen for the experiments. The movement of the compound was from a reservoir of solute dissolved in water located below the sand, through a tension-saturated zone and overlying unsaturated zone, to the soil surface. With the use of a high precision peristaltic pump, constant infiltration rates were applied to the columns. Gas phase and liquid phase TCE concentrations above and below the sand were measured by gas chromatography. The TCE vapor flux from the sand was measured by collecting TCE vapor with an activated carbon trap and extracting the TCE from the carbon with carbon disulfide. The steady state gas fluxes from this system and the results of chloride tracer tests conducted in the columns were used to determine whether the gas and liquid phases within the columns were in equilibrium.

Six infiltration rates—0.219 cm/h, 0.226 cm/h, 0.281 cm/h, 0.422 cm/h, 0.426 cm/h, and 1.34 cm/h—were simulated. We observed TCE vapor fluxes ranging from 0.011 $\mu g/(h \cdot cm^2)$ for an infiltration rate of 0.219 cm/h to 0.006 $\mu g/(h \cdot cm^2)$ for an infiltration rate of 1.34 cm/h. These fluxes were inputs into one-dimensional finite element Galerkin mass transport models. Both equilibrium and nonequilibrium transport models were used. In the nonequilibrium case, the finite element model was used ... conjunction with an optimization program, MINOS (available from the Systems Optimization Laboratory, Department of Operations Research, Stanford University, Stanford, CA 94305), to determine an appropriate soil-gas phase–soil water phase mass transport coefficient, or volatilization rate constant.

An equilibrium formulation using a dispersivity to characterize local variations in liquid flow velocity resulted in predicted vapor fluxes which were controlled by the dissolved-phase dispersive phenomena. This dispersive transport acts counter to the average velocity field. In other words,

dispersion counter to average flow appears to be the predominant transport mechanism of volatile compounds in an equilibrium soil gas-soil water system. This is physically unrealistic.

Two nonequilibrium models were fitted to the columns based on the bottom- and top-end concentrations and measured vapor fluxes. The first nonequilibrium model was the convection-dispersion equation with a first-order rate constant for volatilization. The second model incorporated a "mobile–immobile" formulation to characterize nonuniformities in the flow regime of the infiltrating water. The concentration profiles that were predicted using these transport models were used to calculate concentration gradients. The gradients were employed in Fick's first law to obtain the net vapor fluxes, which were compared with the measured vapor fluxes. The optimal value of the volatilization rate constant for a given column was the value which resulted in a predicted vapor flux which matched the measured vapor flux.

For a given infiltration rate, the optimal value of the volatilization rate constant ranged over three orders of magnitude from 10^{-4} h^{-1} to 10^{-1} h^{-1}, depending upon the assumptions made. Corresponding to each fitted value of the volatilization rate, a concentration profile was generated. Since concentration measurements within the column were unavailable, the fitted values of the volatilization rate constant were rough estimates. To more accurately and precisely measure the volatilization rate constant, a large column study is being conducted.

In this large column study, a column (4 feet tall and 12 inches in outer diameter) is packed with 80 cm of the same coarse sand (ASTM C-190) used in the preliminary experiments. The sand overlies a reservoir of water saturated with the TCE. Above the sand, a drip plate containing 600 30-gauge hypodermic needles, arrayed in a square grid and 1 cm apart, supplies water at constant flowrates down to 0.008 cm/h. The water infiltration rates are regulated by adjusting the height of the water above the needles. At 6 cm intervals, two sets of probes enter the sand at opposite sides of the column. The next set of probes is 6 cm below and 60° shifted from the previous set, so the probes are staggered in a spiral fashion. On each side of the column, a porous ceramic cup tensiometer connected to 1/16 inch stainless steel tubing is filled with water and embedded 8 cm into the column. The tensiometer is capped with a sealed septum at the edge of the column and serves as a lysimeter for water concentration measurements. Two centimeters above the porous cups, a miniature glass funnel, 1/4 inch in inner diameter with a narrow opening, allows for gas phase concentration measurements. The funnel openings are also located 8 cm into the column. The funnels are connected to 1/16 inch stainless steel tubing and capped at the edge of the column with a septum seal. Because of the width of its inner diameter, the funnel remains filled with air for most unsaturated soil states (except for water contents near saturation) due to capillary phenomena. Finally, on one side of the column, another porous cup tensiometer is filled with water and connected to a pressure transducer for matric pressure measurements. The column has twenty-two gas concentration probes and twenty-two water concentration probes and eleven tensiometer-transducer connections. In addition to these probes, gas and water phase concentrations above and below the sand as well as vapor flux measurements are available, as in the 20 cm columns.

The two major factors that are important in modeling transport of dissolved/gas phase organic compounds in unsaturated soils during infiltration are: (1) the degree to which heterogeneities in the velocity of the infiltrating water affect the overall transport process; and (2) the degree to which thermodynamic equilibrium between the gas and the dissolved phase is reached. If thermodynamic equilibrium is not achieved, a quantitative measure of interphase mass transfer is required. The column apparatus, as described, is capable of addressing both of these factors. Because gas phase and liquid phase concentrations can be obtained at essentially the same spatial point at numerous locations within the column, deviations from thermodynamic equilibrium can be observed and quantified. If equilibrium is not achieved, there is sufficient data to accurately estimate a volatilization rate constant. To address the issue of flow heterogeneities in the column, the high spatial resolu-

tion of measurement points allows one to obtain detailed tracer breakthrough data at twenty-two locations within the column.

To date, dry column tests have been conducted to test the precision of gas phase concentration measurements and to select an appropriate tortuosity correction for gas phase diffusion. Column experiments with infiltrating water have been started, and data will be available during the summer of 1990.

The Use of Microbubbles to Enhance Oxygen Transfer to Flowing Ground Water and to Bioreactors

D.L. Michelsen, M. Lotfi, J.A. Kaster and W. Velander
Department of Chemical Engineering
Virginia Polytechnic Institute and State University
Blacksburg, VA 24061

Microbubble generation techniques have been developed for the production of a 55 to 75% dispersion of 50 ± 40 micron microbubbles. The microbubbles can be generated with a low surface tension solution such as a yeast fermentation broth or using as low as a 100 ppm surfactant solution in pure water. For laboratory and modest pilot testing a spinning disk generator providing as much as 1 to 2 liters per minute of microbubbles has proved satisfactory. Several different sized continuous spinning device generator prototypes have been designed, fabricated and tested, with production capabilities ranging from 10 to 80 liters per minute of the dispersion mixture containing 50 to 65% microbubbles.

Analytical procedures have been standardized to measure <u>quality</u> defined as the percent of gas in the gas plus water dispersion. The <u>stability</u>, H (lower the better), has been defined as milliliters of clear liquid interface in a standard 23.5 cm high, 250 ml pyrex glass graduate, one minute after sampling, H', divided by the milliliters (or weight in grams) of water in the 250 ml graduate given as a percentage. These key parameters can be determined quickly by taking a 250 ml sample, weighing it, and measuring clear liquid ml after one minute. Typical H' values of 8 to 30 ml convert to H values of 9.4 to 35.3 if microbubble quality is 66%. <u>Void air</u>, the portion of gas not incorporated into the microbubbles, can also be determined by material balance on the total generation but also by collecting a total of 250 ml of dispersion in a closed system while measuring total dispersion plus void air in an inverted graduate. Bubble size distribution was determined using <u>microscopic techniques</u>. This involved flowing the dispersion through continuous sampling cell, stopping flow, photographing through the microscope directly or photographing the black and white TV image, and subsequently using image analysis techniques to determine distribution. These size distribution results have proved useful for parameter studies.

The use of <u>oxygen</u> microbubbles and straight air sparging for in-situ bioremediation of flowing contaminated ground water has been a subject of continued pilot plant research using a 7 ft high by 7 ft wide, by 5 in. deep (front to back) vertical slice test cell. Previously microbubbles had been shown to flow into saturated soil matrices under slight pressure and then adhere and be retained for long periods of time in the matrix. The pilot testing addressed oxygen transfer and utilization so the cell, typically filled with coarse sand, was treated with a sodium azide solution to kill any biological organisms. Testing was conducted with the water table 2 to 4 ft below the sand surface. A series of two horizontal injectors,

one above the other, provided an aerated, 24 in. high (to the water table), by 5 in. deep and estimated six in. length, vertical zone in the saturated region through which ground water flows horizontally (about 6 inches) with oxygen transfer taking place. A material balance on oxygen was conducted by controlling the oxygen delivered (input) as microbubbles, determining the total oxygen microbubbles retained in the cell at time zero upon injection by measuring water overflow from the cell with no ground water flow. After microbubble injection was completed and cell overflow stopped, anaerobic ground water (dissolved oxygen less than 1 mg/l) was slowly pumped through the cell with transfer of dissolved oxygen to the flowing ground water from either the retained microbubbles or continuously sparged air. This was completed by taking numerous groundwater samples and measuring dissolved oxygen. Testing was conducted for several days and longer. Any oxygen released or vented from the initial microbubble injection was collected from under a clay horizontal layer at the water table interface with an initial oxygen microbubble injection. Initially, 0.002 g moles/hr of oxygen was observed to be transferred to the ground water decreasing with time, and finally, a total of 0.41 g moles of oxygen was transferred over a 44 hour duration. The K_{la} (oxygen transfer coefficient) was found to be 0.15 hr^{-1}. The oxygen balance for a 44 hour run indicated that of the 0.240 g of moles oxygen injected, roughly 38% was lost immediately, another 25% was vented over time, 17% was transferred to the flowing ground water with the final 20% unaccounted for but a portion of that at least visibly dispersed within the saturated soil matrix.

With air sparging the rate of transfer to the ground water was .00067 g mol/hr although the rate dropped as channeling developed to the surface. The mass transfer rate is higher at 0.44 hr^{-1} likely due to continued sparging. Less than 1% of the sparged oxygen in the air was transferred to the flowing ground water.

The use of an air microbubble dispersion to supply oxygen for aerobic fermentation in a standard two liter tank fermenter was also studied. The microbubble dispersion was formed using the natural surfactants formed during the fermentation. Sacchapamyces cervisiae culture was used as the media for yeast fermentation. When comparing the use of microbubble dispersion and standard air sparging to provide oxygen for aerobic bacterial action, it was found that the use of a microbubble dispersion resulted in growth rates equal to or greater than when sparged air was used. The oxygen transfer coefficient with the air microbubble dispersion was found to be 190 hr^{-1}, independent of impeller speed in the 100-580 RPM range, while the oxygen transfer coefficient with air sparging increased from 55 to 132 hr^{-1} over the same range of impeller speeds.

The potential of using standard microbubbles compared to sparged air has also been tested for the chemical oxidation of sulfite to sulfate in the presence of a copper catalyst. After duplicating earlier oxygen transport experiments with air sparging in a 2 liter mix tank, the change to microbubbles resulted in a K_{la} increasing from 1.5 to 5 hr^{-1} l^{-1} (shown to be a function of input mixing energy), to a

range of 90 to 200 hr^{-1} l^{-1} which appeared to be independent of input mixing energy.

The use of microbubbles due to their large surface area (25-90 μm diameter), slower rise velocity in liquid media and surface selectivity (their surface can be charged or neutral) in biological systems were found to be promising. The increase in microbial growth rate and in-situ transfer of oxygen to anaerobic ground water was evidenced from the findings of this research.

EVALUATION OF VADOSE ZONE SOIL GAS SAMPLING TECHNIQUES FOR VOLATILE ORGANIC COMPOUNDS

Qing Zhu

Department of Civil and Environmental Engineering

Utah State University, Logan, Utah 84322

Abstract

Soil vapor monitoring, the sampling and analysis of vapor samples collected from subsurface pore space, has been shown to be an effective means of broadly delineating the extent of contamination in the interval between the land surface and groundwater at many locations contaminated with volatile organic compounds (VOCs). Soil gas concentration measurements are effective due to depends upon the fact that VOCs such as petroleum products and organic industrial solvents, will volatilize from surface spills, leakage from underground storage tanks, and improper waste disposal practices, and travel through the vadose zone by advection and diffusion. Soil gas concentration measurement techniques which have been used for vadose zone VOCs determinations include: flux chambers, ground probes, surface-downholes, and monitoring wells. Surface-downhole sampling methods are most often used for the development of vertical and horizontal profiles of organic vapor plumes.

Because there are many specific parameters (i.e., vapor pressure, solubility, density, boiling point etc.) which influence the determination of VOCs in soil gas, and because many complex interactions occur in the soil gas phase, quantitative soil gas concentrations are of limited value without a detailed understanding of site-specific soil and waste parameters. An evaluation of surface-downhole soil gas sampling techniques was conducted using an experimental laboratory microcosm system consists of large scale glass (15.25 centimeter, 200 centimeter high) column systems (Figure 1) filled with air dried sand. The columns were constructed with six side sampling ports spaced at approximately 40 cm intervals. Surface-downhole sampling probes were incorporated into the original design as shown in Figure 1 to allow comparison the results of there two soil vapor sampling locations. Samples taken from side sampling port were thought to be more accurate because of the shorter sampling distance.

A comparison of the results between the two sampling locations showed that surface-downhole samples were useful for the quantitative determination of the extent and location of subsurface contamination. Overall concentrations obtained from the surface-downhole method were consistently lower than the column-port samples for the eleven VOCs evaluated in this study which have a wide range of physical properties (Figure 2). Correlation of surface-downhole versus column-port samples indicated a negative sampling bias that ranged from -9.7 to -34.9% for the test compounds representative of petroleum products and industrial solvents frequently detected in contaminated groundwater. Regression analysis showed that difference in concentration of all compounds between the surface-downhole and column-port samples was relate to the vapor pressure and boiling point of the compounds. This bias was dependent upon the compound vapor pressure and boiling point. Compounds which have vapor pressure below 1.0 mm Hg (20°C) and boiling points above 179°C are particularly difficult to monitor using surface-downhole soil gas sampling technology yielding the highest sampling bias, i.e.,>-34%. Results of this study suggest that while surface-downhole soil-gas sampling method serve as a preliminary screening technique is effective in selecting locations for detailed sampling and analysis. If this method is used to quantitatively measure the concentration of the VOCs, it should be applied with caution for field activities related to routine leak detection, or contaminate transport model calibration. This consistency of sampling bias over sampling depth among compounds of widely varying vapor pressure and boiling points would be useful as a correction method for subsurface organic vapor concentration determinations in field investigations.

This study evaluated a laboratory scale surface-downhole soil gas sampling monitoring systems by comparing it to samples taken horizontally from the column side, it was also found that the sampling error was independent of the sampling depth, soil-gas sample concentration, and contamination location (i.e., surface spill accident, subsurface tank leaking) based on ANOVA analysis results.

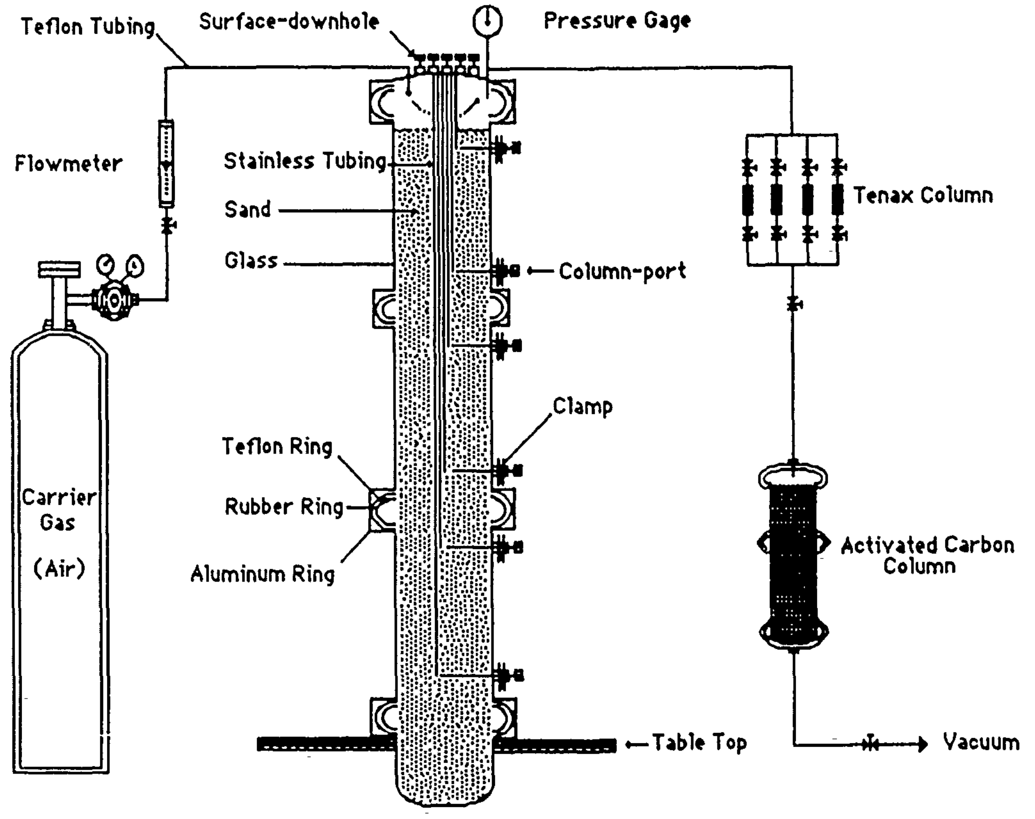

Figure 1. Laboratory microcosm apparatus used in laboratory subsurface soil gas sampling study

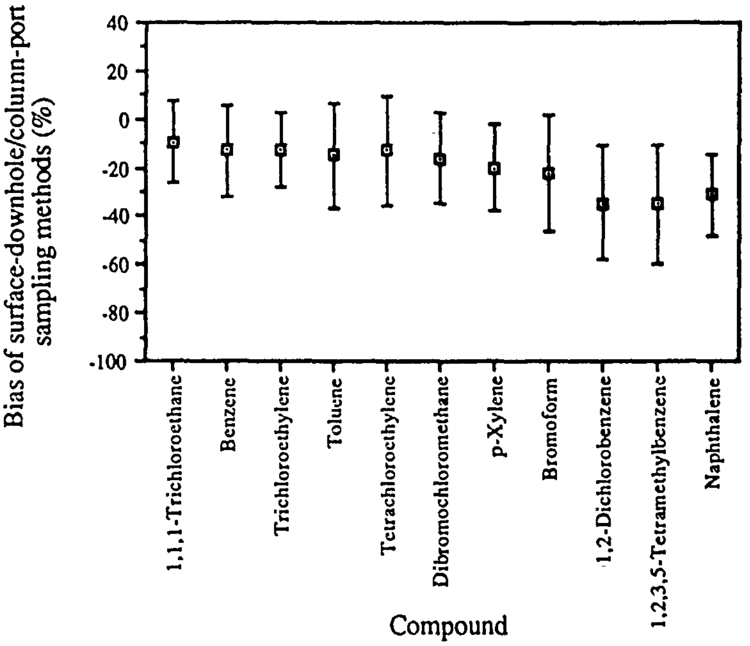

Figure 2. Bias of surface-downhole/column-port sampling methods for eleven compounds

BIOGEOCHEMICAL CYCLES/
SEAS/OCEANS

Correlation of Fractional Foam Coverage With Gas Transport Rates

W. E. Asher

Battelle/Marine Science Laboratory, 439 W. Sequim Bay Road, Sequim, WA 98382.

E. C. Monahan

Marine Sciences Institute, Avery Point, University of Connecticut, Groton, CT 06340.

R. H. Wanninkhof

Lamont-Doherty Geological Observatory, Palisades, NY 10964

Generally, calculating the global flux of a gas into the ocean requires summation of a series of regional fluxes estimated using maps of global wind fields, air/sea gas concentration gradients, and a wind speed parameterization of the gas/liquid mass transport rate, k_L. Because the relationship of k_L with wind speed is poorly known, there may be large errors introduced into the calculation of these regional fluxes through uncertainties in either the relation of k_L with wind speed or the global wind field. Therefore, accurate global maps of k_L would help reduce the uncertainties in the calculation of gas fluxes into and/or out of the ocean. Such maps could be generated from satellite data if k_L could be determined from remotely sensed parameters.

As an initial step in the development of a method for remote prediction of air/sea gas exchange rates, laboratory studies were conducted to investigate the role of bubble plumes in promoting gas/liquid mass transport. Because bubble plumes increase the microwave emissivity of water surfaces, it may be possible to determine oceanic whitecap coverage from satellite-mounted passive microwave radiometers. Correlation of gas exchange velocities with whitecap coverage would then allow estimation of air/sea exchange rates using this satellite data. As an initial step in developing this remote-sensing-based method of determining k_L, the conditions under which the fractional area bubble plume coverage, F_C, may be used as a predictor of k_L were investigated.

The apparatus used in these experiments was a 1.3 m x 1.3 m x 2.6 m acrylic tank equipped with a tipping bucket mechanism. The tipping bucket generated bubble plumes by periodically dumping a volume of water into the tank. Computer control of the tipping bucket allowed accurate variation of the total volume of water in the bucket and frequency of bucket cycles. This provided control of the intensity and duration of the bubble plumes. F_C was calibrated in the tank as a function of bucket spill height and spill volume by analysis of video records of bubble plume surface area. Calibration of F_C allows generation of a known F_C under a variety of conditions including bucket height above the water surface, tipping volume, and salinity.

k_L was measured as a function of F_C in freshwater and seawater for the liquid-phase rate-controlled gases oxygen (O_2), elemental mercury (Hg), sulfur hexafluoride (SF_6), and dimethyl sulfide (DMS). This

suite of gases provided a range of molecular diffusivities to be studied. The transport process was studied as a function of intensity and duration of the bubble plumes.

Measurement of k_L for several gases with varying molecular diffusion coefficients allowed determination of the Schmidt number dependence of the bubble plume-mediated gas exchange process. The results show that the bubble plumes generated by the tipping bucket are very efficient promoters of gas exchange and that k_L is correlated with F_c as suggested by Monahan and Spillane (1984). Although more research is necessary, this suggests that it may be possible to predict air/sea gas exchange rates using satellite measurements of whitecap coverage. In addition, the results suggest that gas transport at the ocean surface may be controlled mainly by breaking waves.

References

Monahan, E. C., and M. C. Spillane, 1984. "The Role of Oceanic Whitecaps in Air-Sea Gas Exchange" In Gas Transfer at Water Surfaces, eds. G. H. Jirka and W. Brutsaert, D. Reidel, Hingham, MA, pp. 495-504.

Acknowledgement

The Battelle/Marine Sciences Laboratory is part of the Pacific Northwest Laboratory, which is operated for the U.S. Department of Energy by Battelle Memorial Institute under Contract DE-AC06-76RLO 1830.

STRUCTURE OF THE DRIFT CURRENT OBSERVED UNDER WIND-GENERATED CAPILLARY-GRAVITY WAVES

Guillemette Caulliez

Institut de Mécanique Statistique de la Turbulence
12 Ave du Général Leclerc, 13003 Marseille (France)

Because of the respective molecular diffusion properties of the air and the water, it is now well established that gas exchange across the air-sea interface is mostly controlled by the turbulent structure of the upper water boundary layer. However, many laboratory or field observations suggest that free surface phenomena, such as wave breaking, bubble clouds, etc., play also a quite significant role. More specifically, the latter are generally assumed to be accountable for the large increase of gas transfer rate over the classical predictions from turbulent flow on solid walls. Among these processes, the generation and development of capillary-gravity waves at the water surface are frequently quoted (Hasse and Liss, 1980; Jahne et al., 1984; McCready and Hanratty, 1984). At the moment, it is undoubted that the associated effects are still misunderstood. In the work presented here, we attempt to bring a new insight to this question by investigating the water velocity field below wind-generated short waves.

The facility where experiments have been carried out is an 8-m x 0.60-m x 0.50-m wind-water channel. The velocity measurements in water were performed with a two-component laser-Doppler velocimeter, equipped with a 2W Argon-ion laser, an electro-acoustic Bragg cell and two frequency trackers. The optical configuration allowed measurement of the longitudinal and vertical flow velocities from a few centimeters to about 0.5 mm from the water level at rest, with a probe volume section 0.1 mm in diameter. The water surface displacements due to waves were recorded simultaneously by means of a thin wire capacitance probe located very close to the LDV measuring point. Special care has been taken during these experiments in the adjustment of the air and water flow function, the cleanness of the water surface and the calibration of the measuring devices. In accordance with our objective, the observations have been conducted at a moderate wind speed of 5 m/s, for four different fetches in the upwind part of the tank where only capillary-gravity wind-waves are present at the water surface.

Results of the mean and fluctuating velocity measurements within 1 cm of the interface and the wave records reveal a very strong coupling between the drift current structure and the surface wave development by the wind. Thus, three typical stages can be defined. In the first one, the wind-generated waves are not perceptible by eye yet, and the water flow is found laminar as shown by the linear vertical mean velocity distribution and the lack of turbulent motions. In the second one, the capillary-gravity waves become visible in some ruffled patches or divergent streaks. It appears clearly from the instantaneous signal observations that the first current instabilities occur inside these areas. This is also confirmed by the large mean velocity decrease in the 2-mm-thick interfacial sublayer and the fast deepening of the whole boundary layer. The third stage is characterized by a fully developed capillary-gravity wave field which covers entirely the water surface. The largest wave amplitude reaches about 2 mm. There, the water surface flow moves to a homogeneous turbulent flow as the close linear-logarithmic shape of the mean velocity profile enables us to state.

With regard to mass transfer, the "turbulent" structure of the drift current in the second growth stage, and to a certain extent in the third one, proves to be of special interest. Through the analysis of the longitudinal and vertical velocity spectra and cross spectra at different depths, the existence of large amplitude motions at the wave frequency within a sublayer of 2 to 5 mm thickness is shown. By comparison with theoretical predictions made on the basis of a linear model which accounts for the mean shear flow, we find that these motions cannot be interpreted only as the orbital motions due to the water surface displacements. Further investigations on their peculiar properties suggest they are related to a type of "convective" disturbances which can be represented schematically by Figure 1 below.

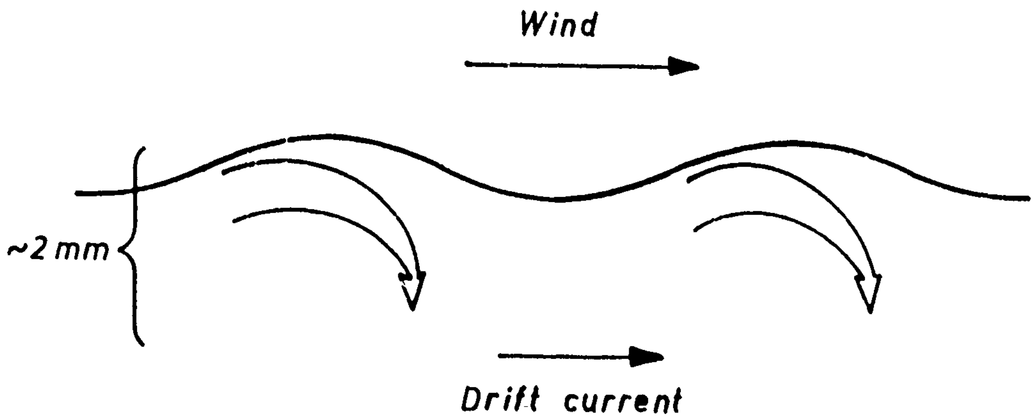

Fig. 1. Schematic picture of "convective" motions under capillary-gravity wind-waves.

These measurements provide confirmation of the facts revealed by Okuda et al. (1976) by means of water flow visualizations where very similar motions were observed under wind-generated capillary-gravity waves. Finally, the flow transport properties are examined by comparing these phenomena to the turbulent spots occurring during the laminar-turbulent transition of a boundary layer flow on solid wall.

In conclusion, the efficiency of such an intermittent process for transferring gas across the ocean or lake air-water interfaces is discussed. It is found to be essentially related with the large-scale turbulent intensity of the wind.

References

Hasse, L., and Liss, P. S., 1980, Tellus, 32, 470-481.

Jähne, B., Huber, W., Dutzi, A., Wais, T., and Ilmberger J., 1984, in "Gas transfer at water surfaces," W. Brutsaert and G. H. Jirka, eds., D. Reidel Publ. Co.

McCready, M. J., and Hanratty, T. J., 1984, in "Gas transfer at water surfaces," W. Brutsaert and G. H. Jirka, eds., D. Reidel Publ. Co.

Okuda, K., Kawai, M. S., Tokuda, M., and Toba, Y., 1976, J. Oceanogr. Soc. Japan, 32, 53-64.

Title: The Role of Breaking Wavelets in Air-Sea Transfer Processes

Author: G. T. Csanady

Affiliation: Department of Oceanography, Old Dominion University

Norfolk, Virginia 23529-0276

Short gravity waves (O 10 cm wavelength) transfer momentum and scalar properties from air flow to the surface layer of the ocean through the following chain of processes:

- The air flow separates from the crests of the wavelets and upon reattachment causes local concentrations of shear stress;
- Shear stress pulses cause surface fluid to overtake the wave, turning wavelets into breakers;
- The flow structure of a breaker is similar to that of a hydraulic jump, containing a roller which interacts with the wave;
- The roller converts wave momentum into shear flow momentum of a trailing turbulent wake (in a wave following frame);
- The roller wave interaction produces the forward leaning, crested and asymmetrical shape of a breaker;
- The shape of the breaker maintains the separation of the air flow above the crest, see above;
- The surface flow in and around the roller is convergent ahead, divergent behind the roller center;
- The magnitude of the surface divergence is comparable to the vorticity in the roller, which is of order stress over viscosity;
- For gases of low diffusivity in water the diffusion boundary layer at the surface is thin compared to the roller depth;
- The thinness of the diffusion boundary layer is maintained by the divergent flow behind the roller;
- Scalar substances are carried downward by plumes ahead of the rollers, their flux being proportional to the square root of surface divergence times diffusivity

Some of these processes can be illustrated by linear theory models. The simplest such model consists of a volume of stagnant fluid, representing a roller in a wave following frame, riding the surface of a stream, which carries a train of wavelets. The calculated surface shape reproduces the forward leaning shape of a breaker, and shows the presence of capillaries ahead of the roller, as

observed. Adding a shear stress pulse makes the model more realistic. Such models demonstrate that flow structures exist on the sea surface with properties quite unlike classical irrotational waves. They play a dominant role in air-sea transfer processes.

Much of the scatter in observed air-sea transfer coefficients can be understood once the importance of breaking vortical wavelets is realized. Interestingly, this leads back to some ideas of Keulegan on mass transfer at a density interface: his non-dimensional number, $u^3/g\prime v$, where u is velocity, $g\prime$ effective gravity, v viscosity, should be an important parameter in any air-sea transfer process. A proper non-dimensional plot of the drag coefficient-wind speed relationship should therefore have the Keulegan number as the abscissa.

On a wind-blown sea surface the density of breaking wavelets is likely to be a function of (long-) wave height, fetch, etc., most importantly the presence or absence of breaking long waves. This may explain some of the observed scatter of gas transfer rates.

New Experimental Results on the Parameters Influencing Air-Sea Gas Exchange

Bernd Jähne
Scripps Institution of Oceanography
Physical Oceanogr. Res. Div., A-030
La Jolla, CA 92093, USA

Introduction

From the early experimental studies of the transfer of gases across the air-sea interface it has been obvious that the wind is the driving force for the exchange process. Yet despite numerous experimental studies in a varity of laboratory facilities and natural water bodies, there is still not a consistent picture of the details of the mechanisms. Both wind-tunnel and field experiments show that there are significant deviations up to a factor two from a straight correlation between the gas transfer velocity to the friction velocity indicating the significant influence of the wave field.

This influence is subject to controversial discussions in the literature. Based on the striking experimental fact that the gas transfer rate is rather insensitive to the scale of the experimental facility and/or theoretical scale considerations, several investigators concluded that small scale waves (especially capillary waves) cause the observed enhancement of the gas exchange rate. *Coantic* [JGR 91, 3925–3943, 1986] and *Back and McCready* [JGR 93, 5143–5152, 1988] propose two different mechanisms. In contrast, *Kitaigorodskii* [J. Phys. Oceanogr. 14, 960–972, 1984] emphasizes the influence of the energy containing large scale waves, which break and may enhance air-sea gas exchange by turbulent patches.

This paper summarizes a number of new experimental results from wind-wave facility studies on the parameters influencing air-sea gas exchange besides the wind speed with emphasize on the wave field.

Description of Experiments

The experiments have been performed in six wind-wave facilities to gain the widest range of wind wave fields possible in laboratory experiments. The smallest facility was one of the circular tunnels of Heidelberg University with an annular water channel with 60 cm outer diameter and a cross-section of 10 cm × 10 cm. The largest facilities include the Delft and Delta flumes of Delft Hydraulics in the Netherlands with water channels of 100 m × 8 m × 1 m and 250 m × 5 m × 5 m, respectively. Both flumes are equipped with hydraulically controlled wave paddles. Thus wind wave field was also combined with regular and random mechanically generated waves.

The gas transfer rates have been determined with different tracers including CO_2, ^3He, ^4He, CH_4, Kr and Xe. In addition, heat was used as a proxy tracer with the controlled flux technique which offers the advantage of *local* measurements of the transfer velocity while conventional techniques only yield values integrated over the whole water surface area of the facility [*Jähne et al.*, Tellus 41B, 177-195, 1989 and this issue].

Wave slope frequency spectra have been obtained in all facilities with a laser slope gauge except the Delta flume where slope distributions have been measured with a reflective slope gauge. In addition, in some of the facilities image sequences of the wave slope have been recorded. (For a detailed description of the optical wave measuring techniques see *Jähne and Waas* [SPIE Conference Proc. 1129, 1989]).

Results

Empirical parameterization of the measured gas exchange rates as a function of friction velocity and wave parameters gives interestings hints on the mechanisms of the gas exchange process.

- *Capillary Waves.* The gas exchange rates do not correlate well with the capillary wave slopes. Significant higher capillary wave slopes were observed in the smaller facilities, but the gas exchange

rates did not increase correspondingly. In contrast, a much better correlation was found between the total mean square slope and the gas exchange rate. Other measurements support this observation. At lower wind speeds, the gas exchange measurements in the Delft flume run more than half a day. During that period it happened occasionally that a slick passed through the measuring area of the controlled flux technique and the laser slope gauge. While the spectral densities of capillary waves decreased by up to a factor ten, the larger scale waves and the transfer velocity were only slightly affected.

- *Fetch Dependence.* The fetch dependence of the gas transfer velocity has been studied in the Karlsruhe wind-wave facility in a range of 2–8 m. In the initial wave generation region at short fetches, the transfer rate increased with fetch. At higher fetches, it kept constant. The mean square slope of the waves shows a coinciding pattern.

- *Large Scale Waves.* In the Delta flume deep water waves with a wavelength of 11 m, a frequency of 0.384 Hz, and amplitudes (crest to trough) between 0.3–1 m were superimposed to wind generated waves. These regular waves showed no significant influence on both the gas transfer velocity and the total mean square slope of the wave field. Experiments with a random JONSWAP-like wave spectrum gave the same result. In both cases no significant wave breaking occured. A significant enhancement of the gas transfer velocity could only be observed in the Delft wind wave facility, when a steep, nearly instable wave of 0.7 Hz generated by a wave maker started breaking over the whole facility after adding a moderate wind of 5.5 m/s.

- *Air Flow Stability.* The outdoor Delta flume allowed a study of the stability of the air flow on the gas exchange rate. At low wind speeds, the exchange rates where significantly lower with a stable (air warmer than water) than with an instable stratification.

Discussion

On the one hand, the results indicate that the influence of waves on the air-sea gas exchange process cannot be restricted to small scale waves only, since there is no good correlation between the gas exchange rate and the spectral density of capillary waves. On the other side they also show that sinusoidal large waves do not influence the gas exchange process at all. The key to a deeper understanding lies in the fact that the gas exchange rate is closely related to the total mean square slope of the waves. This global parameter is a measure for the overall stability of the wave field. This fact emphasizes that the nonlinearity or instability of water waves *of all scales* enhances gas exchange. Thus a realistic conceptual model has to include both small and large scale processes, i. e. to be a synthesis of the models proposed so far.

The experimental data still allow two mechanisms. Either the waves directly dissipate to near-surface turbulence or interact with the turbulent shear current to enhance turbulence.

Enhancement of gas exchange starts with the occurance of water surface waves. If the considerations above are correct, instable waves must occur even at low wind speeds, only less frequent than at higher wind speeds. Such data cannot be obtained from mean wave spectra but a direct analysis of time series or images of the waves. Images of the wave slope at low wind speeds in the Delft wind wave facility indeed show that the water surface is in general quite smooth. From time to time, however, gravity waves with steep crests occur which are accompanied on their lee-side with a steep gravity wave train. The frequency of these events is increasing with wind speeds.

Conclusions

More details about the mechanisms can only be revealed by studies which need much more detailed experimental tools. These studies should include the energy balance in wind waves (especially the dissipation term) and the turbulent flow in the water close to the interface including the temporal and spatial scales of wave-induced turbulence.

Simulation of the Exchange of short-lived reduced Sulphur Compounds between the Ocean and the Atmosphere

Gerhard Kramm and Eberhard Schaller

Fraunhofer-Institut fur Atmosphärische Umweltforschung
D-8100 Garmisch-Partenkirchen, FRG,
Kreuzeckbahnstraße 19

Results from numerical simulations regarding the exchange of short-lived reduced sulphur compounds such as CH_3SCH_3, H_2S, COS and SO_2 between the ocean and the atmosphere will be presented. A meteorological-photochemical model of the marine atmospheric boundary layer (ABL) is used which describes the meteorological processes and photochemical transformations as a function of height above sea surface and time.

The meteorological part of the ABL-model is based on a set of conservation principles such as the continuity equation, the first law of thermodynamics, the equation of motion, the mass conservation equation of water and the conservation equation of turbulent kinetic energy. This model part evaluates the time-varying vertical distributions of wind velocity, potential temperature and specific humididy.

A set of mass conservation equations of the form

$$\frac{\partial c_i}{\partial t} = - \frac{\partial F_{c,i}}{\partial z} + f_i(c_1, \ldots, c_p) \qquad (1)$$

is used to calculate the time-varying distributions of concentrations c_i, i = 1, .., p, of reactive trace constituents. $F_{c,i}$ is the vertical mass flux density and $f_i(c_1, \ldots, c_p)$ the chemical transformation rate which is calculated on the basis of a kinetic mechanism formulated by Sze and Ko (1980). Eq. (1) is solved by the splitting-up method (e.g. Yanenko, 1971) which allows to treat the chemical part and the diffusive parts indepently. The chemical part is described by a "stiff" system of coupled nonlinear ordinary differential equations which is solved by Gear's (1971) backward differentiation formula. The Crank-Nicholson method is applied to treat the diffusive parts.

Subgrid-scale turbulence is parameterized according to a first order closure hypothesis (flux-gradient relationship). The determination of the eddy diffusivity of momentum is based on an analytical-empirical solution of the conservation equation of turbulent kinetic energy. The eddy diffusivities of heat, water vapour and trace constituents are calculated on the basis of the eddy diffusivity of momentum, the turbulent Prandtl number Pr_t and the turbulent Schmidt numbers Sc_t for water vapour and trace constituents.

The vertical transfer in the molecular-turbulent sublayer close to the sea surface is described in accordance to Reichardt's (1951) empirical flux-gradient relationship.

The boundary conditions at the top of the ABL are given by the large-scale features of the free atmosphere, where no fluxes of momentum, sensible heat, water vapour and trace constituents through the upper boundary are prescribed. The lower boundary conditions are formulated for a flow at a fluid interface where the temperature at the interface is determined by solving the surface balance equation for energy.

The concentration of trace constituents at the sea surface are determined by the surface balance equation for mass

$$F_{c,i} - F_{c,i} = 0 \qquad (2)$$

where the vertical exhalation (or sorption) flux density $F_{c,i}$ is given by a gas transfer model of the aqueous boundary layer close to the air-sea interface.

References

Gear, C.W. (1971), 'Numerical initial value problems in ordinary differential equations'. Prentice-Hall. Inc. Englewood Cliffs, New Yersey, p253.

Reichardt, H. (1951), 'Vollständige Darstellung der turbulenten Geschwindigkeitsverteilung in glatten Rohren'. Z. angew. Math. Mech. 31, 208-219.

Sze, N.D.; Ko, M.K.W. (1980), 'Photochemistry of COS, CS_2, CH_3SCH_3 and H_2S: Implications for the atmospheric sulfur cycle. Atmospheric Environment 14, 1223-1239.

Yanenko, N.N. (1971), 'The method of fractional steps'. Springer-Verlag, New York.

SMALL-SCALE WAVE BREAKING AND ITS INFLUENCE ON GAS TRANSFER

by

N. Merzi, M. Servos & M.Donelan

National Water Research Institute
Canada Centre for Inland Waters
P.O. Box 5050, Burlington
Ontario, Canada L7R 4A6

1. INTRODUCTION

Gas transfer at air-water interfaces plays an important rôle in the global biochemical cycle. The exchange of gases, such as carbon dioxide and methane, has significant consequences in the progress of climatic change. High molecular weight organic compounds such as PCBs have impacts on the environment and on human health. Sources and sinks of these compounds on a global scale, and particularly their flux rates at the air-water interface, are not very well known. Mass balance models for any of these compounds in natural water bodies require accurate estimates of the mass transfer velocities across the air-water interface.

Gas transfer at water surfaces depends on the degree of turbulence intensity in the controlling phase. For thermally neutral conditions, the main turbulence creating mechanisms for liquid phase controlled compounds are the velocity shear produced by the application of wind stress at the interface and the breaking of waves of all wavelengths.

The breaking of waves on natural water bodies is among the most commonly observed step changes in entropy. A highly ordered flow becomes unstable and loses energy to turbulence in an often spectacular way. The mixing engendered by deep water breakers that produce whitecaps has an important local effect on the mixing of surface waters. However, whitecaps are generally sparsely distributed and occur in association with the passage of wave groups (Donelan et al.(1972). Small scale wave breaking (the breaking of short gravity and gravity-capillary waves having wave lengths from about 1cm to a few tens of centimeters) is much more uniformly distributed. These small breakers, with overturning crests only a few millimeters high, are sufficient to disturb the thin diffusive sublayer beneath the interface (thickness,

$\delta_D = 10\, \nu\, u_*^{-1}\, Pr^{-1}$; ν is the kinematic viscosity, u_* is the friction velocity, $Pr = \nu/D$ is the Prandtl number, D is the molecular diffusivity of the compound in water). For typical values of u_* and Pr, δ_D is of the order of a millimeter. Small scale wave breaking at this order might be sufficient "to ventilate" the subsurface layer of the water body. Kerman (1984) has estimated that the area covered by these small breakers is 6.4 times that disturbed by whitecaps.

2. EXPERIMENTAL DESIGN

An air-tight recirculating Gas Transfer Flume was designed and constructed in the Canada Centre for Inland Waters for toxic gas transfer studies across the air-water interface as well as studies related to wave mechanics and boundary layer turbulence in both air and water.

The gas transfer flume provides wind speeds from 1 m/s to 22.5 m/s. The test section is 32.2m long: the water depth is designed to be up to 0.25m and the height of the air duct is 0.60m. The system is equipped with a high efficiency HEPA filter and charcoal filter in air and a carbon filter in the water. At the end and/or during the experiment, contaminated air and water can be discharged through these filters.

The aim of this study is to determine the influence of small scale wave breaking on the mass flux of a water phase controlled compound (chlorobenzene). The experiments were conducted in two stages: aero-hydrodynamical measurements and chemical measurements. The mass flux of chlorobenzene was determined as a function free stream wind speed at eight different speeds (U(m/s)= 1.5, 2, 2.5, 3.5, 5, 6, 7, 8). Wind speed was measured with a Pitot-static tube and wave height with a capacitance wave gauge.

Chemical experiments were conducted by making repeated measurements of the concentration of chlorobenzene in water. The general mass flux equation is given by,

$$dCw/dt = -Kol\ (Cw-Ca)/d$$

where Cw is bulk liquid concentration, Ca is bulk gas concentration, Kol is the overall liquid-phase mass transfer velocity, d is the depth of water (or, more precisely, the volume of water divided by the surface area exposed to wind). The flume was operated in the open (or vented) mode, in which air was drawn in from the laboratory and vented to atmosphere. This continuous renewal of the air guarantees that the air concentration, Ca is effectively zero. The integrated mass flux equation then becomes,

$$Cw = Cwo\ \exp(-Kol\ t/d)$$

where Cwo is the initial concentration in the water. The mass transfer velocity for chlorobenzene was determined by measuring the decrease in its concentration with time.

3. RESULTS

The mass transfer velocity of chlorobenzene was calculated on the basis of hourly concentration measurements. It was observed to increase dramatically when small scale wave breaking starts to occur. Other studies also indicate an enhancement of the mass transfer velocity (of water phase controlled compounds) but in terms of wind speed alone. Various results cover the range of 3 to 7 m/s: (Kanwisher, 1963; Liss, 1973; Broecker et al., 1978; Jaehne, 1979; MacKay and Yeun, 1983). They did not provide specific information about the wave field. The difference in results between various studies originates apparently from the different dimensions of the wind tunnels and the fetch of the measurements. In this study, the mass transfer velocity is parametrized in terms of wind and wave properties.

REFERENCES

Broecker, H.C., J. Petermann and W. Siems, 1978: "The influence of wind on CO exchange in a wind-wave tunnel, including the effects of monolayers", J.Mar.Res., 36, 4, 595-610.

Donelan, M.A., M.S. Longuet-Higgins and J.S.Turner, 1972: "Periodicity in whitecaps", Nature, 239, 449-451.

Jaehne, B., K.O. Muennich, and U.Siegenthaler, 1979: "Measurements of gas exchange and momentum transfer in a circular wind-water tunnel", Tellus, 31, 321-329.

Kanwisher, J., 1963: "On the exchange of gases between the atmosphere and the sea", Deep-Sea Res., 10, 195-207.

Kerman, B.R., 1984: "A model of interfacial gas transfer for a well-roughened sea", in Gas Transfer at Water Surfaces, D. Reidel, 311-320.

Liss, P.S., 1973: "Process of gas exchange across an air-water interface", Deep-Sea Res., 20, 221-238.

MacKay, D. and A.T.K. Yeun, 1983: "Mass transfer coefficient correlations for volatilization of organic solutes from water", Environ.Sci.Technol., 17, 4, 211-217.

Further Evidence Supporting the Contention That Oceanic Whitecaps Markedly Enhance the Rate of Air-Sea Gas Exchange

Edward C. Monahan

Marine Sciences Institute
University of Connecticut, Avery Point
Groton, Connecticut 06340

Recent "tipping bucket" experiments carried out in hooded Whitecap Simulation Tank III at Avery Point have provided additional data supporting the hypothesis, put forward at the First International Symposium on Gas Transfer at Water Surfaces by Kerman (1984), and by Monahan and Spillane (1984), that the whitecaps that form when waves break at sea, and the associated buoyant bubble plumes, greatly influence the effective air-sea gas transfer coefficient, or piston velocity, of those gases subject to liquid-phase control.

Monahan and Spillane (1984) put forward an expression, reproduced here as Eq. 1, for the effective piston velocity, k_E, for such gases.

$$k_E = k_m (1 - W_B) + k_t W_B \qquad (1)$$

In this equation, where W_B (W in the notation of the earlier paper) is the fraction of the sea surface covered by mature whitecaps, k_m is the piston velocity identified with gas transfer via molecular diffusion through a viscous surface sub-layer, or "stagnant layer," which is assumed to exist everywhere except in the interior of the whitecaps, and k_t is the piston velocity associated with the turbulent diffusion of gas via the top of the buoyant bubble plume, i.e., through the whitecap.

In recognition of the complex character of gas transfer through smooth and roughened, but whitecap-less, sea surfaces, as recently described by Liss and Merlivat (1986), and by Coantic (1986), Monahan (1989) recently recast Eq. 1 in the manner of Eq. 2 to make the wind speed dependence of k_m explicit.

$$k_E = (k_{m_1}U + K_{m_2}U^2) (1 - W_B) + k_t W_B \qquad (2)$$

Recognizing that the whitecap and bubble plume represent a "low impedance vent" for gas exchange, it is assumed that k_t is much larger than k_m, i.e., than $k_{m_1}U + k_{m_2}U^2$.

In the recent tipping bucket gas evasion experiments, the temporally averaged whitecap coverage, resulting from one spill of the contents of the bucket, i.e., one "breaking wave," every 210s, was only 0.00014 (Mason, et al, 1988). Yet for this modest whitecap coverage, and with the sea water in the tank stirred by means of several

small submerged pumps, the evasion velocity of Rn was found to be 3.7 times the evasion velocity determined for the same gas when the sea water in Whitecap Simulation Tank III was only subject to the stirring action of the small pumps (Torgersen, et al, 1989). (When these experiments were repeated with Hg, the evasion velocity for this gas in the bucket spilling, and stirring, case was determined to be 2.3 times the Hg evasion velocity for the case of stirring alone.)

Making use of the preliminary Radon results, Eq. 1 can be evaluated for the case where W_B equals 0, and likewise for the case where W_B is 0.00014, and the resulting two expressions can be solved for k_m and k_t. The value thus obtained for k_m is 7.9 μms^{-1}, and for k_t is 152 mms^{-1}. The extremely large value found for k_t is in part a reflection of the fact that the optically resolvable whitecap has a smaller lateral extent, and a considerably shorter duration, than does the relevant diffuse bubble plume (Stramska, et al., 1990).

References

Coantic, M., A Model of Gas Transfer Across Air-Water Interfaces with Capillary Waves, J. Geophys. Res., 91, 3925-3943, 1986.

Kerman, B.R., A Model of Interfacial Gas Transfer for a Well-Roughened Sea, in Gas Transfer at Water Surfaces, W. Brutsaert and G.H. Jirka, Eds., D. Reidel Pub., Dordrecht, 311-320, 1984.

Liss, P.S., and L. Merlivat, Air-Sea Gas Exchange Rates: Introduction and Synthesis, in The Role of Air-Sea Exchange in Geochemical Cycling, P. Buat-Menard, Ed., D. Reidel Pub., Dordrecht, 113-127, 1986.

Mason, R., T. Torgersen, W.F. Fitzgerald, M.P. Dowling, J. Kim, E.C. Monahan, M.B. Wilson, and D.K. Woolf, The Role of Breaking Waves in the Control of the Gas Exchange Properties of the Sea Surface, in Oceanic Whitecaps and the Fluxes of Droplets From, Bubbles To, and Gases Through, the Sea Surface, Whitecap Report No. 4, M.S.I., Univ. of Connecticut, Avery Point, 85-94, 1988.

Monahan, E.C., From the Laboratory Tank to the Global Ocean, in Climate and Health Implications of Bubble-Mediated Sea-Air Exchange, E.C. Monahan and M.A. Van Patten, Eds., Connecticut Sea Grant College Program, Avery Point, 43-63, 1989.

Monahan, E.C., and M.C. Spillane, The Role of Oceanic Whitecaps in Air-Sea Gas Exchange, in Gas Transfer at Water Surfaces, W. Brutsaert and G.H. Jirka, Eds., D. Reidel Pub., Dordrecht, 495-503, 1984.

Stramska, M., R. Marks, and E.C. Monahan, Bubble-Mediated Aerosol Production as a Consequence of Wave Breaking in Supersaturated (Hyperoxic) Sea-Water, J. Geophys. Res., 95 (in press), 1990.

Torgersen, T., R. Mason, D. Woolf, J. Benoit, M.P. Dowling, M. Wilson, and E.C. Monahan, The Role of Breaking Waves in the Control of the Gas Exchange Properties of the Sea Surface, in Climate and Health Implications of Bubble-Mediated Sea-Air Exchange, E.C. Monahan and M.A. Van Patten, Eds., Connecticut Sea Grant College Program, Avery Point, 155-162, 1989.

Oceanic CO_2 Uptake and Future Atmospheric CO_2 Concentration based on Lateral Transport Model of the World Ocean

Tsung-Hung Peng
Environmental Sciences Division
Oak Ridge National Laboratory
Oak Ridge, Tennessee 37831

Models of lateral transport of surface water in the Atlantic, Indian, and Pacific oceans are proposed on the basis of the distribution pattern of bomb-produced ^{14}C in the ocean observed during the Geochemical Ocean Section Studies program (GEOSECS 1973-1978). The water column inventories of bomb-produced ^{14}C and the input function of atmospheric time history of bomb-produced ^{14}C are used as constraints for determining the mean CO_2 gas exchange rate in three oceans. These results indicate that the mean CO_2 exchange flux is 22.3 $mol{\cdot}m^{-2}{\cdot}yr^{-1}$in the Atlantic Ocean, 19.4 $mol{\cdot}m^{-2}{\cdot}yr^{-1}$in the Indian Ocean, and 19.2 $mol{\cdot}m^{-2}{\cdot}yr^{-1}$in the Pacific Ocean. The pattern of global water column inventories of bomb-produced ^{14}C suggests that upwelling of bomb-^{14}C-free water from below takes place in the Antarctic, northern Pacific, and equatorial regions, and downwelling of surface waters occurs in the temperate oceans and northern Atlantic. Uptake of excess CO_2 by these models is calculated using the observed Mauna Loa atmospheric CO_2 record as an input function. Results indicate that 35% of fossil-fuel- produced CO_2 is taken up by these model oceans. In addition to fossil fuel CO_2 input, a close match of model-derived atmospheric CO_2 time history with the observed record from Siple ice core and Mauna Loa Observatory requires that a net release of 91.7 x 10^{15} g C from land biosphere is necessary for the period 1800 to 1980 AD. Three scenarios of future CO_2 release from fossil fuel consumption and tropical deforestation have been used for the prediction of future atmospheric CO_2 concentrations. Although these scenarios are designed to obtain an expected double preindustrial CO_2 concentration in years 2030, 2060, and 2090 AD, respectively, the uptake of excess CO_2 by the lateral transport models is so much more efficient than general box-diffusion models that only the highest CO_2 release scenario would lead to a doubling atmospheric CO_2 before 2100 AD.

Research sponsored by U.S. Department of Energy, Carbon Dioxide Research Program, Atmospheric and Climate Change Division, Office of Health and Environmental Research, Budget Activity Number KP 05 00 00 0, under contract DE-AC05-84OR21400 with Martin Marietta Energy Systems, Inc.

Oxygen exchange with saline waters

Michal Shatkay and Joel R. Gat

Isotope Research Department, Weizmann Inst. of Science, Rehovot 76100, Israel.

While gas transport processes across a water-gaseous interface have been the subject of extensive research, gaseous exchange across the interface of a gaseous phase and a saline water phase has hardly been studied. Salinity affects gas exchange both through its effects on gas solubility, surface tension, viscosity etc. as well as through its effects on the stability of the liquid column. Saline water bodies range from the oceans, through evaporated basins and solar ponds to such saline terminal lakes as the Dead Sea. Thus gas transport in saline systems is of high interest and importance for environmental sciences. Furthermore, the comparison between saline systems and fresh water systems gives additional insight into gas exchange processes as a whole. We will report here on few aspects of our studies:

1) the comparative measurement of oxygen exchange (both evasion and invasion) for Dead Sea and fresh water, carried out under controlled temperature, at wind still and a relative humidity of close to 100 % (so that evaporation is negligible).

2) the comparative measurement of oxygen exchange for saline and non saline solutions carried out in a cell where temperature, humidity and the gaseous phase composition are controlled.

3) Preliminary results of the difference in transport rates of oxygen into fresh water/saline solution, when the gas is introduced into the liquid in the form of bubbles.

In the first experiment oxygen was bubbled into the liquid phase prior to the experiment in order to create supersaturation. The subsequent decrease (evasion) in oxygen concentration was monitored till a constant equilibrium value was reached. Prior to the invasion experiment the liquid phase was stripped of its oxygen by bubbling helium through it. The subsequent increase in oxygen concentration was monitored till an equilibrium was established. Solutions used where an artificial Dead Sea solution and double distilled water. Mercuric chloride solution was added to both media to prevent biological activity during the experiments. Experiments were conducted at 31^o C.

The piston velocity was deduced directly from the experimental results, using the Fickian equation ($Flux = K\Delta C$, K being the piston velocity). It was found that for both the invasion and the evasion runs the oxygen flux fluctuated at the very beginning of each experiment before a monotonic decrease set in. In the fresh water case the piston velocity was about the same for the invasion/evasion runs (approximately 3 cm/hour) which is the expected situation where the transport mechanism is identical for both cases (namely probably of molecular diffusion). In the saline case, the invasion flux is smaller and the piston velocity is about three fold lower (1.01 cm/hour and 3.14 cm/hour respectively). For the artificial Dead Sea solution, the diffusion coefficient can be estimated from the relationship $D_{D.S.}/D_{f.w.} = \gamma_{f.w.}/\gamma_{D.S.}$ (Horne 1969), where $D_{D.S.}$ and $D_{F.W.}$ are the diffusion coefficients and $\gamma_{D.S.}$

and $\gamma_{f.w.}$ are the dynamic viscosities of Dead Sea and fresh water respectively at the same temperatures. The ratio of the molecular diffusivities for these different media is about three, suggesting that the difference in the piston velocities can be explained by assuming a diffusion controlled exchange.

In the evasion run the calculated "K" value for the artificial Dead Sea solution changes with time. The persistence of foaming and bubbles in the solution long after active bubbling has ceased, suggests that transport by bubbles played some role in the gas transport out of the solution, at least in the early phase of the run (in the invasion case described above, where residual helium bubbles remained at the beginning of the run, this evidently did not affect the invasion rate of oxygen into the saline solution). The observed decrease in the "K" values with time, finally approaching a value similar to the one measured for the invasion experiment, indicates a change during the experimental run from a bubble transport mechanism to one controlled by diffusion. Discounting the bubble entrainment effect, both these runs indicate a dramatic decrease in the piston velocity in the saline solution. It further seems that for the fresh water case and the given experimental setup, bubbles were less dominant as a transport mechanism (it is indeed observed that foam is more stable under saline conditions). The existence of bubble transport at the beginning stages of the various experiments, could also account for the non monotonic (flux:time) behavior, described above.

The second experiment involved the comparison of oxygen invasion/evasion across the surface of a 240 g/l NaCl solutions and of fresh water. The experiment was carried out in an "environmental chamber" where the gaseous phase was changed during the experiment by flushing, above the liquid surface, with either nitrogen or oxygen. When nitrogen was flushed in, oxygen evasion followed and the decrease in dissolved oxygen was monitored. Later the cell was flushed by pure oxygen and oxygen invasion into the liquid was monitored with time. The bulk of the liquid was well mixed. The 'wind speed' in the cell was lower than 0.05 m/sec, and we could again expect a transport mechanism controlled by molecular diffusion. However, in this experiment, evaporation took place and accompanied gas exchange. The evasion and invasion piston velocities for each liquid were found to be similar within the given experimental error. The ratio of the average piston velocities, $K_{f.w.}/K_{NaCl}$, is 1.23, while the ratio of the respective diffusivities (assuming it to be the inverse of the ratio of the respective dynamic viscosities) is 1.53. $K_{f.w.}$ has the value of 2.98 cm/hour, which is similar to the value reached in the previously described experiment. Thus obviously gas transport in the saline solution is enhanced and is not dependent solely on molecular diffusion. Computation of the Rayleigh number for the saline case and for the fresh water case (Turner 1973) showed that while the fresh water column stability should not have been affected by the evaporation, in the saline case the critical Rayleigh number was reached, and thus the water column had become unstable and was susceptible to vertical convection. This high Rayleigh number is due to an increase in salinity in the top layer in addition to the cooling produced by the evaporation.

A separate experiment was conducted in order to compare the transport of oxygen by bubbles between a saline and a non saline bubble-liquid interface. Fresh water of millipore Q quality and a saline (150 g/l NaCl) solution were stripped of all dissolved oxygen at a given regulated temperature. Air bubbles were subsequently introduced into the fresh water/saline solution, by shaking it for a given amount of time and intensity. The increase in dissolved oxygen concentration was monitored with time. The contents were then not stirred further so as not to perturb the bubbles ascent/coalescence. A control experiment where air bubbles were not introduced into the liquid was also conducted. Its results were subtracted from those of the runs where air bubbles were present. It was found that saturation was approached faster in the saline solutions compared to the fresh water case. A calculation of the gas

flux from a single bubble into a water body could be performed, using the model proposed by Memery and Merlivat (1985). According to this calculation, bubbles of a given radius produced at a given depth will last longer in a saline solution than in fresh water but will contribute less gas to the liquid during their ascent. This seems to be in contradiction to our results for the whole bubble population. We maintain that the reason for the better aeration in the NaCl solution is the bubble population produced by the bubbling event. Photographs of the bubbles populations produced at a given depth below the liquid surface by a bubble diffuser (pore radius < 8 microns) show two orders of magnitude more bubbles for the saline solution than for fresh water. The bubbles for the fresh water case were larger than those found in the saline solution. These differences in bubble populations are attributed to bubble coalescence which occurs in the fresh water case but is inhibited in the NaCl solution. Thus transport assisted by bubbles will exist longer in the NaCl solution than in fresh water and results in a better aeration.

It is concluded that salinity affects gas exchange across a liquid-gaseous interfaces in several manners. Under a Fickian regime the piston velocity is dependent on the diffusion coefficient and is lower in the saline media than in fresh water. When evaporation becomes significant the piston velocity in the saline case can be enhanced due to vertical instability. The opposite could be expected for the case of condensation. Under extreme turbulence, where gas transport by bubbles is dominant, we would expect a higher degree of aeration in a saline water body than in a fresh water body. The latter effects may be dependent on the nature of the salt as well as its concentration.

Reference List

Horne R. A., 1969. Marine Chemistry. Wiley Interscience, 568pp.

Memery L. and Merlivat L., 1985. Tellus, 37:272-285.

Turner J. S., 1973. Buoyancy effects in fluids. Cambridge U. Press, 367pp.

PARAMETRIZATION OF AIR-OCEAN GAS TRANSFER

Alexander V. Soloviev

P.P.Shirshov Institute of Oceanology USSR Academy of Sciences,
23 Krasicova, Moscow 117218, USSR

Air-ocean gas transport substantially depends on parameters of the ocean "Diffusion Boundary Layer" (DBL). Free and forced convection in the upper ocean and surface waves control the DBL thickness and, hence, the gas resistance across the DBL.

Dimensional analysis. I will ignore bubble and droplet production in whitecaps. In the case of stationary weather and wave conditions one can expect the gas transfer coefficient K as follows:

$$K = f(u_*, q_0, \alpha, g, \nu, \mu), \tag{1}$$

where f is a function, u_* the frictional velocity in water, q_0 the the vertical heat flux from the surface of the ocean due to latent and sensible heat fluxes and effective long wave radiation, α the coefficient of thermal expansion, g the acceleration of gravity, ν and μ the coefficients of molecular momentum and gas diffusion in water. A standart dimensional analysis of (1) leads to the following relation:

$$K^+ = F(Rf_0, Sm, W), \tag{2}$$

where $K^+ = K/u_*$, F is a universal fuction of its nondimensional arguments $Rf_0 = \alpha g q_0 \nu / u_*^4$, $Sm = \nu/\mu$ and $W = \nu g/u_*^3$.

Recently Csanady(1990) suggested a conception about the role of surface waves in the air-ocean gas transfer. A renewal model developed by Kudryavtsev and Soloviev(1985) and ideas of Csanady(1990) allow dependence (2) to elucidate.

Renewal model. Following Liu and Businger(1975) and Kudryavtsev and Soloviev(1985) I consider a fluid element adjacent to the ocean surface. Initially it has a uniform temperature and scalar property

concentration equal to the bulk values. As it is exposed to the interface the temperature difference, ΔT, across the thermal DBL and the surface flux, G_0, of a scalar property C are governed by the appropriate molecular diffusion lows (at constant heat flux q_0 and at constant concentration difference ΔC respectively):

$$\Delta T(t) = 2\pi^{-1/2}(t/\varkappa)^{1/2}q_0 \text{ and } G_0(t) = \pi^{-1/2}(t/\mu)^{-1/2}\Delta C, \tag{3}$$

where $\varkappa$ is the molecular diffusivity of heat.

The horizontally averaged temperature difference and surface flux can be defined as follows:

$$\Delta\overline{T} = \int_0^\infty \varphi(t)\Delta T(t)dt \text{ and } \overline{G}_0 = \int_0^\infty \varphi(t)G_0(t)dt. \tag{4}$$

The distribution function $\varphi(t)$ is defined as the fractional are of the surface containing fluid elements which have been in contact with the interface for a time t. Suggestion that all fluid elements have equal exposition time t_* results in the following expressions:

$$\Delta\overline{T} = (4\pi^{-1/2}/3)(t_*/\varkappa)^{1/2}q_0 \text{ and } \overline{G}_0 = 2\pi^{-1/2}(t_*/\mu)^{-1/2}\Delta C. \tag{5}$$

Depending on wind speed I consider 3 separate regimes:

A) Calm and low wind speed conditions ($V_{10} \simeq 0 - 5$ m s^{-1}). The cyclic injections of fluid from the molecular sublayer are of convective nature. The time period of the injections is defined as (Foster 1971):

$$t_* = C_*(\nu/\alpha g(-q_0))^{1/2}, \tag{6}$$

where C_* is a dimensionless constant.

B) Moderate wind speed conditions ($V_{10} \simeq 5 - 12$ m s^{-1}). According to Csanady(1990) the most intense surface renewal is caused on a wind-blown surface by viscous surface stress variations assotiated with breaking wavelets - "rollers". The time period of these variations can be defined as:

$$t_r = C_r\nu/u_*^2, \tag{7}$$

where C_r is dimensionless constant.

C) High wind speed conditions ($V_{10} > 12$ m s^{-1}). Long **wave** breaking suppresses the short wavelets and thus affects the gas transfer at the air-ocean interface (Csanady 1990). At fully developed wind **waves** the time scale of the surface renewal depends on the parameters of

the waves, u_* and g. A dimensional analysis results in the following relation:

$$t_w = C_w u_*/g, \tag{8}$$

where C_w is a dimensionless constant.

Combining (3) with (6), (7) and (8) one can get:

$$\Delta\bar{T}/T_* = \Lambda_0 Pr^{1/2} F_1(Rf_0, W), \tag{9}$$

$$K^+ = A\Lambda_0^{-1} Sm^{-1/2} F_1(Rf_0, W), \tag{10}$$

where $T_* = q_0/u_*$,

$$F_1(Rf_0, W) = \begin{cases} (Rf_0/Rf_{cr})^{1/4} \text{ at } 0 < u_* \leqslant (\alpha g q_0 \nu/Rf_{cr})^{1/4}, \\ 1 \text{ at } (\alpha g q_0 \nu/Rf_{cr})^{1/4} \leqslant u_* \leqslant (\nu g/W_{cr})^{1/3}, \\ (W/W_{cr})^{1/2} \text{ at } u_* > (\nu g/W_{cr})^{1/3}, \end{cases} \tag{11}$$

$A = 8\pi^{-1}/3$, $\Lambda_0 = (4\pi^{-1/2}/3)C_r^{1/2}$, $Rf_{cr} = -(C_*/C_r)^2$ and $W_{cr} = (C_w/C_r)^1$.

According to Kudryavtsev and Soloviev(1985) Rf_0 is the "Surface Richardson Number" which controls transition from free to forced convection (at $Rf_0 = Rf_{cr}$) in the molecular sublayer. The W-number controls transition from "rollers" to long-wave breakings. The values of $\Lambda_0 = 13.3$ and $Rf_{cr} = -1.5 \cdot 10^{-4}$ have been determined by Kudryavtsev and Soloviev(1985) on the thermal DBL data obtained by Grassl(1976). An estimation of critical value $W_{cr} \approx 2.2$ can be obtained taking into account the wind speed value $V_{10} \approx 12$ m s^{-1} at which, according to the vizual Bofort scale, long-wave breaking appears.

Comparison with experimental data. For convenience in practical use I "smoothed" (11) in the following way:

$$F_1(Rf_0, W) = (1 + Rf_0/Rf_{cr})^{1/4}(1 + W_{cr}/W)^{-1/2}. \tag{12}$$

On the figure gas transfer coefficient $K = K^+u_*$ is plotted versus friction velocity u_*. Being obtained under conditions of fully developed wind waves parametrization (10) represents the minimum values of the gas transfer coefficient. Differences between the parametrization and field measurements in the ocean can be explaned by the two main causes: 1) random scatter of experimental points due to problems of gas transfer method and variations of weather conditions; 2) systematic exceeding of the experimental points above the para-

metrization on account of distinction of wind waves from the stage of full development.

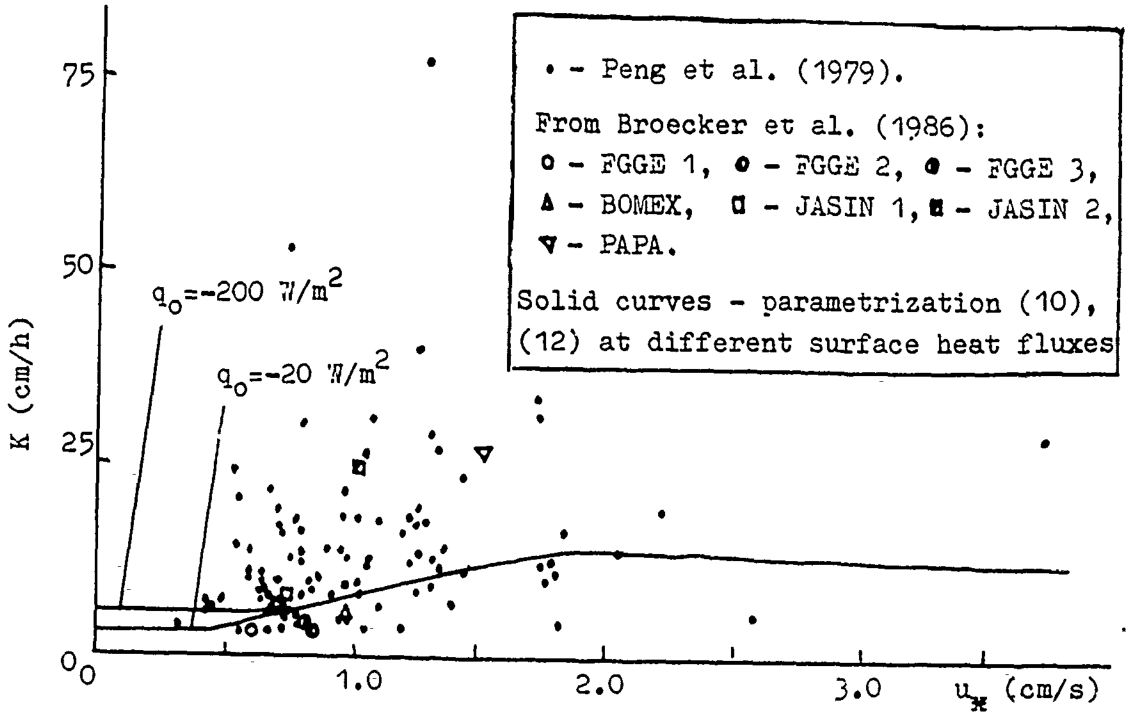

References

Broecker et al.(1986) Isotopic versus micrometeorological ocean CO_2 fluxes: A serious conflict. J. Geophys. Res. 91, 10517-10527.

Csanady G.T.(1990) The role of breaking wavelets in air-sea gas transfer. J. Geophys. Res. (in press).

Grassl H.(1976) The dependence of the measured cool skin of the ocean on wind stress and total heat flux. Boundary-Layer Meteorol. 10, 465-474.

Kudryavtsev V.N. and A.V.Soloviev (1985) On the thermal state of the ocean surface. Fizika Atmosfery i Okeana 17, 1065-1071 (in Russian)

Liu W.T. and J.A.Businger (1975) Temperature profile in molecular sublayer near the interface of a fluid in turbulent motion. Geophysical Research Letters 2, 403 - 404

Peng T.H., W.S.Broecker, G.G.Mathieu, Y.H.Li and A.E.Bainbrige (1979) Radon evasion rates in the Atlantic and Pacific Oceans as determined during GEOSECS program. J. Geophys.Res. 84, 2471 - 2486

ARTIFICIAL AERATION

NUMERICAL STUDY OF INTERACTING SWIRLED STREAMS IN THE MIXING CHAMBER OF COUNTERVORTEX AERATOR

Abramov N.N.
Achmetov V.K., Candidate of physico-mathematical sciences
Volshanik V.V., Candidate of technical sciences
Karelin V.Ya., Doctor of technical sciences
Levanov A.V., Candidate of technical sciences
Mordasov A.P., Candidate of technical sciences
Perekalsky V.M., Candidate of physico-mathematical sciences

Moscow Engineering and Construction Institute, the USSR

Various devices for forming of air (gas) saturated stream may be used in the systems of fluid stream aeration. But usage of so called countervortex aerators is thought of as the most attractive one. For their action they depend on intencive interaction of two concentric fluid streams rotating oppositely within a cylinder mixing chamber. Air stream which is automaticaly sucked from atmosphere into aerator space at the expense of rarefaction zones presence in swirled streams of fluid is splited into numerous bubbles. It provides for formation of greate area of phases contact surfaces and for intencive oxygen dissolution in water. Tests of model and production prototypes of countervortex aerators have shown that the dissolved oxygen content of water increases by 2-6 mg/l within their running-water part depending on initial oxygen content of aerating fluid massif.

Study of hydraulical and mass-transferal fenomena taking place in countervortex aerator space has for an object to improve its effectivness and to make engineering analysis more accurate. In view of extreme complexity of processes occuring in an aerator mixing chamber we start this study from the examination of the simpler case of interaction of two concentric opposite swirled streams consisting of viscous, incompressible fluid without bubble gas phase in cylinder pipe.

The study of streams mixing mechanism was conducted for two cases. In the first case three streams were supplied to inlet of mixing chamber: the stream stabilizing the central axial one (the stream "A") and two external coaxial swirled streams (the streams "B" and "C"). In the second case there was no stream "A" and the central hole was closed.

The study was conducted on the basis of Navier-Stokes equation complete system solution which, in cylindrical coordinates "z", "r", "φ" with reference to variables: current function , vartex and velocity rotational component V with existing stream axial symmetry, may be written as follows:

$$r^2 \left[\frac{\partial \omega}{\partial t} + \frac{\partial}{\partial z} \left(\frac{\omega}{r} \frac{\partial \psi}{\partial r} \right) - \frac{\partial}{\partial r} \left(\frac{\omega}{r} \frac{\partial \psi}{\partial z} \right) \right] - r \frac{\partial V_\varphi^2}{\partial z} =$$

$$= \frac{\partial}{\partial z} \left[r^3 \frac{\partial}{\partial z} \left(\frac{1}{R_e} \frac{\omega}{r} \right) \right] + \frac{\partial}{\partial r} \left[r^3 \frac{\partial}{\partial r} \left(\frac{1}{R_e} \frac{\omega}{r} \right) \right],$$

$$r \frac{\partial (V_\varphi r)}{\partial t} + \frac{\partial}{\partial z} \left(V_\varphi r \frac{\partial \psi}{\partial r} \right) - \frac{\partial}{\partial r} \left(V_\varphi r \frac{\partial \psi}{\partial r} \right) =$$

$$= \frac{\partial}{\partial z}\left[\frac{1}{R_e} r^3 \frac{\partial}{\partial z}\left(\frac{V_\varphi}{r}\right)\right] + \frac{\partial}{\partial r}\left[\frac{1}{R_e} r^3 \frac{\partial}{\partial r}\left(\frac{V_\varphi}{r}\right)\right],$$

$$\frac{1}{r}\frac{\partial^2\psi}{\partial z^2} - \frac{1}{r^2}\frac{\partial\psi}{\partial r} + \frac{1}{r}\frac{\partial^2\psi}{\partial r^2} = -\omega .$$

Functions ω and ψ are connected with components of axial(V_z) and radial (V_r) velocities by relationships:

$$V_z = \frac{1}{r}\frac{\partial\psi}{\partial r}, \quad V_r = -\frac{1}{r}\frac{\partial\psi}{\partial z}, \quad \omega = \frac{\partial V_r}{\partial z} - \frac{\partial V_z}{\partial r} .$$

Reynolds number (R_e) was defined by average stream-rate velocity(V) at the mixing chamber inlet and by the chamber radius.

The flow was considered in cylinder area Γ ($0 < z < z_k$, $0 < r < 1$). At the area Γ entrance, with z=0 and with existance of the stream "A", for all three streams (A,B and C) velocity axial component was given in the form of Poiseuille parabolic profile and radial component was taken to be zero. Rotational component for the stream "A" was also taken as V_φ =0 and for the streams "B" and "C" trapezoidal profiles V_φ was given, such that $|V_\varphi|_B = \pm |V_\varphi|_C$. Swirling intensiveness was specified by swirling angle α, defining as $tg\,\alpha = (V_\varphi|_{z=0})/V$. At the outlet from the area Γ, with $z=z_k$, gentle boundary conditions were established: at axis r=0 - stream symmetry condition, at the mixing chamber walls - adhesion conditions. In the case of the stream "A" nonexistance and insted of it, with z=0, there was a solid wall it was also given adhesion conditions at this wall.

The problem was solved by finite-difference method of establishment. Diffusion members were approximated by central differences and convective ones - under hybrid cheme. Difference equations were solved by means of method of successive upper relaxation. Calculations were conducted with $R_e < 500$.

Comparison of interaction development of swirled streams with opposite swirling and with one-way one showes that the mixture is much more effective with opposite swirling of streams spending for mixing in the chamber with a length of 1-2 calibres up to 80-90% of the total swirling energy. With one-way swirling it is occured merging of streams into single "monovortex" with the slow decrease of swirling. This conclusion is in good accord with experimental studies conducted before. With the small initial values of streams swirling ($\alpha \sim 20^\circ$) and with moderate Reynolds number ($R_e \sim 200$) interaction of streams with opposite and one-way swirlings is in practice identical. Difference between two ways of mixing arrangement increase with swirling angle increase.

It is shown that the axial stream has a stabilizing effect on swirled streams interaction in the mixing chamber with the great Reynolds numbers. With a small swirling and with the moderate Reynolds numbers the axial stream is also involved in "monovortex" (with one-way swirling) or it merges with internal swirled stream (with opposite swirling). Swirling rate is raised at the symmetry axis and the central rotating zone is structured into vortex core. With increase of R_e and swirling rate the initial position of vortex core moves downstream but it is not collapsed with one-way swirling and in practice it is absent with opposite one.

It has been revealed two forms of stream instationarity. In the first case the stream instability appeares in the form of pul-

sating recirculative zone within internal swirled stream. Hereat only recirculative zone is instationary with the general stationarity of the stream in the mixing chamber. In the second case instationarity of the whole bulk of mixing streams is observed. It is characteristically for interaction of opposite swirled streams with the great initial swirling. In certain working regimes appearance of two forms of instationarity simultaneously is possible.

Recirculative zone appearing in the stream is a prototype of vapour-air core which is formed under the action of centrifugal forces and causes the stream discontinuity. It may be supposed that the vapour-air core shall behave similarly to recirculative zone.

Later on it is planned to carry out numerical studies of turbulent interacting swirled streams with reference to examined aerators on the basis of Reynolds equations system and of turbulence differential model.

Factors Influencing Gas Transfer in Diffused Aeration Systems and their Application to Hypolimnetic Aeration

K.I. Ashley

Fisheries Research and Development Section,
Ministry of Environment, Province of British Columbia,
University of British Columbia, Vancouver, B.C., Canada, V6T 1W5

D.S. Mavinic and K.J. Hall

Environmental Engineering Group, Dept. of Civil Engineering,
University of British Columbia, Vancouver, B.C., Canada, V6T 1W5

A series of laboratory and field experiments were conducted to examine the effect of several design variables on the oxygenation capacity of full lift hypolimnetic aeration systems. The design variables included (1) depth of air injection; (2) surface area of the separator box; (3) overall air flow rate; (4) air flow rate per diffuser and (5) diffuser orifice diameter. The laboratory experiments used non-steady state gas transfer methodology to examine the effect of air flow rate, air flow rate per diffuser, orifice diameter and reduced tank surface area on the overall oxygen transfer coefficient (K_La_{20}, hr^{-1}); standard oxygen transfer rate (OTs, g O_2/hr); transfer efficiency (E_o, %) and energy efficiency (E_p, g O_2/kW-hr). The laboratory experiments were conducted in two different test tanks, a 70 L vertical cylinder and a 239 L rectangular tank. The field experiments examined the effect of diffuser depth, orifice diameter and reduced separator box surface area on the oxygen input per cycle (mg/L); daily oxygen load (kg O_2/day); transfer efficiency (E_o, %); energy efficiency (E_p, kg O_2/kW-hr) and water velocity (m/sec) in a full lift hypolimnetic aerator. The field experiments were conducted in a small (max. depth = 9.0 m; volume = 178,000 m^3) naturally eutrophic lake.

The laboratory experiments demonstrated that K_La_{20}, OT_s, E_o and E_p increased in value with increasing air flow rate in the coarse bubble diffusers, which had an orifice size range from 397 μ to 3175 μ diameter. In the fine bubble diffusers, 40 μ and 140 μ diameter pore size, K_La_{20} and OT_s increased with air flow rate; however, E_o and E_p were not significantly different. The orifice size experiments indicated that K_La_{20}, OT_s, E_o and E_p increased in value as orifice diameter decreased from 3175 μ to 140 μ diameter; however, there was no significant difference between the 140 μ and 40 μ pore diameter silica glass diffusers. Photographic analysis of the bubbles revealed a similar trend towards decreasing bubble size as orifice diameter decreased from 3175 μ to 140 μ. A reduction in air flow rate per fine bubble diffuser (40 μ and 140 μ diameter pore size) significantly increased K_La_{20}, OT_s, E_o and E_p. A reduction in tank surface area had a minimal effect on K_La_{20}, OT_s,

E_0 and E_p in the two tank configurations (70 L and 239 L) with different surface area to volume ratios (0.94 and 2.2 m^{-1}).

The field experiments demonstrated that increased depth of air release increased the oxygen input per cycle and water velocity in a full lift hypolimnetic aerator, which, in turn increased the daily oxygen load, E_0 and E_p. The orifice size experiments indicated that the 140 μ diameter pore size significantly increased oxygen input per cycle, daily oxygen load, E_0 and E_p; however, the size range in the coarse bubble diffusers (794 μ to 3175 μ) exhibited similar but reduced oxygen transfer characteristics. Under field conditions, the difference in bubble size generated by orifice diameters in the 794 μ to 3175 μ range was too small to have a significant effect in the full lift hypolimnetic aerator, because of their smaller surface area to volume ratio and the coalescing nature of the air-water mixture in the inflow tube. A reduction in surface area in the separator box had no effect on the oxygenation capacity of the hypolimnetic aerator.

These experiments indicate the majority of oxygen transfer in full lift hypolimnetic aerators occurs in the inflow tube, and separator box design modifications would be required to increase the surface transfer component of the overall oxygen transfer process. Options include increasing the relative size of the separator box and installing additional mechanical surface aerators inside the separator box. The most cost-effective method for increasing the oxygenation capacity of full lift hypolimnetic aerators is to redesign the diffuser to produce bubbles in the 2-3 mm diameter size range.

TITLE : The use of a deep shaft for the waste water treatment plant of ORGAMOL S.A.

AUTHOR : Roger P. Favre, dipl. Eng. FIT, Zurich, (Switzerland), Locher & Co. Inc. Zurich

AFFILIATION : M. ASCE, AG4

Orgamol SA waste water plant

Orgamol SA produces 40 to 80 different basic compounds a month for the international pharmaceutical industry. Industrial waste water from the plants is highly loaded (2800 kg BOD_5/d for a water volume of only 350 m3/d) and its p_H can vary over the whole scale.
The waste water is therefore first neutralized at the plant, then pumped to a buffer tank of 1100 m3 capacity so as to homogenize as far as possible the waste water and to permit continuous operation of the treatment plant over the weekend.
At present, the treatment plant features only a first stage, as this has to be thoroughly tested before designing the second stage to fit.

Deep shaft

This first stage consists mainly of a deep shaft (30 m deep) with a total capacity of 300 m3, where the mixed liquor is aerated under pressure. The aerated mixed liquor flows to a combined flotation/settling tank from where the sludge is either recirculated or removed when in excess.
The deep shaft takes the place of a conventional aeration basin.
The concentration of dissolved oxygen in the reactor-room is controlled by a variable speed pump of 45 kW which drives the mixed liquor through a multiple injector. Atmospheric oxygen is aspired at the injector outlet and the air/water mix is driven down. The volumetric air/water relationship is a linear function of the pump's speed. Maximum depth reached is 30 m.
The water/air mix then rises in the annulus and drives the mixed liquor in the reactor room.

Oxygen transfer in deep shaft

Pressure and flow charts of the deep shaft are presented and discussed.
Oxygen transfer data, based on measured oxygen input and reduced saturation values show interesting curves.
Their possible mathematical interpretation is discussed.
Comparison between tran-:er in water and in mixed liquor is made and -factor .s c .lculated.

Advantages and limitation of the deepshaft as an aeration unit for biological degradatio..

The energy consumption is on a par with other systems. But surface is smaller, so less land, less surfactants/antifoaming agents, less surface to cover in case of odors. A higher -factor means a better Oxygen use.
But oxygen transfer is limited by partial pressure so that an economical balance has to be found.

TITLE : OXYGEN AND NITROGEN TRANSFER IN LAKE AERATION LONG-TERM RESULTS IN VARIOUS SWISS LAKES

AUTHOR : ROGER P. FAVRE dipl. Eng. FIT, Zürich, (Switzerland), LOCHER & CO, INC. ZURICH

AFFILIATION: M. ASCE, AGU

1. Eutrophication in Swisslakes

In Switzerland, there are 70 natural and 96 artificial lakes (of over 0.1 km2) spread at altitudes varying between 250 m and 2500 m. All natural lakes and at least half the artificial ones between 250 and 750 m are eutrophic.

Eutrophication can very often be traced to an excess of nutrients, mainly P - phosphor - in our case. That led to a boom of sewage treatment plants and their extension with P-elimination stages. Now P-content has been stabilized or is slowly regressing. But the goal of 30 mg/m3 is far from being reached.

Main reasons are agricultural P-input and P release from the sediments. The former calls for external measures and political decisions, the latter can be dealt with by lake reaeration.

2. Aeration systems

Basically, there are 2 ways to aerate a lake

- an "open" system where bubble columns are produced through perforated plates, etc. Pure oxygen rises freely in summer and compressed air is used in winter.

- a "closed" system which uses atmospheric air throughout the year.

The Locher equipment belongs to the second category.

A flow diagram is shown and discussed.

3. Oxygen transfer with LOCHER equipment

Oxygen is transferred in two stages:

- in the pipe leading the air-water mixture down from the nozzle.

- in the air-lift (riser).

From the pressure chart, it is easy to calculate, for the average local atmospheric pressure and daily temperatures, the corresponding oxygen saturation values.

Measured oxygen transfer data are presented.

The main parameters are:

- the depth reached

- the volumetric air / water relationship

- the contact time

Interesting is a chart which shows the optimum parameter combination.

The respective pressure and transfer diagrams of lake Wilen and lake Hütten equipments are presented and discussed.

4. Results of oxygen transfer/presentation of lakes

Lake Wilen 1981 - 1990
Lake Hütten 1983 - 1990

The oxygen profiles are presented in chronologic series and oxygen uptake is discussed. Other relevant profiles (temperature, P, NH_4) are shown.

A special case:

Lake Türlen is a lake which lies in the lee of a ridge. The wind is not strong enough so that the fall and spring circulation are incomplete. A simple device induces complete overturn in the fall and maintains surface oxygen transfer during the winter period, even when the lake is frozen.

5. Nitrogen transfer

Results of measurements made in Lake Wilen are shown and a possible yearly mechanism is presented. Nitrogen profiles are shown.

6. Transfer of carbon dioxide and other gases

   Some ideas are presented based on yearly variations of p_H. Possible stripping of other gases is discussed.

7. Conclusion

   A healthy lake has a healthy sediment. Comparison between systems, further possibilities.

SIDESTREAM ELEVATED POOL AERATION STATION DESIGN

by Bill Macaitis

Assistant Chief Engineer, Metropolitan Water Reclamation District of Greater Chicago, 111 E. Erie, Chicago, Il. 60611

ABSTRACT: In the early 1970's the Metropolitan Water Reclamation District of Greater Chicago (MWRDGC) developed a plan for a system of instream aeration stations to insure maintenance of waterway dissolved oxygen standards and as an alternative to advanced wastewater treatment at the District's three largest water reclamation plants. Two diffused air instream aeration stations were constructed and are operational. These operate by bubbling air through diffuser plate batteries located in the waterway adjacent to the waterway banks. A total of ten diffused instream aeration stations were planned. Subsequent to the construction of the first two instream aeration stations, a review of the station's design was made with the purpose of reducing operational costs, simplifying operation and reducing impacts on waterway navigation.

A Sidestream Elevated Pool Aeration (SEPA) design was selected as a cost and environmentally effective alternative to the diffuser stations. The SEPA design involves the utilization of low head, high volume screw pumps to lift up to 50 percent (576 cfs maximum) of the waterway flow to a series of elevated shallow pools located adjacent to the waterway and connected by weirs. Aeration is achieved while pumping, in the shallow pools and at the waterfalls. The SEPA discharge flow is designed to be within 95% of dissolved oxygen saturation. Water is pumped from the bottom of the channel and discharged to the surface to maximize oxygen transfer and the mixing of the SEPA and bypass flows.

Five SEPA stations having a total pumping capacity of 2022 cfs and a cost of $35.4 million are planned to be constructed by the District. The stations will have a design capacity of 49,700 lb O_2/day and will aerate a 42 mile reach of the waterway system during warm weather months. These stations are an alternative to $300 million in advanced wastewater treatment projects.

The five SEPA stations were one element of a 1987 Water Quality Proposal report to the Illinois Pollution Control Board. This report was coauthored by the Illinois Environmental Protection Agency and the MWRDGC with the assistance of the United States Environmental Pollution Control Agency

(USEPA). The SEPA stations and an implementation schedule are a condition of the USEPA NPDES permit issued to the MWRDGC for its Calumet Water Reclamation Plant (354 MGD). Two stations are under construction and are scheduled to be completed in the spring of 1991. The remaining three stations have a 1990 construction start date and are to be completed in the spring of 1992.

A full vertical scale pilot station was constructed by the District adjacent to the waterway and operated for two years to verify the SEPA concept and obtain design data. Waterway water quality data and the mathematical modeling of the waterway were used to determine the necessary number, capacity and location of the SEPA stations. Additionally, four hydraulic scale models of planned stations and the adjacent waterway were constructed during design to optimize the mixing characterist cs of the stations and to prevent short circuiting between the intake and discharge channels of the stations.

The stations will be unmanned. They will be remotely operated from the MWRDGC's Calumet Water Reclamation Plant by radio control. Waterway DO concentration and temperature data will be automatically taken from upstream and downstream of each station and telemetered to the Calumet plant for operation.

The water elevation of the highest pool will range from 12 to 15 ft. above the waterway elevation. Three stations will each have four waterfalls of 3.0 ft. in height, and two stations will each have three waterfalls of 5.0 ft. in height.

Four of the stations are located on the MWRDGC's canal system and will operate with waterway elevations which are controlled by lock and dam structures and which during the design condition, dry weather, the waterway elevation will be maintained at a constant elevation approximating -2.0 ft. Chicago City Datum (CCD). Zero CCD is the approximate average elevation of Lake Michigan. The stations located on the MWRDGC canal system will each use two to five screw pumps of up to ten feet in diameter. Screw pumps were found to be cost effective for the stations and have the water quality advantage of aerating the station flow during pumping.

Station #1 is located upstream of the lock and dam system, and the waterway at this location approximates Lake Michigan's water elevation. The elevation of Lake Michigan at Chicago has ranged from El.-2.8 to 3.4 ft. CCD. Sustained high or low Lake levels can range over a period of years. Because the efficiency of an axial column pump is only affected to a small degree by the intake elevation ranges found at station #1, four submerged axial pumps with a total capacity of 100 cfs were selected as cost effective for Station #1. The pumping capacity of the stations will range

from 86 to 576 cfs.

Fish populations are not significant in the canal system. Relatively high fish populations have been measured at Station #1. A vertical moving fish barrier screen is being installed at Station #1, and provisions have been included in the designs of the canal stations to allow for the future addition of fish barriers.

The station locations range from highly urban to relatively remote. In order to implement the five station SEPA project it was important that the adjacent communities not view these water quality facilities as a liability. The stations will not be fenced and are lighted. Multipurpose active and passive recreational, environmental and navigational uses have been integrated into the station designs. The design themes for the stations were chosen to be compatible with the surrounding land use. The stations where sited on MWRDGC land which was originally purchased to construct the modified river and canal system, and the station land provisions range from 2.0 to 20.0 acres.

Station #1, which is bracketed by an industrial area and wetlands, will have a pump house similar to the architecture of surrounding modern industrial buildings but will also have a constructed 4.0 acre wetland, a protected heron rookery and a nature path with bridges through the station. Station #2, which at 86 cfs capacity is the smallest station, is designed as a 22 ft. high waterfall (water is pumped to the upper portion of the waterfall system in limited quantities for aesthetic purposes) on a wooded high bank at a bend in the waterway. Station #3 is located in a highly populated area and is designed as an urban park. The adjacent municipality of Blue Island will operate the station as a park with the MWRDGC operating and maintaining the water quality elements of the facility. Station #4 has a more passive park character, and it is hoped a local municipality will eventually assume the general maintenance responsiblity for this station. Station #5, which with a 576 cfs capacity is the largest of the five,is located at the junction of two waterways, and its most significant feature will be a lighthouse.

DESIGN OF MECHANICAL AERATION SYSTEMS FOR RESERVOIR TAILWATER ENHANCEMENT

Richard E. Price and Edward B. Meyer

U.S. Army Engineer Waterways Experiment Station

ABSTRACT

Many large reservoir projects, such as Corps of Engineer Reservoirs, experience low dissolved oxygen (DO) levels in the tailwater during the stratified periods of the year. In some cases, the loss of DO has resulted in fish kills in the tailwaters and downstream. A variety of alternatives have been investigated to alleviate the low DO conditions in the tailwater. Some techniques involve reaeration of low DO in the reservoir prior to release, such as localized mixing to enhance release of epilimnetic water or hypolimnetic oxygenation. Methods to enhance reaeration of the water as it passes through the structure such as turbine venting or penstock oxygen injection have also been successful at some projects. However, few techniques have been developed for tailwater reaeration. Therefore, some research effort was directed at developing design guidance for mechanical aeration systems which would be suited to tailwater environments.

A variety of mechanical aeration devices, which are designed primarily for wastewater treatment facilities, are available commercially and may be suited for some tailwater aeration applications. However, the performance criteria usually given with this type of equipment is in the form of an efficiency rating on a per horsepower (Hp) basis (oxygen in pounds/Hp/hr). This works well if the design application calls for a system capable of delivering a given volume of oxygen in a specified time period to satisfy a DO demand due to biochemical oxygen demanding materials. In reservoir tailwater environments however, the driving force for reaeration is controlled primarily by the DO deficit, rather than biochemical oxygen demanding components. Since the efficiency per Hp for most devices has been developed, a means of relating a mechanical aeration device's oxygen delivery rate to the DO deficit would provide a method for designing mechanical aeration systems for tailwater environments.

The recommended model for analysis of oxygen transfer data is the two-film model (ASCE, 1983). This model is also appropriate for describing the reaeration process with mechanical aeration systems in reservoir tailwaters. Upon integration, the logarithmic form of the model is as follows:

$$\ln \frac{C_\infty - C}{C_\infty - C_0} = -K_L a \ t \qquad (1)$$

where:

C_∞^* = average dissolved oxygen (DO) saturation concentration, mg/l
$K_L a$ = apparent volumetric mass transfer coefficient, t^{-1}
C_0 = DO concentration at $t = 0$, mg/l
C = average DO concentration, mg/l
t = time, hr.

This form of the model can be rearranged in terms of the ratio of the final deficit to the initial deficit and substituting the hydraulic residence time (V/Q) for time (t) as follows:

$$\frac{D_f}{D_i} = \exp\left[-K_La(V/Q)\right] \tag{2}$$

where:

D_f = final deficit (C_∞^* - C), mg/l
D_i = initial deficit (C_∞^* - C_0), mg/l
V = volume of aeration basin, mil gal
Q = flow through rate, mil gal/hr

Using this form of the model, the amount of DO deficit that can be satisfied for any given reservoir tailwater can be determined. The DO in the release, the basin volume and release volume are usually known, however, since the K_La for each type of aeration device in a given tailwater would be different, it is usually determined from pilot tests using a proposed aeration system under proposed field conditions. By rearranging the equation used to determine the Oxygen Transfer Rate (OTR) for an aerator using data from pilot tests , a K_La can be computed using the following equation:

$$K_La = [(OTR)(Hp)]/[(8.34)(Q)(C_\infty)] \tag{3}$$

where:

OTR = oxygen transfer rate, lbs O_2/Hp/hr
Hp = total horsepower of aeration system, Hp.

With a K_La computed using equation 3, equation 2 can then be used to determine the deficit satisfaction with a given aeration system.

This approach was used to compute the K_La for pilot tests of aspirating aerators in a tailwater environment and tests of aerators in other applications, including wastewater facilities. The predicted K_La compared favorably to the observed K_La for tailwater tests. Results also indicate that the quotient of the final deficit to initial deficit can be used to evaluate mechanical aeration devices for tailwater applications.

References

American Society of Civil Engineers 1983. "Development of Standard Procedures for Evaluating Oxygen Transfer Devices," Prepared for Municipal Environmental Research Lab., EPA, Cincinnati, OH.

Oxygen Transfer with a Bubbleless Membrane Aerator

Michael J. Semmens and Tariq Ahmed
Department of Civil and Mineral Engineering
University of Minnesota
Minneapolis MN 55455

The objective that the manufacturers of aeration devices strive for is to provide the maximum oxygen transfer at the lowest cost. The effectiveness of oxygen transfer is evaluated in two ways: by the oxygen utilization efficiency, and the pounds of oxygen transferred per horsepower - hour. The oxygen utilization efficiency is a measure of the fraction of the oxygen delivered to the water that is actually transferred into the water. A high efficiency is clearly desirable. For example, higher efficiencies may be achieved by using an aerator that produces smaller bubbles, however this can only be achieved with a greater power input, which means that we must consider the ratio of oxygen transfer to the power input. The lbs. O2 transferred/HP-hr is a measure of the operating cost of the aerator. As the value of this ratio goes up the operating cost of putting a certain amount of oxygen into the water goes down. Generally it is true to say that as the oxygen utilization efficiency goes up the operating cost goes up as well.

Bubbleless aeration using a sealed membrane pressurized with pure oxygen is characterized by having an oxygen utilization efficiency of 100% irrespective of the power input. Thus at low power inputs the ratio of lbs. O2 transferred/HP-hr can be large. It is this feature of membrane aeration that makes it attractive and we have spent approximately a year studying aeration using hollow fibers of polypropylene filled with oxygen.

Experimental:

The bubbleless membrane aerator employs the use of oxygen filled hollow fibers that are made of microporous polypropylene (Hoechst Celanese, Charlotte, N.C.) to affect the gas transfer. This membrane had a fiber diameter of 400 microns and a wall thickness of about 12 microns. Approximately 40-60% of the surface of the membrane is made up of 0.02-0.05 micron holes. When the membrane fiber is immersed in water it does not wet owing to the hydrophobic nature of the polymer. Thus all the pores remain dry and air filled. Gases and volatile components may transfer across the membrane wall through these pores, however the water, and nonvolatile components in solution are rejected by the membrane. Since the membrane is gas filled, transport through the membrane is by gaseous diffusion through the pores which is approximately 5 orders of magnitude faster than diffusion in liquids, oxygen transfer remains liquid film controlled just as it is in conventional aeration. The membrane therefore presents no impediment to oxygen transfer.
The oxygen is transferred across the membrane by diffusion and water flowing past the membrane is enriched in oxygen.

The aerator tested is schematically depicted below in Figure 1. For the field tests a pump forces water through a PVC pipe and over the fibers. Approximately 1000 hollow fibers measuring up to about 2.6 meters in length were fitted to a regulated oxygen supply.

The fibers were sealed at the downstream end such that the oxygen delivered to the fibers cannot escape from the fibers to form bubbles. However, the oxygen contained in the fibers may diffuse across the membrane walls and into the water flowing past on the outside. The fibers are individually sealed at the downstream end and thus they are each

free to move independently with the local flow patterns. The flow past the fibers tends to induce a waving motion in the membrane fibers that appears to encourage mass transfer between the fiber and the surrounding water.

The results of our field tests on the bubbleless membrane aerator will be presented. The membrane aerator was tested in a lake water aeration application and also for the supplemental aeration of a secondary effluent. The results of these field test transfer data will be compared with clean water test data and operating difficulties experienced in field application will be discussed.

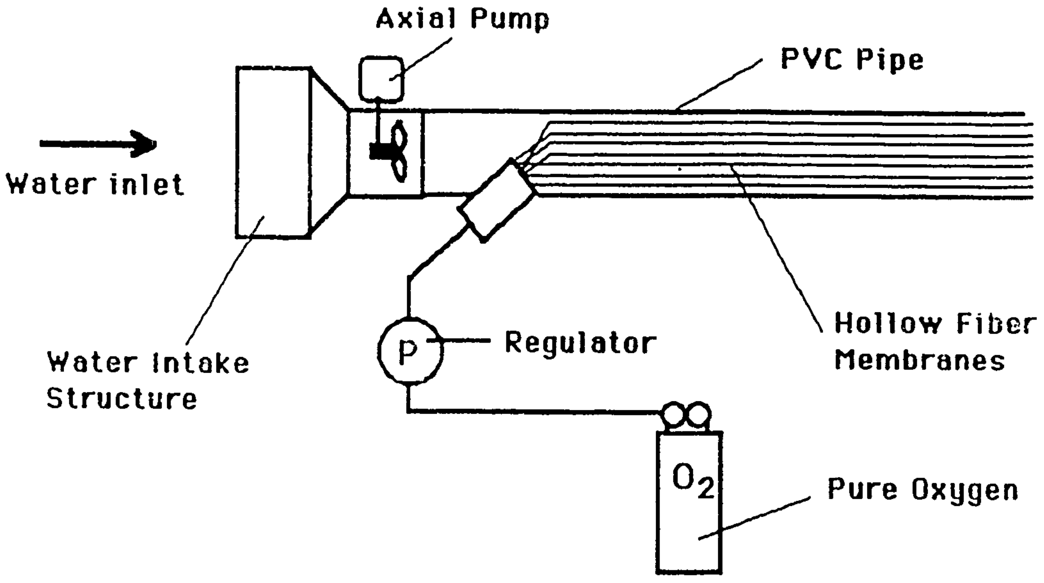

FIGURE 1: A SCHEMATIC REPRESENTATION OF THE BUBBLELESS AERATION DEVICE

Performance of an Aerator Based on Jet Pump-Aspirator Principles

Charles C. S. Song
Professor
University of Minnesota
Department of Civil and
Mineral Engineering
Mississippi River and 3rd Ave. SE
Minneapolis, Minnesota 55414-2196

and

Dominic S. Arbisi
Consultant
Aeras Water Systems, Inc.
4510 W. 77th Street
Suite 101
Minneapolis, Minn. 55435

The principle of jet pump has been widely applied in industry to pump not only liquids, but also, solids and gases. A jet pump depends primarily on the momentum of a high speed liquid jet to drive the material being pumped. On the other hand, the commonly available spray devices or aspirators depend on the low pressure generated according to the Bernoulli principle to drive the material to be pumped. By a suitable combination of the two principles, it should be possible to optimize the efficiency of a pump.

The Aeras Water System Inc. is committed to developing an efficient Aerator system based on the principles of jet-pump and aspirator for environmental applications. A preliminary design of such a device has been completed. A prototype will be manufactured and tested under a laboratory controlled conditions immediately. The primary objective of the test will be to evaluate the pumping characteristics involving, among other variables, the water and air pumping rates, jet momentum, and approximate (mean) air bubble size under various submergence and other ambient conditions. Unlike a conventional pump for which, head-discharged characteristics is of primary importance, the overall efficiency of an aerator depends also on the air pumping rate, air bubble size and the momentum of the air-water jet. The last quantity affects the current in the receiving water body and, hence, the mixing and the residence time of the injected air.

This paper will describe the design principle and present the experimental results.

THEORETICAL INVESTIGATION OF BUBBLE PLUMES FOR LAKE REHABITATION BY RE-OXYGENATION

by

Gee Tsang

National Hydrology Research Institute,
Saskatoon, Saskatchewan, Canada. S7K 3H5

Eutrophication of lakes has led to overgrowth of algae and aquatic weeds in them. As the dead algae and weeds accumulated on the lake bottom decay, dissolved oxygen is extracted from the lower layers of the lake water. This leads to oxygen depletion in the bottom layers of the lake and the destruction of habitate for fishes and other aquatic lives. In extreme cases, the lake can be biologically dead excekt for some bateria and fungi.

To rehabitate the oxygen depleted lakes, experiments have been conducted in Canada and in Switzland to re-oxygenate the lakes with bubble plumes. While in Switzland (Muller and Hugi, 1989), air bubble plumes were used in the summer and oxygen plumes were used in the winter, in Canada, pure oxygen plumes were used for both seasons (Prepas and Murphy, 1987). As of today, the Canadian experiments were mainly addressed to biological and chemical concerns. Physical investigation was lacking to guide the effective use of the bubble plumes and the development of a practical and economical technology. This paper will report the physical investigation which was undertaken to fill the above gap. It is anticipated that both laboratory and field experiments will be undertaken under the guidance of the knowledge learned from the present physical investigation.

Gas plumes have been widely used in engineering applications. Besides used for reaeration and stripping volatile compounds from water, they were used for water mixing, freezing suppression, wave breakers as well as oil-spill barriers. The physical properties of bubble plumes have been studied and modelled by Kobus (1968), Ditmars and Cederwall (1974) and Milgram (1983). These researchers treated the bubble plume as an entity and tried to model the vertical velocity distribution, density distribution, Variation of the centre-line velocity with height, the mass flux, the buoyancy flux and the momentum flux. Although the detailed treatments of the problem were unique and different assumptions were used by the researchers, their basic approach to solve the problem was the same, namely in considering or assuming that

1. The conservation of momentum is observed,
2. The buoyancy flux is produced by the rising gas bubbles,
3. The gas bubbles undergo isothermal expansion as they rise,
4. The characteristics of the bubbles are independent of the conditions at the orifice, and

5. The gas is not absorbed by the ambient water.

In the present theoretical investigation, because the nature of application of the oxygen or air bubble plumes, the plume gas will definitely be absorbed and point 5 above will obviously no longer apply. The flux of oxygen across the bubble boundary is assumed to be proportional to the difference between the partial pressure of oxygen in the bubble and the equilibrium partial pressure that would otherwise produce the concentration of oxygen in the ambient water according to Henry's law. As the initial oxygen bubbles rise, other dissolved gases are stripped into them and render the bubbles to be of mixed gas. The stripping process is also governed by the same law and having the same formulation.

Because the total mass transfer of gases between the bubbles and the ambient water is greatly affected by the total gases/water area, the number of bubbles will be an important parameter and the assumption that the characteristics of the bubbles are independent of the initial conditions of the plume (point 4 above) will also become invalid. An equation is established relating the initial energy flux to the initial number of bubbles. This number is assumed not to change as the bubbles rise, shrinking or expanding as governed by absorption and isothermal expansion.

Presently the theoretical investigation is still in progress. Some interesting conclusions, however, have been drawn which should provide ample opportunity for the participants to discuss and debate during the conference.

References:

Ditmars, J.D. and Cederwall, K., 1974, Analysis of Air-Bubble Plumes, Proceedings of 14th Coastal Engineering Conference, June 24-28, Copenhagen, Demark, Vol.III, pp.2209-2226.

Kobus, H.E., 1968, Analysis of the Flow Induced by Air-Bubble Systems, Proceedings of 11th Conference on Coastal Engineering, Sept., London, Vol. II, pp.1016-1031.

Milgram, J.H., 1983, Mean Flow in Round Bubble Plumes, Journal of Fluid Mechanics, Vol. 133, pp.345-376.

Muller, A. and Hugi, C., 1989, Design of an Instrument for Measuring Density, Size and Velocity of Rising Air Bubbles, Proceedings of Workshop on Instrumentation for Hydraulics Laboratories, International Association for Hydraulic Research (IAHR), Aug. 16-18, Burlington, Ontario, Canada, pp 61-70.

Prepas, E.E. and Murphy, T.P., 1987, Proposal to Aerate the North Basin of Amisk Lake, Summer, 1988, A Proposal submitted to the Ministry of Fish and Wildlife, Alberta, Canada. (Unpublished).

WATER SURFACE FLOW PATTERNS INDUCED BY A BUBBLE PLUME

K. Zic and H. G. Stefan
St. Anthony Falls Hydraulic Laboratory
University of Minnesota, Minneapolis, MN

Aeration of stratified (or non-stratified) lakes is a common method to increase dissolved oxygen in the water. In this method gas is transferred from rising bubbles to water, but there is also increased reaeration at the water surface due to the surface flow and turbulence induced by the bubble plume. Results of laboratory experiments and numerical simulations will be presented to give some information on surface temperatures and surface velocities induced by air bubble plumes. Experiments and simulations were conducted for temperature stratified laboratory tanks simulating "typical" mid-summer conditions in temperate lakes.

In the experiments the time evolution and the spatial distribution of water temperatures on the water surface were measured. Of particular interest for surface gas transfer are the development of the upwelling region and the water temperature induced by the bubble plume. Infrared photographs of the surface temperature show the axisymmetrical nature of the flow. It has been found that there is a distinct nearfield and farfield with a size of the nearfield of the order of the lake depth.

The 2-D numerical model provides additional information about the flow field which would be difficult to obtain from the experiments. The flow patterns by means of the velocity vectors, streamlines and temperature contours will be presented and analyzed. The transition from the stratified flow patterns to the one of the well-mixed water body will be presented.

The turbulence fluctuations in the measurements and simulations will be presented and related to the governing parameters.

No gas transfer rates were calculated.

UNIT PROCESSES

GAS HOLD-UP AND MASS TRANSFER IN BCR WITH AND WITHOUT RECIRCULATION LOOP

U. K. Ghosh and S. N. Upadhyay

Department of Chemical Engineering and Technology
Banaras Hindu University, India

Bubble column reactors (BCR) with or without internal recirculation loop are being widely used in many chemical and biochemical processes due to their simple design, absence of mechanical moving parts and high efficiency for mixing, heat and mass transfer. Deep shaft reactor is a direct application of such reactors to wastewater treatment.

The degree of circulation in bubble column reactors depends upon a number of parameters, such as the size of the equipment, the nature of the phases involved, the velocities of the phases, the nature of internals within the equipment, and many others. Flow regime, bubble size distribution and coalesence characteristics, gas hold-up, interfacial mass transfer coefficents, gas liquid interfacial area, dispersion coefficients, heat transfer and particle fluid mass transfer characteristics are important design parameters for all types of bubble column reactors. A thorough knowledge of these interdependent parameters is necessary for a proper scale-up of these reactors.

In the present work, an attempt has been made to compare the gas hold-up and solid-liquid mass transfer characteristics of bubble column reactors with and without recirculation loops. Some additional data on gas hold-up and mass transfer are also reported. Fluids used are water, 0.5 and 1% aqueous CMC and 60% propylene glycol. Bubble columns used are 14.5 to 65 cm in diameter and 190 to 290 cm in height. Correlations for gas hold-up and mass transfer coefficients are presented.

SIMULATION BY WATER-TEST OF THE ARGON ENTRAINMENT IN THE SODIUM OF A BREEDER

J. Guidez and G. Cognet

French Atomic Commission
13100 St. Paul lez Durance

The fast breeder reactors use sodium as coolant and argon as gas-blanket above sodium the free surface; thus, gas entrainment is always possible in nominal or accidental conditions.

For example at nominal conditions, vortices may appear at the free surface of sodium and entrain gas. The spillway, used to lick bath the main vessel with "cold sodium" (400°C), is also a source of argon bubbles in the sodium (circulation).

Furthermore accidental operation can also create a temporary modification of the bubbles' concentration. For example, there is a bell around the SPXI Heat Exchanges. This bell is filled with pressurized argon which avoids the circulation of sodium between the hot and the cold plena. If the argon pressure accidently decreases, sodium can irrupt inside the bell and entrain a part of the imprisoned gas.

The main consequences of the argon circulation are both neutronic perturbations, with possibilities of plant shutdown, and measurement perturbations (acoustic monitoring or ultra-sonic measurements).

So, it is necessary during the project studies to predict the maximum level of gas in the sodium in the nominal and accidental situations.

For practical reasons (visualization and measurement technics) it is easier for experimentalists to simulate the sodium/argon couple, with the water/air couple. A majority of diphasic phenomena can be simulated with the respect of four adimensional numbers:

- The Reynolds number (for the hydraulic simulation).
- The Froude number (when a free surface exists).
- The Weber number (for the surface tension).
- The Euler number (for the gas pressure).

The simultaneous respect of these four numbers between sodium and water is not possible. On the contrary for one scale value ($\hat{L} = 0.61$ for sodium at 430°C and water at 20°C), it is possible to respect the Froude and the Weber. In that case the distortion on the Reynolds remains supportable (1/7 in.), especially for high turbulent circulation. The other scales are then $\hat{Q} = 0.3$ for the flow-rate, $\hat{t} = 0.78$ for the time, and $\hat{P} = 0.76$ for the pressure.

So it is possible with water tests to have a good simulation of the diphasic effects in sodium. An application is shown with the results of a mockup, named SIRENA. In that case, the test was in geometrical similarity with the Super Phenix heat exchanger bell at the scale 0.62. When the pressure decreases in the bell the water levels climb up, go up, and when the siphon begins to be in circulation, a part of the gas is entrained. The test shows the large influences of some parameters as the initial flow-rate and shows clearly two different phenomena. At first the bubbles are created by a

classical "spillway effect." Then the flow rate increases, a siphon-circulation occurs, a free surface is created and big vortices entrain a part of the remaining gas. Comparisons with test results at nominal scale, in sodium, on the Super Phenix plant were made and show good agreement with the tests SIRENA.

In other cases, if the dimensions of the studied phenomena are too large, the choice of a scale of 0.62 is not yet possible for economic reasons. For example, the study of the vortices at the free surface of the plant is not possible at this scale, and bigger distortions on the similarity rules are unavoidable. Practically no distortion is taken on the Froude number, but a bigger distortion is taken on the Reynolds number and some small distorsion is accepted on the Weber number.

As an example, some results are shown on a water mock-up at scale 1/8th of the hot pool of the european fast reactor project: Colchi III. The test shows vortices at the free surface with gas entrainment. An explanation of the cause of this phenomenon was found and a modification of the internal structures is shown that suppresses the gas entrainment by vortices. A comparison of the hydraulic circulations in the two cases is made, that explains the results obtained.

As a conclusion, it appears that the global methodology to quantify the gas entrainment in the fast breeder reactor studies is clear. Either the phenomenon is local (siphon, spillway, etc.) and a water-test at scale 0.62 gives results directly transferable for the plant, or the phenomena occur on a large scale (pool free surface, for example) and water tests are made at a smaller scale to modify the hydraulic circulation in order to suppress gas entrainment.

Title: Enhancement of Gas-Liquid Mass-Transfer Rate in Process Reactors

Authors: Uzi Mann, Himanshu Zinzuwadia and Charles Forster

Affiliation: Texas Tech University, Lubbock, TX 79409

The performance of many gas-liquid process reactors is limited by the rate the gas reactant is transferred into the liquid. To improve the transfer rate it is necessary to break the gas phase into small bubbles to generate a large gas-liquid interface area. This is achieved by an agitated tank configuration whose standard design is based on the use of vertical baffles (usually four) along the tank wall, and selection of an appropriate agitator (see Figure 1). To ensure formation of small gas bubbles and to enhance the mixing of the reacting broth high level of shear is generated by the impeller.

The standard design of agitated gas-liquid reactors has three main drawbacks: (i) Excessive shear level is generated near the impeller in order to maintain good mixing throughout large reactors. Beside the many high agitation power associated with high shear, in reactors (e.g., bioreactors processing mammalian cells) a limit on the maximum shear generated is imposed. To reduce the shear the agitator speed is reduced, but this results in low gas-liquid transfer rate. (ii) Undesirable flow patterns generated by the baffles causing low gas holdup and small interfacial area. (iii) Inflexible design - the impeller design dominates the reactor operation.

A modified design, utilizing horizontal (radial) baffles at the liquid surface has been investigated. Horizontal baffles prevent vortex formation and generate less shear than standard baffles. In addition, the flow patterns generated by the horizontal baffles induce surface aeration and increase gas holdup in the tank, thus improving the gas-liquid mass transfer rate.

Experiments conducted on a 7 gallon reactor (1 ft ID, 1.5 ft. height) showed that the gas-liquid mass transfer rate improved by a factor of 1.6 to 2.3 over that in an identical reactor with standard baffles operated in the same conditions, while the agitation power was 30% lower. (See Figure 2).

The paper will describe the design and operating experience with horizontal baffles as well as an analysis of the experimental results.

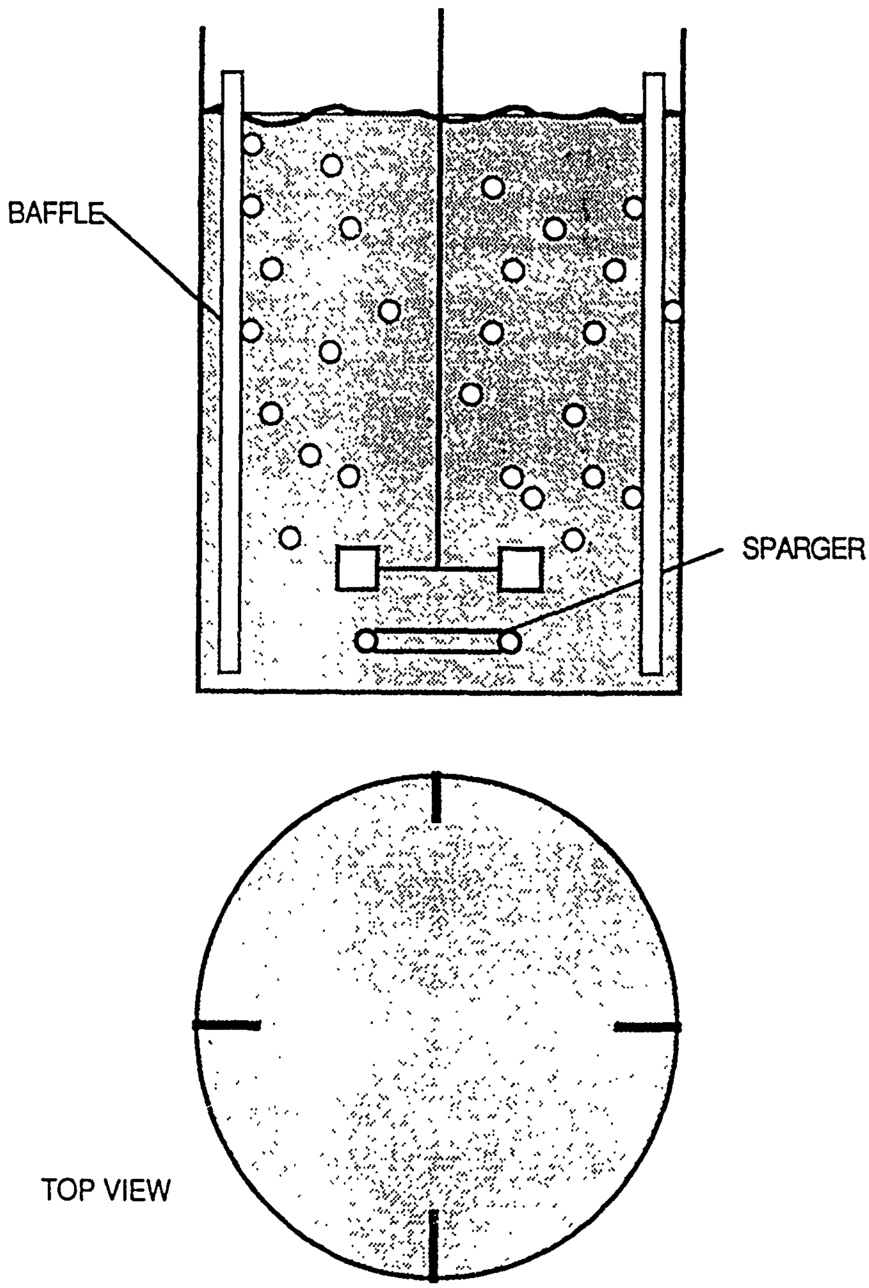

Standard Design of Agitated Reactor

12-081

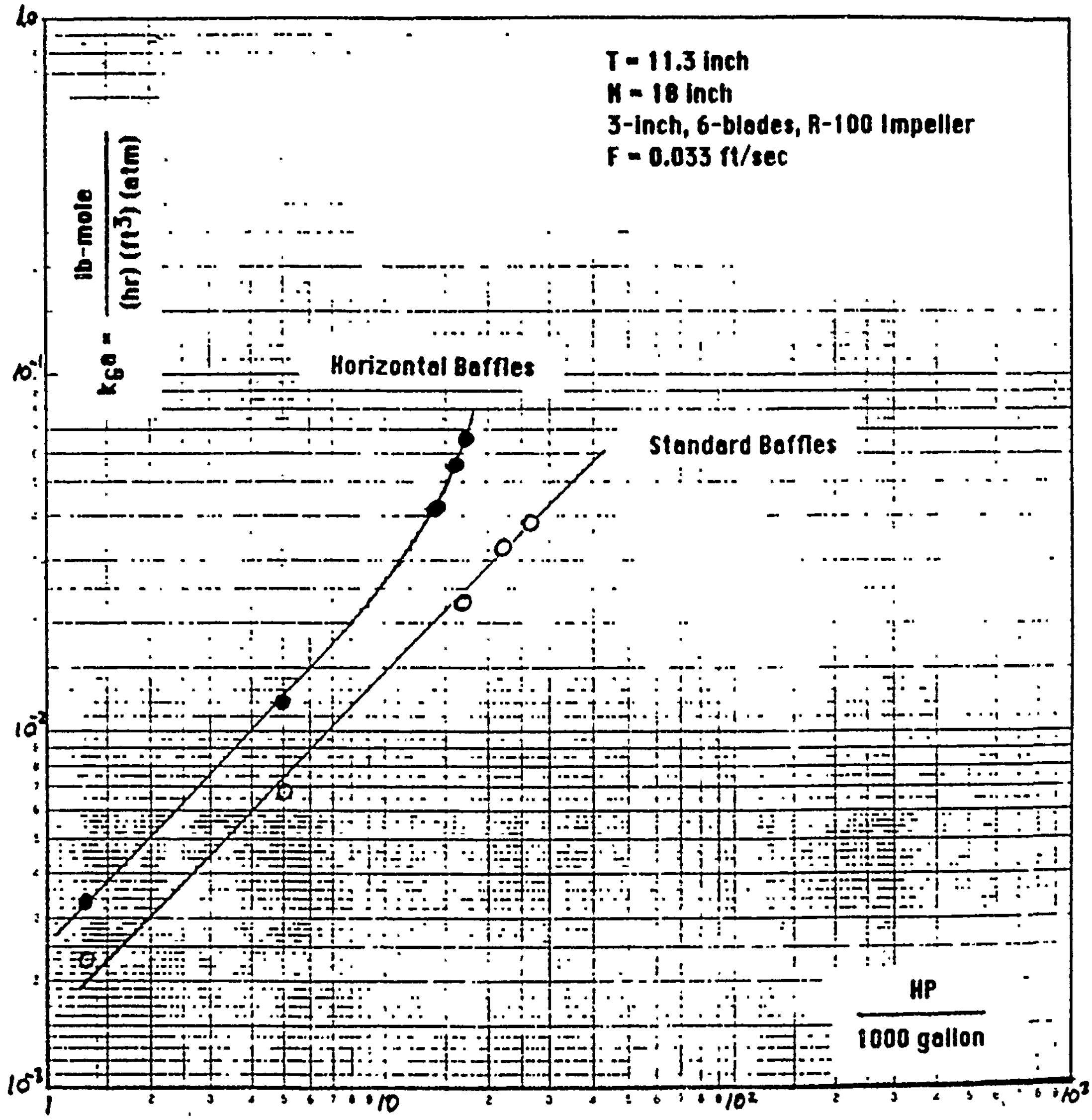

Performance Comparison Between Reactors Equipped with Horizontal and Standard Baffles

Full Logarithmic, 3 × 3 Cycles

STEADY TURBULENT GAS DESORPTION IN SURFACE CONDENSER TUBES

Mahmood Naghash
Bechtel Corporation, Gaithersburg, MD

C. Samuel Martin
Georgia Institute of Technology, Atlanta, GA

The hydraulic and thermal performance of the cooling water systems of the thermal power plants are greatly affected by the desorption of the dissolved gas of the cooling water. During steady-flow conditions, more often the pressure in the upper tubes of the condenser is sub-atmospheric creating a super-saturation condition if the water is initially saturated at the intake. The combined effect of pressure reduction and water temperature rise along the condenser tubes increases the degree of super-saturation favoring higher longitudinal rates of gas desorption. If the released air is not removed completely by the action of vacuum pumps, its accumulation in the upper tube rows can cause blockage, thus reducing the effective cooling surface and lowering the condenser efficiency. Furthermore, the deaerated discharge water in conjunction with its temperature rise creates ecological problems in the receiving water bodies.

There is very limited literature available quantifying the turbulent mass transfer in the pipelines even for no heat transfer effect. An experimental and mathematical investigation of turbulent mass transfer in a horizontal tube with no effect of temperature is reported by Naghash [1989]. In this study, by maintaining upstream pressure atmospheric and the downstream pressure sub-atmospheric, a turbulent gas desorption is generated along a 32 m long, 26 mm diameter pipe. Then the cross sectional average volume of the free gas along the pipe is measured experimentally for a variety of test conditions. The experimental findings are then used to test a one-dimensional two-phase flow equation model derived for this purpose. The objective of present study is to include the heat transfer effect in the mathematical formulation and to investigate the problem numerically.

A one-dimensional steady two-phase separated flow model in conjunction with mass transfer equation and an associated turbulent mass transfer coefficient model introduced by Naghash [1989] are utilized to represent the numerical model. The heat transfer relation along the condenser tube is presented through the Log Mean Temperature Difference (LMTD) relation available for the surface condensers. The set of mathematical relations are then integrated numerically in conjunction with the boundary conditions.

In the first part of this investigation the numerical predictions are compared against the experimental results of Naghash [1989] to demonstrate the influence of heat addition. Then the effect of a number of variables on the gas desorption rate including variation of pressure, degree of saturation, temperature, and sensitivity to the mass transfer coefficient model multiplier are evaluated numerically. The surface condenser design data are obtained from the Heat Exchange Institute Standards for Steam Surface Condensers [1984].

REFERENCES

Naghash, M., "Steady Turbulent Gas Desorption in a Horizontal Pipeline", Ph.D. Thesis, Georgia Institute of Technology, Atlanta, Georgia, March 1989.

"Heat Exchange Institute Standards for Steam Surface Condensers", Eighth Edition, Heat Exchange Institute, Cleveland Ohio, January 1984.

THE BEST HOLLOW FIBRE CONTACTOR

S. R. Wickramasinghe, M. J. Semmens* & E. L. Cussler

Departments of Chemical Engineering & Materials Science and Civil and Mineral Engineering*

Abstract

Traditional membrane devices have been developed using a plate and frame or spiral wound geometry. In the early 70s the hollow fibre geometry was introduced. These fibres consisted of small diameter tubes (3-400 mm). The walls were made of the same polymeric materials commonly used for flat membranes thus the walls of these hollow fibres had the same properties as the corresponding flat membranes.

Current hollow fibre modules are designed like small shell and tube heat exchangers. They consist of a glass or plastic shell containing a bundle of hollow fibres. At each end of the shell the fibres are embedded in a potting material made of polyurethane or an epoxy . Two distinct phases flow independently in the module. One phase flows inside the lumen of the fibres; the other flows outside the fibres. In most hollow fibre devices a parallel flow configuration has been used. D'Elia et al. (1986), Prasad et al. (1986) and Yang & Cussler (1986) however report experiments using a cross flow configuration.

Hollow fibre contactors can allow rapid mass transfer compared to conventional equipment. For example acid gas treatment with hollow fibre modules can take place more than ten times faster than in packed towers, (Zhang & Cussler, 1985). Liquid-liquid extraction with hollow fibre modules can occur more than one hundred times faster than in packed towers, (Kiani et al, 1984). While the rates observed in extraction are comparable to those in centrifugal extraction they are achieved at much lower equipment costs.

The aim of this project is to design the 'best' hollow fibre contactor by maximising the mass transferred per operating cost of the module. In the past, the design of hollow fibre contactors was based upon maximising the mass transferred per unit volume. The system considered here is the de-oxygenation of water. This system has many interesting commercial applications including the pretreatment of boiler feed water, the de-oxygenation of bottled beverages and the de-oxygenation of sea water for secondary oil recovery (Balasundaram et al. (1989)).

The overall operating cost of a hollow fibre contactor is given by the membrane cost and the power cost of pumping the two phases through the unit. Results for a volatile solute within the fibres are included here.

Both graphs show a sharp decrease in the COST/MASS TRANSFERRED with increasing fibre diameter. This is due to the decrease in pumping cost as the fibre diameter is increased. In both cases a minimum is reached. Then at intermediate fibre diameters the COST/MASS TRANSFERRED increases due to the rising membrane cost. It can be seen that the optimum fibre

diameter decreases with increasing membrane cost. This can be rationalised in terms of the opposing nature of the membrane cost and power cost. As the fibre length increases, the value of the optimum fibre diameter increases. This shows that the increase in the minimum cost with increasing fibre length is due mainly to higher pumping costs.

Results obtained from modelling a volatile and non-volatile solute in various module geometries are presented. The method of Lagrange multipliers is used to find an overall minimum COST/MASS TRANSFERRED. Experimental results are then compared with the predictions obtained. The 'best' hollow fibre contactor is then described. The usefulness of the various mass transfer correlations available in the literature is discussed as well as the direction of future work.

References

1. Balasundaram, V., Porter, J. E. and Ramshaw, C., (1989), 'Process Intensification: A Rotary Seawater Deaerator', *AIChE Annual Meeting*.

2. D'Elia, N. A., Dahuron, L. and Cussler, E. L., (1986), 'Liquid-liquid Extractions with Microporous Hollow Fibres', *J. Memb. Science*, 29, 309-319.

3. Kiani, A., Bhave, R. R. and Sirkar, K. K., (1984), 'Solvent Extraction with Immobilised Interfaces in a Microporous Hydrophobic Membrane', *J. Memb. Sci.*, 20, 125-145.

4. Prasad, R., Bhave, R. R., Kiani, A. and Sirkar, K. K., (1986), 'Further Studies on Solvent Extraction with Immobilized Interfaces in a Microporous Hydrophobic Membrane,' J. Memb. Sci., 26, 79.

5. Yang, M.C. and Cussler, E. L., (1986), 'Designing Hollow Fibre Contactors', *AIChE J.*, 32, 1910-1916.

6. Zhang, Qi and Cussler, E. L., (1985), 'Microporous Hollow Fibres for Gas Absorption', *J. Memb. Sci.*, 23, 321-332.

VOLATILE SOLUTE WITHIN FIBRES
VARIATION OF MEMBRANE COST

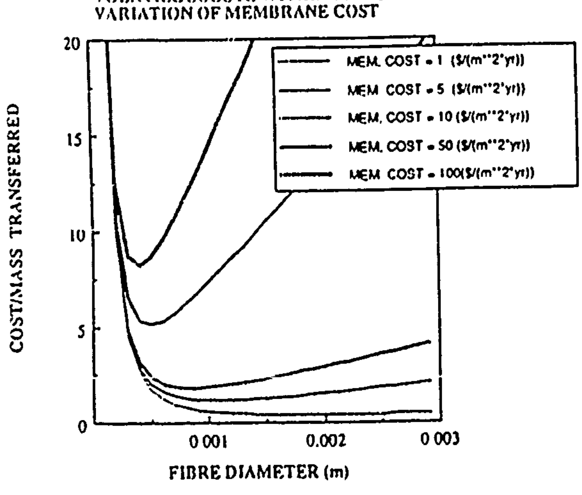

VOLATILE SOLUTE WITHIN FIBRES
VARIATION OF FIBRE LENGTH

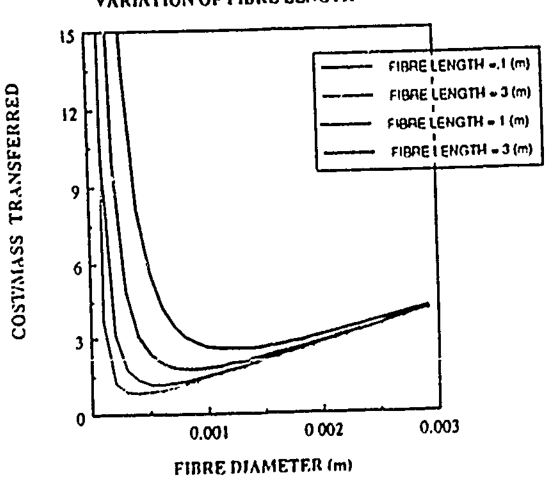

WATER/WASTEWATER TREATMENT

USE OF A GAS TRANSFER MODEL TO EXAMINE ALTERNATIVE CONTROL STRATEGIES FOR AN OXYGEN ACTIVATED SLUDGE TREATMENT PLANT

R. C. Clifft

Department of Engineering, Arkansas State University,
P. O. Box 1740, State University, Arkansas, 72467, U.S.A.

A large number of wastewater treatment plants that utilize high purity oxygen ($\geq$ 90%) have been constructed since the late 1960's. The oxygen activated sludge (OAS) process is the most widely used version and involves the continuous feeding of high purity oxygen, influent wastewater, and recycled sludge to a staged closed-tank reactor. As shown in Figure 1, the conventional scheme for controlling oxygen utilization consists of varying the oxygen feed rate to maintain a constant pressure in the first stage (usually 2 to 6 mm Hg above atmospheric pressure) and regulating the exit gas flow manually or automatically to maintain the exit gas composition at approximately 50 percent oxygen (Albertsson et al., 1978). An operating pressure above existing atmospheric conditions is required to vent nitrogen and carbon dioxide which accumulate in the reactor and to force the high purity oxygen through the series of stages.

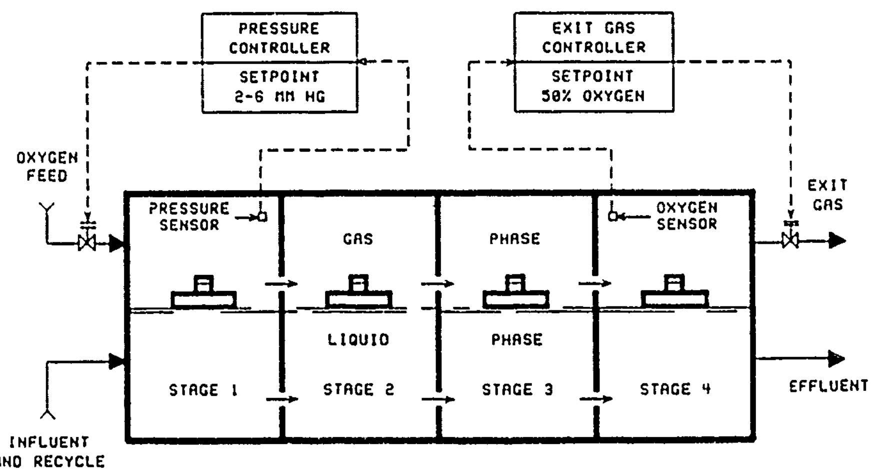

FIGURE 1. Conventional Control Strategy

The conventional control method usually provides for about 75 to 85 percent utilization of the oxygen feed by the biological reactions (Clifft and Barnett, 1988). This is a considerable improvement over very early attempts to use high purity oxygen, but there are several disadvantages of the conventional control method. Because the system

operates with a slight positive pressure in the gas phase, losses of oxygen by leakage through cracks in the concrete reactor cover can be significant. A direct means for controlling the dissolved oxygen (DO) in the effluent mixed liquor does not exist, so significant amounts of oxygen can be lost through the exit gas line and the mixed liquor effluent. Reactor volume disturbances as a result of influent lift station operation have also been documented which cause the conventional oxygen feed controller to be ineffective (Norman et al., 1985).

The purpose of this paper is to review the operational inadequacies of the conventional oxygen control scheme and to examine the potential benefits of two alternative control strategies. One alternative is the patented vacuum exhaust control (VEC) strategy as shown in Figure 2 (Clifft and Garrett, 1988). This strategy controls the oxygen feed in a conventional manner, but the setpoint pressure in the first stage is reduced to atmospheric pressure (0.0 mm Hg differential pressure). Since a pressure drop through the gas phase is required, subsequent stages operate with a slight negative pressure which eliminates potential oxygen losses through gas phase leaks. In order to prevent DO depletions and minimize oxygen losses through the exit gas line, an exhaust apparatus is used to control the exit gas flow rate. A DO signal from probes located in the last stage (or the clarifier stilling well) is used to regulate the exit gas flow. This method of controlling the exit gas is superior to the conventional control method because the exit gas flow is not limited by the reactor gas phase pressure. Also, existing pl' . -an be retrofitted to implement the VEC strategy very easily.

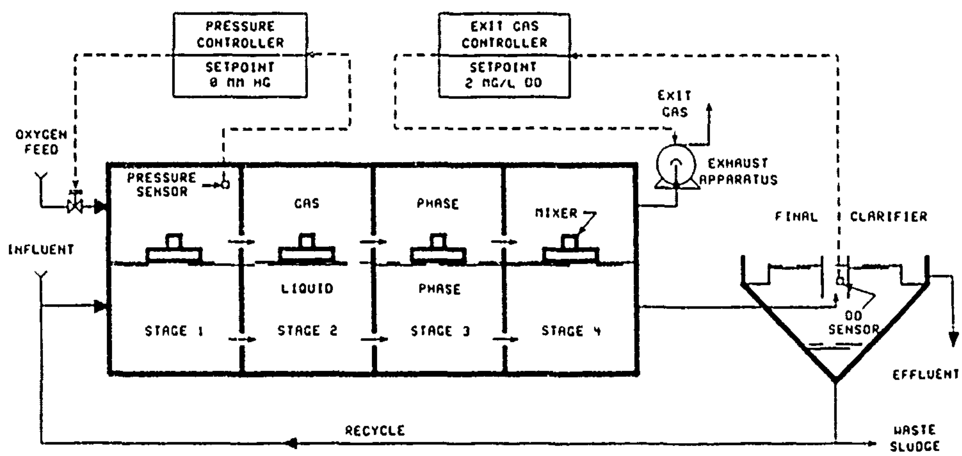

FIGURE 2. VEC Control Strategy

Some plants have experienced problems with the conventional oxygen feed controller which is also utilized in the VEC strategy. The problem appears to be associated with liquid level changes in the reactor caused by lift station pumps during peak flows. When high influent flows occur, the liquid level in the reactor increase suddenly and compresses the gas phase causing an increase in pressure. When the conventional controller senses an increased pressure, it reduces the oxygen feed to the system in an attempt to bring the pressure back to the setpoint. This is the opposite action that is needed since as more wastewater is brought into the reactor, oxygen demands increase requiring more oxygen feed. To alleviate this problem a new oxygen feed control strategy is examined which utilizes a DO probe in the last stage of the reactor to control the

oxygen feed rate. The new oxygen feed control strategy does not attempt to control gas phase pressure, but it adjusts the oxygen feed rate in an effort to maintain a constant effluent DO. The advantage of this control scheme is that it is not affected by disturbances in the reactor liquid volume.

A dynamic model for gas transfer in OAS plants (Clifft and Andrews, 1986) is used in this paper to compare the conventional and alternative control strategies. The model describes the transfer of oxygen, nitrogen, and carbon dioxide between phases and accounts for equilibrium changes in the carbon dioxide-bicarbonate buffering system. Gas transfer is modeled using the two-film theory with consideration of direct interfacial oxygen transfer and inert gases (Clifft and Barnett, 1988). Since the basic model developed by Clifft and Andrews assumes a constant volume reactor, the model used in this work was modified to account for slight volume changes caused by varying influent flows. This modification was necessary in order to examine variations in the gas phase pressure for simulations of the new oxygen feed control strategy.

The model was calibrated for the 12 MGD OAS plant serving the City of Hot Springs, Arkansas, and simulations of the conventional and alternative control strategies are presented for a 24 hour period. Typical variations in influent flow and reactor oxygen uptake rates are examined for the Hot Springs plant under dry and wet weather conditions. The simulation results indicate that the oxygen utilization efficiency can be significantly improved when the alternative control strategies are employed. Using the conventional control strategy, the present oxygen utilization efficiency for the Hot Springs plant is approximately 67 percent during dry weather. The VEC and new oxygen feed control strategies increase the efficiency to more than 85 percent. Thus, a significant cost savings can be achieved since the oxygen generating facilities are equipped with turndown capability. Annual savings for the Hot Springs plant are projected to exceed $50,000 if alternative control strategies are implemented.

REFERENCES

1. Albertsson, J. G., Grunert, W. E., Nehov, N. T., and Scaccia, C., "Oxygenation Equipment and Reactor Design for UNOX Systems," In: The Use of High Purity Oxygen in the Activated Sludge Process, Vol. II, J. R. WcWhirter (Ed.), Chemical Rubber Co. Press, Inc., Cleveland, OH (1978).

2. Clifft, R. C., and Andrews, J. F., "Gas-Liquid Interactions in Oxygen Activated Sludge," Journ. Envir. Engr. Div., ASCE, 112:61 (1986).

3. Clifft, R. C. and Barnett, M. W., "Gas Transfer Kinetics in Oxygen Activated Sludge," Journ. Envir. Engr. Div., ASCE, 114:415 (1988).

4. Clifft, R. C. and Garrett, M. T., "Improved Oxygen Dissolution Control for Oxygen Activated Sludge," Water Sci. and Tech., 20:101 (1988).

5. Norman, T., Borchart, R. J., Garrett, M. T., Ahmad, Z., and Hayre, G., "Startup and Interim Operation of Houston's 69th Street Wastewater Complex", Instrumentation and Control of Water and Wastewater Treatment and Transport Systems, Proceedings of the 4th IAWPRC Workshop, Houston, TX (1985).

VOLUMETRIC MASS TRANSFER COEFFICIENT AND HYDRODYNAMICS IN AIR-WATER AIR LIFT REACTORS

M. Díaz, I.I. Ugartemendia, J.C. García, A.G. Lavín.

Dpt. of Chemical Engineering. Univ. of Oviedo. Oviedo. Spain.

Oxygen transfer from air to water is an important subject in municipal water treatment works because of its low cost-to-oxidation capacity ratio. Impellers and bubblers are mainly in use, but other process reactors like the air-lift ones must be tested. For waste water treatment, diferent configurations can be considered, air lift pipes, air lift towers with downflow section, distribution of air lift pipes in lagoons, weirs in lagoons ..., each one of them having a diferent efficiency per unit power in terms of oxygen supply, good mixing, or uniform distribution of solids.

A 'sufficient' oxygen transfer for a given water will depend mainly on the volumetric mass transfer coefficient K_La and on the concentration gradient. The K_La value will be a fûntion of mass transfer equipment, flow rates and physical properties, while oxygen gradient will depend on the complexion degree and on hydrodynamics. Hydrodynamics, including the downflow can give rise to sustained or fastly low concentration gradients.

To study mass transfer and hydrodynamics an air lift tower with 4 m height has been built. It consists of a square column of 60 cm x 60 cm with a centered tube of 8 cm diameter with the inlet air in the bottom. Flow rates of gas and liquid can be measured and controlled with a computer and sampling is also prepared. Volumetric mass transfer coefficient have been measured by the oxygen absorption method. Hydrodynamics in the downflow was followed by stimulus-response method with image analysis of video.

The K_La values in the global set-up with the up and down flows, have been determined for different air flow rates. The values obtained by measures at different heights in the column are afected with a delay time, function of the type of downflow and its flow rate.

A separate determination of the K_La value in the upflow has been made with a 2 m length tube as a function of gas flow rate. Previously, the induced liquid flow rate had been obtained and heterogeneity in the column was characterized optically. The K_La coefficient was correlated as a function of gas flow rate and on the concentration of a solid of high porosity. The selected solids are cubes of high porosity poliestyrene of E=0.97 that makes density similar to that of water, like flocs but also that can be used as a support, and that will need a low energy consumption for suspension

and mixing.

For modeling of the resulting mass transfer in the pilot air lift studies of downflow must be made a coloured stimulus inyection in the upper water surface at two distances from pipe for different gas flow rates. Correlation of results has been made in terms of a mixing time for each experiment . Specific models for the semicontinuous G-L system must be introduced, although a simple dispersion value can be obtained from the analysis of the expansion of coloured zone.

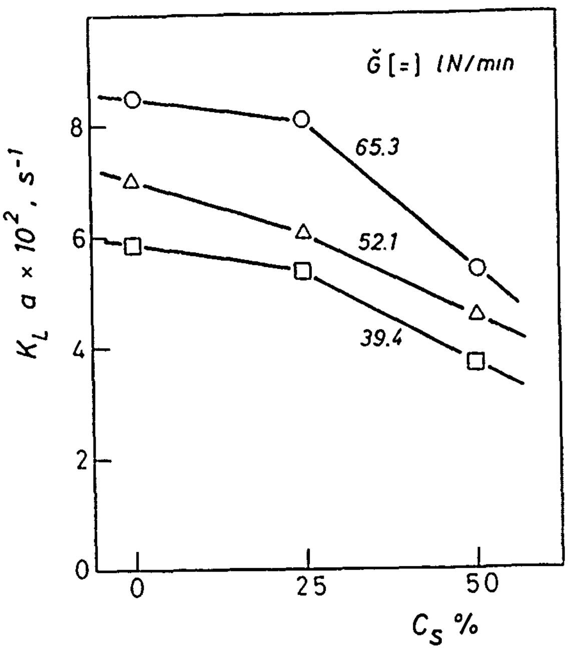

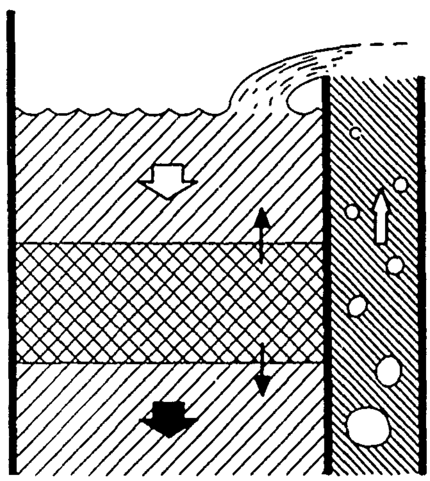

Refs.:

- M. Díaz, D. Saenz, F. Varona, "Pressure Drop for Air Lift Pumps", Latinoam. J. of Chem. Eng., Nº 16, pp. 335-350, (1986).

- M.E. Orazem, L.T. Fan, L.E. Erickson, "Bubble Flow in the Downflow Section of an Airlift Tower.", Biotechnology and Bioengineering, Vol. XXI, 1579 (1979).

- M.Y. Chisti, M. Moo-Young, "Airlift Reactors: Characteris - tics, Applications and Design Considerations." Chem. Eng. Comm., Vol. 60, pp 195-242, (1987).

Mercury behavior in a wastewater sludge incineration process

Dianne Dorland
Department of Chemical Processing Engineering
University of Minnesota, Duluth
Duluth, Minnesota 55812

Joseph Stepun
Western Lake Superior Sanitary District
Duluth, Minnesota 55806

ABSTRACT

The Western Lake Superior Sanitary District (WLSSD) in Duluth, Minnesota utilizes solid waste as fuel to incinerate wastewater treatment sludge, conserving energy resources while reducing landfill loading requirements. The District's solid waste processing facility was completed in 1981 and processes over 300 tons of solid waste per day from residential, commercial, and industrial sources. After processing and removal of non-combustible materials, such as metal and glass, the system produces an average of 150 tons of refuse derived fuel (RDF) each operating day. The wastewater treatment sludge is incinerated with RDF in a fluidized bed reactor.

With the incineration of solid wastes, however, some wastes are recycled and constituents such as heavy metals have increased concentrations in effluent streams. Independent studies in the St. Louis Bay (Duluth-superior Harbor), indicate significant concentrations of mercury in the water column in the area of the WLSSD water effluent. Sediments are known to accumulate heavy metals that may contribute to overlying water, and surface sediment samples at the WLSSD site have also been shown to contain substantial amounts of mercury, cadmium, lead, copper, nickel, chromium, zinc, and arsenic. Of these metals, mercury is the only one that indisputably biomagnifies through the food chain. In addition, unlike most other metals, mercury is efficiently transformed into its most toxic form (methyl mercury) in an aquatic environment and metal contamination of fish has been a public health concern in St. Louis Bay for some time. Revised National Pollution Discharge Elimination System (NPDES) guidelines will require new discharge effluent levels, and operational changes are needed to meet the new guidelines. A decrease in the heavy metal component in the water effluent from WLSSD would also aid in lowering mercury levels in the St. Louis Bay, promoting continuing efforts to improve the water quality in this area. The objective of this research was to determine mercury partitioning between the gas and water phases during the wastewater treatment/incineration process. This information would then be utilized in the development of a mercury removal process for the WLSSD facility.

A preliminary evaluation of the process flows and compositions in the plant was used to determine overall and unit mass balances streams with high metal concentrations. The incinerated sludge and solid waste produce a gas stream which leaves the fluidized bed incinerator and passes through dry ash removal cyclones. The hot gas stream passes through a wet venturi scrubber and a sieve tray column to remove remaining particulates and pollutant gases. Scrubbed particulates in the form of a dilute sludge are then recycled to the wastewater treatment process.

Mass balance calculations indicated that approximately 50% of the total mercury left the process in the gas stream and approximately 50% was contained in the wastewater

effluent at a concentration of 100-400 ng/L. The principal form of mercury in the stack gas appears to be elemental mercury. In the wastewater effluent, mercury is present at equilibrium in the +2 oxidation state and is considered to be complexed as the Hg^{+2} cation. In the scrubbing process, the pH of the aqueous system is appreciably lower than that of the final effluent and species such as chlorine complexes may be favored over hydroxide complexes. Forms of methyl mercury are not expected as an incineration product, but would favor the gaseous phase due to their high volatility. Organic complexation of mercury in the wastewater effluent to yield methyl mercury forms may occur after effluent discharge into the natural waters of the bay.

The scrubbing system was identified as a critical area for heavy metal accumulation based on the process flow stream evaluation. In the recycled water to the venturi scrubber, total mercury concentrations were 22,000 ng/L. Initial laboratory tests indicated a high percentage of the mercury associated with the particulates on fly asn in this stream. Three primary methods of mercury removal were considered for application in this process: removal of solids with adsorbed mercury, precipitation, and adsorption. Precipitation and coagulation were subsequently tested for mercury removal efficiency with a series of chemicals and coagulants including lime, alum, ferric sulfate, ferric chloride, cationic polymer, and anionic polymer. The removal of solids with adsorbed mercury appeared to be the most efficient method with over 90% removal of total mercury. Precipitation reactions did not appear to increase the removal efficiencies, indicating that the mercury was not independently available for reaction.

Initial plant tests have been run using alum and anionic polymer resulting in a mercury removal efficiency of 84%. Plant tests with lime are also planned because of the anticipated benefit in terms of reduced corrosivity and phosphorous control in other process streams. Further plant tests with added lime in the incineration process are being considered. Their purpose would be to alter plant process conditions to favor a reducing environment, yielding mercury speciation more soluble in water and subsequently promoting higher removal of total mercury in the aqueous scrubbing process.

This paper presents a process description, the results of the laboratory testing to choose a mercury removal method appropriate for the plant process, and the results of initial plant trials for mercury removal. Mercury partitioning is correlated with process variables such as temperature, pH, phase, chemical oxygen demand, total dissolved solids content, and fly ash composition. An outline of plant process evaluations and suggestions for further study are also discussed.

Title: Optimization of Oxygen Mass Transfer Rate in Biological Wastewater Treatment

Author: Mr. Tapan Kumar (Environmental Engineer, CCJM, P.C.)

Affiliation: Member of AICHE, WPCF

The function of an aeration tank in the activated sludge system is to transfer oxygen to the liquid at such a rate that oxygen never becomes the limiting factor in process operation (i.e., never limits the rate of organic utilization or other metabolic functions). The mechanism of transporting oxygen from gas to microbial cells so as to maintain the microbes at the maximum respiratory activity is vital to an effectively functioning aerobic system.

Oxygen transport is not simply a transport process since the oxygen, once in solution, is utilized by the microorganisms. The method of **dynamic reaeration** was used to measure the oxygen transfer coefficient, making use of the unsteady state technique in the presence of active, oxygen consuming microorganisms. The following three different experimental set-up, under varying process parameters were used to evaluate the oxygen transfer efficiencies: biological system with a bubble column (Figure 1), biological system with a packed column (Figure 2), and biological system with a mechanical high shearing device (Figure 3).

The mass transfer rate of oxygen to the aerated biomass sludge (K_La) in the bubble column was 0.54 min^{-1} (Table 1). When the experiment with a concurrent flow in the packed column was used as a recirculation loop, the K_La value was increased to 6.86 min^{-1}. The packed column affected the K_La value greatly because the packing of 3 mm glass beads broke the air bubbles into very fine bubbles. The flocs were also broken so that oxygen could easily reach the center of the smaller flocs. Both processes increased the interfacial area of contact and thereby the mass transfer rate. The use of a mechanical high shearing device provided shear and turbulence to the aerated biomass sludge to better disperse air into the liquor, and hence yielded a high mass transfer rate with a value of 3.50 min^{-1}.

Table 1 shows that the mechanical shearing affects the K_La value greatly. The use of a centrifugal pump as the mechanical shearing device increased the K_La value to 3.50 min^{-1}. When the packed column was used with a peristaltic pump, the K_La value was 2.76 min^{-1}. It showed the use of a centrifugal pump resulted in higher mass transfer rate than the packed column when other parameters were kept the same.

Table 1

Comparison of Mass Transfer Rate for Different Systems

Biological System	F_1 (ml/min)	K_La (min^{-1})	σ_{n-1}
Bubble column	-	0.54	0.02
Packed column* with the peristaltic pump	885	2.76	0.18
Mechanical high shearing saturator using a centrifugal pump	885	3.50	0.14
Packed column* with the centrifugal pump	870	6.86	0.61

Note: F_1 = Flow rate of liquid
K_La = Mass transfer rate of oxygen to the aerated biomass sludge
Air flow rate = 188 ml/min
* = Packed column with an effective length of packing of 325 mm with 3 mm glass beads and ID = 26 mm
σ_{n-1} = standard deviation in K_La values

The dynamic reaeration method yielded very reliable results and required the least complicated measuring equipment for determining the oxygen transfer rate. The recirculation of aeration liquor by a mechanical high shearing device and the use of a packed bed column produced surface and subsurface turbulence, resulted in smaller size bubbles, and diffused air through the liquid mass, resulting in longer contact time. The oxygen transfer was increased significantly using these techniques.

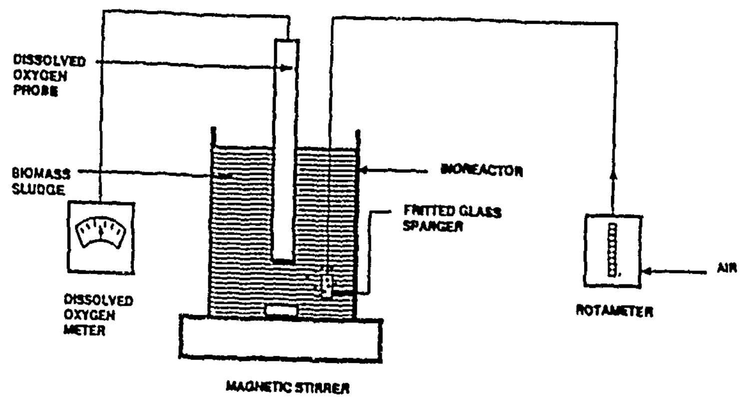

FIGURE 1. BIOLOGICAL SYSTEM WITH A BUBBLE COLUMN.

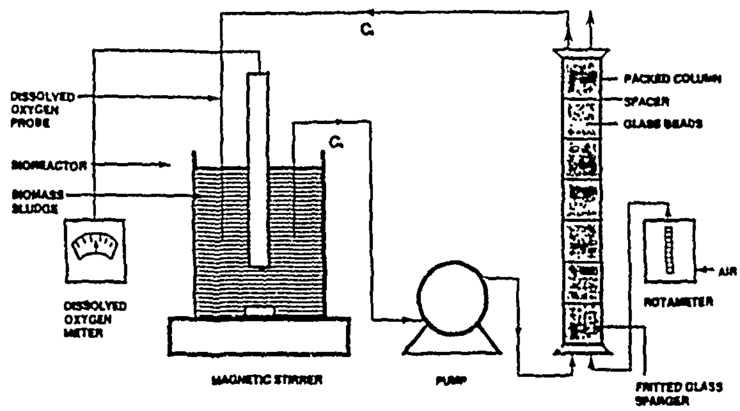

FIGURE 2. BIOLOGICAL SYSTEM WITH A PACKED COLUMN IN THE RECIRCULATION LOOP.

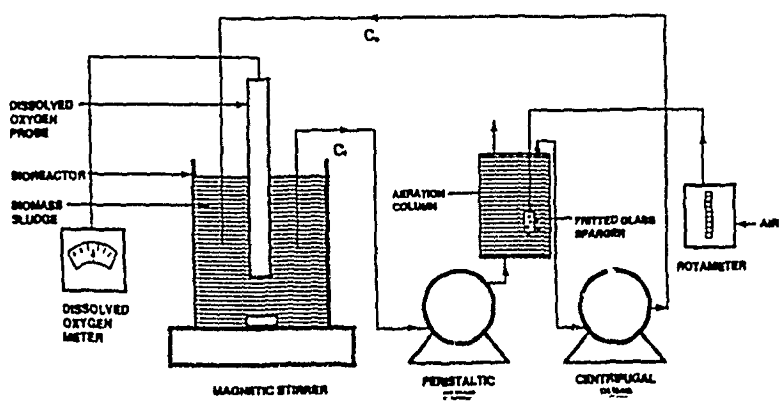

FIGURE 3. BIOLOGICAL SYSTEM WITH A MECHANICAL HIGH SHEARING SATURATOR.

CATALYTIC LIQUID-PHASE OXIDATION OF ORGANICALLY POLLUTED WATERS

Janez Levec

Department of Chemistry and Chemical Engineering
University of Ljubljana, 61000 Ljubljana, Yugoslavia

Many wastewater streams originating in the chemical process industries contain organic pollutants which are either poorly biodegradable or are found in concentrations so high that the conventional biological treatment can not be applied directly. Other than biological and chemical oxidation processes several systems are used, or are in various stages of development. For example, thermal liquid-phase is known to have a great potential in advanced waste treatment facilities. However, reaction conditions such as 200-300°C and 70-130 bar, and the presence of wide range of oxygenated compounds which are highly corrosive materials, drastically affect the economics of the process. Oxidation of dilute aqueous solutions of organic pollutants by using solid catalysts offers an alternate process to thermal liquid-phase oxidation as a means of purifying wastewaters. In this process organics are oxidized to carbon dioxide in a three-phase reaction system at milder conditions than in the thermal process.

The aim of this work is to present experimental results of the catalytic oxidation of dilute aqueous solutions of model organic pollutants such as phenol, 2-chlorophenol, 4-nitrophenol, tertiary buthyl alcohol, and methyl vinyl ketone over a proprietary catalyst. A two-level approach was used: (1) in a slurry system intrinsic oxidation kinetics was evaluated, and (2) in an integral trickle-bed reactor the interaction of intrinsic kinetics, intraparticle, interphase, and intrareactor mass transport was studied. Only the first approach will be discussed in details.

The kinetic runs were carried out in a two liters autoclave reactor equipped with magnetically driven turbine type impeller and temperature and pressure control units. In a typical run 60-100 mesh size catalyst was charged into the reactor containing known amount the dilute aqueous solution of a model pollutant. The back pressure regulator was set and the content of reactor was brought to the reaction conditions. Then air/oxygen was sparged continuously through the suspension at a metered rate. Representative samples were withdrawn periodically and the catalyst was immediately separated by centrifugation from the aqueous phase. The aqueous phase was analyzed by conventional HPLC/GC methods for the residual content of organics.

The results of these experiments demonstrate that the above model pollutants can easily be converted via intermediates to carbon dioxide at relative mild reaction conditions: temperature of 130°C and oxygen partial pressure of 3 bar only. The catalyst employed exhibites an induction period for all organics but nitrophenol. The reaction undergoes the induction period and transition to much higher, steady state activity regime. The oxidation reaction is first order with respect to particular organic pollutant in both regimes. The oxygen dependency is shifted from first order in the induction period to one-half in the steady state activity regime.

Global reaction rates from differential trickle-bed operation and conversions from integral reactor were compared with predictions of global rates and integral conversions by using available mass transfer information. These quantitative comparisons between predicted and experimental global rates and conversions suggest that the available literature information may not fulfill the needs for an ab initio design of trickle-bed reactor, neither to determine whether such a reactor is an optimum choice in removal of organic pollutants from wastewaters by catalytic oxidation. In particular, more complete studies are needed with water near its boiling point in order to evaluate the effect of direct contact of air/oxygen with catalyst particle. In the trickle-bed runs the proprietary catalyst in a cylindrical form (3 x 3 mm) was employed in a 40 mm I.D. reactor operated at 130-150°C and 6-30 bar.

HIGH EFFICIENCY AMMONIA STRIPPING - A NOVEL APPROACH

Syed Obaid-ur-Rehman
Department of Chemical Engineering
King Saud University, P.O. Box 800,
Riyadh 11421, Saudi Arabia

and

Shafkat A. Beg
Department of Chemical Engineering
King Fahd University of Petroleum & Minerals,
Dhahran 31261, Saudi Arabia

INTRODUCTION

Ammonia is one of the pollutants that is dealt with in particular in any wastewater management program. This is primarily due to the various deleterious effects that it exerts on receiving waters. Various physio-chemical and biological processes (breakpoint chlorination, selective ion exchange, ammonia stripping and biological nitrification-denitrification) are available for ammonia removal from wastewaters. The ammonia stripping offers several advantages over the other available processes. These include, simplicity of operation, lower capital and treatment cost, high degree of removal and no liquid or solid wastes for disposal.

The ammonia stripping process can be simply defined as a unit process in which air and wastewater are brought into contact with each other for the purpose of transferring ammonia from wastewater to air. The efficiency of the ammonia stripping process primarily depends on the way the two phases are brought into contact with each other. In large scale water treatment applications, packed columns, spray towers, and holding ponds have been extensively employed for ammonia stripping. Severe operational problems are reported for packed column ammonia stripping. These include, $CaCO_3$ scale deposition, biological oxidation of ammonia to nitrates in the aerobic towers and relatively poor performance in cold weather(1-4). Previous studies have indicated that high ammonia removal efficiencies in the spray towers can only be achieved at very low hydraulic loadings and significantly high air to water ratios(1-4). Furthermore, the holding ponds were found to be low efficiency systems with a very high reliance on the wind velocity.

THIS COMMUNICATION

In this communication, a cocurrent wetted butterfly valve scrubber system is introduced for air stripping of ammonia from waste waters. The wetted butterfly valve scrubber system (Figure 1) consist of a pneumatic atomizing section, a cyclone separator, reservoirs for feed and treated water, and other control auxiliaries. A Sutorbilt 5L series blower driven by a 10 hp, 1725 rpm Reliance motor assembly was used to provide a maximum air flowrate of 500 SCFM through the scrubber with a maximum water flowrate of about 10 GPM.

Detailed mass transfer studies for ammonia stripping in the proposed system have been carried out. The data is reported in terms of removal efficiency and number and height of transfer units. The effects of pressure drop, gas and hydraulic loading on the performance of the system have also been included.

It has been concluded that the proposed system, being a cocurrent liquid atomizing system, not only provides very high relative velocities between the two phases, but also provides very high interfacial areas for interphase mass transfer. In addition, it also offers high removal efficiencies for ammonia, both at high hydraulic loading and lower air to water ratios.

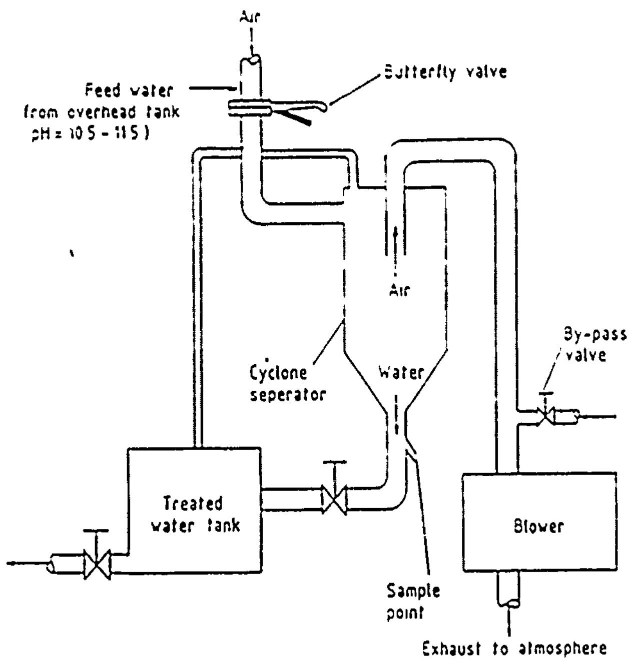

Figure 1 : The Proposed Wetted Butterfly Valve Scrubber System.

REFERENCES

1. Slechta, A.F. and Culp, R.L., "Water Reclamation Studies at the South Lake Tahoe Public Utility District", JWPCF, 39, 5, 787(1967).

2. Reeves, A.F., "Nitrogen Removal: A Literature Review:", JWPCF, 44, 10, 1895(1972).

3. Atkins Jr., P.F. and Scherger, D.A., "A Review of Physical-Chemical Methods for Nitrogen Removal from Wastewaters", Prog. Wat. Technol., 8, Nos. 4/5, 713(1977).

4. Beg, S.A. and Obaid-ur-Rehman, S., "Ammonia Removal by Air Stripping-From Origin to Present State of Technology", The Journ. of Envirom. Sci. & Technol. (Submitted).